Expanding technological horizons for treatment and staging early oesophageal cancer



Paul Wolfson

Department of Targeted Intervention

Division of Surgery & Interventional Science

UCL

December 2024

A thesis submitted for the degree of Doctor of Philosophy

Statement of Originality

I, Paul Wolfson confirm that the work presented in this thesis is my own. Where information has been derived from other sources, I confirm that this has been indicated in the thesis.

Abstract

<u>Background</u>

Barrett's dysplasia confers significantly greater risk of developing oesophageal adenocarcinoma (OAC) which has poor outcomes. Radiofrequency ablation (RFA) has become established therapy for Barrett's dysplasia. Long-term data is lacking. Staging is the most accurate reflection of cancer prognosis. Accuracy of this staging is conflicting.

I aim to establish if:

- I. outcomes from RFA are durable and reduce the risk of developing OAC
- II. T2N0 oesophageal cancer staging is accurate
- III. x-ray phase imaging (XPCI) can stage and grade oesophageal tissues

Methods

Analysis of the UK RFA registry was conducted to calculate rates of invasive cancer, clearance rates of dysplasia (CR-D) and intestinal metaplasia (CR-IM). Accuracy of oesophageal cancer staging was established using a systematic review. To grade and stage oesophageal tissues XPCI techniques were used.

Results

Ten-years after RFA therapy, cancer rate was 4.1%. CR-D and CR-IM after 2 years of therapy were 88% and 62.6%. Persistance rates were 5.9% from CR-D and 18.7% from CR-IM at 8 years, most recurrences occurred within 2 years.

Impact statement

My PhD began as a project to investigate the use of x-ray phase contrast imaging within oesophageal tissues. This project was and remains the only use of this novel technique to both grade and stage oesophageal tumours. Whilst performing this work I developed my interest in the accuracy of current staging techniques and worked to publish the long-term outcomes from the largest UK registry focusing on early treatment of oesophageal pre-cancerous lesions.

I have published research from my thesis has been published in a number of peer-reviewed journals and have authored/co-first authored three articles. Work is ongoing to publish remaining data from some of my work particularly the use of x-ray phase contrast imaging to identify different tissue types.

The greatest impact from my work was publishing the 10-year outcomes from the UK National Halo Radiofrequency Ablation Registry [1]. This paper, published in *Gastrointestinal Endoscopy*, has been cited over 30 times as of December 2024, was the culmination of more than 10 years work across the county. It remains the largest study of its kind with data from over 2,500 patients included. It confirmed that a widely established treatment for Barrett's dysplasia is both safe and efficacious, reducing cancer risk by more than 90%. This work has profound implications for the potential 160 million people with Barrett's oesophagus.

Further published work includes my meta analysis *Accuracy of clinical staging for T2NO oesophageal cancer: systematic review and meta-analysis* [2]has been cited 10 times and *T staging esophageal tumours with x rays* [3].

I have had work accepted at both national and international conferences. I presented my work on the HALO RFA registry as an oral presentation at the British Society of Gastroenterology Meeting in 2019. Unfortunately, I was never able to present my work at the Digestive Disease Week 2020 due to COVID-19 pandemic.

List of publications

- P. Wolfson *et al.*, "Endoscopic eradication therapy for Barrett's esophagus—related neoplasia: a final 10-year report from the UK National HALO Radiofrequency Ablation Registry," *Gastrointest Endosc*, vol. 96, no. 2, pp. 223–233, Aug. 2022, doi: 10.1016/J.GIE.2022.02.016.
- P. Wolfson *et al.*, "Accuracy of clinical staging for T2N0 oesophageal cancer: Systematic review and meta-analysis," *Diseases of the Esophagus*, vol. 34, no. 8, pp. 1–12, 2021, doi: 10.1093/dote/doab002.
- T. Partridge et al., "T staging esophageal tumors with x rays," Optica, vol. 11, no. 4, p. 569, Apr. 2024, doi: 10.1364/OPTICA.501948.

List of abstracts

- P. Wolfson *et al.*, "P240 Accuracy of clinical staging for T2N0 oesophageal cancer: systematic review and meta-analysis," Gut, 70, A166.1-A166, 2021, doi: 10.1136/gutjnl-2020-bsgcampus.314.
- P. Wolfson *et al.,* "O29 Time to CRD and subsequent relapses: ten year follow up from the UK patient registry," Gut, 70, A16-A17, 2021, doi: 10.1136/gutjnl-2020-bsgcampus.29.
- P. Wolfson *et al.*, "P239 X-ray phase contrast imaging for staging oesophageal tumours: preliminary results from the VIOLIN study," Gut, 70, A165.2-A166, 2021, doi: 10.1136/gutjnl-2020-bsgcampus.313.
- P. Wolfson *et al.*, "OTU-18 Using X-ray phase contrast imaging to identify oesophageal pathology", Gut, 68, A134.1-A134, 2019 doi: 10.1136/gutjnl-2019-BSGAbstracts.253.

UCL Research Paper Declaration Form

referencing the doctoral candidate's own published work(s)

Please use this form to declare if parts of your thesis are already available in another format, e.g. if data, text, or figures:

- have been uploaded to a preprint server
- are in submission to a peer-reviewed publication
- have been published in a peer-reviewed publication, e.g. journal, textbook.

This form should be completed as many times as necessary. For instance, if you have seven thesis chapters, two of which containing material that has already been published, you would complete this form twice.

- 1. For a research manuscript that has already been published
 - a) What is the title of the manuscript?

Endoscopic eradication therapy for Barrett's esophagus-related neoplasia: a final 10-year report from the UK National HALO Radiofrequency Ablation Registry

b) Please include a link to or doi for the work

https://pubmed.ncbi.nlm.nih.gov/ 35189088/

c) Where was the work published?

Gastrointestinal Endoscopy

d) Who published the work? (e.g. OUP)

Elsevier

e) When was the work published?

February 2018

f) List the manuscript's authors in the order they appear on the publication

Paul Wolfson, Kai Man Alexander Ho, Ash Wilson, Hazel McBain, Aine Hogan, Gideon Lipman, Jason Dunn, Rehan Haidry, Marco Novelli, Alessandro Olivo, Laurence B Lovat;

g) Was the work peer reviewed?

Yes

h) Have you retained the copyright?

Νo

i) Was an earlier form of the manuscript uploaded to a preprint server? (e.g. medRxiv). If 'Yes', please give a link or doi)

No

If 'No', please seek permission from the relevant publisher and check the box next to the below statement:

Ø

I acknowledge permission of the publisher named under **1d** to include in this thesis portions of the publication named as included in **1c**.

- 2. For a research manuscript prepared for publication but that has not yet been published (if already published, please skip to section 3)
 - a) What is the current title of the manuscript?

Click or tap here to enter text.

b) Has the manuscript been uploaded to a preprint server? (e.g. medRxiv; if 'Yes', please give a link or doi)

Click or tap here to enter text.

c) Where is the work intended to be published? (e.g. journal names)

Click or tap here to enter text.

d) List the manuscript's authors in the intended authorship order

Click or tap here to enter text.

e) Stage of publication (e.g. in submission)

Click or tap here to enter text.

3. For multi-authored work, please give a statement of contribution covering all authors (if single-author, please skip to section 4)

I was responsible for analysing the data obtained through the UK registry. I drafted the final manuscript. Rehan Haidry, Gideon Lipman, Jason Dunn and Marco Novelli all worked to establish and publish on earlier work from this registry. Kai Man Alexander Ho, Ash Wilson, Hazel McBain, Aine Hogan and Alessandro Olivo all assisted with data analysis and drafting this manuscript. Laurence Lovat was founded the UK registry, guided all analysis and assisted with drafting of the final work.

4. In which chapter(s) of your thesis can this material be found?

Chapter 3

5. e-Signatures confirming that the information above is accurate (this form should be co-signed by the supervisor/ senior author unless this is not appropriate, e.g. if the paper was a single-author work)

Candidate Paul Wolfson Date 09/12/2024

Supervisor/ Senior Author (where appropriate)
Prof Laurence B. Lovat
Date 18/12/2024

UCL Research Paper Declaration Form

referencing the doctoral candidate's own published work(s)

Please use this form to declare if parts of your thesis are already available in another format, e.g. if data. text, or figures:

- · have been uploaded to a preprint server
- are in submission to a peer-reviewed publication
- have been published in a peer-reviewed publication, e.g. journal, textbook.

This form should be completed as many times as necessary. For instance, if you have seven thesis chapters, two of which containing material that has already been published, you would complete this form twice.

- 1. For a research manuscript that has already been published (if not yet published, please skip to section 2)
 - a) What is the title of the manuscript?

Accuracy of clinical staging for T2NO oesophageal cancer: systematic review and meta-analysis

b) Please include a link to or doi for the work

https://pubmed.ncbi.nlm.nih.gov/33618359/

c) Where was the work published?

Diseases of the Esophagus

d) Who published the work? (e.g. OUP)

Oxford University Press

e) When was the work published?

August 2021

- f) List the manuscript's authors in the order they appear on the publication Paul Wolfson, Kai Man Alexander Ho, Paul Basset, Rehan Haidry, Alessandro Olivo, Laurence B Lovat, Sarmed S Sami
 - g) Was the work peer reviewed? Yes
 - h) Have you retained the copyright?

No

i) Was an earlier form of the manuscript uploaded to a preprint server? (e.g. medRxiv). If 'Yes', please give a link or doi)

No

If 'No', please seek permission from the relevant publisher and check the box next to the below statement:

冈

I acknowledge permission of the publisher named under **1d** to include in this thesis portions of the publication named as included in **1c**.

- 2. For a research manuscript prepared for publication but that has not yet been published (if already published, please skip to section 3)
 - a) What is the current title of the manuscript?

Click or tap here to enter text.

b) Has the manuscript been uploaded to a preprint server? (e.g. medRxiv; if 'Yes', please give a link or doi)

Click or tap here to enter text.

- c) Where is the work intended to be published? (e.g. journal names) Click or tap here to enter text.
- d) List the manuscript's authors in the intended authorship order Click or tap here to enter text.
- e) Stage of publication (e.g. in submission)

Click or tap here to enter text.

3. For multi-authored work, please give a statement of contribution covering all authors (if single-author, please skip to section 4)

I, along with Professor Laurence Lovat and Dr Sarmed Sami conceived and drafted the study. I collected the data and performed the initial searches. Dr Alex Ho and I collected the data. Dr Sarmed Sami and Dr Paul Bassett assisted me with the data analysis and interpretation. I wrote the initial draft which was reviewed by Professor Laurence Lovat, Dr Sarmed Sami and Dr Alex Ho.

- 4. In which chapter(s) of your thesis can this material be found? Chapter 4
- **5. e-Signatures confirming that the information above is accurate** (this form should be co-signed by the supervisor/ senior author unless this is not appropriate, e.g. if the paper was a single-author work)

Candidate

Paul Wolfson

Date 09/12/2024

Supervisor/ Senior Author (where appropriate)

Prof Laurence B. Lovat

Date 18/12/2024

UCL Research Paper Declaration Form

referencing the doctoral candidate's own published work(s)

Please use this form to declare if parts of your thesis are already available in another format, e.g. if data, text, or figures:

- have been uploaded to a preprint server
- are in submission to a peer-reviewed publication
- have been published in a peer-reviewed publication, e.g. journal, textbook.

This form should be completed as many times as necessary. For instance, if you have seven thesis chapters, two of which containing material that has already been published, you would complete this form twice.

- **6.** For a research manuscript that has already been published (if not yet published, please skip to section 2)
- j) What is the title of the manuscript?T staging esophageal tumors with x rays
- k) Please include a link to or doi for the work https://opg.optica.org/optica/fulltext.cfm?uri=optica-11-4-569&id=549214
- I) Where was the work published?Optica
- m) Who published the work? (e.g. OUP) Optica publishing group
 - n) When was the work published? April 2024
- o) List the manuscript's authors in the order they appear on the publication T. Partridge, P. Wolfson, J. Jiang, L. Massimi, A. Astolfo, N. Djurabekova, S. Savvidis, C. J. Maughan Jones, C. K. Hagen, E. Millard, W. Shorrock, R. M. Waltham, I. G. Haig, D. Bate, K. M. A. Ho, H. Mc Bain, A. Wilson, A. Hogan, H. Delaney, A. Liyadipita, A. P. Levine, K. Dawas, B. Mohammadi, Y. A. Qureshi, M. D. Chouhan, S. A. Taylor, M. Mughal, P. R. T. Munro, M. Endrizzi, M. Novelli, L. B. Lovat, and A. Olivo
 - p) Was the work peer reviewed?
 Yes
- q) Have you retained the copyright? No
 - r) Was an earlier form of the manuscript uploaded to a preprint server? (e.g. medRxiv). If 'Yes', please give a link or doi)
 No

If 'No', please seek permission from the relevant publisher and check the box next to the below statement:

X

I acknowledge permission of the publisher named under **1d** to include in this thesis portions of the publication named as included in **1c**.

- 7. For a research manuscript prepared for publication but that has not yet been published (if already published, please skip to section 3)
 - f) What is the current title of the manuscript?

Click or tap here to enter text.

g) Has the manuscript been uploaded to a preprint server? (e.g. medRxiv; if 'Yes', please give a link or doi)

Click or tap here to enter text.

- h) Where is the work intended to be published? (e.g. journal names) Click or tap here to enter text.
- i) List the manuscript's authors in the intended authorship order Click or tap here to enter text.
- j) **Stage of publication** (e.g. in submission) Click or tap here to enter text.
- 8. For multi-authored work, please give a statement of contribution covering all authors (if single-author, please skip to section 4)

The system setups were designed and refined by Professor Sandro Olivo and his Advanced X-ray Imaging Group (AXIm). Much of the refinement for this project was led by Dr Jinxing Jiang, Dr Michela Esposito and Dr Tom Partridge. I led on all tissue acquirement and specimen holder development.

- 9. In which chapter(s) of your thesis can this material be found?
 Chapter 8
- 10. e-Signatures confirming that the information above is accurate (this form should be co-signed by the supervisor/ senior author unless this is not appropriate, e.g. if the paper was a single-author work)
 Candidate

Paul Wolfson

Date 09/12/2024

Supervisor/ Senior Author (where appropriate)

Prof Laurence B. Lovat

Date 18/12/2024

Acknowledgements

Firstly, I would like to thank my supervisors, Professor Laurence Lovat and Professor Sandro Olivo. Their expertise, knowledge and guidance have helped me through the challenges the last 3 and a half years have generated. I am indebted to them for providing me with the opportunity to work in such ground-breaking research.

I would also like to thank Professor Marco Novelli for his assistance and humour throughout these years. His expertise in histology research has proved to be invaluable through this journey.

I am grateful to all members of the Advanced X-ray Imaging group at UCL. In particular I would like to thank Dr Jinxing Jiang, for his tireless work and for developing many of the techniques I relied on, and Dr Thomas Partridge who has seen this project to a close. I would also like to thank Dr Charlotte Maughan-Jones, Dr Michela Esposito and Dr Savvas Savvidis for their commitment and efforts to this project.

I would like to thank members of the GENIE team. In particular Dr Alex Ho for his support and statistical advice, as well as Hazel McBain, Aine Hogan and Vanessa Ward for their assistance and entertainment throughout.

My biggest thank you is for my family. Thank you to my parents for their help and support. To my Uncle Ian without who's financial assistance I was unlikely to be able to have made such a career choice. To my children, Ella, Maya and Ethan who have always helped me to keep all challenges in perspective. Finally, my best friend and wife Debra who supports me through thick and thin.

Table of contents

Statement of originality	2
Abstract	3
Impact statement	4
Acknowledgements	12
List of Figures	24
List of Tables	33
List of Abbreviations	35
Chapter 1 Introduction	38
1.1 Oesophageal cancer	38
1.1.1 Disease prevalence and impact	38
1.1.1.1 Risk factors	39
1.1.1.1.1 Age	39
1.1.1.1.2 Smoking	39
1.1.1.1.3 Ethnicity	40
1.1.1.1.4 Sex	40
1.1.1.1.5 Alcohol	41
1.1.1.1.6 Obesity	42
1.1.1.1.7 Abdominal obesity	43
1.1.1.7.1 Weight loss	44
1.1.1.1.8 Hormones	44
1.1.1.1.9 Metabolic syndrome	45
1.1.1.1.10 Barrett's oesophagus	45

1.1.2 Management of oesophageal cancer	46
1.1.2.1 Diagnosis and staging	46
1.1.2.2 Accuracy of staging	49
1.1.2.3 Staging technologies	50
1.1.2.3.1 Computerised Tomography	50
1.1.2.3.2 Endoscopic ultrasound	50
1.1.2.3.3 Laparoscopy	50
1.1.2.3.4 Novel techniques	51
1.1.2.3.4.1 Magnetic resonance imaging	51
1.1.2.3.4.2 X-ray Phase Contrast Imaging	51
1.1.3 Treatment of oesophageal cancer	51
1.1.3.1 Endoscopic endotherapy	52
1.1.3.2 Chemotherapy and radiotherapy	52
1.1.3.2.1 Outcomes of chemotherapy and radiotherapy	52
1.1.3.3 Surgery	53
1.1.3.3.1 Outcomes of surgery	54
1.1.3.4 Best supportive care	55
1.2 Barrett's oesophagus	55
1.2.1 Definition	55
1 2 2 Rarrett's pesophagus disease progression	57

1.2.3	Vienna clas	sification			58
1.2.3.1	Low gra	ade dysplas	sia		59
1.2.3.2	2 High gr	ade dyspla	sia		59
1.2.3.3	3 Intram	ucosal carc	inoma		60
1.2.4	Surveillance	e in Barrett	's oesophagus		60
1.2.5	Treatment	of early	oesophageal	adenocarcinoma	and Barrett's
oesopha	gus associat	ed dysplasi	a		62
1.2.5.1	Endosc	opic Muco	sal Resection		63
1.2.5.2	2 Endosc	opic subm	ucosal dissection	on	64
1.2.5.3	B Photod	lynamic the	erapy		65
1.2.5.4	l Radiofr	requency a	blation		65
1.2.5.5	5 Cryoth	erapy			66
1.2.5.6	S Argon I	photo coag	ulation		68
1.2.6	Radiofreque	ency ablati	on		68
1.2.7	Gastrointes	tinal histop	oathology		70
1.2.7.1	. Oesoph	nageal histo	opathology		70
1.2.8	Histology				71
1.2.8.1	L Backgro	ound			71
1.2.8.2	2 Fixatio	n			72
1.2.8.3	3 Trimmi	ng			73
1.2.8.4	l Pre-em	bedding			73

	1.2.8.5	5 Embedding	74
	1.2.8.6	6 Sectioning	75
	1.2.8.7	7 Staining	75
1.	2.9	Cost	75
1.3	The	UK RFA Registry	76
1.	3.1	Study protocol	78
1.	3.2	Data collection	80
1.	3.3	Previous publications and outcomes	81
1.4	Phy	sics of x-rays	82
1.	4.1	Background	82
1.	4.2	What are x-rays	83
1.	4.3	Attenuation	83
1.	4.4	Image quality in imaging	86
	1.4.4.1	1 Signal to noise ratio	86
	1.4.4.2	2 Resolution	88
	1.4.4.3	3 Contrast to noise ratio	88
1.	4.5	Clinical X-ray setup	89
	1.4.5.1	1 Source	89
	1.4.5.2	2 Detectors	91
	1 /	F 2.1 Crosstalk	01

	1.4.5.	3 Summary of limitations	92
1.5	X-ra	y phase contrast imaging	92
1.5	5.1	Phase contrast imaging methods	93
	1.5.1.	1 Edge Illumination (EI)	93
	1.5.	1.1.1 Masks	94
	1.5.1.	2 Free space propagation	96
	1.5.1.	Research applications of phase contrast imaging	97
1.5	5.2	Synchrotron radiation	100
Chapte	er 2	Aims and objectives	102
2.1	Aim		102
2.2	Obj	ectives	103
Chapte	er 3	The UK RFA Registry	105
3.1	Вас	kground	106
3.2	Aim	S	107
3.3	Me	thods	108
3.3	3.1	Inclusion criteria	109
3.3	3.2	Exclusion criteria	109
3.3	3.3	Data analysis	113
	3.3.3.	1 Data download and worksheet setup	113
	3.3.3.	2 Initial data organisation	114

	3.3.3.3	Histology grade identification11	5
	3.3.3.4	Therapy11	.5
	3.3.3.5	Identification of CR-D and CR-IM11	.5
	3.3.3.6	Worked examples11	.7
	3.3.3.6.1	1 Example patient 1:11	.7
	3.3.3.6.2	2 Example patient 2:11	.7
	3.3.3.6.3	3 Example patient 3:11	8.
	3.3.3.7	Outputs	8.
	3.3.3.8	Time to CR-D and CR-IM11	8.
3.4	Results .	11	9
3	.4.1 Obj	ective 1: One versus two biopsies12	.0
	3.4.1.1	Clearance of dysplasia12	0.
	3.4.1.2	Recurrence of dysplasia from clearance of dysplasia12	.1
	3.4.1.3	Discussion	.2
3	.4.2 Obj	ective 2: Detailed analyses12	.3
	3.4.2.1	Clearance of dysplasia12	.5
	3.4.2.2	Recurrence of dysplasia from clearance of dysplasia12	.6
	3.4.2.3	Clearance of dysplasia after recurrence (CR-D2)12	8.
	3.4.2.4	Clearance of intestinal metaplasia12	9
	3.4.2.5	Recurrence of intestinal metaplasia (IM) from clearance of	of
	intestinal r	metaplasia (CR-IM)13	0

3	3.4.2.6	Clearance of Intestinal Metaplasia after a previous recurrence (CR-
I	IM2)	131	
3	3.4.2.7	Primary EMRs, Dilatations and rescue therapy	L32
3.4	1.3	Objective 3: Invasive cancer	L33
3.5	Disc	ussion1	L35
3.5	5.1	Implications for clinical practice	L38
3.5	5.2	Conclusions	L39
Chapte	r 4	Accuracy of clinical staging for T2NO oesophageal cancer: Systema	atic
Review	and N	Meta-analysis 1	l41
4.1	Intro	oduction1	L41
4.2	Mat	erials and methods1	L43
4.2	2.1	Search strategy1	L44
4.2	2.2	Study selection and outcome measures	L44
4.2	2.3	Statistical analysis1	L46
4.2	2.4	Heterogeneity, subgroup analyses, and publication bias	L46
4.3	Obje	ective 4: Results	L47
4.3	3.1	Characteristics of included studies	L47
4.3	3.2	Outcomes	l51
2	4.3.2.1	L T&N staging1	l51
2	4.3.2.2	2 T stage accuracy1	L54
2	4.3.2.3	3 T downstaging1	156

4.3.2	.4 T upstaging	158
4.3.2	.5 N upstaging	160
4.4 Dis	scussion	161
4.4.1	Principal findings	161
4.4.2	Study strengths and limitations	163
4.4.3	Implications for clinical practice	164
4.4.4	Conclusions	165
Chapter 5	XPCI Methods	166
5.1 Int	roduction	166
5.2 Sys	stem setups	166
5.2.1	UCL molybdenum system	167
5.2.2	HICF system using El	168
5.2.3	UCL copper system using Free Space Propagation	170
5.2.4	Diamond light source Beamline i13-1	171
5.3 Hu	man specimens	171
5.3.1	Biobank	173
5.3.2	Fresh tissue	173
5.4 Sar	mple containers	174
5.4.1	Prevention of movement	174
5.4.2	Fit into the field of view of different XPCI systems	174

5.4.3 Minimise attenuation174
5.4.4 Sample types
5.4.4.1 Biopsies
5.4.4.1.1 CT imaging
5.4.4.1.1.1 Synchrotron setup
5.4.4.1.1.2 UCL lab setup176
5.4.4.2 Oesophagectomies
5.4.4.2.1 Prototypes
5.4.4.2.1.1 Prototype 1
5.4.4.2.1.2 Prototype 2180
5.4.4.2.1.3 Prototype 3181
5.4.4.3 EMRs and ESDs
5.5 Summary
Chapter 6 Preliminary oesophageal work189
6.1 Introduction
6.2 Aim189
6.3 Methods190
6.4 Results
6.5 Discussion
Chapter 7 Preliminary biopsy work194

	7.1	Introduction				
	7.2	Aim1				
	7.3	Met	hods	. 194		
	7.4	Resu	ults	. 195		
	7.5	Disc	ussion	. 196		
C	hapter	8	VIOLIN – Oesophagectomies and Endoscopic Resections	. 197		
	8.1	Aims	S	. 197		
	8.2	Intro	oduction	. 197		
	8.3	Met	hods	. 198		
	8.4	Resu	ults	. 201		
	8.4.	1	Oesophagectomies	. 201		
	8.4.	2	Endoscopic resections	. 208		
	8.5	Disc	ussion	. 209		
	8.5.	1	Oesophagectomies	. 209		
	8.5.	2	Endoscopic resections	. 210		
C	hapter	9	VIOLIN – Biopsies	. 212		
	9.1	Aims	S	. 212		
	9.2	Intro	oduction	. 212		
	9.3	Met	hods	. 214		
	9 4	Reci	ılts	215		

9.5	Discussion	219
Chapter	10 Discussion	221
10.1	Assess existing technologies used in the treatment and staging of OAC.	221
10.2	Using XPCI to grade and stage oesophageal cancers	223
10.3	Limitations	225
10.4	Ideas for future work	226
10.5	Conclusions	228
Chapter	11 References	229

List of figures

Figure 1.1: Partially obstructing oesophageal tumour seen in the lower oesophagus
at OGD [54]46
Figure 1.2: Siewert classification of distal oesophageal tumours [56]
Figure 1.3: A – T1-T3 OAC; B – T4 OAC; C – nodal spread; D – metastatic spread
(adapted from [59])49
Figure 1.4: Showing surgical treatment of oesophageal cancer [73]54
Figure 1.5: Showing progression of disease from normal squamous epithelium to OAC
(adapted from [98])59
Figure 1.6: Image showing Seattle protocol biopsies. The Xx represent biopsies that
should be taken (adapted from [102])61
Figure 1.7: Image showing cap and snare and band ligation EMR techniques [113] 64
Figure 1.8: Showing available RFA catheters. From left to right: 360 balloon catheter;
ultra-long focal catheter; 90° focal catheter; 60° focal catheter; channel endoscopic
catheter [122]66
Figure 1.9: Stages of modern histological processing72
Figure 1.10: Map of the 28 sites submitting data to the UK RFA Registry. Those sites
highlighted in red have undergone additional review by the primary site77
Figure 1.11: UK HALO RFA registry study protocol [123]79
Figure 1.12: Example online CRFs for HALO registry. Left-hand image shows a test
patient CRF including baseline demographic data, previous therapy and BO length.
Right hand image shows procedure CRF including length of current BO, any therapy
performed and histology results if biopsies taken81

Figure 1.13: Electromagnetic spectrum [151]83
Figure 1.14: Schematic diagram showing contrast generation using attenuation [150]
84
Figure 1.15: Formula showing how contrast is generated using attentuation. I_2 is the
intensity of the signal detected in the shadow of the imaged object. I_1 is the intensity
of the signal immediately outside the object
Figure 1.16: Attenuation coefficients of air, metal and different human tissues 85
Figure 1.17: The setup for planar radiography [152]86
Figure 1.18: A – image taken with no antiscatter grid. B – image taken with antiscatter
grid[154]87
Figure 1.19: Schematic diagram of an x-ray tube[153]90
Figure 1.22: Image showing refraction of X-ray (shown by dashed line – "new path of
x-ray") relative to original path of x-ray. The angle of refraction is shown by "r" 92
Figure 1.23: Schematic diagram showing EI setup [159]
Figure 1.24: Left hand image shows a representation of a non-skipped mask; Right
hand image shows a representation of a skipped mask95
Figure 1.25: Showing dithering of a specimen. The sample is shown in two positions
as it is moved relative to the setup96
Figure 1.26: Schematic diagram showing FSP [150]
Figure 1.27: Images of left breast with a suspicious mass seen on DM image (a) and
corresponding zoom image (c). MSR image (b) depicting spiculated mass more clearly
and corresponding zoom image (d) [66]:98
Figure 1.20: Hutch at DLS, Oxfordshire101
Figure 1.21: Schematic diagram of a synchrotron[165]

Figure 3.1: Flow diagram indicating included and excluded patients. Of the patients
132 excluded for not having had treatment or not having LGD, HGD or IMC prior to
treatment, 9 had proven invasive cancer prior to therapy, 30 never had RFA therapy
and the remaining 93 excluded had no confirmed evidence of having dysplasia112
Figure 3.2: Flow diagram illustrating data outputs, linking and processing 114
Figure 3.3: Example patients to illustrate the effects of using one biopsy vs two
biopsies
Figure 3.4: Kaplan Meier graph showing rate of CR-D using the one biopsy method
and the two-biopsy method. Log rank score = 0.018
Figure 3.5: Kaplan Meier graph showing rate of recurrence of dysplasia from CR-D
patients achieving CR-D using both one biopsy and two biopsy methods. Log rank
score p=2.58E-05
Figure 3.6: Graph showing absolute number of recurrences of dysplasia from CR-D
and cumulative recurrences from CR-D per year of follow up for the one biopsy and
two biopsy methods. Black trendline indicates the difference in the cumulative
number of recurrences of dysplasia from CR-D between the two methods 122
Figure 3.7: Kaplan Meier graph showing rate of CR-D for those patients initially
treated for LGD, HGD and IMC125
Figure 3.8: Kaplan Meier graph showing rate of recurrence of dysplasia from CR-D for
those patients initially treated for LGD, HGD and IMC. Log rank score between IMC
and LGD p = 0.4. All other comparisons Log Rank Score p = N.S. Please note that the
y axis is truncated at 80% for ease of viewing
Figure 3.9: Highlighting the time intervals of follow-up compared. Red arrow
indicates the first time interval. Green arrow shows the second time interval. 127

Figure 3.10: Kaplan Meier graph showing rate of CR-D2 in initial 2 years of therapy
(combined for all initial histology types)
Figure 3.11: Kaplan Meier graph showing rate of CR-IM for those patients initially
treated for LGD, HGD and IMC
Figure 3.12: Kaplan Meier graph showing rate of recurrence of IM from CR-IM for
those patients initially treated for LGD, HGD and IMC. Initial disease severity did not
affect rates of CR-IM. Please note that the y axis is truncated at 60% for ease of
viewing
Figure 3.13: Kaplan Meier graph showing rate of CR-IM2 in initial 2 years of therapy
(combined for all initial histology types)
Figure 3.14: Showing the likelihood of treatment success for each RFA procedure.
Figure 3.15: Kaplan Meier graph of entire cohort showing rate of invasive cancers at
10 years from the start of treatment in patients treated with RFA. The y axis is
truncated at 80% for ease of viewing
Figure 4.1: Flow diagram of the search strategy and selection of studies148
Figure 4.2: Quality Assessment of Diagnostic Accuracy Studies (QUADAS-2) tool for
the 18 studies included in the meta-analysis
Figure 4.3: Forest plot for combined T/N stage accuracy
Figure 4.4: Funnel plot for combined T/N stage accuracy
Figure 4.5: Forest plots for secondary outcomes. A, T stage accuracy; B, T
downstaging
Figure 4.6: Funnel plot for T stage accuracy
Figure 4.7: Funnel plot for T downstaging

Figure 4.8: Forest plots for secondary outcomes. A , T upstaging; B , N upstaging 158
Figure 4.9: Funnel plot for T upstaging
Figure 4.10: Funnel plot for N upstaging
Figure 5.1: showing UCL XPCI- CT system [65] . A) A photograph of the system
showing the source, sample mask (M1), sample stage, detector mask (M2) and
detector. B) A top-down schematic representation of the system with non-skipped
masks in place
Figure 5.2: Images showing HICF machine. Left-hand image shows entire machine
with radiation shielded enclosure. Right-hand image shows sample stage and masks.
Figure 5.3: Schematic diagram to show the effect of increasing the distance between
the sample and detector. Placing the detector at position 2 (red arrow) increases the
sample to detector distance (relative to position 1 – blue arrow). This increases the
x-ray deviation at position 2 relative to position 1 (shown by the relative difference
in lengths of the blue and red dotted lines
Figure 5.4: Schematic diagram of UCL copper source and monochromator for FSP
Figure 5.5: Image of UCL copper system for FSP
Figure 5.6: Image of DLS beamline i13-1
Figure 5.7: Diagram showing source of different specimens – note there were two
sources of biopsies (highlighted in orange)
Figure 5.8: Pipette tip containing biopsies for CT imaging at DLS176

Figure 5.9: Schematic diagram showing biopsy setup for scanning. Microbeads were
attached to the outside of the capillary. The setup could contain a single biopsy or
two biopsies as depicted here
Figure 5.10: Oesophagectomy specimen with anatomical landmarks labelled 178
Figure 5.11: Graph showing distribution of measurements for oesophagectomy
specimens
Figure 5.12: Prototype oesophagectomy holder – with central core and funnel region
Figure 5.13: Scaffold for oesophagectomies
Figure 5.14: Image depicting spiralised 3D printing technique
Figure 5.15: Prototype 2 container with lid. Printed with spiralised method 181
Figure 5.16: Image highlighting week regions of prototype 2
Figure 5.17: Prototype 3 and lid showing a less flared cone reducing the angle at the
weak points seen in prototype 2
Figure 5.18: Oesophagectomy specimen showing area of gastric tissue that could be
removed
Figure 5.19: Schematic diagram showing how oesophagectomy specimens were held
for imaging
Figure 5.20: Projections of 3D printed PLA container. Image A yellow box shows an
example area outside the container; Image B yellow box shows an example area
inside the container
Figure 5.21: Graph showing the percentage of photons attenuated by different
104

Figure 5.22: Cap and snare EMR technique highlighting relatively uniform size of
resection specimens
Figure 5.23: Schematic diagram showing different positions for imaging EMR and ESD
specimens. The submucosa is illustrated in blue and mucosa in orange185
Figure 5.24: Schematic diagram of a theoretical setup that shows the effect of
specimen orientation on photon attenuation
Figure 5.25: Schematic diagram showing how endoscopic resections were held for
imaging
Figure 5.26: Container and lid for smaller specimens – EMRs, ESDs and porcine
oesophagus
Figure 6.1: Porcine oesophageal tissue attached to scaffold with sutures190
Figure 6.2: Schematic diagram showing sections of porcine oesophagus
Figure 6.3: Reconstructed CT slice from samples A, B and C
Figure 7.1: Flow chart showing method for preliminary biopsy experiment 195
Figure 7.2: Results from preliminary biopsy work. Image A shows a slice from the first
scan CT (biopsy in formalin). Image B shows a slice from the second scan CT (biopsy
in ethanol). Image C shows a slice from the third scan CT (biopsy in formalin). The
inserted pictures in the bottom right of each image show the biopsy mounted in the
capillary195
Figure 8.1: Example CT slices from S07 (images A and B) and S08 (images C and D).
Images A and B show some degree of contrast through the soft tissue although not
enough to identify tissue layers clearly or tumour. Images C and D show minimal
contrast. In addition, motion artifacts can be observed in images C and D 201

Figure 8.2: CT slices from an oesophagectomy that showed clear contrast throughout
the tissue layers. Image A shows normal oesophageal tissue with matched histology
in image D. Image C shows tumour starting to destroy the tissue layers between 10
and 12 o'clock. These changes are matched in the histology shown in image E. Image
C shows near complete loss of tissue layers circumferentially (most marked in the top
half of the specimen). This is matched to histology in image F202
Figure 8.3: This shows CT slices from two different specimens. Image A shows a T1b
tumour extending from 9 o'clock to 11 o'clock. Image B shows matching histology.
Image C shows an early T2 tumour extending from 11 o'clock to 3 o'clock. Image D
shows matching histology
Figure 8.4: Shows CT slices from two different specimens. Image A shows a T2 tumour
extending from 7 o'clock to 11 o'clock. Image B shows matching histology. Image C
shows a T3 tumour extending from 10 o'clock to 12 o'clock. Image D shows matching
histology
Figure 8.5: CT slices from a normal region of oesophagectomy. Each image depicts
the same region. Images A, B, C and D show slices from 2, 4, 10 and 15 hour CT scans.
Figure 8.6: CT slices from an abnormal region of oesophagectomy. Each image
depicts the same region. Images A, B, C and D show slices from 2, 4, 10 and 15 hour
CT scans
Figure 8.7: Shows endoscopic resections. Image A is an EMR with matching histology
in image D. Images B and C show two ESD specimens with matching histology in
images E and F, respectively208

Figure 9.1: Images from matched scans. Images on the left side are synchrotron CT
slices and images on the right side are CT slices using a conventional source. Images
A and B show a squamous biopsy, images C and D show a biopsy containing NDBO;
images E and F show a biopsy containing DBO; images G and H show a biopsy
containing adenocarcinoma216
Figure 9.2: Images showing matched images of a NDE biopsy. The arrows highlight
matched features. Image A shows a slice from the synchrotron CT. Image B shows a
slice from serial sectioning of the biopsy
Figure 9.3: Images showing HGD. Image A shows a slice from the synchrotron CT.
Image B shows a slice from the lab CT. Image C shows a slice from serial sectioning of
the highsy 218

List of Tables

Table 1.1: TNM staging for OAC (eighth edition) [57]
Table 1.2: Showing staging of OAC49
Table 1.3: Vienna classification
Table 1.4: Godkar and Bancroft techniques for tissue processing prior to embedding
74
Table 1.5: List of the 28 sites submitting data to the UK RFA Registry. Those site
highlighted in red have undergone additional review by the primary site
Table 3.1: Showing each analysis, number of recruits included and specific exclusion
criteria
Table 3.2: Showing number of patients reaching CR-D and CR-IM within specific time
frames from the start of RFA treatment. The 24-month cut off applied is highlighted
in yellow119
Table 3.3: Demographic and outcome data of all 1,175 patients with BO included in
CR-D and CR-IM analysis of UK HALO RFA registry 124
Table 4.1: Search strategy
Table 4.2: Summary of included studies (n=20)
Table 4.3: Summary of characteristics of patients included in the analysis 15
Table 4.4: Meta-analysis results for all studies combined
Table 4.5: Accuracy of combined T/N stage by study subgroup
Table 4.6: Accuracy of T stage by study subgroup
Table 4.7: T downstaging by study subgroup
Table 4.8: T upstaging by study subgroup
Table 4.9: Nunstaging by study subgroup

Table 6.1: Protocol for porcine oesophagus processing	191
Table 8.1: Showing scan parameters for endoscopic resection and oe	sophagectomy
specimens	200

List of abbreviations

ABS Acrylonitrile Butadiene Styrene

A.H. Alex Ho

ALA 5-aminolevulinic acid

APC Argon plasma coagulation

AXIm Advanced X-ray imaging group

BMI Body Mass index

BO Barrett's Oesophagus

CNR Contrast to noise ratio

CR Computed radiography

CR-D Complete reversal of dysplasia

CRFs Case record files

CR-HGD Complete reversal of HGD

CR-IM Complete reversal of IM

CRT Chemoradiotherapy

CT Computerised tomography

DBO Dysplastic Barrett's Oesophagus

DLS Diamond Light Source

DM Digital mammography

DR Digital radiography

EET Endoscopic endotherapy

El Edge illumination

EMR Endoscopic mucosal resection

EUS Endoscopic ultrasound

FoV Field of view

FSP Free space propagation

GI Gastrointestinal

GM Glandular Mucosa

GOJ Gastro-oesophageal junction

H&E Haemotoxylin and eosin

HGD High grade dysplasia

HIPS High impact polystyrene

HR Hazard ratio

HRT Hormonal replacement therapy

HU Hounsfield units

IBD Inflammatory bowel disease

IM Intestinal metaplasia

IMC Intramucosal carcinoma

IQR Interquartile range

kVp Kilovoltage peak

LGD Low grade dysplasia

LINAC Linear accelerator

LNSC Liquid nitrogen spray cryotherapy

MRI Magnetic resonance imaging

MSR Mammography with synchrotron radiation

NAT Neoadjuvant therapy

NS Not specified

NDBO Non-dysplastic Barrett's Oesophagus

OAC Oesophageal adenocarcinoma

OGD Oesophago-gastro-duodenoscopy

OR Odds ratio

OSCC Oesophageal squamous cell carcinoma

PC Polycarbonate

PDT Photodynamic therapy

PET Positron emission tomography

PLA Polylactic acid

P.W. Paul Wolfson

RCT Randomised control trial

RFA Radiofrequency ablation

RR Relative Risk

SCC Squamous cell carcinoma

SNR Signal to noise ratio

S.S.S Sarmed S. Sami

TNM Tumour, Node, Metastasis

UCL University College London

UCLH University College London Hospital

UK United Kingdom

US Ultrasound

USA United States of America

XPCI X-ray Phase Contrast Imaging

Chapter 1 Introduction

1.1 Oesophageal cancer

1.1.1 Disease prevalence and impact

Oesophageal cancer is the 13th most common cancer but the 7th most common cause of cancer death in the United Kingdom (UK). In men it is the 9th most common cancer but the fourth commonest cause of death [4]. It accounts for 9,000 new cancer cases in the UK every year of which men account for two thirds of new cases. Incidence rates have risen 6% since the 1990s, this has been driven by an increased incidence in males of 10% (the incidence in women has decreased by 9% over this time period) [4].

Oesophageal cancer predominantly comprises of two histological types, adenocarcinoma (OAC) and squamous cell carcinoma (SCC). In the UK 55% of cases are currently due to adenocarcinoma [4] and this proportion is continuing to rise. Worldwide 87% of cases are due to SCC [5].

Since the 1970s UK mortality rates have increased by 41% although over the last decade mortality rates have decreased by 9%. Five-year survival has been rising very slowly over the last 50 years but is still very low [4]. Recent data has showed that 5-year survival in men increased from 4% during the 1970s to 16% in 2010. In women 5 year survival has increased from 5% to 15% over the same time period [4].

This high mortality rate and poor 5-year survival data reflects the fact that most oesophageal cancers are diagnosed at a late stage. Survival data shows in the UK

those patients with stage 1 disease have a 52.8% 5 year survival compared to 29.9% and 16.3% for those with stage 2 or stage 3 disease [4].

The majority (70-80%) of patients diagnosed with oesophageal cancer are diagnosed at a later stage (stage 3 or 4) in the UK with only 21-30% being diagnosed at stage 1 or 2 [4], [6], [7], [8]. Staging of oesophageal adenocarcinoma (OAC) is discussed further in section 1.1.2.1.

1.1.1.1 Risk factors

1.1.1.1.1 Age

The main risk factor for developing OAC is age, with 41% of new cases in the UK being in people older than 75 years [6], [7], [9], [10]. Incidence is highest in 85-89 year olds with case rates reaching 178/100,000 [6], [7], [9], [10].

1.1.1.1.2 Smoking

Smoking is associated with increased risk of developing oesophageal cancer in both SCC and OAC [11], [12]. There is a dose-response relationship such that the odds ratio (OR) compared with never cigarette smokers is 1.3 for smokers with a <15 pack-year history; 2.19 for smokers with a 15-29 pack-year history; 2.38 for smokers with a 30-44 pack-year history and 2.73 for smokers with a >45 pack-year history [13]. This additional risk occurs for both men and women.

1.1.1.1.3 Ethnicity

The highest incidence of OAC is seen in white population groups with rates ranging from 13.9 to 14.4 per 100,000 for males and 5.5 to 5.7 per 100,000 for females. In contrast the incidence in the Black population is 6.0 to 10.2 per 100,000 for males and 2.1 to 4.5 for females. The incidence is even lower in the Asian population with a rate of 3.6 to 6.1 per 100,000 for males and 2.5 to 4.5 per 100,000 for females [14].

1.1.1.1.4 Sex

As mentioned previously, in the UK two-thirds of cases of oesophageal cancer are detected in men [4]. For OAC the male to female rate has been reported to be as high as 7-20:1 in one retrospective study from the United States of America (USA) [14] with the highest ratio between sexes seen in those aged 50-59 years, followed by a decline in older ages. This publication used population-based cancer registries in the National Cancer Institute's SEER (Surveillance, Epidemiology, and End Results) program. This increased ratio between men and women was seen in all ethnic groups.

It is unclear what causes this marked difference. It has been hypothesised that the difference may be due to the effects of sex hormones with oestrogen being protective and testosterone being harmful. The highest ratio of cancer incidence between sexes being at or within a decade of menopause may add weight to this hypothesis [15], [16].

If oestrogen is protective, then taking exogenous oestrogens in the form of contraception or hormonal replacement therapy (HRT) should further reduce the risk

of developing OAC. A number of studies have been performed looking at this with variable results [17], [18], [19], [20], [21]. A 2014 meta-analysis reported a statistically significant 25% decreased risk of OAC for users of HRT (OR 0.75 95% CI: 0.58–0.98) and a borderline significant odds reduction for those taking oral contraceptives (OR 0.76, 95% CI 0.57–1.00) [22].

The evidence suggesting testosterone is harmful is weaker. One retrospective cohort study looked at the effect of anti-androgens, used for the treatment of prostate cancer. This study looked at over 100,000 patients they observed 14 cases of OAC in patients treated with anti-androgens compared to the expected 16 with a standardised incident ratio of 0.9 (95% CI 0.5-1.5).

There appears to be no significant association between gastroesophageal reflux symptoms and sex. This has been demonstrated in both cross sectional and longitudinal studies [23], [24], [25], although men are more likely to have erosive reflux disease [26]. Whether or not this is a factor in explaining the increased incidence of OAC in men is still not clear.

1.1.1.1.5 Alcohol

Alcohol is a recognised carcinogen for a number of cancers [27]. Some evidence suggests alcohol consumption confers additional risk, although this link is more established with oesophageal squamous cell carcinoma (OSCC) than OAC. A 2015 meta-analysis found even light alcohol consumption was associated with increased risk of developing OSCC (Relative risk [RR] 1.26 95%CI 1.06-1.50). The risk was greater for moderate alcohol consumption (RR 2.23 95%CI 1.87-2.65) and heavy alcohol

consumption (RR 4.95 95%CI 3.86-6.34). An epidemiological study published in 2015 attributed 44.7% of OSCC to alcohol consumption [28].

The association between OAC and alcohol consumption is less well established. There is evidence to suggest light alcohol consumption is associated with reduced risk of developing OAC (RR 0.86 95%CI 0.76-0.98). Moderate and heavy alcohol consumption was not associated with significantly increased risk of developing OAC, RR 0.97 (95%CI 0.78-1.22) and RR 1.15 (95%CI 0.95-1.39) [29].

The BEACON consortium found no association between increased alcohol consumption and oesophageal and oesophagogastric adenocarcinoma [30]. They also found moderate levels of alcohol consumption (0.5-1 drink/day) to be protective relative to non-drinking for both OAC (OR 0.59 95%CI 0.39-0.88) and oesophagogastric adenocarcinoma (OR 0.64 95%CI 0.45-0.90).

1.1.1.1.6 Obesity

The risk of developing OAC increases with increased body mass index (BMI). This correlation has been demonstrated to have a linear relationship [31], [32]. It is hypothesised that the obesity epidemic is driving the increasing incidence of OAC although early rises in the incidence of OAC predate the rise in obesity rates in Western populations [33], [34].

A 2013 meta-analysis calculated the RR of developing OAC in people who are overweight (BMI 25-30Kg/m²) or obese (BMI \geq 30Kg/m²) [31]. They found the RR was 1.71 (95% CI 1.50–1.96) for the overweight cohort and 2.34 (95% CI 1.95–2.81) for

the obese group. In addition, the authors found that for every 5-point increase in BMI the RR was 1.11 (95% CI 1.09–1.14).

One of the leading theories behind this link is that the rising incidence of OAC is driven by increased oesophageal reflux secondary to the mechanical effect seen in obesity [35]. It is hypothesised that this is through increased intra-abdominal pressure [36] and reduced lower oesophageal sphincter pressure [37]. This increased reflux leads to chronic oesophageal inflammation and so predisposes individuals to developing Barrett's oesophagus (BO) (section 1.2).

It should be noted that obesity does not appear to be a risk factor for development of BO independent of reflux symptoms [38]. Also, the risk of developing OAC increases in obesity even in people that have never experienced symptoms of reflux [39] [40].

1.1.1.1.7 Abdominal obesity

A 2013 meta-analysis found a significant association between BO and central obesity even after adjusting for BMI (OR 1.88; 95% CI 1.20-2.95) [41]. The study also found that a high level of central adiposity was associated with a higher risk of developing OAC (OR, 2.51; 95% CI, 1.56–4.04), albeit with substantial heterogenicity between the included studies (I²=62%) and some delay between central adiposity measurement and diagnosis of OAC.

A study looking at the Norwegian Cancer Registry found an increased hazard rate of OAC with increased waist circumference a (HR=2.48, 95% CI: 1.27-4.85) [42].

1.1.1.1.7.1 Weight loss

No study to date has demonstrated a significant risk reduction in individuals who undergo weight loss. This is largely due to the complexity in identifying large numbers of patients that will undergo weight loss and then following them up long-term. One Swedish study identified patients that had undergone obesity surgery and compared the incidence of OAC in this population versus a cohort of obese individuals who did not undergo obesity surgery [43]. No significant difference was seen in the standardised incidence ratio. The lack of significance is likely due to the relatively few cases of OAC seen in the surgery cohort (n=8) and the median follow up being 3.7 years. There is a more established association between reduced symptoms of reflux and weight loss.

Other hypotheses for the link between obesity and oesophageal cancer suggest a more systemic effect of obesity either through hormones or metabolic effects [44].

1.1.1.1.8 Hormones

Some association has been shown between raised levels of leptin and an increased risk of progressing from BO to OAC. One prospective cohort study for which data collection was between 1995 and 2009 reported higher leptin levels were associated significantly with an increased risk of OAC within 3 years (HR, 2.51; 95% CI, 1.09-5.81; P = .03) [45]. This additional risk was eliminated when those with high grade dysplasia (HGD) were analysed separately. It should also be noted that leptin levels were higher in women and leptin correlated strongly with BMI.

1.1.1.1.9 Metabolic syndrome

A North American study looking at the SEER database found an association between OAC and metabolic syndrome (defined as three of: elevated waist circumference/central obesity/obesity, elevated triglycerides, lowered high-density lipoprotein cholesterol, high blood pressure and elevated fasting glucose). This association was significant when comparing cases of OAC with population controls but was not significant when compared with BO controls [46]. The previously mentioned Norwegian study found a significant association between metabolic syndrome and gastric adenocarcinoma (Hazard ratio [HR] =1.44, 95% CI: 1.14-1.82) but not with oesophageal cancers, either adenocarcinoma (HR=1.32, 95% CI: 0.77-2.26) or SCC (HR=1.08, 95% CI: 0.64-1.83), possibly due to the limited number of cases detected (OAC n=62; OSCC n=64, gastric adenocarcinoma n= 373) [42].

1.1.1.1.10 Barrett's oesophagus

BO is the only known premalignant state of OAC [47]. The risk of developing OAC is 11 times higher in patients with BO compared with the rest of the population [48]. However, the annual cancer conversion rate from BO to OAC is low (<0.5%/year). Much of this data is from case series with small numbers of patients [49], [50], [51], [52]. A recent meta-analysis gave an annual risk of developing OAC of 0.33% in patients with non-dysplastic Barrett's oesophagus (NDBO) [51].

1.1.2 Management of oesophageal cancer

1.1.2.1 Diagnosis and staging

To confirm a diagnosis of oesophageal cancer histological assessment is required. Tissue is usually obtained via an oesophago-gastro-duodenoscopy (OGD) (Figure 1.1) during which at least six biopsies should be taken according to national guidelines [53].

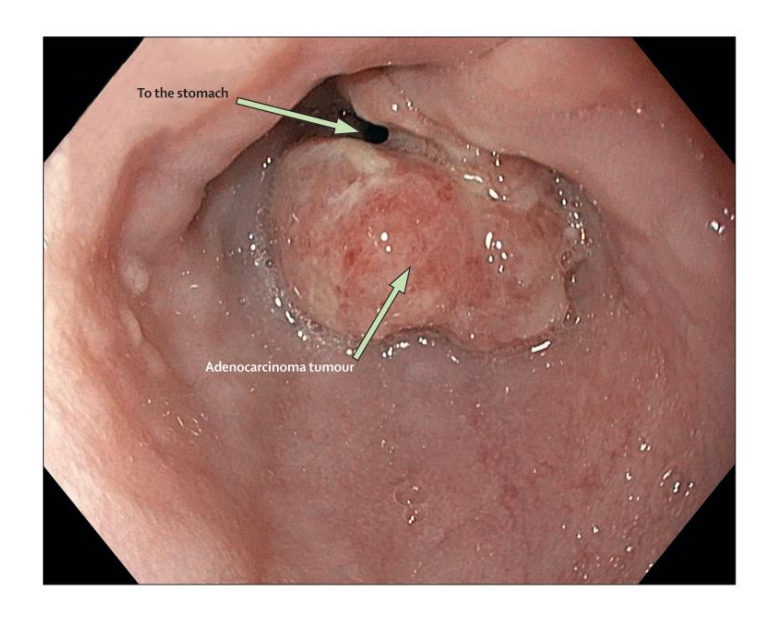


Figure 1.1: Partially obstructing oesophageal tumour seen in the lower oesophagus at OGD [54]

The position of the tumour should be identified and recorded to guide potential targeted therapy, either surgery or radiotherapy. The standard method used to define tumour position is the Siewert classification (Figure 1.2). This system categorises oesophageal tumours according to their anatomical relationship with the gastro-oesophageal junction (GOJ).

Distal oesophageal tumours above the GOJ are defined as Siewert I, tumours at the GOJ are defined as Siewert II and gastric carcinomas that extend beyond the cardia

but also infiltrate the GOJ are defined as Siewert III (Figure 1.2). Although this practice is established there is some criticism of this system [55]. Frequently the GOJ can be difficult to visualise endoscopically or radiologically, the anatomy can be distorted, either by the tumour or a hiatus hernia and large tumours can reach across two Siewert groups.

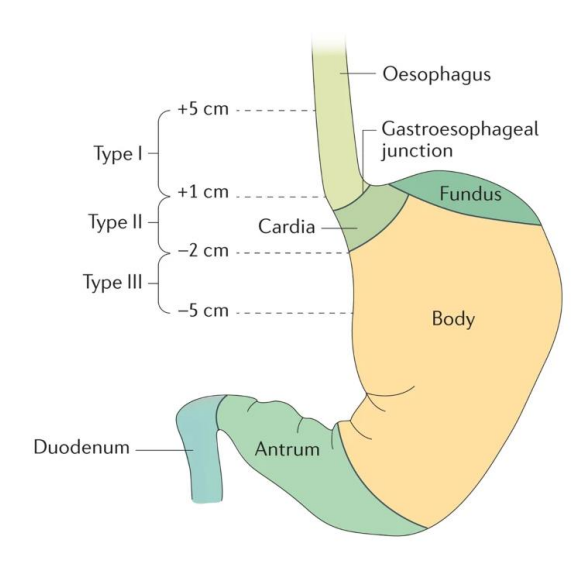


Figure 1.2: Siewert classification of distal oesophageal tumours [56].

Initial staging of oesophageal tumours should include a computerised tomography (CT) scan of the thorax, abdomen and pelvis. Other staging modalities that can be used to inform the clinical picture include positron emission tomography (PET), endoscopic ultrasound (EUS), therapeutic endoscopy and laparoscopy. Following this all cases should be discussed at a multidisciplinary meeting [53].

The precise stage of OAC is defined by the Tumour, Node, Metastasis system (TNM).

The eighth edition published in 2016 is shown below in Table 1.1 and Figure 1.3 [57].

Clinical staging is the most accurate reflection of cancer prognosis, it guides therapy and is a survival reference point [57]. As therapeutic options have expanded accurate

clinical staging has become increasingly important [58]. Clinical staging is referred to as cTNM with pathological staging, staging of resection specimens, referred to as pTNM. If patients have been offered neoadjuvant therapy (NAT), chemotherapy or radiotherapy, prior to resection this is referred to as ypTNM.

Table 1.1: TNM staging for OAC (eighth edition) [57]

Category				
Tumour	Тх	No evidence of primary tumour		
	Tis	High grade dysplasia, defined as malignant cells confined by the basement membrane		
	T1a	Tumour invades the lamina propria or muscularis mucosae		
	T1b	Tumour invades the submucosa		
	T2	Tumour invades the muscularis propria		
	Т3	Tumour invades adventitia		
	T4a	Tumour invades the pleura, pericardium, azygos vein, diaphragm, or peritoneum		
	T4b	Tumour invades other adjacent structures, such as aorta, vertebral body, or trachea		
Node	NX	Regional lymph nodes cannot be assessed		
	N0	No regional lymph node metastasis		
	N1	Metastasis in 1–2 regional lymph nodes		
	N2	Metastasis in 3–6 regional lymph nodes		
	N3	Metastasis in 7 or more regional lymph nodes		
Metastases	M0	No distant metastasis		
	M1	Distant metastasis		

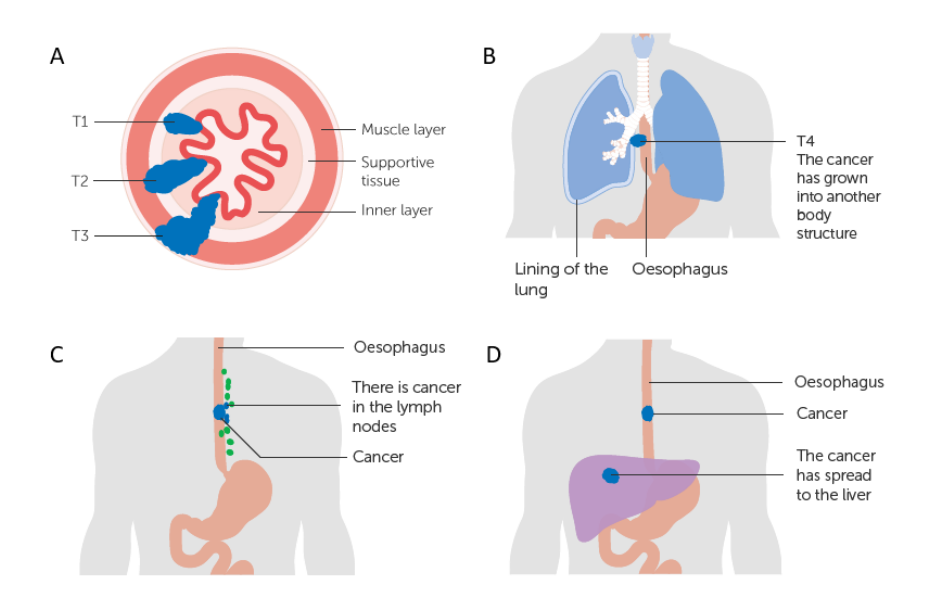


Figure 1.3: A – T1-T3 OAC; B – T4 OAC; C – nodal spread; D – metastatic spread (adapted from [59])

Table 1.2: Showing staging of OAC

Stage	Tumour	Node	Metastasis
0	Tis	N0	M0
1	T1	N0	M0
24	T2	N0	M0
2A	T3	N0	M0
20	T1	N1	M0
2B	T2	N1	M0
2	T3	N1	M0
3	T4	Any N	M0
4A	Any T	Any N	M1a
4B	Any T	Any N	M1b

1.1.2.2 Accuracy of staging

To calculate accuracy of clinical staging (cTNM), pathology (pTNM) is used as the reference standard. This means only data from patients that undergo a resection without NAT can be included in these calculations. When comparing post-operative

pathological staging to clinical staging the accuracy ranges from 6-42% [60], [61], [62].

This could relate to limitations in technologies used to stage oesophageal cancers.

1.1.2.3 Staging technologies

1.1.2.3.1 Computerised Tomography

Conventional contrast-enhanced CT of the chest, abdomen and pelvis should be the initial investigation to determine if there is distant spread or irresectable disease [53]. These studies should be performed in such a way that images can be reformatted in different planes to assist with staging accuracy. This is particularly of value to determine T3 or T4 disease, as this allows for more precise evaluation of tumour invasion into surrounding tissues [53].

1.1.2.3.2 Endoscopic ultrasound

EUS is a highly operator dependent technique and is best performed by experienced technicians [53]. EUS can assist with tumour and nodal staging. To complete the examination the endoscope needs to traverse the entire length of the tumour. Even small luminal tumours may be enough to prevent passage of the endoscope limiting this technique. EUS fine needle aspiration (FNA) cytology of suspicious lymph nodes can improve accuracy [63].

1.1.2.3.3 Laparoscopy

In cases when no overt metastatic disease has been identified and curative treatment remains a possibility, laparoscopy should be performed. This allows direct

visualisation of the abdominal cavity to identify presence of peritoneal and hepatic metastases. Laparoscopy provides additional clinical information in ~17% of junctional and distal oesophageal tumours [64].

1.1.2.3.4 Novel techniques

1.1.2.3.4.1 Magnetic resonance imaging

Currently, magnetic resonance imaging (MRI) is not used for routine clinical staging of oesophageal cancers, other than to characterise indeterminate liver lesions. Studies to date are yet to show MRI offers an advantage over CT and EUS in oesophageal cancer staging [53].

1.1.2.3.4.2 X-ray Phase Contrast Imaging

X-ray Phase Contrast Imaging (XPCI) is a novel technique which makes use of refraction of x-rays. This differs from clinical x-ray techniques which use attenuation to generate contrast. Currently this modality has primarily been applied to ex-vivo specimens [65]. Some promising in-vivo work has been conducted in breast cancer tumour staging and characterisation [66]. XPCI will be discussed in more detail in section 1.5.

1.1.3 Treatment of oesophageal cancer

Treatment options for oesophageal cancer include endoscopic endotherapy (EET), chemotherapy and radiotherapy, surgery (with or without neo-adjuvant or adjuvant therapy) and best supportive (symptomatic management). Therapeutic options

should consider the stage of cancer as well as the performance and nutritional status of the patient.

1.1.3.1 Endoscopic endotherapy

Curative EET can be offered to patients with T1a disease either in the form of endoscopic mucosal resection (EMR) or endoscopic submucosal dissection (ESD) [67]. This will be discussed in more detail in section 1.2.5 as much of this therapy is also used for treatment of BO.

1.1.3.2 Chemotherapy and radiotherapy

Chemotherapy with and without radiotherapy can be offered in several clinical scenarios: firstly, as NAT to downstage disease to enable curative surgery; secondly, for patients who are unsuitable, due to co-morbidities or fitness for surgery, or unwilling to have surgical resection radical chemo-radiotherapy can be offered with curative intent; thirdly definative treatment with chemoradiation can be offered for patietns with OSCC. Finally, patients with extensive disease can be offered palliative chemo-radiotherapy can be offered with a view to extending survival [53].

1.1.3.2.1 Outcomes of chemotherapy and radiotherapy

Chemoradiotherapy (CRT) offers significant benefit for patients going on to potentially curative surgery. This was demonstrated in the CROSS trial [68] in which patients were randomised to CRT + surgery or to surgery alone. Those in the CRT + surgery group had a median overall survival of 49.4 months versus 24.0 months in the surgery group. It should be noted that this study did include patients with OSCC

(23%) who derived greater benefit from the CRT. In addition, up to $1/3^{rd}$ of patients did not see a substantial reduction in tumour size.

Few studies have evaluated the role of palliative chemotherapy. Much of what is understood regarding palliative chemotherapy is inferred from trials containing a mixture of oesophageal, junctional and gastric cancers [69]. Chemotherapy extends overall survival to 11.0 months from 4.3 months relative to best supportive care [70]. The median survival for patients with advanced OAC is <1 year [71]. When offering CRT for the purpose of extending survival it is important to consider this. In this clinical scenario intensity and side effect profile of the therapy offered must be carefully considered by both clinician and patient.

1.1.3.3 Surgery

In disease staged >cT1a and <cT2N0M0 surgery is the treatment of choice [67] although some recent data has shown T1b adenocarcinoma can be treated endoscopically[72]. Several surgical approaches exist and include both transthoracic (Ivor-Lewis procedure) and minimally invasive transhiatal approaches. NAT can be used to downstage disease >T2N0M0. If successful downstaging is achieved, i.e. achieving post chemotherapy disease stage <cT2N0M0, this may allow curative surgery to be performed.

Surgical removal of the oesophageal tumour (Figure 1.4) initially involves mobilisation of the oesophagus and stomach, the oesophagus (containing the tumour) is then resected, finally the stomach is pulled into the chest and an anastomosis is formed between this and the proximal oesophagus. Typically, during

resection of the oesophagus and formation of the anastomosis the thorax is opened, and the right lung is collapsed requiring ventilation of the patient during surgery to be performed on a single lung.

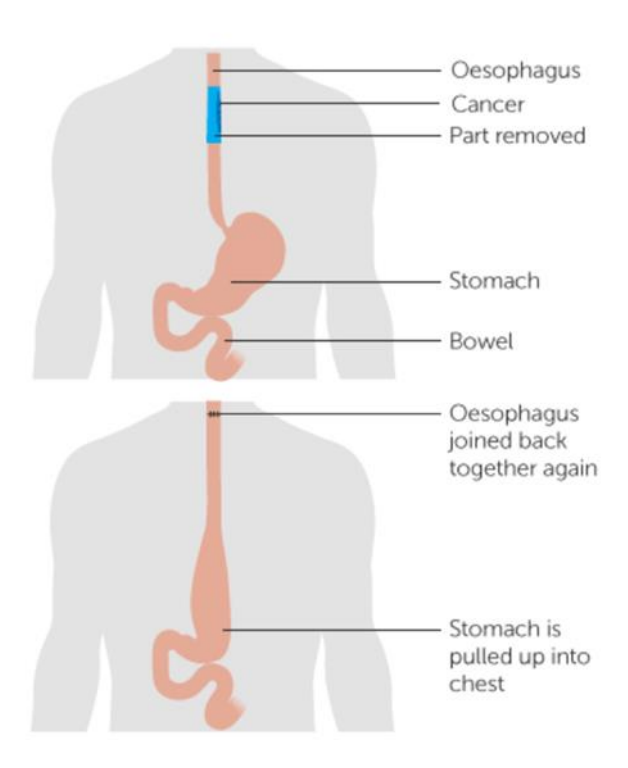


Figure 1.4: Showing surgical treatment of oesophageal cancer [73]

1.1.3.3.1 Outcomes of surgery

Oesophagectomy is one of the most complex and extensive surgical procedures performed for cancer therapy. Historically mortality rates have historically been over 10% but with improvements in patient selection, optimisation of patients preoperatively and improvement of anaesthetic support and surgical techniques this has reduced to less than 5% [74], [75].

Long term outcomes, measured by patient morbidity, quality of life and 5-year mortality, remain poor. Morbidity of any grade affects up to two thirds of patients

[76]. Within 30-days of surgery the most common causes of morbidity are respiratory complications (pneumonia, pneumothorax and acute respiratory distress syndrome) and surgical complications (anastomotic leak and post-operative strictures).

Five-year survival following oesophagectomy has improved over the past 30 years. According to one study from the UK, median survival is now 52 months with a 5 year survival of nearly 50% [77]. This survival rate has doubled over the past 30 years. There is increasing evidence that the outcomes for both mortality and morbidity are improved with newer surgical techniques such as minimally invasive and robotic surgery [78].

1.1.3.4 Best supportive care

Best supportive care aims to control symptoms of patients with advanced disease in whom systemic therapy is deemed not to be of benefit. Endoscopic therapy options include dilatation, YAG laser, argon plasma coagulation (APC) and oesophageal stenting [53]. In addition palliative radiotherapy can be used to stop bleeding although the evidence for this is mostly inferred from treatment of gastric cancers [79].

1.2 Barrett's oesophagus

1.2.1 Definition

BO occurs when the normal distal squamous epithelial lining is replaced by metaplastic columnar epithelium. The diagnosis should be visible endoscopically,

with the metaplastic tissue evident ≥1 cm above the GOJ and confirmed histopathologically from oesophageal biopsies [80].

It should be noted that UK guidelines do not require the presence of intestinal metaplasia (IM) on biopsies for confirmation of BO whereas guidelines from the USA require this [80] [81]. The explanation for the UK approach is to avoid underdiagnosis of BO due to the chance of a sampling error not detecting IM. The risk of this error is greater in shorter segments of BO and when fewer biopsies are taken.

The precise role of IM in development of OAC is not fully understood. Two early pathological studies including patients that developed OAC showed that the presence of IM conferred a significantly higher cancer risk [82], [83]. It should be noted that these studies contained less than 50 patients between them.

Two more recent studies have looked at tissue from patients that have developed OAC. The first by Takubo et al [84] looked at EMR specimens. These resections had been performed to treat early oesophageal cancers. The authors looked at the surrounding mucosa and found that of the 113 that had an oesophageal origin 64 (56.6%) had no evidence of IM. The second study reviewed all patients that had lower oesophageal biopsies at a single centre. In total, 379 were found to have IM (IM group) whilst 309 had glandular mucosa alone (GM group). In the IM group 17 (4.5%) went on to develop OAC compared with 11 (3.6%) from the GM group [85]. This difference was not statistically significant.

The risk factors for developing BO are very similar to those for developing OAC. These vary across the large number of studies that have looked at this. They include male gender [26], older age [86], abdominal circumference [87], obesity [88], family history of BO or OAC [89], [90], and a history of reflux disease [86]. A personalised multifactor risk prediction model has recently been created to help diagnose BO by our laboratory [91].

1.2.2 Barrett's oesophagus disease progression

OAC in BO usually arises from an area of tissue with a precursor lesion. This region of tissue is known as "dysplastic". Dysplasia means abnormal growth or development of cells [92] and can occur in any region of BO. This process is known as the metaplasia-dysplasia-carcinoma sequence [93].

This hypothesis is supported by the widespread presence of dysplasia in specimens with invasive OAC. Prospective studies have demonstrated that in patients with invasive cancer, preceding biopsies were associated with ever increasing severity and extent of dysplasia [94].

The drivers for this pathway are complex and include activation of certain oncogenes alongside suppression of tumour suppressor genes [95].

It is due to wide acceptance of this theory that surveillance of BO is justified. By accepting this process BO surveillance aims to detect dysplasia prior to the development of OAC. BO surveillance will be discussed at a later point (see section 1.2.4).

1.2.3 Vienna classification

The Vienna classification has been used to categorise regions of BO (Table 1.3). Introduced in 1998 at the World Congress of Gastroenterology it categorises BO into 5 distinct categories, namely; Negative for dysplasia, Indefinite for dypslasia, Non-invasive low grade neoplasia (including low grade dysplasia (LGD)), Non-invasive high grade neoplasia (including HGD and carcinoma in situ), and Invasive neoplasia (including intramucosal carcinoma (IMC) and submucosal carcinoma or beyond) [96].

Table 1.3: Vienna classification

rable 1.5. Vienna classification	
Category 1	Negative for neoplasia/dysplasia
Category 2	Indefinite for neoplasia/dysplasia
Category 3	Non-invasive low-grade neoplasia
	Low-grade adenoma/dysplasia
Category 4	Non-invasive high-grade neoplasia
	4.1 High grade adenoma/dysplasia
	4.2 Non-invasive carcinoma (carcinoma
	in situ)
	4.3 Suspicious for invasive carcinoma
Category 5	Invasive neoplasia
	5.1 IMC
	5.2 Submucosal carcinoma or beyond

Biopsies that are negative for dysplasia should show normal surface maturation (Figure 1.5). Some nuclear alteration is acceptable in the bases of the pits. To complete this assessment it is important the tissue is embedded in wax correctly [97].

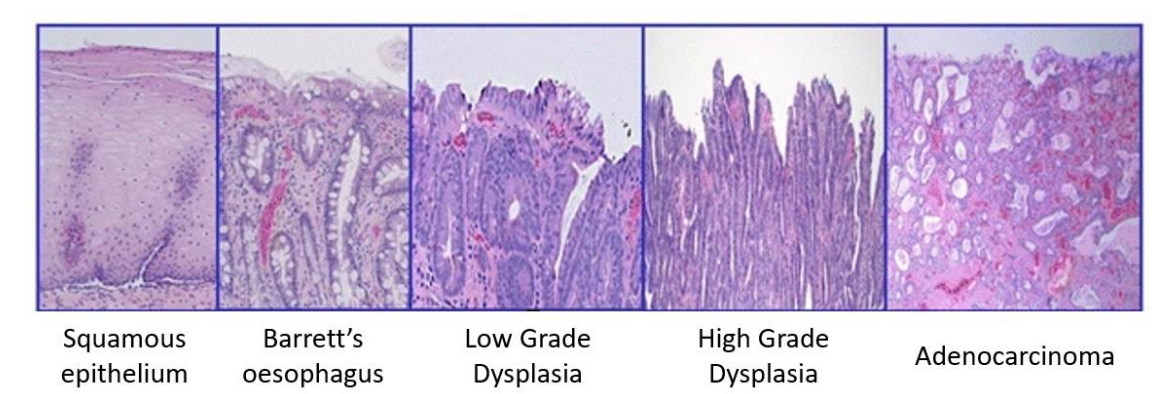


Figure 1.5: Showing progression of disease from normal squamous epithelium to OAC (adapted from [98]).

Indefinite for dysplasia incorporates a level of uncertainty into the diagnosis. When introduced, in 1983, for evaluation of epithelial changes in inflammatory bowel disease (IBD) this was a novel approach [99]. In addition, grading a biopsy as indefinite for dysplasia can reflect that the tissue is inflamed, or artefact has impeded interpretation. Typically, this category should only be used in a small percentage of cases.

1.2.3.1 Low grade dysplasia

LGD has larger nuclei than non-dysplastic tissue. There should be little inflammation to be confident of the diagnosis. There can sometimes be effacement in the region where LGD and NDBO meet, similar to tubular adenomas in lower GI pathology. The long axes of the enlarged nuclei should remain vertical and so maintain their polarity.

1.2.3.2 High grade dysplasia

HGD appears darker relative to non-dysplastic tissue in the sample. Nuclei often are more rounded and seem less regularly arranged as they have lost their relationship to the basement membrane. Performing immunohistochemistry to assess for TP53 overexpression can assist with identifying HGD.

1.2.3.3 Intramucosal carcinoma

IMC is present if there is invasion into the mucosa. This is staged as T1a OAC. Invasion into the submucosa is staged as T1b. IMC can only be diagnosed on biopsies that include submucosa as it is the absence of invasion into the submucosa that truly confirms IMC. Some institutions will diagnose IMC on specimens only containing mucosa. They do this with the understanding that this diagnosis of IMC will lead to an EMR being performed which will enable more accurate histological staging of the lesion [97].

Identifying these subtle abnormalities requires a high level of skill and experience. A demonstration of this challenge is the recommendation that two independent GI pathologists review any diagnosis of dysplasia[80].

1.2.4 Surveillance in Barrett's oesophagus

As mentioned, the metaplasia-dysplasia-carcinoma sequence is the basis for surveillance. The rationale being to detect early dysplastic changes or cancer at a stage when intervention can be curative.

Surveillance currently takes the form of frequent interval endoscopies with the frequency dictated by endoscopic and histopathological factors. UK guidelines recommend endoscopies every 2-3 years if the length of BO is ≥3cm and every 3-5 years if the length of BO is <3cm with IM [80].

There is a lack of evidence from RCTs to demonstrate the efficacy of surveillance.

Results from the BOSS Trial a randomised study comparing 2-yearly endoscopic

surveillance against 'at the time of need' endoscopy over a 10-year period showed surveillance did not improve overall survival or cancer-specific survival [100].

Surveillance endoscopies typically consist of a period of inspection using white light endoscopy and image enhancing techniques (such as narrow band imaging and optical zoom) followed by biopsies being taken. There is evidence that longer time inspecting segments of BO are associated with increased detection of HGD and OAC [101]. If any visible lesions are identified these should be biopsied. Following this, Seattle protocol biopsies should be taken consisting of quadrantic biopsies every 1-2cm.

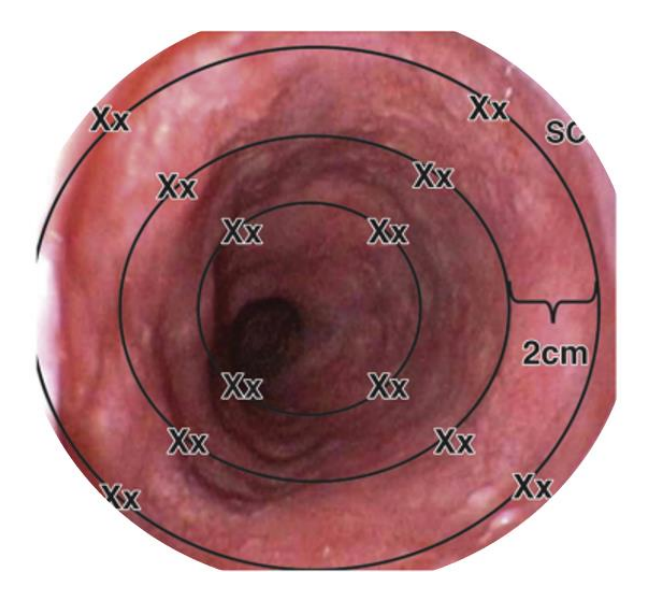


Figure 1.6: Image showing Seattle protocol biopsies. The Xx represent biopsies that should be taken (adapted from [102]).

Although Seattle protocol is recommended by national guidelines adherence ranges from 10% to 79% with poorer compliance in longer BO segments [103], [104], [105]. Seattle protocol only samples up to 5% of the BO segment meaning focal dysplasia

can be missed. This protocol generates large quantities of biopsies for histopathology laboratories and pathologists to process, which is associated with high financial and labour costs.

1.2.5 Treatment of early oesophageal adenocarcinoma and Barrett's oesophagus associated dysplasia

Historically, early oesophageal cancers required radical surgical treatment, namely oesophagectomy. Over the past 20 years newer less invasive therapies have been introduced with less associated morbidity and mortality.

Current treatment guidelines recommend removal of any visible lesions using a resection technique, either EMR or ESD, followed by ablation of the remaining Barrett's segment [80]. The theory underlying this ablation is to avoid the risk of leaving a metachronous lesion in the residual BO. Ablative techniques include photodynamic therapy (PDT), radiofrequency ablation (RFA), APC and cryotherapy.

Ablative therapies aim to eradicate the existing pathological columnar lined mucosa, which contains IM, dysplasia or neoplasia. This is then replaced by new squamous mucosa (neo-squamous regeneration).

The most widely used endpoints for therapy are complete reversal of dysplasia (CR-D) and complete reversal of IM (CR-IM).

1.2.5.1 Endoscopic Mucosal Resection

Although EMR is primarily used for resection of visible lesions in dysplastic BO it can also be used for diagnostic purposes. The steps for EMR (along with other resection techniques including ESD) are to identify a lesion, mark around it with diathermy followed by stepwise resection of the previously marked region. Since the original EMR technique was introduced in the 1990s for treating early OSCC [106], several other techniques have been developed. The most practised of these techniques are cap and snare and band ligation (Figure 1.7). Both these techniques make use of a cap on the end of the endoscope into which the mucosa is sucked into, creating a pseudo-polyp. This is then resected using a snare. The size of resection specimens is limited by the size of the cap and so lesions larger than this need to be resected piecemeal. The typical size of each resection specimen is 9-13mm [107].

Both cap and snare and band ligation appear to have similar efficacy of 85-98% [108], [109], [110]. No significant difference has been seen in the complication rates or depth of resection. This was demonstrated in two recent randomised control trials RCTs [111], [112].

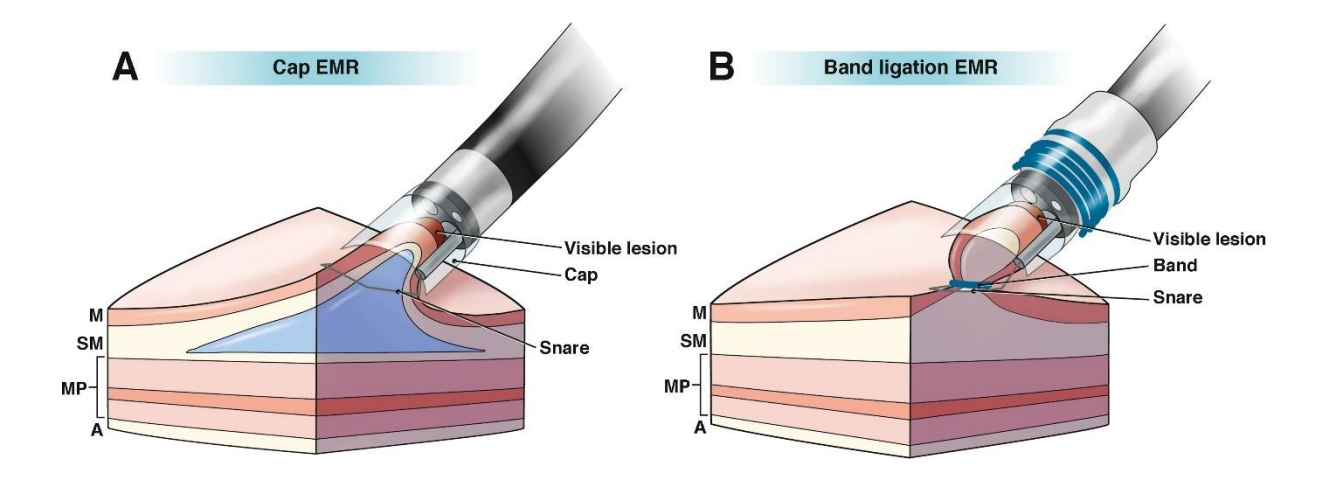


Figure 1.7: Image showing cap and snare and band ligation EMR techniques [113]

When circumferential resections are performed the stricture rate can be up to 88% whereas for resection limited to less than 50% of the circumference of the mucosa, symptomatic stricture is rare [114], [115]. For this reason resection is only recommended for visible lesions before the remaining mucosa is ablated [80].

1.2.5.2 Endoscopic submucosal dissection

ESD is a technique used to resect larger lesions in a single piece or *en bloc*. It is a highly technical procedure requiring extensive training. Lesions are removed by dissecting through the submucosa using a modified needle knife.

A 2009 meta-analysis comparing ESD with EMR in the GI tract. Curative resection rates for ESD was 65.8% versus 50.6% for EMR (OR 3.53, 95 %CI 2.57 – 4.84) [116]. Local recurrence rate for ESD was 0.3% versus 5.2% for EMR (OR 0.09, 95 %CI 0.04 – 0.18). However, ESD was both more time consuming and associated with significantly higher rates of complications including procedure-related bleeding (9.2% vs 5.8%; OR 2.20, 95 %CI 1.58 – 3.07) and perforation rates (4.5% vs 1.0%; OR 4.09, 95 %CI 2.47 – 6.80).

1.2.5.3 Photodynamic therapy

PDT, along with direct laser therapy and APC, was one of the first ablative therapies used to treat dysplastic BO. This involves administration of a photosensitising drug followed by application of light via a laser. The resulting photosensitivity reaction acts to eradicate the dysplastic tissue.

Two different photosensitising agents have been trialled. 5-aminolevulinic acid (ALA) and Photofrin. PDT has been demonstrated to be efficacious in several RCTs. A phase three trial from the USA randomly assigned patients to a Photofrin-PDT plus proton-pump inhibitor group or omeprazole alone [117]. The rate of complete reversal of HGD (CR-HGD) was 77% in the PDT treatment arm compared with 39% in the omeprazole alone group (p<0.0001). Another study looked at ALA-PDT vs Photofrin-PDT [118]. The rate of CR-HGD was significantly higher with ALA-PDT than with Photofin-PDT in segments of BO <6cm.

Unfortunately, although PDT has been found to be efficacious the side effect profile has been prohibitive to mainstream clinical use. The most common side effects are stricturing (up to 50% if more than one course of PDT was required [119], [120]) and photosensitivity reactions.

1.2.5.4 Radiofrequency ablation

The most established ablative therapy is RFA. RFA has increasingly been used for treatment of BO since 2005 [121]. RFA applies thermal energy to tissues via a probe this leads to necrosis of the target tissue. This energy is generated using a medium

frequency alternating current and is applied via a balloon catheter or a focal device.

This device can be attached to the outside of the endoscope or passed through the endoscope working channel (Figure 1.8).



Figure 1.8: Showing available RFA catheters. From left to right: 360 balloon catheter; ultra-long focal catheter; 90° focal catheter; 60° focal catheter; channel endoscopic catheter [122]

RFA has been demonstrated to have high treatment success rates as well as good durability [121], [123], [124], although long-term data is lacking. This will be discussed further in section 1.2.6.

1.2.5.5 Cryotherapy

Where RFA uses thermal energy to destroy tissues, cryotherapy uses a freezing agent to cause ischaemic necrosis of the treated region. This process is caused by intracellular and extracellular ice forming which on thawing causes apoptosis of the treated cells.

When cryoablation was initially introduced, the freezing agent used was liquid nitrogen. This was applied directly to the mucosa using a spray catheter [125]. One of the disadvantages of this technique were the large volumes of gas used during

therapy. This required placement of a nasogastric tube to decompress the stomach.

Despite this in an early trial a single case of gastric perforation was recorded [126].

A new balloon device has been manufactured by Pentax (Pentax Medical C2 CryoBalloon Focal Ablation System) using nitrous oxide. Rather than applying a freezing agent directly to the tissues the freezing agent is applied indirectly through a balloon catheter. This avoids large volumes of gas being introduced into the patient.

Work is ongoing to establish the efficacy of cryoablation. There is some evidence suggesting cryoablation is efficacious albeit in trials with small sample sizes. In an early trial in 2005, all 11 patients treated achieved CR-D and CR-IM [125]. A 2015 study containing 44 subjects achieved CR-D in 95.6% of patients with LGD and 91.3% of patients with HGD. The rate of CR-IM was 55% [127]. Ramay et al published 5-year follow up data for 40 treatment naïve patients that had undergone cryoablation using a liquid nitrogen catheter spray. At 5 years, CR-D was 80% and CR-IM was 65% [128].

A retrospective cohort study [129], published in 2021, compared RFA with cryoablation, using liquid nitrogen spray cryotherapy (LNSC). This showed the rate of CR-D or CR-IM did not differ significantly between the RFA and LNSC groups (CR-D 81% vs. 71.0%, p = 0.14; CR-IM 64% vs. 66%, p = 0.78). In this study LGD was highest grade of neoplasia for 60% of the patients. In addition, although the patient groups were very similar in their baseline characteristics patients were not randomised to either intervention.

1.2.5.6 Argon photo coagulation

APC uses thermal ablation to treat targeted areas. Argon gas, which is passed through a catheter that is introduced into the endoscope working channel, is used to conduct electrical current to the tissue. APC is typically used as an adjunct to other ablative therapies as, although it is low cost it is more suitable for treating small regions of residual disease rather than field ablation.

Ablation using APC has been shown to be significantly superior to surveillance in increasing recurrence-free survival following endoscopic resection (ER). Secondary lesions were identified in 3% of patients in the APC group vs 37.7% in the surveillance group (p = 0.005).

Data from a feasibility study (BRIDE) compared APC with RFA [130]. 76 patients were randomised to either APC or RFA. The study found longer residual lengths of BO in the group treated with APC (mean 1.3cm vs 1.7cm), these results were non-significant. There was no difference in rates of CR-D at 12-months (12.5% RFA versus 11.5% APC, OR 1.10, 95% CI 0.22-5.4).

1.2.6 Radiofrequency ablation

RFA uses directly applied thermal energy to ablate the surface 500µm of mucosa. This ablation is uniform across the mucosa and treats the mucosa alone, the site of BO related dysplasia. By treating BO to a uniform depth, and so avoiding ablating the submucosa, RFA is associated with fewer strictures than other modalities such as PDT.

As shown previously (Figure 1.8) there are a range of devices produced by Medtronic.

This range allows specific areas of BO to be treated, from focal ablation with a channel catheter to a 360° field with a balloon catheter.

A 2013 systematic review and meta-analysis of efficacy and durability of RFA for BO identified 18 studies reporting on efficacy and 6 studies reporting durability [131]. The efficacy data included 3802 patients. CR-IM was achieved in 78% of patients (95% CI, 70%–86%) and CR-D was achieved in 91% (95% CI, 87%–95%). These endpoints were confirmed with a single endoscopy in all but one study. Oesophageal stricture was the most common adverse event, occurring in 5% of patients (95% CI, 3% - 7%). Durability data was limited with just 540 patients followed up for a median 1.5 years. Cancer occurred in 0.7% of patients during follow-up.

Between 2007 and 2010 the EURO-II trial collected data for combined therapy with first (primary) endoscopic resection followed by field ablation with RFA [132]. Across 13 European sites 132 patients had a median of 3 RFA (interquartile range (IQR) 3-4) treatments following primary ER. CR-IM was achieved in 87% of patients. After a median of 27 months IM had recurred in 8% of patients. Strictures occurred in 6% of patients after RFA.

A 2021 meta-analysis [133], reported high levels CR-D and CR-IM at the completion of endoscopic therapy (CR-D 95.9 [95% CI 91.7-98.7]%; CR-IM 90.9 [95% CI 83-96.6]%). After 3.4 years of follow up the rate of CR-D was 89% (95% CI 73.4-98.2%) and CR-IM was 77.8% (95% CI 65.6-88%). Only two studies provided data for follow

up greater than 5 years, with a combined rate of CR-D 50% (95% CI 41.5-58.5%). Further long-term durability data is lacking.

1.2.7 Gastrointestinal histopathology

Biopsies and cytology taken at the time of endoscopy provide vital diagnostic evidence. Histology is the gold standard for a number of gastrointestinal (GI) pathologies, including IBD, cancers and coeliac disease. It should be noted that GI endoscopy accounts for up to one third of a department's entire histopathology work load [134].

Histology often provides more than diagnostic value. Histology assists with guiding therapeutic options (tumour markers in cancers), prognosis (IBD) and surveillance intervals (colonic polyps).

1.2.7.1 Oesophageal histopathology

Histopathology is a critical tool in caring for patients with upper GI pathology, especially with regard to BO and BO related neoplasia. Pathological assessment is the gold standard for grading BO related disease as recommended by national and international guidelines [80], [135], [136].

As mentioned previously BO is the only known premalignant state of OAC [47]. BO is a condition in which the distal squamous epithelium is replaced by metaplastic columnar epithelium. Although this metaplastic change is visible endoscopically current guidelines recommend biopsies every 2cm to assess for any dysplastic changes. Dysplastic changes in BO increase the risk of developing OAC

Experts in upper GI endoscopy increasingly find that dysplasia can be visualised using endoscopic imaging enhancement techniques [137]. It has been suggested that in the future these techniques may remove the need to take Seattle protocol biopsies. Currently biopsies remain an essential part of guidelines [80], [135], [136].

1.2.8 Histology

Histology is the gold standard for diagnosing both OAC and BO. The processing of tissue for histology from patient to a diagnosis is complex and expensive.

1.2.8.1 Background

Histology is a branch of anatomy that deals the minute structure of animal and plant tissues as discernible the microscope [138]. Histopathology is a branch of pathology that is concerned with the tissue changes characteristic of disease [139].

Histological assessment requires precise tissue preparation and a microscope to improve magnification and resolution. Tissue processing involves multiple steps including, fixation, sectioning and staining (Figure 1.9). Much of current practice was introduced in the 19th century and is largely unchanged since then.

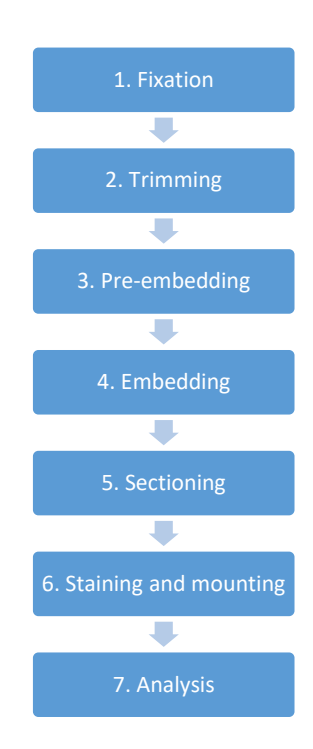


Figure 1.9: Stages of modern histological processing

1.2.8.2 Fixation

The first stage of histological processing is fixation. The purpose of fixation is to preserve tissues and to slow down tissue degradation. It is a vital step to ensure tissue cellular architecture and composition is preserved prior to subsequent processing. It is crucial that fixation occurs immediately specimens are resected to minimise damage to the tissues.

Tissue fixation is a complex gradual process that is not fully understood but comprises of two parts. The first is the diffusion of the fixative into the tissues and the second is the chemical effect of the fixative on the tissues themselves. Ideally a fixative would preserve all aspects of a specimen, including physical structure and chemical activities. Several different chemicals can be used with slightly varying properties.

The most commonly used fixative used in modern tissue processing is formalin. Typically 10% formalin solution. This solution comprises of 3.7% formaldehyde in water with 1% methanol. It acts of tissues by cross-linking proteins. Alcohols such as methanol and ethanol can also be used as fixatives. These work by denaturing proteins in specimens.

Since fixation is a gradual process dependent on diffusion of the fixative into the tissues, the speed of histological processing is determined by the size, shape and type of the specimen, temperature, pressure and volume of fixative solution[140].

1.2.8.3 Trimming

Trimming ensures tissue samples are the adequate size and orientation. This is important to ensure that subsequent stages can take place. Some specific tissues require additional processing steps at this point, one example being teeth and bones that need to be decalcified.

1.2.8.4 Pre-embedding

The aim of pre-embedding is to replace water in the tissues with paraffin wax. The use of paraffin wax in histological processing began in the 19^{th} century. Wax ensures the tissue is supported prior to sectioning and enables cutting of thin sections (typically $3-5\mu m$).

Paraffin wax used in histological processing has a melting point between 56°C and 58°C. This temperature is not high enough to cause damage to the structures or the microscopic details of the tissues. Water and paraffin wax are immiscible meaning

the water in tissues needs to be replaced with a different reagent prior to the wax infiltration. The specific steps used vary but, in all cases, different grades of alcohol are used to replace the water in the tissues. The different grades ensure this process occurs slowly, minimising the chance of critical damage to the tissues caused by rapid dehydration. Two typical processes for pre-embedding are seen below (Table 1.1).

Table 1.4: Godkar and Bancroft techniques for tissue processing prior to embedding.

	GODKAR		BANCROFT	
STEPS	Reagents	Number of changes	Reagents	Number of changes
DEHYDRATION	80% alcohol	2	70% alcohol	1
CLEARING	90% alcohol	1	95% alcohol	2
IMPREGNATION	100% alcohol	3	100% alcohol	3
	Xylene	2	100% alcohol	1
	Paraffin	2	Xylene	2
			Paraffin	3

Once all the water has been removed from the tissues the alcohol is replaced by xylene, a solvent in which liquid paraffin wax easily dissolves. Much of this work is automated using a piece of equipment known as a tissue processor.

1.2.8.5 Embedding

After infiltration with paraffin wax specimens are placed inside a mould which is then filled with liquid paraffin creating a solid block of wax with the specimen in the middle. This is performed using an embedding station. Once the paraffin block is cooled the specimen is ready for sectioning. It should be noted that this stage is vital to ensure correct orientation of the specimen prior to sectioning.

1.2.8.6 Sectioning

Sectioning is a process by which 3-5 μ m thin samples from each specimen are made. This is done using a specialised piece of equipment known as a microtome. The microtome consists of a holder for the paraffin block and a precision knife.

The block is cut into ribbons (serial sections). Once a ribbon is cut it is floated across a warm water bath before the section is lifted onto a glass slide. These sections are then allowed to dry in a laboratory oven.

1.2.8.7 Staining

To visualise microscopic details in sections chemicals are added to generate contrast. Various staining mediums are used in modern histology. Most of them were originally introduced during the late 19th century and early 20th century. The most used in modern clinical practice is haemotoxylin and eosin (H&E). Once staining has been performed a cover slip is mounted over the slide to protect the tissue.

1.2.9 Cost

The processing of specimens for histological assessment is a complex procedure with multiple steps, several of which are labour intensive, increasing both the time and financial cost.

Pathology costs range from 2-5% of health care costs in the Western World and these costs are rising [141]. In the UK the cost of histopathology specimens ranges from £21.40 to £773.70 per specimen [142]. Assessment of biopsies is responsible for

about 25% of the workload of histopathology departments in large 'district general' hospitals in the UK [143]. The number of histopathology specimens in the UK has increased annually by 4.5% [144] and the case load is increasing in complexity. This additional complexity is in part due to additional tests being required, including immunohistochemistry and tumour markers. In addition, there are increasing numbers of cases requiring precise diagnosis of early cancers and precancerous lesions, which are more time consuming to interpret.

One of the impacts of this increasing work load has been increased turnaround times for specimens in the lab [144]. This is the time from a specimen being collected till a result is available. The number of patients waiting more than six weeks, a key performance marker, for a result increased 16.5% annually between 2010/11 and 2015/16. Histopathology turnaround times are particularly vulnerable to increased demands due to the highly manual nature of the work and the time it takes to train staff. This is compounded by an ongoing shortage of consultant histopathology consultants. Technological solutions such as digital pathology along with advances in machine learning are advancing which aim to resolve some of these issues [145].

1.3 The UK RFA Registry

The UK RFA Registry was founded in 2008 to audit outcomes of patients undergoing RFA for dysplastic BO and Barrett's associated neoplasia. Twenty-eight sites have been registered to be included in the registry (Figure 1.10 & Table 1.5). These sites were recognised and nominated by their local cancer networks. Subsequently they were approved by the CLRN. These sites recorded demographic and clinical details

relevant to patients Barrett's therapy. Ethical approval was granted by the Joint University College London (UCL) / University College London Hospital (UCLH) Committee on the Ethics of Human Research (REC REF 08/H0714/27). The UK registry is registered at ISRCTN 93069556.



Figure 1.10: Map of the 28 sites submitting data to the UK RFA Registry. Those sites highlighted in red have undergone additional review by the primary site.

Table 1.5: List of the 28 sites submitting data to the UK RFA Registry. Those sites highlighted in red have undergone additional review by the primary site.

Addenbrooke's Hospital	Plymouth Hospital NHS Trust	
Aintree University Hospital	Queen Alexandra Hospital, Portsmouth	
Belfast City Hospital	Queen Elizabeth Hospital Birmingham	
Bradford Teaching Hospitals NHS	Royal Bournemouth and Christchurch	
Foundation Trust	Hospitals NHS Foundation Trust	
County Durham & Darlington NHS	Royal Infirmary of Edinburgh	
Foundation Trust		
Frimley Park Hospital	Royal Liverpool University Hospital	
Glasgow Royal Infirmary	Salford Royal NHS Foundation Trust	
Gloucestershire Royal Hospital	Southampton University Hospital	
Guys and St Thomas' NHS Foundation	St James's Hospital, Dublin	
Trust		
John Radcliffe Hospital	St Mary's Hospital, London	
Manchester Royal Infirmary	The London Clinic	
Newcastle Upon Tyne Hospital	The Royal Wolverhampton NHS Trust	
Norfolk and Norwich University Hospital	University College London Hospital	
Nottingham University Hospitals NHS	West Hertfordshire NHS Trust	
Trust		

1.3.1 Study protocol

Prior to recruitment all patients had a diagnostic endoscopy including Seattle protocol biopsies. Following this endoscopic resection took place if clinically indicated. At this point they were entered into the study protocol shown in Figure 1.11.

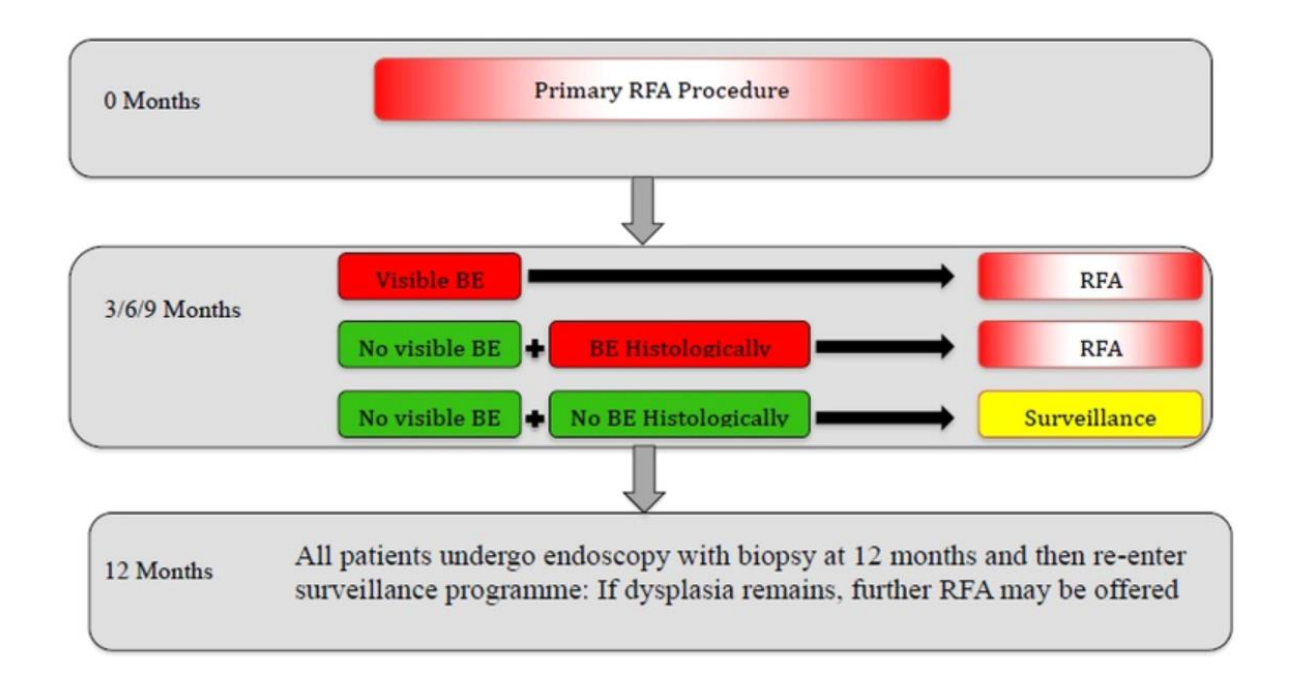


Figure 1.11: UK HALO RFA registry study protocol [123]

Following completion of the protocol, not all patients achieve CR-D or CR-IM.

Patients could then have further endoscopic therapy according to patient and clinician preference. Patients that achieved CR-D and CR-IM continued to have surveillance endoscopies.

The post-RFA surveillance protocol consisted of 3-monthly intervals for the first year, 6-monthly intervals for the second year and annually thereafter. To detect recurrence, biopsies were taken from 1cm below the GOJ and from the previously treated BO segment according to the Seattle protocol. Recurrence of CR-IM was defined as IM on biopsies taken more than 5mm above the GOJ.

If dysplasia or IM was detected at any of these surveillance procedures further EET was considered. This included APC, RFA, YAG laser or endoscopic resection (EMR or ESD).

1.3.2 Data collection

Data collection for the RFA registry was performed by local teams at each site. Initially this was completed using paper case record files (CRFs) which were faxed to the central site (UCLH). By 2011 this system was replaced with an online database (www.treatbarretts.com/doctor) allowing real-time data submission.

This data was pseudo-anonymised with only the local sites able to identify individual patients. Data collected included baseline demographics, previous endoscopic resection and BO length at recruitment (Figure 1.12). After each endoscopy, treatment data was recorded via procedure CRFs (Figure 1.12). These recorded the current length of BO, the type of treatment that was applied and outcomes of any biopsies taken. Data could be extracted from the database in the form of Excel worksheets allowing analysis of patient and procedure specific data.

patient: h28p1 patient info		procedure	
		procedure info: 19695	
Patient ID	H28P1 (edit patient info)	Procedure ID	19695 (edit procedure info)
Hospital	Example Hospital	Patient ID	H28P1
Sex	m	Procedure Date	25/10/2021
DoB	19/06/1945 (76)	Halo Ablation No	1
Ethnicity	Caucasian	Top of gastric folds at	40cm
Date of Informed Consent		Top of Barrett's C at Top of Barrett's M at	38cm 36cm
Prior Ablation	No	Top of islands at	34cm
Prior Argon Plasma Coagulation (APC)	No	Barretts C	2
Prior PDT	Yes	Barretts M	4
PDT Type	ALA	Stricture Pre Rx	No
Prior Resection	Yes	Stricture dilated today	No
EMRduringHALO	No	Bx Taken	Yes
EMRafterHALO	No	Rx Performed	Yes
Prior Resection Info		Rx Type	H360,Halo 60
Prior Dilatation	No	Histology Highest Grade	High Grade Dysplasia
Other relevant history	Other	Patient Taking PPI	No
Worst Ever Grade	High Grade Dysplasia	PPI Type	Omerazole
BE Length C	7	PPI Dose	40
BE Length M	9	PPI Freq	2
PATIENT NOTES	,	CR BE	1
PPI TYPE	Omerazole	CR D	1
PPI DOSE	40	CR IM	0
PPI FREO	2	12 Month Protocol	0
Adverse Events	No	Further follow up	Yes
Adverse Events Details		Why no further follow	
Date BE diagnosed	02/05/2018	up arranged	
Date HGD diagnosed	02/05/2018	EUS Done	No
Date of referral	23/01/2018	Complication (adverse	No
Referral source	Physician	event) Complications	
Referring hospital			
In surveillance program? Yes		Complication (AE) Details	

Figure 1.12: Example online CRFs for HALO registry. Left-hand image shows a test patient CRF including baseline demographic data, previous therapy and BO length. Right hand image shows procedure CRF including length of current BO, any therapy performed and histology results if biopsies taken

1.3.3 Previous publications and outcomes

The UK national HALO RFA registry has been the source of several highly cited papers. The first of these papers was published in 2013 and confirmed efficacy for RFA to treat dysplastic BO. Of 335 patients with BO and neoplasia, after 12 months of RFA therapy 81% achieved CR-D and 62% were clear of BO [146]. A subsequent paper published in 2014 included 500 patients who completed RFA therapy. This compared rates of CR-D and CR-IM in two time periods (2008-2010 and 2011-2013) [147]. Overall rates of CR-D and CR-IM improved significantly between these two time periods (CR-D 77% to 92% and CR-IM 56% to 83%; p=0.013). In 2015 the team published data comparing efficacy and durability of EET. The rates of CR-D and CR-D a

IM were not significantly different for patients with HGD or IMC (HGD 88% and 76% respectively; IMC 87% and 75% respectively; p =0.7). The durability of these outcomes was assessed at a median of 24 months after starting treatment. There were slightly higher rates of recurrence of IM for patients with IMC although this was not significant (p=0.08) [148]. Although long term follow-up data have been collected, no new analyses have been done in the last 7 years. The Registry closed to recruitment in 2020.

1.4 Physics of x-rays

1.4.1 Background

As I have shown there are several modalities which aim to detect pathological abnormalities. They all have limitations including modalities using x-rays.

X-ray has been used clinically since the 19th century [149] after its discovery by Röntgen. The physical principle used to generate image contrast has remained the same since then [150] and underlies all historical and current uses of x-rays in clinical practice.

Most clinical x-ray-based imaging consists of planar radiography and three-dimensional x-ray tomography (CT). In addition, there are specialised applications such as mammography and fluoroscopy which make use of adapted instruments. Furthermore, all these techniques can make use of contrast agents such as air.

1.4.2 What are x-rays

X-rays are a form of electromagnetic radiation (Figure 1.13) which is an oscillation of electric and magnetic fields that travel at the speed of light. X-rays have a frequency between 3 x 10^{16} and 3 x 10^{19} Hz (30 petahertz to 30 exahertz) and can be described both as an electromagnetic wave and as a wave of particles called photons.

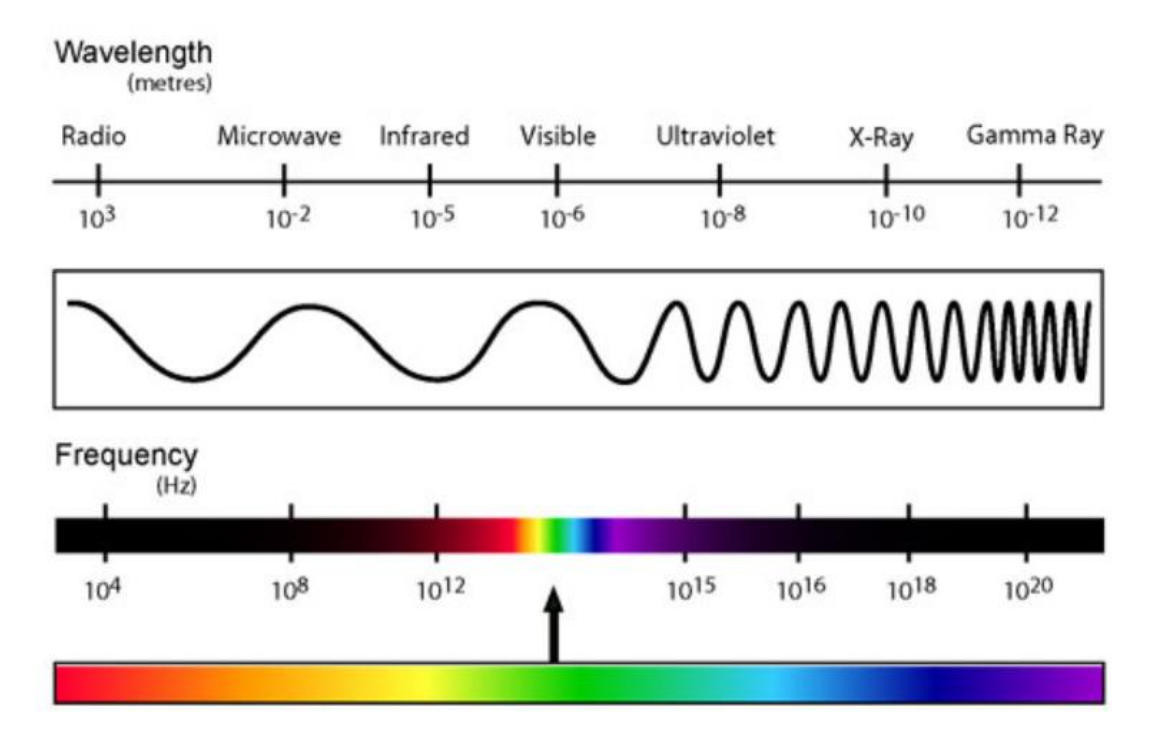


Figure 1.13: Electromagnetic spectrum [151]

X-rays have varying physical properties that can alter their application. Some of these properties are easier to describe as properties of a wave and some as the properties of a particle.

1.4.3 Attenuation

The underlying principle to generate contrast in clinical x-ray-based imaging is attenuation. This uses the number of x-rays that pass-through a given material to generate contrast.

The number of x-rays a material absorbs is called the attenuation coefficient, which is proportional to the electron density of that material. This is called the Z value of the material. Contrast is generated by the difference in absorption of x-rays by different materials. The result of this is that if two materials with similar electron densities are x-rayed side by side little contrast is generated.

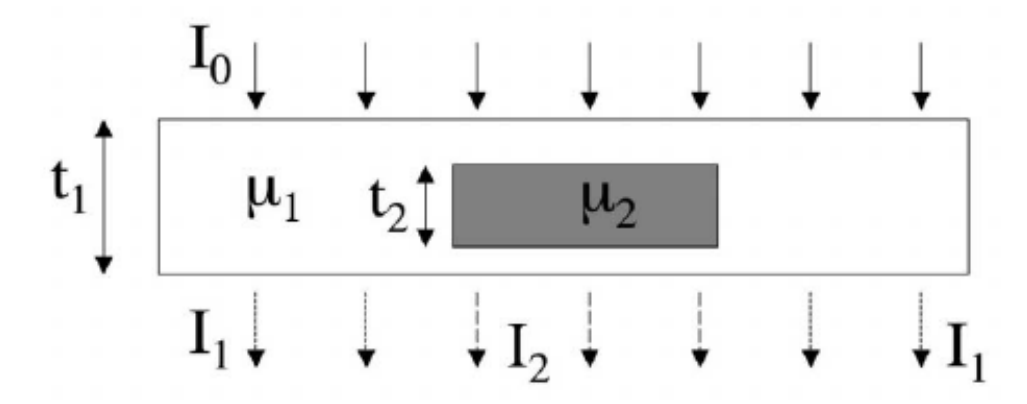


Figure 1.14: Schematic diagram showing contrast generation using attenuation [150]

Figure 1.14 shows contrast formation using attenuation based x-ray imaging [150]. This can be calculated by the formula below (Figure 1.15). I_2 is the intensity of the signal detected in the shadow of the imaged object. I_1 is the intensity of the signal immediately outside the object. The attenuation coefficient of the background and the object are labelled μ_1 and μ_2 . The thickness of the background and object are labelled t_1 and t_2 .

$$C_{att} = \frac{I_1 - I_2}{I_1}$$

Figure 1.15: Formula showing how contrast is generated using attentuation. I_2 is the intensity of the signal detected in the shadow of the imaged object. I_1 is the intensity of the signal immediately outside the object.

Clinical x-ray makes use of the difference in attenuation between two neighbouring tissues to generate contrast. Bone and calcification attenuate a much higher

proportion of x-rays relative to soft tissues (i.e., muscle or solid organs) which in turn are more attenuating than air filled tissues (i.e., lungs or bowel).

Figure 1.16 shows the attenuation coefficient of different materials (including a range of human tissues). Hounsfield Units (HU) are given which is a linear scale of attenuation coefficients. As can be seen soft tissues including kidney, muscle and liver have very similar attenuation properties.

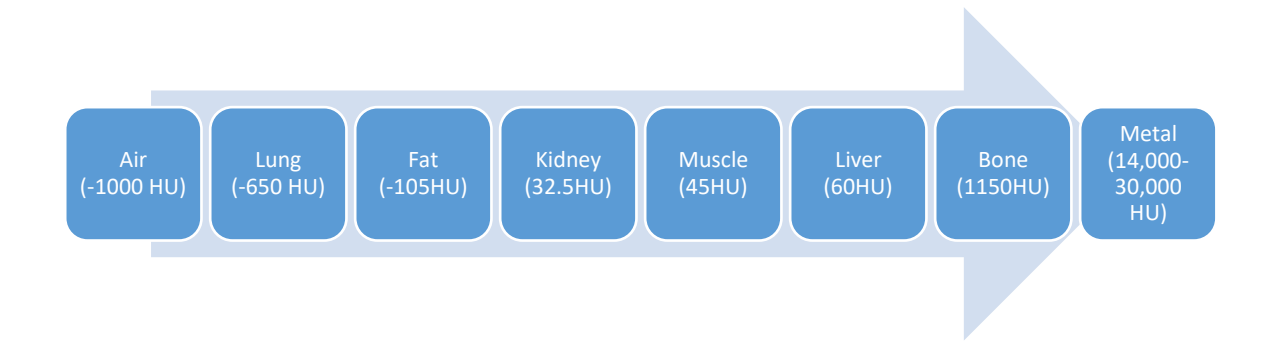


Figure 1.16: Attenuation coefficients of air, metal and different human tissues

Figure 1.17 shows the setup for planar radiography [152]. An x-ray source produces an x-ray beam which is directed at the region of interest. The targeting of this region can be assisted by using a collimator, a device which reduces the size and shape of the beam so enabling the x-ray beam to be targeted more precisely. After passing through the subject the x-rays may pass through an anti-scatter grid before reaching the detector.

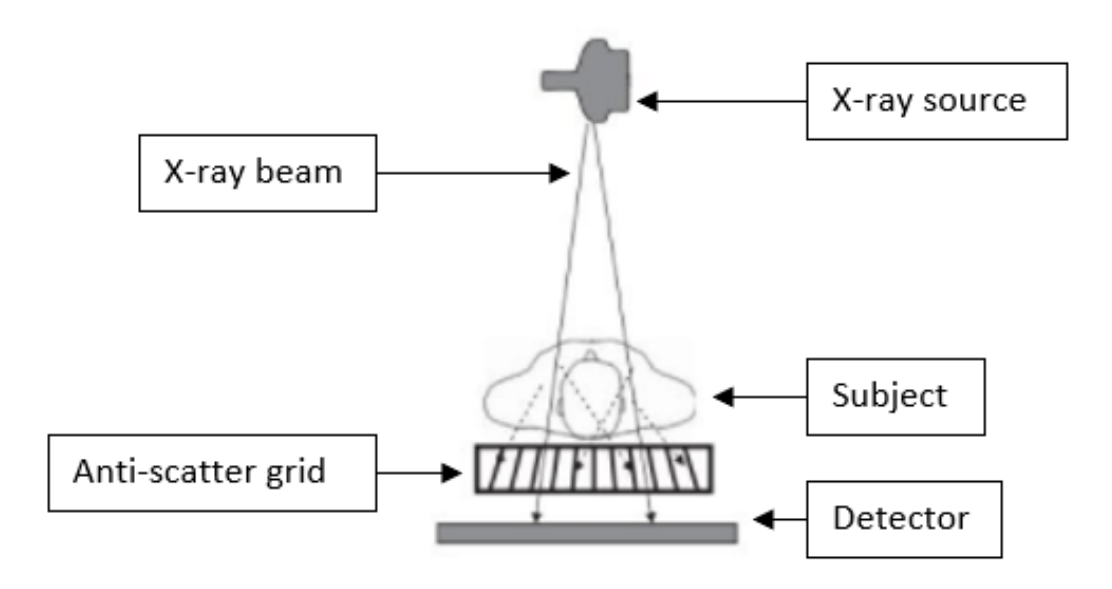


Figure 1.17: The setup for planar radiography [152]

1.4.4 Image quality in imaging

In imaging the most common quantitative parameters to measure image quality are the signal to noise ratio (SNR), spatial resolution and contrast to noise ratio (CNR). The equipment used and operational considerations play a large role in this.

1.4.4.1 Signal to noise ratio

Noise in imaging is any recorded signal that is detected which is not related to the actual signal one is trying to measure [153]. The SNR is the ratio of true signal to this noise. Factors that affect the SNR in x-ray imaging are:

 Quantum noise – natural random variation in the number of photons emitted from the x-ray source. Scattering - scatter occurs when photons interact with a medium and are
deviated from their original path. As scattered x-rays deviate in an irregular
manner, they provide limited clinical information, rather they increase
background noise and so reduce signal related to the imaged object (Figure
1.18). Antiscatter grids are used to minimise this source of noise in medical
imaging.

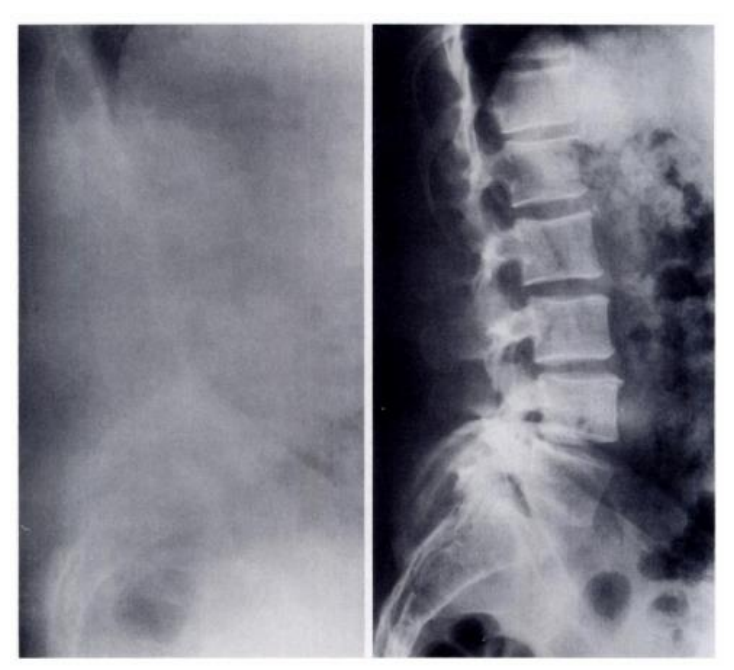


Figure 1.18: A – image taken with no antiscatter grid. B – image taken with antiscatter grid[154]

- The x-ray tube current (mA) and exposure time (influences the number of photons in any given period). The SNR is proportional to the square root of the product of these quantities [153].
- Tube Kilovoltage peak (kVp) As kVp increases more higher energy photons
 are emitted. Higher energy photons penetrate tissues more readily and
 therefore increase the recorded signal at the detector.

- The tissue being imaged. If this is thicker or more attenuating this will reduce the SNR as more x-rays fail to reach the detector.
- The efficiency of the detector

A lower SNR results in images having a grainy appearance.

1.4.4.2 Resolution

Resolution is the smallest distance between two features that allows the features to be individually visible rather than as a single larger shape.

1.4.4.3 Contrast to noise ratio

Whereas SNR is the signal in any given pixel individually contrast is the signal difference between two tissues.

$$C_{AB} = |S_A - S_B|$$

Where C_{AB} is the contrast between tissues A and B, and S_A and S_B are the signals from tissues A and B respectively. The contrast to noise ratio is the SNR of tissue A minus the SNR of tissue B.

$$CNR_{AB} = |SNR_A - SNR_B|$$

This shows that although the contrast between two tissues is dependent on both the method of imaging and the inherent properties of that tissue the background noise also contributes.

1.4.5 Clinical X-ray setup

1.4.5.1 Source

X-rays can be produced from a variety of sources, both natural and man-made.

Clinical x-rays and most laboratory x-rays sources are produced from x-ray tubes.

An x-ray tube (Figure 1.19) comprises of a cathode, anode and vacuum. An electric current is passed through the negatively charged cathode, which is formed by a small helix of tungsten wire. When the wire temperature reaches over 2000°C electrons are emitted from its surface. A high voltage is applied to the anode which accelerates the electrons towards the anode. The higher the voltage applied the higher the potential difference between the cathode and anode, and so the higher velocity at which electrons strike the anode. The anode rotates to reduce localised heating. The apparatus is enclosed in a vacuum to allow electrons to have an unimpeded path between the cathode and anode.

These electrons produce x-rays either by colliding with inner shell electrons in the anode or when slowed by the nucleus of the atoms in the anode.

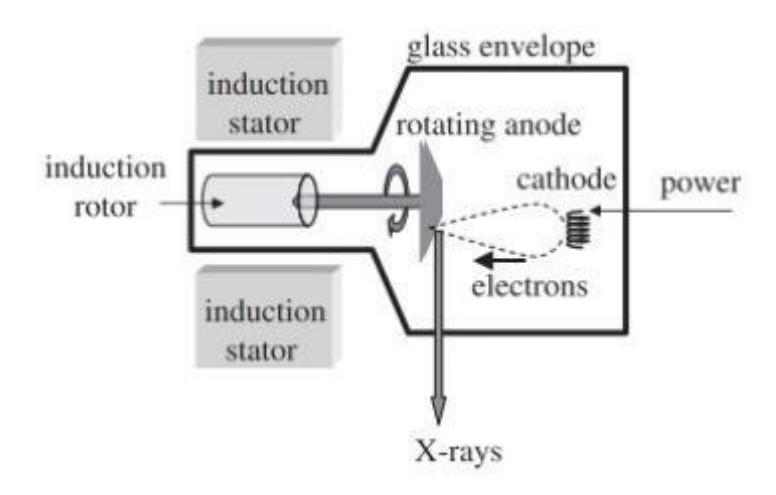


Figure 1.19: Schematic diagram of an x-ray tube[153]

It should be noted that the x-rays produced by an x-ray tube form a spectrum. This spectrum is determined by the material used to form the anode and the voltage applied to the x-ray tube. In most clinical x-ray modalities tungsten is used, but to generate lower powered x-rays such as those used in mammography a molybdenum source is used. The spectrum can be modified by using certain parameters as well as filters to select out low energy x-rays but is not continuously tuneable. X-rays produced from synchrotron sources do not have these limitations.

The parameters relating to the x-ray tube that can be modified include:

mA – current applied to the cathode. This increases the number of electrons emitted which in turn increases the number of photons emitted from the anode. It should be noted that another way to increase the number photons passing through an imaged medium is to increase the exposure time.

kVp – the maximum voltage applied across the x-ray tube. This is proportional to the highest energy of the resulting x-ray emission spectrum.

1.4.5.2 Detectors

Historically x-ray films comprising of an emulsion of silver bromide were used. Clinically there are two forms of detectors, computed radiography (CR) instrumentation and digital radiography (DR). CR uses a detector plate which forms a 'latent' image of the projection. This can then be fed into a CR reader. DR detectors can be indirect or direct. Indirect detectors use a scintillator to convert x-rays into light which is then converted into voltage using two-dimensional photodiodes.

It should be noted that there is an effective limit to the number of pixels in a detector both due to quantity of data produced and the increased cost of larger detectors. This means that although resolution can be increased by reducing pixel size this leads to a decrease in the field of view (FoV).

1.4.5.2.1 Crosstalk

Crosstalk is the occurrence of a signal that is detected in one pixel creating an effect in another pixel. This is a common phenomenon in electronics but materialises in detectors by reducing the resolution. Measures to reduce this effect will thus improve resolution. One such measure is using skipped masks in an edge illumination (EI) phase contrast setup which will be discussed in more detail in section 1.5.1.1.1.

1.4.5.3 Summary of limitations

In summary there are several limitations for conventional x-ray imaging. This includes the source, detector and even the mechanism for generating contrast, attenuation.

1.5 X-ray phase contrast imaging

Synchrotron radiation has allowed for the advancement of x-ray-based imaging techniques that are now being attempted using conventional x-ray sources. One such technique is XPCI which uses refraction of x-rays as they pass through a medium

Phase contrast imaging is a technique that uses a different effect of a material on an x-ray, refraction (Figure 1.20). This describes the change in direction of the wave through a specimen rather than attenuation. The phase shift of x-rays as they pass through a material, discovered in the 1960s [155], has been shown to provide much higher contrast between soft tissues than attenuation-based imaging [156], [157].

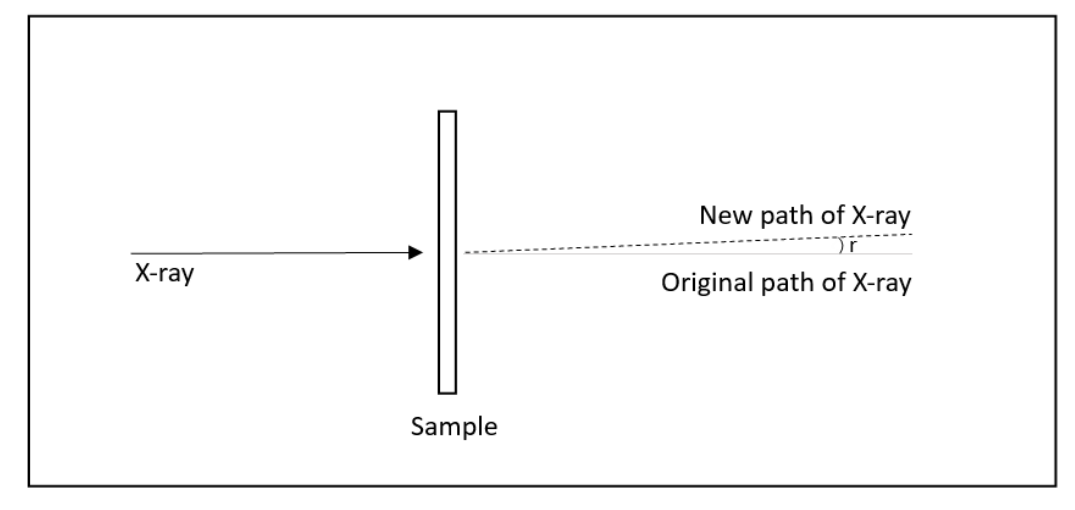


Figure 1.20: Image showing refraction of X-ray (shown by dashed line – "new path of x-ray") relative to original path of x-ray. The angle of refraction is shown by "r".

The phase shift (delta) for most materials is 1000 times greater than the attenuation properties (beta). This suggests that phase contrast imaging will be highly sensitive to small changes in the structure and composition of a given tissue and so enable better contrast between similar tissue types. The phase shift is typically of the order of a microradian (a difference of 1mm at a distance of 1km) [150]. To detect such minute effects an extremely high level of precision is required. This is one of the major limitations to this technology so far. This precision extends to all aspects of the x-ray setup, including the x-ray source used.

As synchrotrons are able to produce x-rays with high flux and coherence much of the early research using XPCI has been performed at these centres.

1.5.1 Phase contrast imaging methods

Different techniques have been developed which make use of this refraction of x-rays. These make use of the deviation in the wave due to the presence of a sample to either increase or decrease the signal intensity hitting a detector. Two of the most used techniques are EI and free space propagation (FSP).

1.5.1.1 Edge Illumination (EI)

El uses a pair of structured masks to implement the technique (Figure 1.21). The first is placed in front of the sample to create micro-beamlets of radiation, the second mask is placed immediately before the detector [158]. This second mask is placed so that it partially conceals a column of pixels on the detector. When an object is present refraction of the micro-beamlets alters the beam intensity hitting the pixel,

and so changes the signal generated. It should be noted that this setup is only sensitive to horizontal deviation of photons. Vertical deviation does not cause a change in signal intensity.

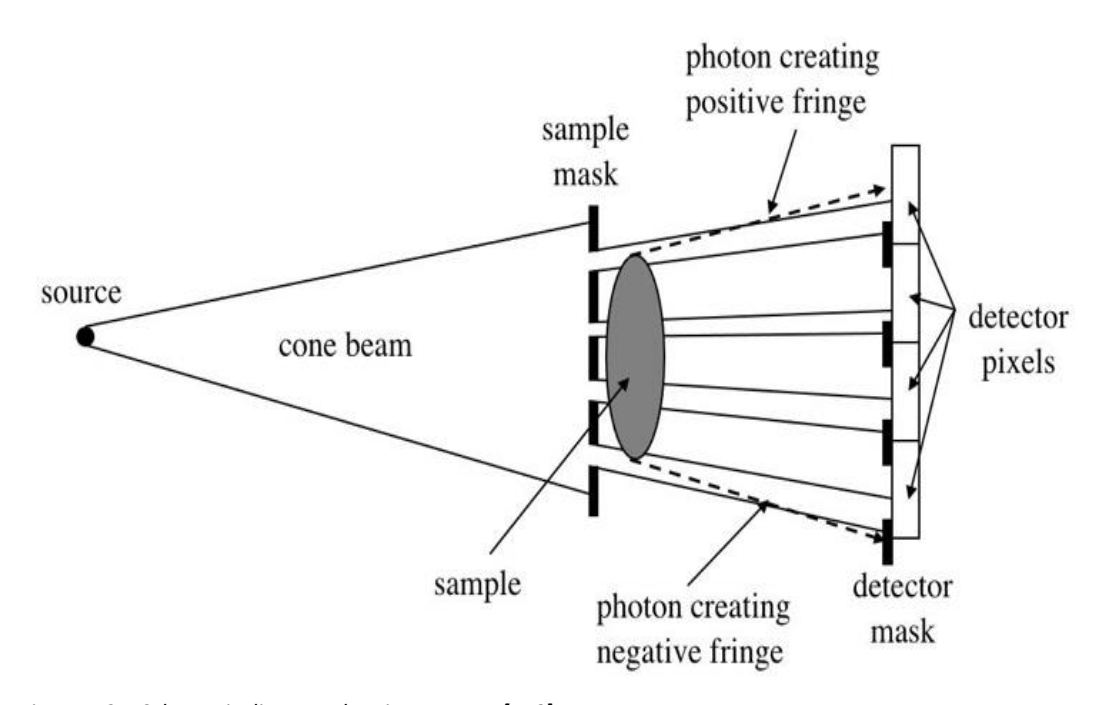


Figure 1.21: Schematic diagram showing El setup [159]

1.5.1.1.1 Masks

The masks are made from a material that is highly attenuating of x-rays, this is typically gold overlayed on a graphite substrate. The physical properties of these masks play an integral role in signal generation. Two critical measurements are the period and aperture sizes.

The apertures (the light regions in Figure 1.22 indicated by blue arrows) are gaps in the mask through which x-rays can pass. The period is the grey region (indicated by red arrows). This is the total distance between the start of two apertures.

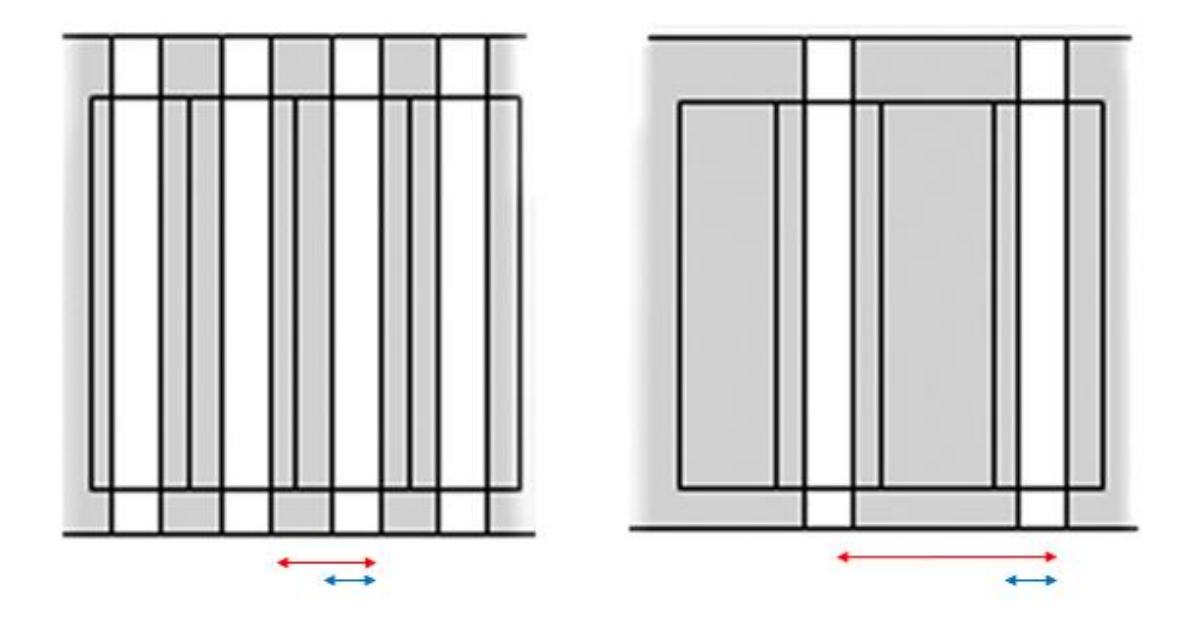


Figure 1.22: Left hand image shows a representation of a non-skipped mask; Right hand image shows a representation of a skipped mask

Two designs of paired masks are used. Non-skipped masks (Figure 1.22) are designed so that the apertures are aligned to every column of pixels on the detector. This allows every pixel to detect a signal. However, due to crosstalk between adjacent pixels this can lead to a reduction in resolution.

A second design of mask, known as a skipped mask, (Figure 1.22) has the same aperture dimensions but the period is wider. This prevents photons from hitting every other column of pixels and so eliminates crosstalk between adjacent pixels.

Using a skipped mask means smaller regions of the sample are imaged (i.e those regions through which the beamlets pass). To avoid this the sample can be moved relative to the entire setup (masks, source and detector - Figure 1.23). This allows the whole sample to be imaged in its entirety using a number of projections. This technique is known as dithering. Increasing the number of dithering steps increases the sensitivity of the setup and so increases the resolution of the images obtained.

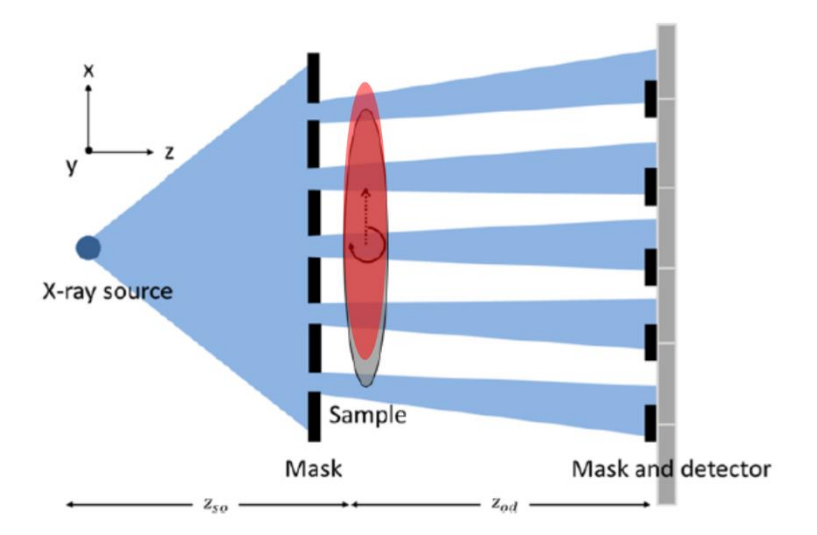


Figure 1.23: Showing dithering of a specimen. The sample is shown in two positions as it is moved relative to the setup

1.5.1.2 Free space propagation

A second XPCI technique commonly used is FSP. This uses a highly coherent source eliminating the need for any optical elements (such as masks). When x-ray waves pass through a sample they are distorted, these interfere with regions of the wave that have not passed through the sample Figure 1.24. The interference between these two regions result in regions of varying x-ray intensity which provide the signal through the detector [150]. To maximise this signal, the object-detector distance must be optimised.

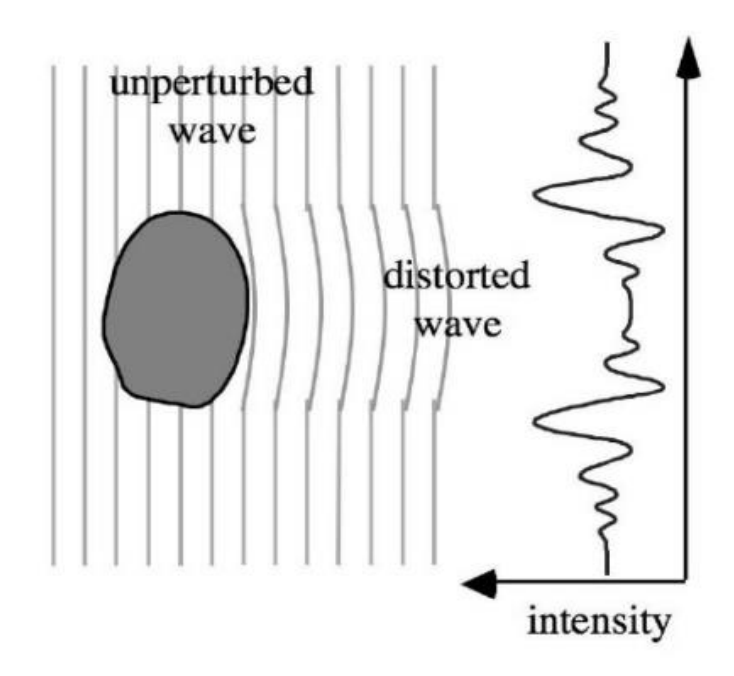


Figure 1.24: Schematic diagram showing FSP [150]

1.5.1.3 Research applications of phase contrast imaging

XPCI has been used successfully both at synchrotrons and in laboratory settings. One of the most notable pieces of research came from the Elettra synchrotron in Trieste [66]. In this unique project the team performed *in vivo* mammography with synchrotron radiation (MSR). This study included 47 patients who had equivocal results after undergoing routine clinical investigations for breast abnormalities digital mammography (DM) and ultrasound (US). Due to the increased resolution (Figure 1.25) seen in MSR the sensitivity, specificity and positive-predictive value of MSR was significantly greater than DM (sensitivity DM 0.79, MSR 0.86; specificity DM 0.53, MSR 0.95; positive predictive value DM 0.55, MSR 0.93). A further advantage of MSR is the low radiation dose each patient was exposed to due to the high x-ray energies used.

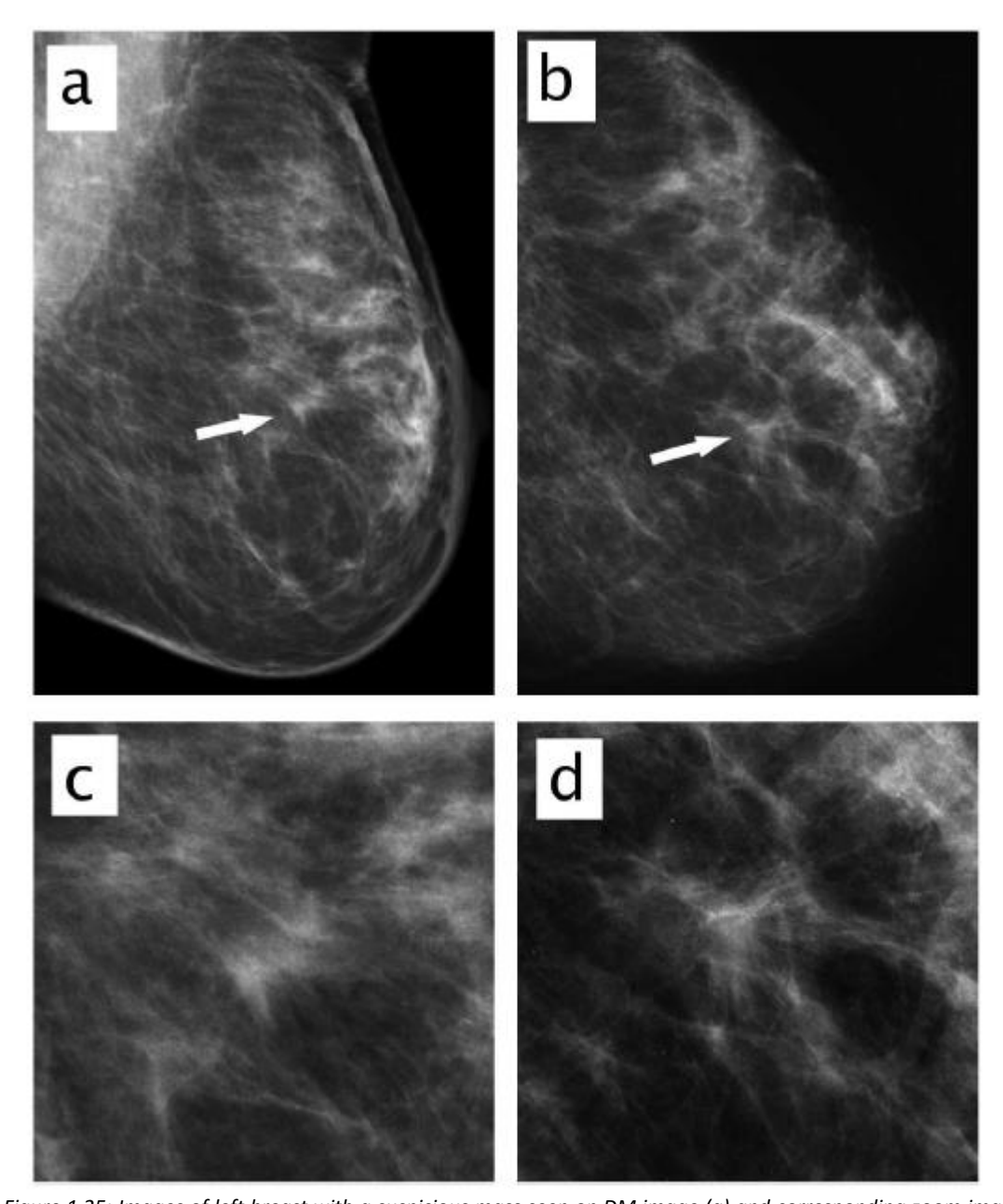


Figure 1.25: Images of left breast with a suspicious mass seen on DM image (a) and corresponding zoom image (c). MSR image (b) depicting spiculated mass more clearly and corresponding zoom image (d) [66]:

EI has been shown to detect features invisible to conventional x-rays using a laboratory x-ray source. Applications have included ability to identify small lesions in rat cartilage as well as tissue layers in decellularized rat oesophagus [160], [161]. A recent paper introduced the possibility of using EI to scan specimens intraoperatively allowing rapid detection of tumour margins [65].

FSP has been performed using synchrotrons and conventional laboratory sources.

Researchers have used this technique to a wide variety of applications. This includes identification of medicines, orthopaedic diagnosis and imaging animal tissue [162], [163], [164].

1.5.2 Synchrotron radiation

The overall quality of an x-ray beam is described by its brilliance. Several factors combine to determine this quality: firstly, the number of photons emitted per second, called flux; secondly, the distribution of the spectrum emitted; thirdly, the amount the wave of photons spreads out is known as collimation; and finally the size of the source area. Synchrotrons produce x-rays many orders of brilliance greater than conventional x-ray tubes.

Synchrotron radiation describes radiation emitted from charged particles travelling along curved pathways (Figure 1.27). Synchrotrons are cyclic particle accelerators built as research tools by governments due to their huge building costs (typically >£100 million) and large running costs. The largest particle accelerator, the Large Hadron Collider, has a \$1 billion per year operating budget. Diamond Light Source (DLS) located in Oxfordshire is the UK's national synchrotron (Figure 1.26).



Figure 1.26: Hutch at DLS, Oxfordshire

Synchrotrons use magnets to control a particle beam around a fixed loop. The particles are forced around this loop by magnets. In a synchrotron this loop is typically not a circle but is a polygon comprising of many sides. Electromagnetic radiation is emitted at each bend of the beam as the electrons are accelerated perpendicular to their velocity. In a synchrotron this is achieved by an array of magnets which allows this radiation to be controlled.

Synchrotrons produce synchrotron radiation which spans a wide frequency range from infrared to high power x-rays. This emitted radiation can be fine-tuned to a specific wavelength.

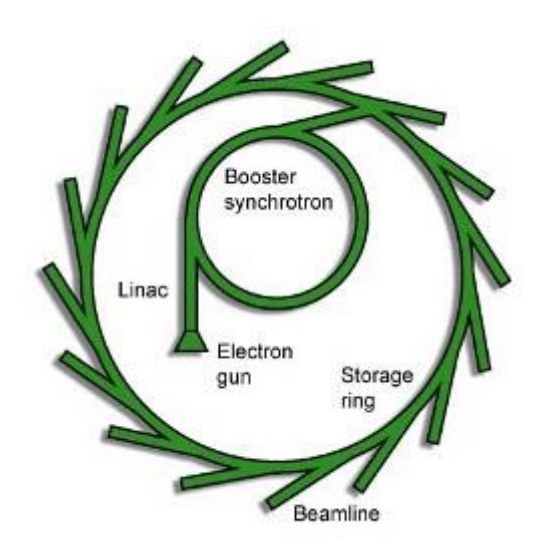


Figure 1.27: Schematic diagram of a synchrotron[165]

Synchrotrons consist of several features as seen in Figure 1.27:

 Electron gun - generates electrons it is similar to a cathode ray tube in an old television set

- Linear accelerator (LINAC) is a linear particle accelerator that accelerates the particles into the booster synchrotron
- Booster synchrotron a circular accelerator that continues to accelerate the electrons almost to the speed of light
- Storage ring maintained at a low pressure. In this ring the electrons pass through magnets which alter their path leading to radiation being emitted.
- Beamlines radiation emitted by electrons is directed toward these
 experimental halls. It is inside these that the radiation can be filtered and
 focused. The final point of these is the experimental hutch where the sample
 sits and the experiment is carried out. Different beamlines are optimised for
 specific tasks such as imaging (including XPCI), spectroscopy or
 crystallography

Chapter 2 Aims and objectives

2.1 Aim

The principal aim of this research was to assess existing technologies used in the treatment and staging of OAC and to apply a new imaging technique, namely XPCI, to both grade and stage dysplasia and invasive OAC. If successful, this would provide insight into areas of weakness in the investigation and management of OAC. Chapters 3 and 4 assess current clinical technologies. Materials and methods for XPCI are discussed in Chapter 5. This includes system setups and sample preparation. Chapter 6 and 7 address using XPCI to stage OAC and identify specific oesophageal tissue types.

2.2 Objectives

Objective 1: Following radiofrequency ablation for dysplastic Barrett's oesophagus, to explore whether the definition of CR-D and its durability are affected if the diagnosis is based on endoscopic sampling at a single time point, or from two consecutive procedures.

Objective 2: Given RFA is now such an established part of therapy are CR-D and CR-IM outcomes durable?

Objective 3: Does RFA reduce overall cancer risk after long-term follow-up?

Objective 4: For patients who have developed oesophageal cancer that penetrates deeper into the oesophageal wall, and is therefore not amenable to endoscopic therapy, how accurate is the current imaging strategy to stage the disease?

Objective 5: Can novel XPCI imaging identify if complete removal of OACs (clear margins) has been achieved and to identify the number, position and possible infiltration state of surrounding lymph nodes.

Objective 6: If it is possible to image entire oesophageal cancer specimens, can XPCI also identify more subtle abnormalities? Specifically, can it determine if the entire region of BO related dysplasia or neoplasia has been removed following endoscopic therapy, and whether it has penetrated into the submucosa?

Objective 7: Finally, given that XPCI can image tissue on multiple scales, can it differentiate four types of oesophageal tissue from biopsy samples: squamous, NDBO, dysplastic Barrett's Oesophagus (DBO) and adenocarcinoma.

Chapter 3 The UK RFA Registry

Parts of the work in this chapter have been published in *Endoscopic eradication* therapy for Barrett's esophagus-related neoplasia: a final 10-year report from the UK National HALO Radiofrequency Ablation Registry [166]. The HALO registry was setup and maintained by Professor Laurence Lovat since 2008, with ongoing contributions from 28 centres across the UK. Ash Wilson reviewed the accuracy of data entry. Professor Laurence Lovat and Dr Rehan Haidry assisted with study design and amendments. I reviewed all the raw data, conducted the preliminary and final analyses, authored the first draft and made amendments as suggested by my coauthors and reviewers.

This chapter addresses the following objectives:

Objective 1: Following radiofrequency ablation for dysplastic Barrett's oesophagus, to explore whether our understanding of the definition of CR-D and its durability are affected if the diagnosis is based on endoscopic sampling at a single time point, or from two consecutive procedures.

Objective 2: Given RFA is now such an established part of therapy are CR-D and CR-IM outcomes durable?

Objective 3: Does RFA reduce overall cancer risk after long-term follow-up?

3.1 Background

The incidence of OAC continues to rise in the Western world [11], [167] but five year survival has only shown modest improvement in the past 40 years despite advances in diagnosis and therapeutics [4]. Dysplasia arising in BO is the only known premalignant condition of OAC albeit with a low risk of progression to invasive cancer [48]. Improvement in patient access, referral pathways and ultimately endoscopic imaging have led to an increased number of patients being detected at an early stage where potentially curative intervention can be initiated. Surgery with oesophagectomy and lymph node clearance was previously the standard treatment for HGD. While this remains the intervention of choice for patients with locoregional disease, mortality and morbidity remains significant [168], [169] so over the past 20 years there has been a paradigm shift in pursuing a minimally invasive approach focused on organ preservation to treat early stage disease and avoid the adverse events related with surgery but to also deliver curative treatment. EET appears to confer a similar medium term survival rate for IMC (stage T1a) disease as oesophagectomy and is being increasingly used in older and less fit patients [170].

The initial treatment modality for early-stage oesophageal neoplasia is endoscopic resection to remove and accurately stage visible neoplasia. Several large scale series have shown short and medium-term success of this approach [171], [172]. A drawback of monotherapy is the risk of metachronous neoplasia arising in the residual metaplastic BO of up to 20% [173]. As a result, a dual EET therapeutic algorithm is now widely implemented with clearance of visible neoplastic lesions by endoscopic resection followed by field ablation of the entire BO field to remove both

neoplasia and IM. Several ablative techniques have been explored including YAG laser and APC [174] but RFA (Medtronic, USA) has gained the most traction due to high quality safety and efficacy data showing short and medium-term success and durability [132], [146] . Since the introduction of RFA in 2005, consensus has developed amongst most international societies that following endoscopic resection, field ablation with RFA is indicated to achieve clearance of disease and ensure long-term safety from progressing to invasive cancer [175], [176]. Due to the relatively recent introduction of RFA to mainstream clinical practice long-term follow up data (>5 years) is lacking. In addition, it remains unclear if a single endoscopy is sufficient to confirm treatment success.

3.2 Aims

CR-D is an endpoint for endoscopic therapy of BO. Despite this, consensus is lacking if CR-D should be measured at a single time point (one endoscopy) or two. In a 2021 systematic review [133], treatment outcomes for RFA therapy were measured using a single endoscopy in all but one of the studies included.

Objective 1: Following radiofrequency ablation for dysplastic Barrett's oesophagus, to explore whether our understanding of the definition of CR-D and its durability are affected if the diagnosis is based on endoscopic sampling at a single time point, or from two consecutive procedures.

OAC primarily arises from DBO for which endoscopic treatment is well established in the UK. This therapy, including RFA, has been ongoing for more than ten years. RFA has been shown to be efficacious with more than 80% of patients being free of dysplasia and more than 70% free of IM at the completion of therapy. There is limited long-term follow up of these outcomes.

Objective 2: Given RFA is now such an established part of therapy are CR-D and CR-IM outcomes durable?

Objective 3: Does RFA reduce overall cancer risk after long-term follow-up?

3.3 Methods

The UK RFA registry has collected data from patients being treated for dysplastic BO undergoing endoscopic therapy at 28 specialist centres across the UK. Details of these centres and entry requirement was previously described in section 1.3. Data were entered by each site initially using paper CRFs but later into a dedicated webbased database. Ethical approval was granted by the Joint UCL/UCLH Committee on the Ethics of Human Research in 2008 (REC REF 08/H0714/27) although most patients were enrolled from 2010 onwards. The UK registry is registered at ISRCTN 93069556. The ten highest recruiting sites were all subjected to further data review by the primary site.

3.3.1 Inclusion criteria

Analysis was conducted for patients in whom LGD, HGD or IMC was confirmed histologically by two expert pathologists prior to beginning EET. Patients recruited from its inception in January 2008 until January 2018 were included (Figure 3.1).

Only males and non-pregnant females over the age of 18 with no contraindications to endoscopy were considered for enrolment. All patients gave written informed consent. Patients were required to attend for treatment and surveillance procedures at regular intervals.

3.3.2 Exclusion criteria

Each analysis that was conducted had specific exclusion criteria. These are shown in Table 3.1. Thirty-eight patients in the registry had previously failed PDT an earlier type of endotherapy. These patients were excluded from all analyses. Patients were excluded from all analyses except time to invasive cancer from the start of RFA therapy if duration of follow up was less than 18 months from recruitment.

Significant data entry gaps were defined as time intervals of greater than 18 months between two consecutive endoscopies despite a patient continuing to have dysplasia or time intervals between two therapeutic endoscopies greater than 1 year prior to primary endpoints being reached. In these cases, the patient's data were censored at the endoscopy prior to the data gap for all analyses except when reviewing the time to developing invasive cancer.

Patients not from the ten highest recruiting centres were excluded from analyses except overall cancer rates due to additional data review not being possible at these sites.

Table 3.1: Showing each analysis, number of recruits included and specific exclusion criteria.

	Analysis	Number included (n)	Sites	Exclusion
1	One versus two biopsies	1,175	Ten highest recruiting centres	- PDT - <18 months f/u from time of recruitment - Significant data gaps*
2	CR-D & CR-IM** (plus recurrences; CR-D2 and CR-IM2)	1,175	Ten highest recruiting centres	- PDT - <18 months f/u from time of recruitment - Significant data gaps*
3	Whole cohort cancer analysis	2,535	All	- PDT

^{*} Significant data gaps - time intervals of greater than 18 months between two consecutive endoscopies in a patient with ongoing dysplasia; time intervals between two therapeutic endoscopies greater than 1 year prior to CR-D or CR-IM being achieved

^{**} Some additional data was collected prior to this completion to extend follow-up time for this cohort

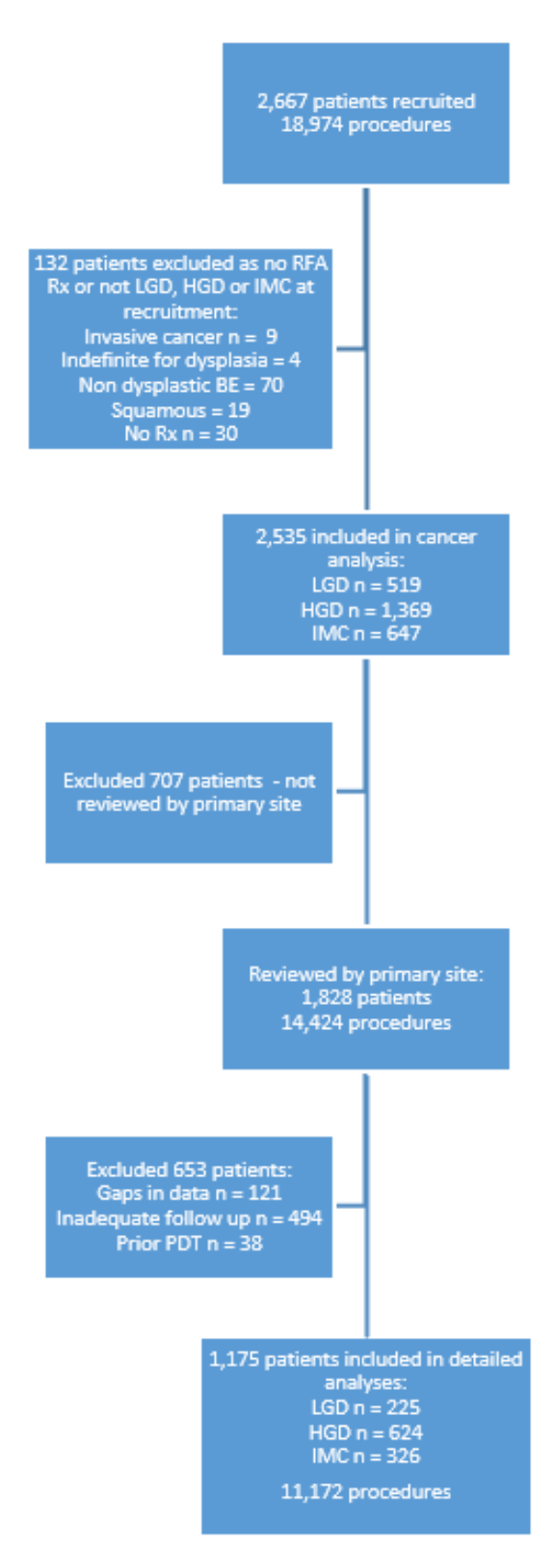


Figure 3.1: Flow diagram indicating included and excluded patients. Of the patients 132 excluded for not having had treatment or not having LGD, HGD or IMC prior to treatment, 9 had proven invasive cancer prior to therapy, 30 never had RFA therapy and the remaining 93 excluded had no confirmed evidence of having dysplasia.

3.3.3 Data analysis

The data was primarily analysed using Microsoft Excel (Excel 2010, Microsoft, Redmond, Wash). This includes all time-dependent data Kaplan-Meier survival analysis with Log Rank test. Supplementary analyses were conducted using R Studio (R Studio 1.2.1335; R Studio PBC, Boston, MA) and GraphPad Prism (GraphPad Prism version 9.2.0 for Windows, GraphPad Software, San Diego, California USA, www.graphpad.com). Data were assessed for normality, following which parametric or non-parametric tests were applied.

To allow automation of the analyses the worksheets required modification from their standard form. This was a complex task but can be summarised into several stages.

Also, this served to assist with identifying data entry errors and gaps.

3.3.3.1 Data download and worksheet setup

The output from the database exported data to two spreadsheets – one containing procedure data ("doctor_procedure") and the other containing patient specific details at the time of enrolment ("doctor_patients"). In order to complete the required data analyses these sheets needed to be linked and to export the data to a third sheet ("Patient level data") (Figure 3.2).

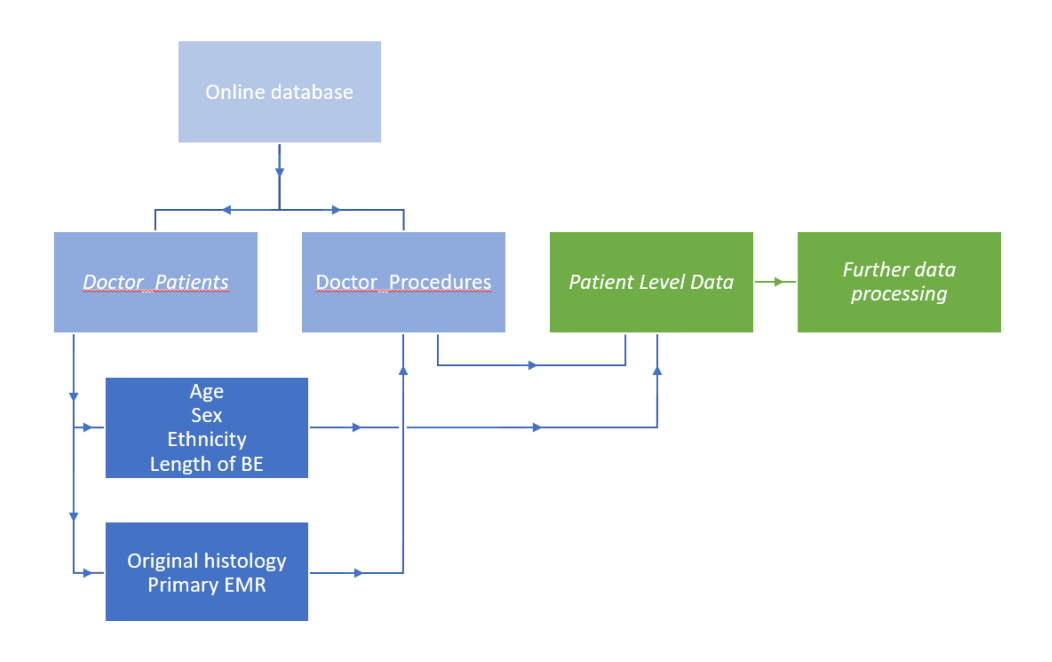


Figure 3.2: Flow diagram illustrating data outputs, linking and processing

3.3.3.2 Initial data organisation

The first step was to order the datasheet containing procedure specific data according to patient ID and date of procedure. All procedures were then numbered for each specific patient and given a unique identifier (e.g "PatientID_ProcedureNumber"; "2_1"). This allowed automated calculation of time intervals between procedures or therapy, cumulative time from the start of therapy or from endpoints, identification of first therapeutic procedure, number of procedures or ablations and identification of significant data gaps.

Multiple data entry points needed to be linked from the "doctor_patients" output sheet (Figure 3.2). This included initial histology, demographic details (age, sex and ethnicity) and if primary EMR had been performed.

3.3.3.3 Histology grade identification

After the initial histology at recruitment was linked, the highest-grade histology prior to therapy was identified. This was used to categorise patients into cohorts with IMC, HGD or LGD.

Each procedure had a histology grade assigned to it. If no histology was taken at a procedure or if the histology was reported as "indefinite for dysplasia" the histology from the preceding procedure was presumed to still be present. If "invasive cancer" was listed as the histological subtype but the patient went on to have successful endotherapy, "invasive cancer" was recategorized to "IMC".

3.3.3.4 Therapy

All procedures involving endoscopic therapy were identified and placed into one of 4 categories:

- 1) Endoscopic resection EMR or ESD
- 2) RFA -H360, H90, Halo 60, TTS RFA catheter, Halo Ultra
- 3) Other ablative therapy YAG laser, APC
- 4) Dilatation

3.3.3.5 Identification of CR-D and CR-IM

Algorithms were introduced into the worksheet to identify procedures as either achieving an endpoint, not achieving an endpoint or being equivocal. Equivocal procedures were identified in the event that there was insufficient evidence to

confirm an endpoint being reached, i.e. in the event of no biopsies being taken (Figure 3.3).

Specific rules were introduced at this point for endpoints according to the definitions used for CR-D and CR-IM.

- CR-D
 - o Biopsies clear of dysplasia
- CR-IM
 - Residual BO tongues measuring less than 3cm and the absence of IM
 (if BO >3cm in length presence of IM is assumed)
 - o COMO BO and presence of IM (IM of the GOJ)

Using this categorisation of each procedure, a status for each subject was given at every procedure. This identified subjects at each procedure as undergoing treatment, clear of dysplasia or IM, or having had recurrence of IM or dysplasia. For CR-D this processing was completed twice, using either histology from one endoscopy to confirm end points or including histology from two consecutive endoscopies to confirm endpoints.

When using two consecutive endoscopies to confirm endpoints the time to reach CRD was calculated to the first of the two procedures that initially identified successful treatment (see example patient 1 - Figure 3.3). This was performed to allow direct comparison between the two methods. For both methods recurrences were identified after a single procedure of recurrence.

3.3.3.6 Worked examples

Procedure	Procedure status	Patient status - One	Patient status - Two	Procedure	Procedure status	Patient status - One	Patient status - Two
		biopsy method	biopsy method			biopsy method	biopsy method
1	HGD	Ongoing Rx	Ongoing Rx	1	HGD	Ongoing Rx	Ongoing Rx
2	HGD	Ongoing Rx	Ongoing Rx	2	HGD	Ongoing Rx	Ongoing Rx
3	HGD	Ongoing Rx	Ongoing Rx	3	Equivocal (no biopsy)	Ongoing Rx	Ongoing Rx
4	No dysplasia	CRD	CRD	4	HGD	Ongoing Rx	Ongoing Rx
5	No dysplasia	Remission	Remission	5	No dysplasia	CRD	Ongoing Rx
6	No dysplasia	Remission	Remission	6	Equivocal (no biopsy)	Remission	Ongoing Rx
				_	uco	I - CONTRACTOR CONTRACTOR	
				7	HGD	Recurence	Ongoing Rx
				8	No dysplasia	CR-D2	CRD CRD
Example Pa	tient 2			7 8 9			
Example Pa		Patient status - One	Patient status - Two	7 8 9	No dysplasia	CR-D2	CRD
Example Pa Procedure	Procedure status	Patient status - One biopsy method	Patient status - Two		No dysplasia Equivocal (no biopsy)	CR-D2 Remission	CRD Remission
					No dysplasia Equivocal (no biopsy)	CR-D2 Remission	CRD Remission
Procedure 1	Procedure status	biopsy method	biopsy method		No dysplasia Equivocal (no biopsy)	CR-D2 Remission	CRD Remission
Procedure 1 2	Procedure status	biopsy method Ongoing Rx	biopsy method Ongoing Rx		No dysplasia Equivocal (no biopsy)	CR-D2 Remission	CRD Remission
Procedure 1 2 3	Procedure status HGD HGD	biopsy method Ongoing Rx Ongoing Rx	biopsy method Ongoing Rx Ongoing Rx		No dysplasia Equivocal (no biopsy)	CR-D2 Remission	CRD Remission
	Procedure status HGD HGD No dysplasia	biopsy method Ongoing Rx Ongoing Rx CRD	Diopsy method Ongoing Rx Ongoing Rx Ongoing Rx		No dysplasia Equivocal (no biopsy)	CR-D2 Remission	CRD Remission

Figure 3.3: Example patients to illustrate the effects of using one biopsy vs two biopsies

3.3.3.6.1 Example patient 1:

This patient achieves CR-D at the 4^{th} procedure using the one biopsy method. Using the two-biopsy method CR-D is not confirmed until the 5^{th} procedure but is counted from the 4^{th} procedure to allow direct comparison.

3.3.3.6.2 Example patient 2:

Using the one biopsy method this patient achieves CR-D at the 3rd procedure but immediately has recurrence at the 4th procedure as there is evidence of dysplasia. At the 5th procedure CR-D2 is achieved as there is no evidence of dysplasia.

Using two biopsies to confirm absence of dysplasia means that although the 3rd procedure has no evidence of dysplasia this is not identified as CR-D as the fourth procedure is not clear of dysplasia. CR-D is achieved at the 5th procedure as both this and the 6th procedure show no evidence of dysplasia.

3.3.3.6.3 Example patient **3**:

This patient shows the effect of procedures being identified as equivocal. The 3rd and 6th procedures are identified as equivocal therefore the status of the patient is continued. Crucially as the 9th procedure is equivocal this is not used to confirm CR-D (using the two biopsy method). The 10th procedure is when CR-D is confirmed but CR-D is counted from the 8th procedure as this was the first of the two procedures that identified successful treatment.

3.3.3.7 Outputs

Once endpoints were identified this enabled calculation of further clinical information such as time to endpoint, number of therapeutic procedures, nature of therapy and follow-up time.

3.3.3.8 Time to CR-D and CR-IM

One of the issues identified when analysing the data was patients achieving CR-D and CR-IM after extended period of therapy. Often these patients were having intermittent treatment (one ablative therapy/year) or had even stopped therapy entirely. The number of patients reaching CR-D and CR-IM at set time points is shown below in Table 3.2.

Table 3.2: Showing number of patients reaching CR-D and CR-IM within specific time frames from the start of RFA treatment. The 24-month cut off applied is highlighted in yellow.

	CR-D		CR-IM	
Months	Number of	Additional	Number of	Additional
of	patients	patients included	patients	patients included
therapy	reaching	relative to	reaching	relative to
	endpoint	previous time cut	endpoint	previous time cut
		off		off
15	898		328	
18	980	82	488	160
21	1014	34	628	140
24	1031	17	729	101
30	1054	23	877	148
36	1058	4	923	46

To limit the effect of this a 24-month cut off was applied (shown in yellow) from commencement of therapy to this cohort. This ensured the recurrence data reflected typical modern practice.

3.4 Results

Please note these analyses were performed at different times with slight variations in the dataset. For example, additional data was collected prior to data analysis of CR-D, CR-IM and subsequent recurrences.

3.4.1 Objective 1: One versus two biopsies

3.4.1.1 Clearance of dysplasia

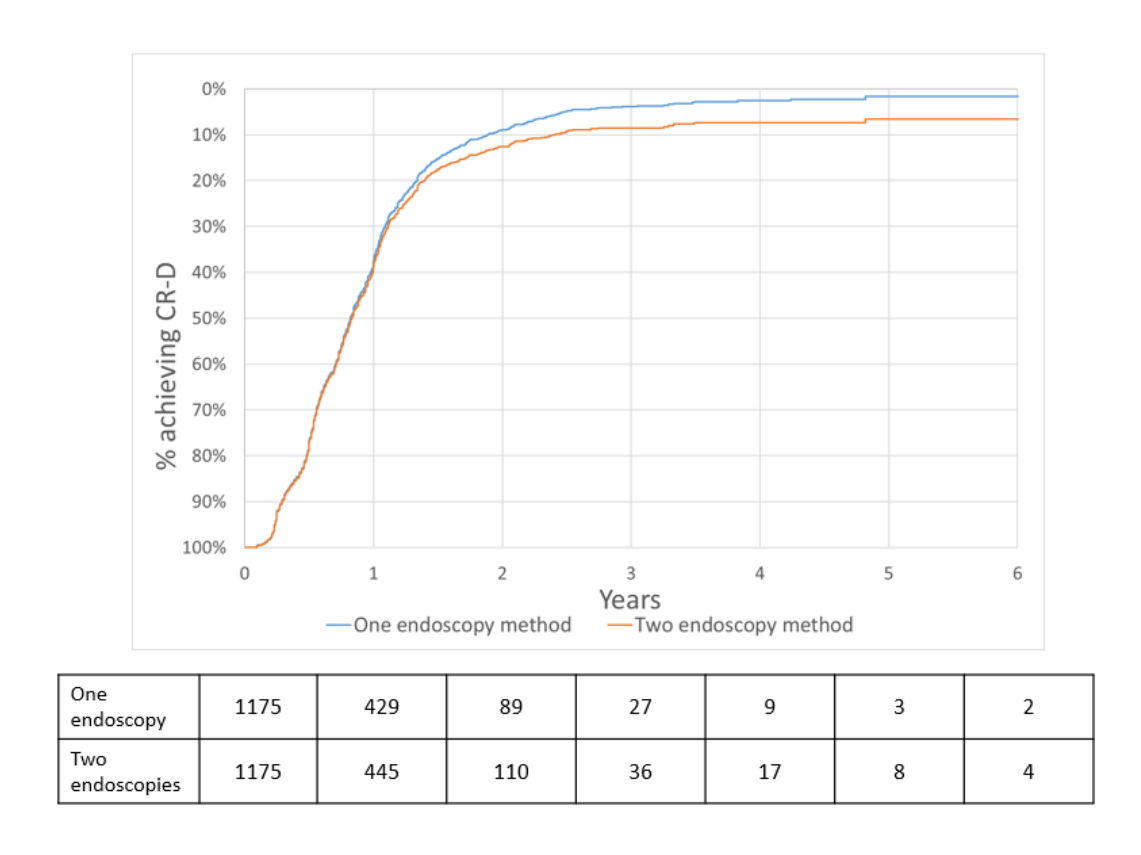


Figure 3.4: Kaplan Meier graph showing rate of CR-D using the one biopsy method and the two-biopsy method. Log rank score = 0.018.

As Figure 3.4 shows there is a significant difference between the rate of CR-D when using one biopsy or two biopsies (Log rank score = 0.018). The Kaplan Meier rate of CR-D for the whole cohort was 63.3% using one endoscopy and 62.2% using two consecutive endoscopies at 1 year, 91.1% using one endoscopy and 87.4% using two consecutive endoscopies at 2 years and 99.2% using one endoscopy and 95.6% using two consecutive endoscopies at 6 years.

3.4.1.2 Recurrence of dysplasia from clearance of dysplasia

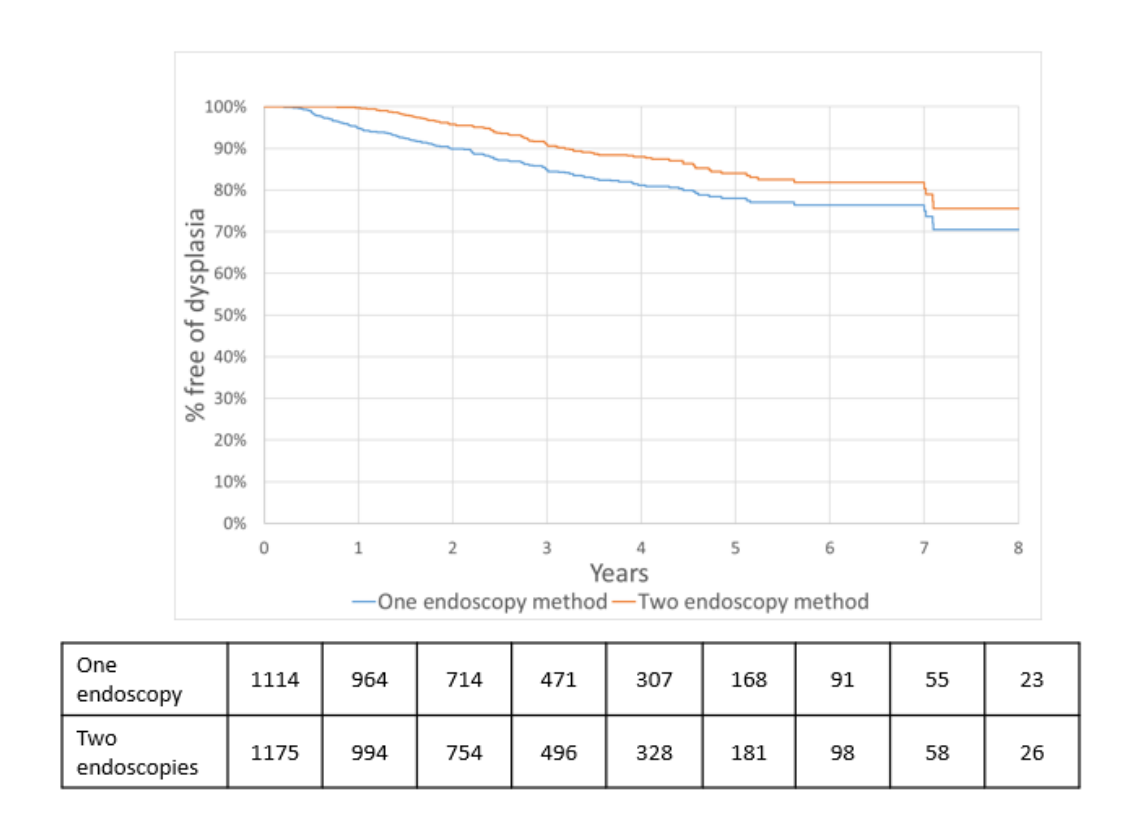


Figure 3.5: Kaplan Meier graph showing rate of recurrence of dysplasia from CR-D patients achieving CR-D using both one biopsy and two biopsy methods. Log rank score p=2.58E-05.

As Figure 3.5 shows there is a significant difference between the rates of recurrence of dysplasia from CR-D when comparing those that achieved CR-D using both the one and two consecutive endoscopies methods (Log rank score P<0.00001). The Kaplan Meier rate of recurrence of dysplasia from CR-D when using the patients that had achieved CR-D using one endoscopy was 5.2% after one year, 10.1% after two years and 29.5% after 8 years. For the patients that achieved CR-D using two consecutive endoscopies the rate of recurrence of dysplasia was 0.3% after one year, 4.2% after two years and 24.4% after 8 years.

The difference between these two KM curves becomes nearly fully established within 2 years of patients achieving CR-D (Figure 3.6). This suggests that this significant

D. In this two-year period there are 100 recurrences using the one endoscopy method compared with 38 in the two consecutive endoscopies method. The absolute difference in recurrences between the two methods reaches 62 by the end of the second year. This difference remains stable between 62 and 67 for the remainder of the follow-up period.

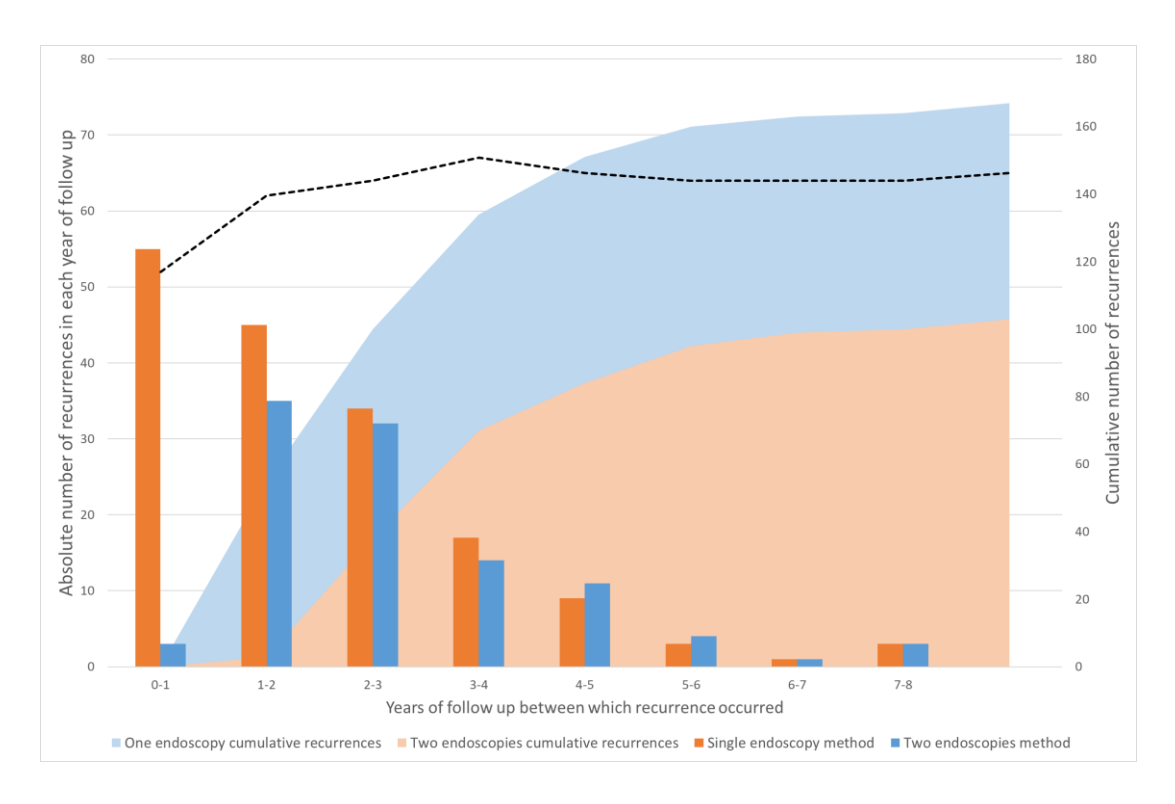


Figure 3.6: Graph showing absolute number of recurrences of dysplasia from CR-D and cumulative recurrences from CR-D per year of follow up for the one biopsy and two biopsy methods. Black trendline indicates the difference in the cumulative number of recurrences of dysplasia from CR-D between the two methods.

3.4.1.3 Discussion

By using these two methods to calculate survival curves and performing a $\chi 2$ analysis I was able to show a statistically significant difference in the results (Figure 3.4 & Figure 3.5). These indicate using a single endoscopy to confirm CR-D leads to significantly higher clearance rates (p value = 0.018) when compared with the two

consecutive endoscopies method. However, the recurrence rate of dysplasia from CR-D was significantly different (P<0.00001). This suggests that using a single endoscopy to confirm a treatment endpoint is a less reliable method than two consecutive endoscopies for confirming a clinical endpoint. This serves to reduce early recurrences.

It is widely understood that surveillance with or without Seattle protocol biopsies carries risk of missed pathology especially in longer BO segments[177]. Using histology from two consecutive endoscopies reduces this risk and provides more accurate staging of disease. This accuracy is vital when a patient is moved from a treatment pathway to interval surveillance.

3.4.2 Objective 2: Detailed analyses

The demographic data for all patients from sites that were included in the detailed analyses is shown in Table 3.3: Demographic and outcome data of all 1,175 patients with BO included in CR-D and CR-IM analysis of UK HALO RFA registryTable 3.3. These analyses were all performed using the two-biopsy method. Prior to therapy, LGD was the highest histological grade for 225 patients, HGD for 624 patients and IMC for 326 patients. The mean length of BO segment was 5.2cm (range, 1-20cm).

Table 3.3: Demographic and outcome data of all 1,175 patients with BO included in CR-D and CR-IM analysis of UK HALO RFA registry

Variable	Value
No. of Patients	1,175
Age, y	
Mean ± SD	67.2 ± 9.4
Range	37.7-90.8
Sex, n (%)	
Male	970 (83)
Female	205 (17)
Ethnicity, n (%)	
White	1,094 (93)
Missing data	81 (7)
Histological grade at study entry, n (%)	
LGD	225 (19)
HGD	624 (53)
IMC	326 (28)
Length of BO: C (Prague Classification), cm,	3.2 ± 3.6 (0-19)
mean ± SD (range)	
Length of BO: M (Prague Classification), cm,	5.2 ± 3.4 (1-20)
mean ± SD (range)	
Received primary EMR (prior to RFA), n (%)	
Yes	646 (55)
No	529 (45)

3.4.2.1 Clearance of dysplasia

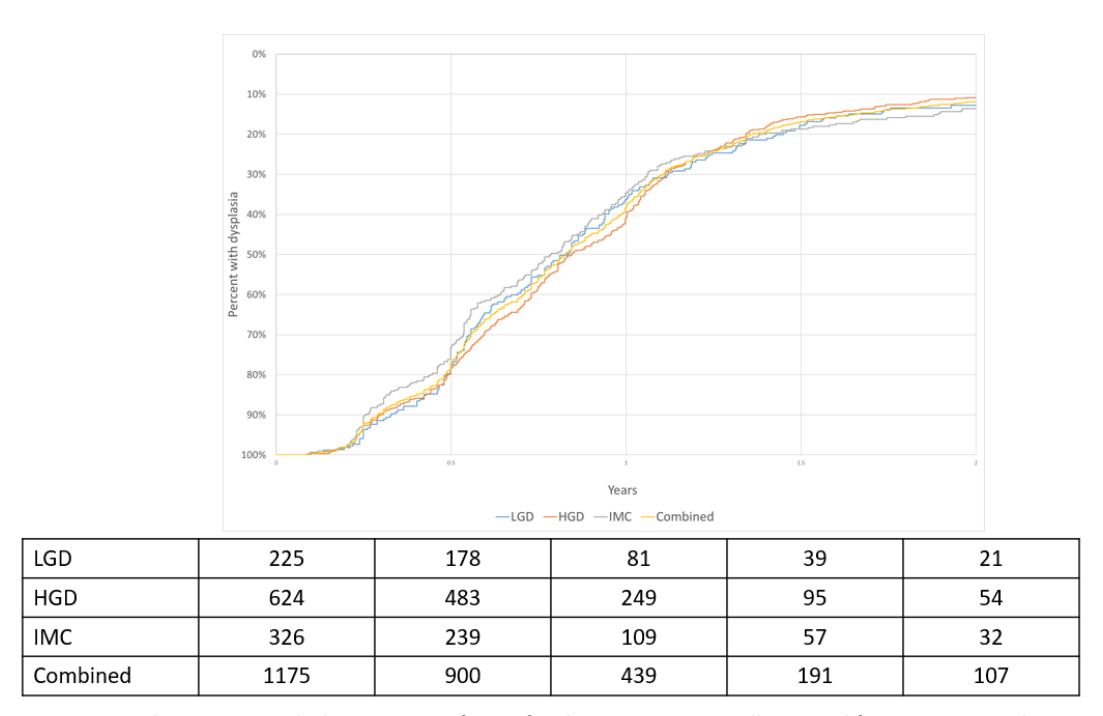


Figure 3.7: Kaplan Meier graph showing rate of CR-D for those patients initially treated for LGD, HGD and IMC.

Within 24 months of initiating EET 1031/1175 patients (88.0%) achieved CR-D. There was no significant difference in remission rates by initial disease severity with LGD achieving 87.2%; HGD, 89.1% and IMC, 86.4% (Log Rank p = N.S.).

Younger patients were significantly more likely to achieve CR-D with mean age 66 years (95% CI 66 - 67 years) vs 69 years (95% CI 67 - 71 years) for those that did not (unpaired two tailed t test p = 0.003). Patients with shorter Barrett's segments also had a higher clearance of dysplasia, median initial maximum length 4cm (IQR 2-7 cm) vs 7cm (IQR 4- 10 cm) where dysplasia remained (Mann-Whitney U test p < 0.0001).

The mean number of ablations was 3.15 (95% CI 3.04 - 3.25) for the whole cohort, 2.83 (95% CI 2.75 - 2.91) for those achieving CR-D and 5.42 (95% CI 4.95 - 5.89) for those not achieving CR-D.

3.4.2.2 Recurrence of dysplasia from clearance of dysplasia

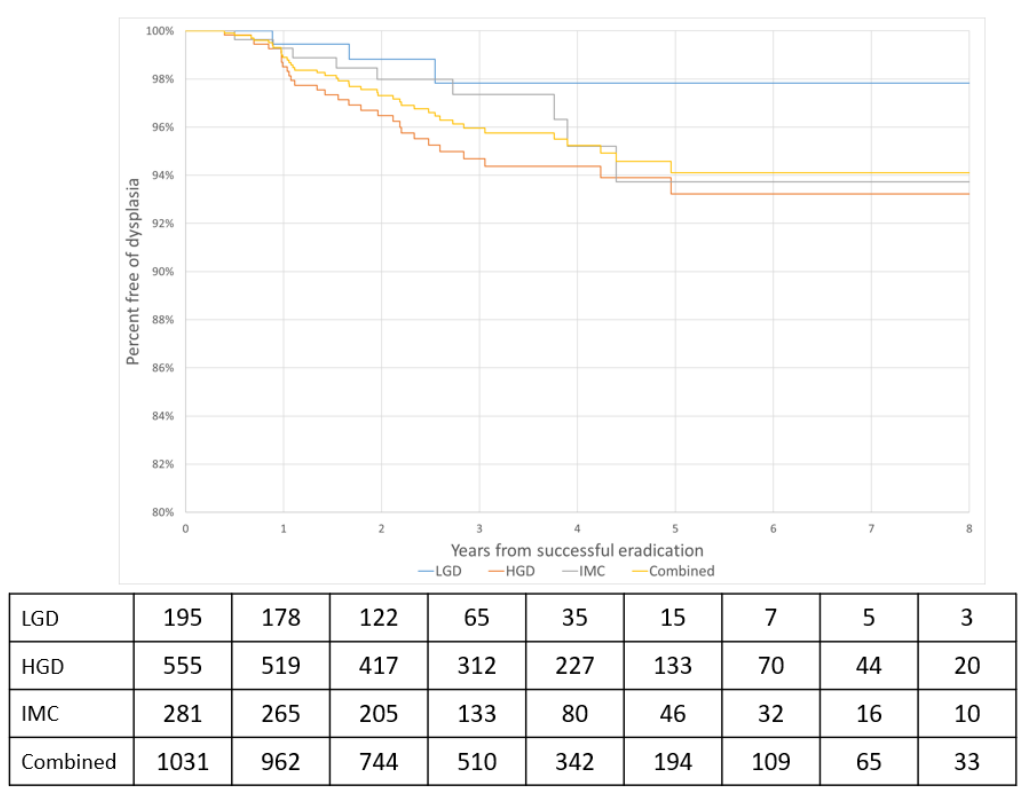


Figure 3.8: Kaplan Meier graph showing rate of recurrence of dysplasia from CR-D for those patients initially treated for LGD, HGD and IMC. Log rank score between IMC and LGD p = 0.4. All other comparisons Log Rank Score p = N.S. Please note that the y axis is truncated at 80% for ease of viewing.

The Kaplan Meier rate of recurrence of dysplasia from CR-D for the whole cohort was 1.1% at 1 year, 2.7% at 2 years and 5.9% at 8 years. There was no difference by histological subtype with 0.5% at 1 year for LGD patients, 1.5% HGD and 0.7% for patients treated for IMC (Figure 3.8). At 2 years the recurrence rates were 1.2%, 3.5% and 2.0% respectively which increased to 2.2%, 6.8% and 6.3% after 8 years. Log Rank Score showed a significantly higher recurrence rate for patients with IMC than LGD

(p = 0.04) but there was no statistically significant difference between any of the other groups.

Dysplasia recurrence rates were not related to patient age or initial length of BO. Mean age of those relapsing from CR-D was 67 years (95% CI 65-70 years) vs 66 years (95% CI 66-67 years) for those that did not (unpaired two-tailed t-test p=0.51). Median initial maximum length of BO for those in whom dysplasia recurred was 5cm (IQR 3-8 cm) vs 4cm (IQR 2-7 cm) for those that did not (Mann-Whitney U test p=0.18). Most recurrences (34/41, 82.9%) occurred within three years.



Figure 3.9: Highlighting the time intervals of follow-up compared. Red arrow indicates the first time interval. Green arrow shows the second time interval.

To ensure the high rate of recurrences was not due to fewer surveillance endoscopies after 3 years of follow up I reviewed the number of procedures within three years of achieving CR-D (Figure 3.9). This was compared to the number of procedures in subsequent follow up. Within the first 3 years of follow up the median number was 5 procedures (IQR 4-6) compared with 1 procedure (IQR 0-2) from the end of this 3-year time period to the end of follow-up. There were 2,802 procedures within the first three years of follow up versus 821 procedures in subsequent years. Within the first 3 years of follow up the number of procedures per year was 1.06 procedures/year versus 0.79 procedures/year in subsequent follow up. The number

of recurrences/procedure/year remained substantially higher within 3 years of follow up at 32.1 vs 8.9 in subsequent follow up.

3.4.2.3 Clearance of dysplasia after recurrence (CR-D2)

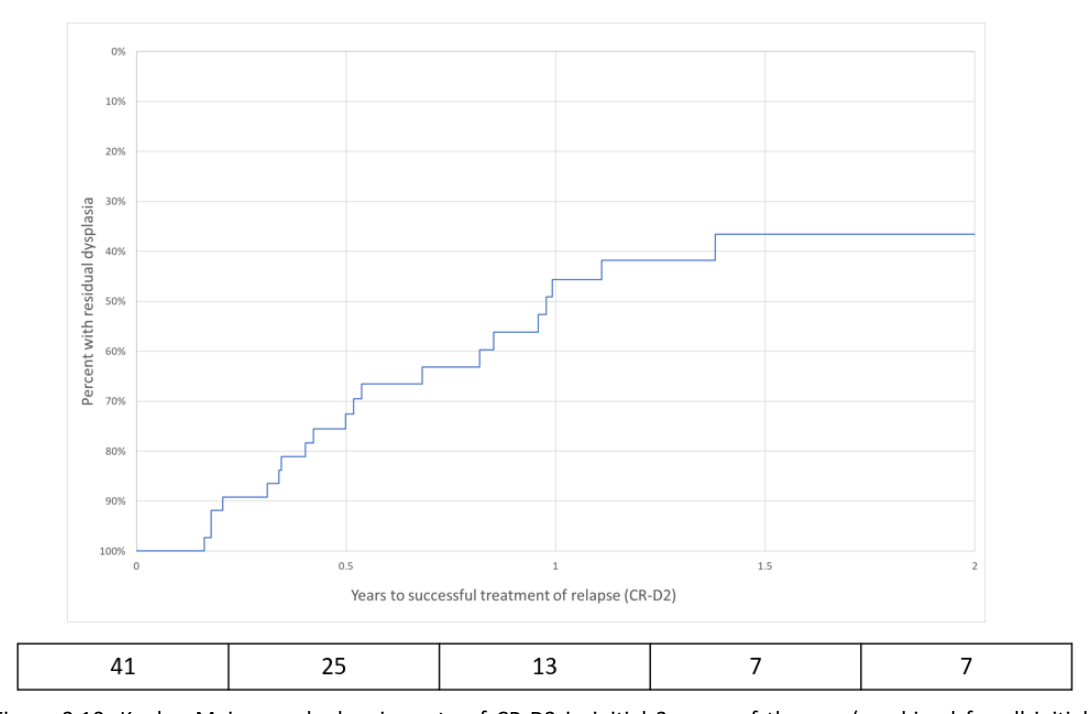
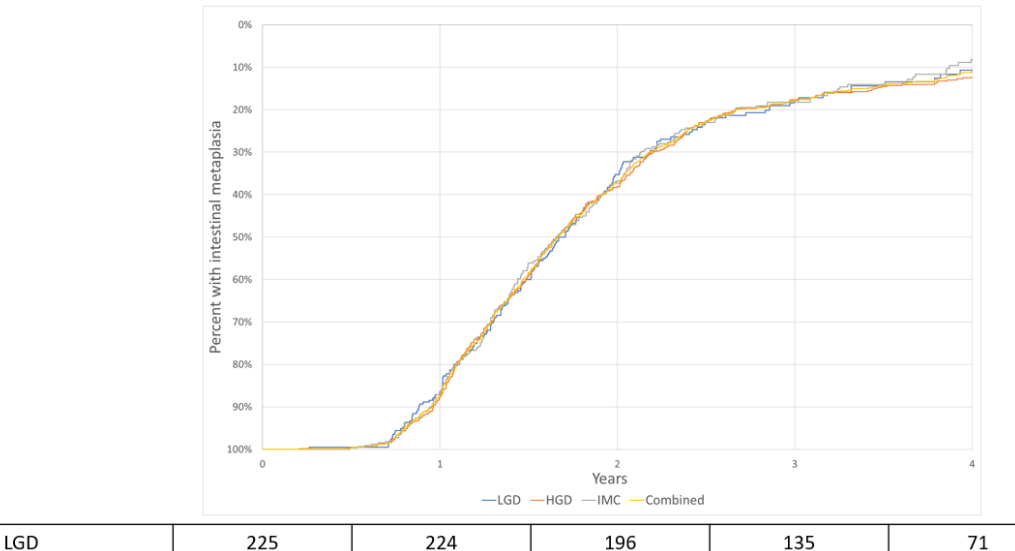


Figure 3.10: Kaplan Meier graph showing rate of CR-D2 in initial 2 years of therapy (combined for all initial histology types).

For patients who were initially successfully treated and then had recurrence of dysplasia, CR-D2 was achieved in 54.4% after 1 year and 63.4% after 2 years (Figure 3.10). In this relatively small group of patients, none of those successfully achieving CRD-2 developed invasive cancer during follow-up.

3.4.2.4 Clearance of intestinal metaplasia



HGD IMC Combined

Figure 3.11: Kaplan Meier graph showing rate of CR-IM for those patients initially treated for LGD, HGD and IMC.

Within two years of starting therapy, 729/1175 (62.7%) patients achieved CR-IM. Initial disease severity did not affect this, with CR-IM achieved by 65.2% of LGD patients; HGD, 62.0% and IMC, 63.5% (Log Rank p = N.S.). After four years of therapy, 971/1175 (82.6%) patients achieved CR-IM. When separated by histological subtype CR-IM was achieved by 89.3% of LGD patients, 87.8% of HGD patients and 91.9% IMC patients (Log Rank p = N.S.).

CR-IM was more likely in younger patients and those with shorter lengths of BO, 4cm (IQR 2-6 cm) vs 6cm (IQR 3-8cm) (Mann-Whitney U test p <0.0001). Age did not impact the likelihood of CR-IM. The mean age for those achieving CR-IM was 66 years (95%CI 66-67 years) vs 67 years (95%CI 66-68 years) for those not achieving CR-IM (unpaired two -tailed t test p = 0.08).

3.4.2.5 Recurrence of intestinal metaplasia (IM) from clearance of intestinal metaplasia (CR-IM)

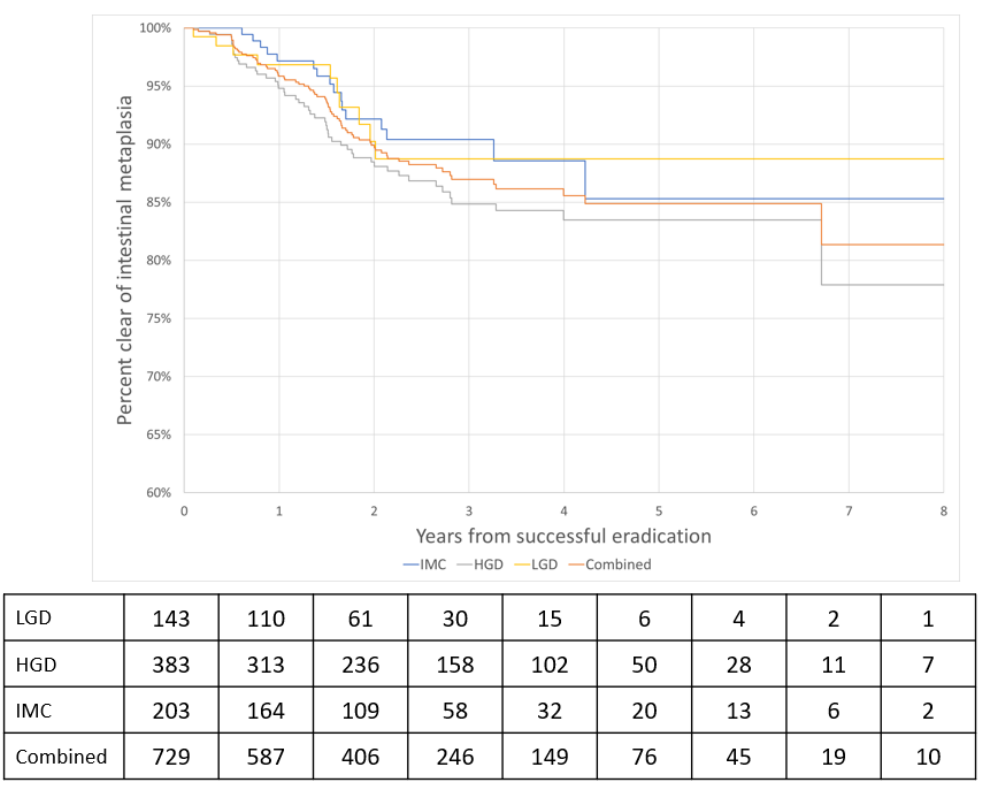


Figure 3.12: Kaplan Meier graph showing rate of recurrence of IM from CR-IM for those patients initially treated for LGD, HGD and IMC. Initial disease severity did not affect rates of CR-IM. Please note that the y axis is truncated at 60% for ease of viewing.

The rate of recurrence of IM from CR-IM for the whole cohort was 4.2% at 1 year, 10.1% at 2 years and 18.7% at 8 years. The rate of recurrence at one year was 3.2% in patients with LGD; 5.2% in HGD and 2.8% in IMC patients (Figure 3.12). At 2 years the recurrence rates were 9.8%, 11.9% and 11.4% respectively which increased to 11.3%, 22.1% and 14.7% after 8 years. The rate of recurrence was significantly higher for patients who originally presented with HGD than LGD (Log Rank p = 0.004) but there was no significant difference between IMC and HGD (Log Rank p = 0.481) or IMC and LGD (Log Rank p = 0.907).

There was also no significant difference in age or length of BO prior to RFA of those that had a recurrence of IM and maintained remission from CR-IM at 66 years (95% CI 63-68) vs 66 years (95% CI 66 – 67 years, unpaired t-test p = 0.70). Similarly, the initial median maximum length of BO was identical at 4cm (IQR 2.25-6.75cm) vs 4cm (IQR 2-6cm, Mann-Whitney U test p 0.45). Although age and length of Barrett's segment were not predictors of recurrence of IM, 78.4% of patients with recurrence of IM did so within two years (n=74).

3.4.2.6 Clearance of Intestinal Metaplasia after a previous recurrence (CR-IM2)

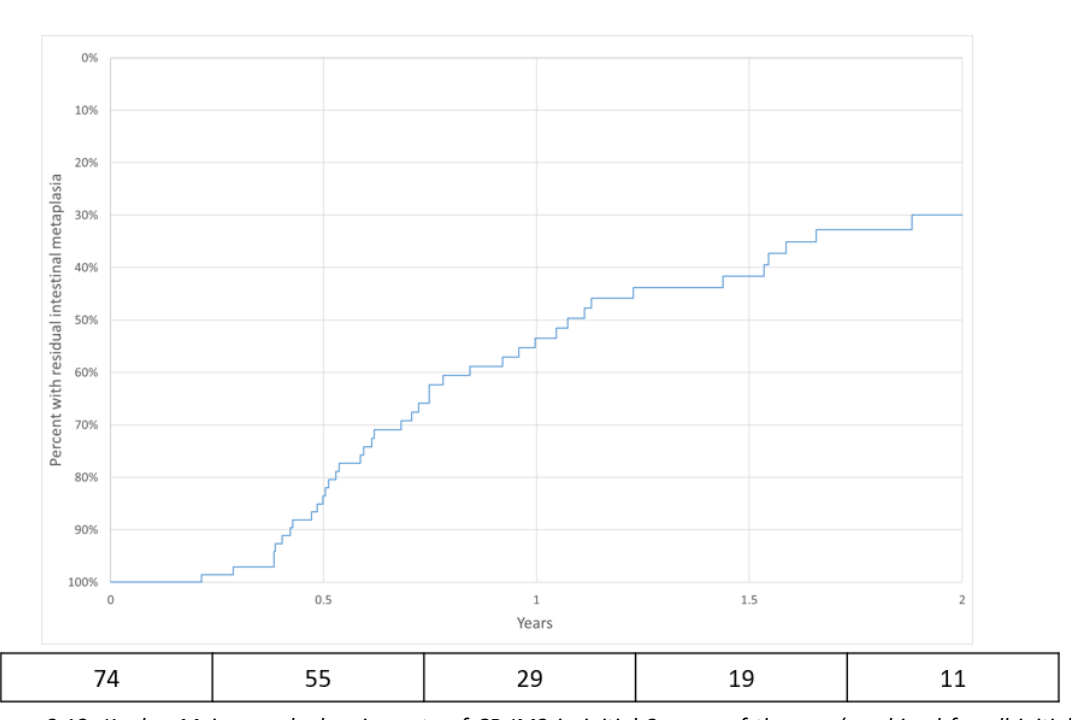


Figure 3.13: Kaplan Meier graph showing rate of CR-IM2 in initial 2 years of therapy (combined for all initial histology types).

For patients that had recurrence of IM (n=74) the rate of CR-IM2 following further treatment was 46.5% after 1 year and 70.0% after 2 years (Figure 3.13).

3.4.2.7 Primary EMRs, Dilatations and rescue therapy

Primary EMR (EMR prior to any RFA therapy) was performed in 646/1175 (55.0%) of patients. The rate of CR-D at 24 months was unchanged at 87.6% versus 88.1% (X² p=0.80) for patients without primary EMR, but rescue therapy was much more likely if an EMR had been done before RFA started at 41.2% versus 17.2% (X² p<0.00001).

Rescue therapy (EMR, APC or YAG laser) during or after reaching CR-D was required by 360 patients (30.6%) and primarily consisted of EMRs (n=351). CR-D was achieved in 287 patients (79.7%). Compared to the patients not having rescue therapy (n=815, 69.4%) where the overall CR-D was 91.4%. CR-D was significantly lower in the group that required rescue therapy (X^2 p<0.001).

During and following EET, 144 (12%) patients required one or more dilatations; 68 required one, 25 required 2 and 51 required more than 2 dilatations.

Median number of ablations per centimetre of BO rose with disease severity. Patients with LGD had 0.80 ablations/cm BO, HGD 1.00 ablations/cm and IMC 1.19 ablations/cm BO. (p<0.0001, Wilcoxon signed rank test). The number of EMRs/cm of BO was also proportional to initial disease severity: LGD 0.08 EMRs/cm BO, HGD 0.24 EMRs/cm BO and IMC 0.45 EMRs/cm BO (p<0.001, Wilcoxon signed rank test).

The number of ablative procedures per cm of BO was higher for patients achieving CR-D (1.00 vs 0.64, Wilcoxon signed rank p <0.001). The same was true for those reaching CR-IM (1.37 ablations/cm BO vs 0.83, Wilcoxon signed rank p <0.001).

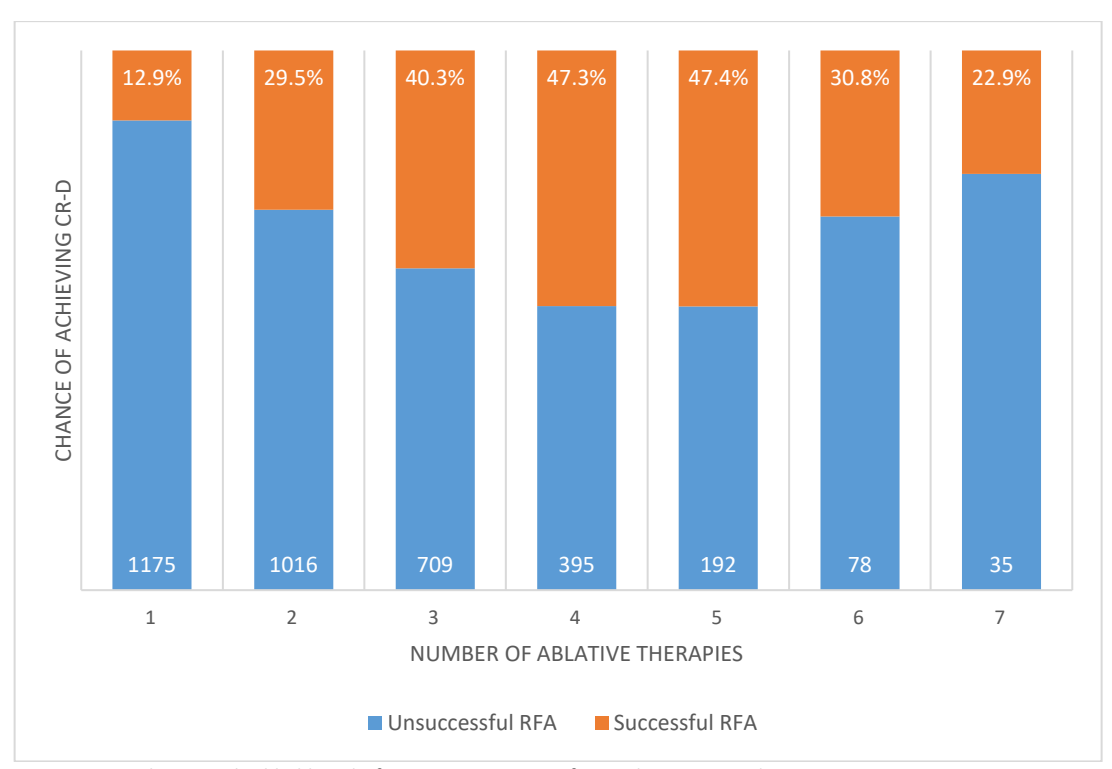


Figure 3.14: Showing the likelihood of treatment success for each RFA procedure.

I calculated the chance of each successive RFA procedure achieving CR-D if this had not yet been achieved. After a single RFA procedure CR-D occurred in 12.9%. Procedural success rose progressively for each procedure until the 5th where it reached 47.4% of patients still being treated (Figure 3.14). Subsequently, the chance of each successive ablation leading to CR-D reduced.

3.4.3 Objective 3: Invasive cancer

One year after patients had started RFA therapy the Kaplan Meier rate of invasive cancer in the entire cohort of 2535 patients was 0.5%. After 2 years follow up this was 1.2% and at ten years was 4.1% (Figure 3.15).

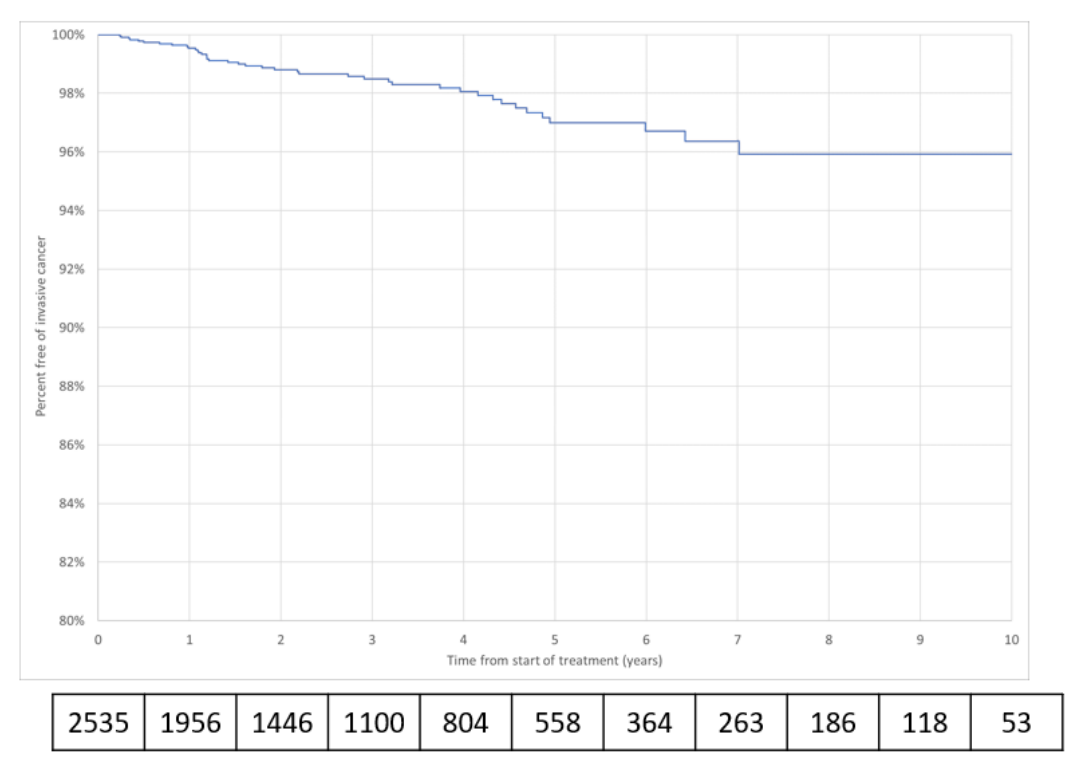


Figure 3.15: Kaplan Meier graph of entire cohort showing rate of invasive cancers at 10 years from the start of treatment in patients treated with RFA. The y axis is truncated at 80% for ease of viewing.

During follow up 41 (1.6%) patients developed invasive cancer. Four were initially being treated for LGD (0.7% of the LGD cohort), 24 for HGD (1.8%) and 13 for IMC (2.0%) (X^2 p = N.S). Of these 41 patients 22 progressed to invasive cancer within 18 months of initiating EET.

Eleven of the 41 these patients initially achieved CR-D at two consecutive endoscopies but subsequently developed invasive cancer. The other 30 patients never achieved CR-D and developed invasive cancer after a median 433.5 days (IQR 310-765 days). They received a median 2 ablations (IQR 2-3.75) before developing cancer.

Follow up time for the whole cohort was 7,856 patient-years, a crude incidence rate of 0.52 per 100 patient years. The crude incidence rate in patients with LGD was 0.20

per 100 patient years and the combined crude incidence rate in patients with HGD and IMC was 0.63 patient years. This difference was significant (X^2 P = 0.015).

3.5 Discussion

The UK RFA registry has followed up a large cohort of patients for 10 years after commencing RFA therapy enabling us to publish from one of the most extensive datasets. It is well established that endoscopic treatment of dysplastic BO is initially successful in up to 90% of patients [124], [178]. What is less well understood is how long that benefit lasts and if this contributes to a substantial reduction in progression to cancer.

This study confirms durable reversal of dysplasia and BO with RFA which reduces cancer risk by more than 90% compared to historical control data of 6-19% per annum [119], [179], [180]. The KM rate of progression to EAC in this cohort was <5% after 10 year follow up. More RFA is needed for patients with longer segments of BO or more advanced initial disease.

Most recurrences occur within 3 years. Initial disease severity, age, and length of BO prior to EET were not reliable predictors of recurrence of dysplasia or IM but new nodules appearing during RFA which require EMR are associated with a small reduction in treatment success. These recurrences occur more than 3 times more frequently within the first 3 years of therapy even when accounting for the greater surveillance offered to patients during this time period.

I have shown here that even when patients have recurrence of dysplasia or IM established EET techniques remain efficacious, with over 50% of patients being successfully retreated.

This work dramatically expands the published literature in long-term follow up for EET in BO. The US RFA Patient Registry reported a median 2.7 year follow up of 4982 patients, but only 1305 had dysplasia [181]. A systematic review and meta-analysis published this year was only able to report on 794 patients followed up for an average of 3.4 years (range 27-69.7 months) [133], highlighting this lack of long-term follow up.

There is only one, recently published Dutch study, with 10 year follow up data on 1386 patients [182]. The larger cohort produces almost identical findings of 1.6% at 10 years. The rates of recurrence of dysplasia or IM were higher than those published by the Dutch team. This may be explained by the longer length of BO treated and lower proportion of patients with LGD in this cohort.

This study including 2,535 patients is the largest looking at RFA outcomes, either short or long term. I included data from 28 sites enabling this study to represent clinical practice across the UK as well as a range of demographics.

This work followed up 1,175 patients from 10 sites with more precision. This data collection was comprehensive and verified. The authors were able to review every endoscopic procedure, reducing missing data and minimizing individual reporting errors. The large number of patients excluded from these analyses does limit this

data somewhat but it was felt this was necessary to ensure the most accurate data was used.

Due to the nature of a long-term multi-centre study, there was some variability in practice across the sites. Where practice led to large time gaps in data collection these patients were excluded or censored. This led to a substantial number of exclusions, but also enabled a more accurate assessment of the long-term effects of EET in BO. A limitation is that patients were followed up by their recruiting site. If patients presented to other hospitals with any of the outcomes or had further therapy this data will not have been collected.

I reviewed the differences between patients with early and more advanced disease extensively. Median length of LGD was greater than for both other groups yet the number of EMRs per centimetre of BO was lower, suggesting those with LGD needed less EET therapy than those with more advanced disease. This argues for earlier therapy which would be easier to perform and require less treatment episodes.

A systematic review published in 2021 included 13 papers, only one of which used two consecutive endoscopies to confirm clinical endpoints [133]. The endpoints measured were complete reversal of neoplasia (absence of IMC or HGD and CR-IM). The rate of recurrence of IM was 37.1% for 1204 patients after 3.4 years of follow up. For the cohort I have studied, the rate of recurrence was 13.8% after the same time interval.

3.5.1 Implications for clinical practice

EET is primarily used to prevent progression to EAC. In this cohort of 2,535 patients only 41 patients developed invasive cancer throughout the entire study period. For patients with HGD the crude incidence was 0.53 per 100 patient-years which is a tenfold reduction in cancer incidence compared with a meta-analysis calculating annual cancer risk [183]. The crude incidence rate for IMC was 0.97 per 100 patient-years respectively. This compares favourably with the original randomised controlled trial [124], [180].

The results I present here show low rates of recurrence of dysplasia across all histological subgroups at 8 years after end of treatment, with most of these recurrences occurring within 2 years of completion of EET. Age and length of BO segment at the start of EET are not predictors of recurrence risk suggesting that these should not be used to stratify the risk of recurrence. It is also possible to successfully treat most patients that have recurrence of dysplasia or IM. This data suggests that continuing annual surveillance endoscopies, as recommended by societal guidelines [80], [184], beyond 2 years may offer little additional benefit whilst providing no evidence that the histological subtype prior to EET should be used to guide surveillance intervals [185]. These findings confirm previous work from our laboratory recommending more intense earlier surveillance, which is reduced over time [186].

The likelihood of achieving CR-D reduces rapidly after 5 ablative episodes, suggesting that these patients may have refractory disease and alternative intervention should

be considered. This must be understood in the context of additional risk of stricturing with further procedures. In this cohort the risk of stricturing following EET requiring dilatation remained within limits suggested by a recent consensus publication [187].

Clinicians may be undertreating those with longer segments of BO. Although the number of ablative procedures per patient is comparable between those that achieve CR-D and those that do not, the number of ablative procedures per cm of BO is higher for patients achieving CR-D than for those not achieving this. For CR-IM this difference is even more substantial. Coupled with what is already understood about cancer progression risks, this suggests clinicians should be more active in the treatment of individuals with longer Barrett's segments and those with high grade disease (either HGD or IMC).

Recently, some endoscopists have advocated ESD as routine treatment [188]. This technique is harder to learn than EMR and has a higher risk profile. This work suggests that EMR with RFA should remain the standard of care, although in specific circumstances operators might want to consider ESD, particularly for patients who develop new lesions after RFA has commenced, although even here, the success of rescue EMR is still very high.

3.5.2 Conclusions

I show here RFA provides durable outcomes in BE as well as reducing rates of invasive cancers. In addition, I have shown that using two consecutive endoscopies to confirm clinical outcomes is a more reliable measure of defining remission.

In addition, I show here long-term benefit of EET in reducing rates of invasive cancer in a large cohort of patients, with RFA alone achieving excellent results in selected patients. Durability is high with most recurrences occurring shortly after completion of therapy and being treatable with the same modality. EET with RFA is now firmly established as the primary therapy for dysplastic BO. In addition, I have confirmed that the durability of CR-D is affected by how remission is defined. The more reliable measure is using histology from two consecutive endoscopies. I would advocate applying this to clinical practice.

Chapter 4 Accuracy of clinical staging for T2N0 oesophageal cancer: Systematic Review and Meta-analysis.

Much of this work was published in *Accuracy of clinical staging for T2NO oesophageal cancer: systematic review and meta-analysis* [189]. I, along with Professor Laurence Lovat and Dr Sarmed Sami conceived and drafted the study. I collected the data and performed the initial searches. Dr Alex Ho and I collected the data. Dr Sarmed Sami and Dr Paul Bassett assisted me with the data analysis and interpretation. I wrote the initial draft which was reviewed by Professor Laurence Lovat, Dr Sarmed Sami and Dr Alex Ho.

This chapter addresses the following objectives:

Objective 4: For patients who have developed oesophageal cancer that penetrates deeper into the oesophageal wall, and is therefore not amenable to endoscopic therapy, how accurate is the current imaging strategy to stage the disease?

4.1 Introduction

Endotherapy for oesophageal dysplasia and early cancers has advanced substantially over the past 10 years. Despite this oesophageal cancer is the 7th most common cause of cancer worldwide and the 6th most common cause of overall cancer mortality [190]. In men in the UK it is the 4th most common. 5-year survival has only shown modest improvement since the 1970s despite advances in diagnostic and therapeutic options [4].

Clinical staging is the most accurate reflection of cancer prognosis, it guides therapy and is a survival reference point [57]. Accurate staging has become increasingly important as the options for therapy have increased [58]. Specifically, endoscopic therapy is now a viable treatment option for T1NO disease as shown in the previous chapter. For more advanced disease, surgery is the modality of choice.

A number of recent studies assessing oesophageal cancer therapy have shown differing results, especially with regards to the benefits of neoadjuvant chemotherapy and radiotherapy prior to surgery. One prospective RCT suggested that neoadjuvant CRT reduced mortality and increased disease-free survival in patients with locally advanced oesophageal cancer (T1N1M0 or T2–3N0–1M0) [191]. However, in patients with T2N0 disease the benefit is less clear, with a recent European multicentre retrospective study demonstrating that NAT had no impact on recurrence, disease-free survival and overall survival [192]. A major limitation of those studies has been the variable accuracy of clinical staging for T2N0 disease reported in the literature. When compared to post-operative pathological staging as the reference standard, clinical staging can be accurate in as low as 6% or as high as 42% of patients depending on which study is considered [60], [61], [62].

Clinical staging of oesophageal cancer uses a number of modalities (see section 1.1.2.3) [67], [193], [194]. This includes any combination of EUS, CT, US, PET, and laparoscopy. A number of studies and systematic reviews have evaluated the accuracy of these tests individually [195], [196], [197]. While this information is useful it does not accurately reflect clinical practice when modalities are used in combination.

Accurate clinical staging of oesophageal cancer is vital to ensure appropriate therapeutic decisions are made both to direct clinical care and to enable precision research. Clinical staging of T2 oesophageal cancer (cT2) is of particular significance for two reasons. Firstly, patients with cancers that are >cT2N0 undergo different treatment pathways to those with <cT2N0, therefore this threshold has a significant clinical application. Patients with >cT2N0 are typically offered neoadjuvant chemotherapy in addition to surgery, patients with cT2N0 may be offered surgery alone and patients with <cT2N0 may be offered endotherapy [67], [193], [194]. Secondly, when assessing the accuracy of staging, pathology is used as the reference standard. If NAT if offered to patients, as recommended by guidelines, this may downstage the cancer which will affect the pathological staging. Patients with <T2N0M0 disease usually undergo endoscopic therapy and therefore seldom undergo full clinical staging [67], [193], [194]. For these reasons, I decided to only include patients with cT2N0M0 disease.

In summary, precise data on accuracy of clinical staging remain lacking. Moreover, data on the understaging and overstaging of T2NO oesophageal cancer are also lacking. This has major implications for treatment decisions and patient survival among other factors. I aimed to address these knowledge gaps by a systematic review and meta-analysis of the relevant literature.

4.2 Materials and methods

This study was conducted according to guidance provided by the Cochrane Collaboration handbook for systematic reviews [198] and followed a pre-specified

protocol. The study was prospectively registered on the PROSPERO international database (CRD42019157635).

4.2.1 Search strategy

The Ovid MEDLINE, Ovid EMBASE and The Cochrane Library databases were searched for studies published from database inception to 1 June 2019 for relevant articles evaluating staging accuracy in oesophageal cancer. No restrictions were applied to the search algorithm (Table 4.1).

Table 4.1: Search strategy

Chistrategy		
Number	Defined Search	
#1	Esophag*	
#2	Oesophag*	
#3	1 or 2	
#4	Cancer	
#5	Adenocarcinoma	
#6	Carcinoma	
#7	3 or 4 or 5	
#8	T2*	
#9	Stag*	
#10	8 or 9	
#11	3 and 7 and 10	

4.2.2 Study selection and outcome measures

I included studies that met the following criteria:

- 1. Performed in cohorts of adult patients defined as 18 years or older
- 2. Provided data on T2 oesophageal cancer staging accuracy
- 3. Used multiple imaging modalities to assess clinical staging

- 4. Compared clinical staging to pathological staging as the reference standard test
- 5. Provided sufficient data to allow the calculation of staging accuracy

Accuracy was defined as the proportion of patients with correct clinical staging prior to surgery using post-operative pathological staging as the reference standard. The primary outcome was diagnostic accuracy of combined T and N staging. Secondary outcomes were accuracy of T stage only; percentage T downstaged; percentage T upstaged and percentage N upstaged.

I was only evaluated patients with cT2N0M0 and were unable to calculate sensitivity and specificity values as these require the number of false negatives for a given test. These data were not available, because incorrectly staged patients as >T2N0 would have typically undergone NAT, therefore their post-operative pathological staging may not reflect their pre-operative stage.

All titles and abstracts identified by the primary searches were screened by two reviewers (Paul Wolfson (P.W.) ad Alex Ho (A.H.)). Full-text articles of potentially eligible studies were read and assessed for inclusion. Data was then independently extracted by P.W. and A.H. before entry into a standardised pro forma (Excel 2010; Microsoft, Redmond, Wash). Disparity between the data collected was resolved by discussion and if no agreement was reached a third investigator (Sarmed S. Sami (S.S.S.)) was consulted. The corresponding authors of the primary studies were contacted to ask for any missing data.

Variables for each study were collected as follows: Year of publication, years of recruitment, number of centres, population studied (age, sex, sample size, cancer subtype), country of origin, study design, imaging modalities used.

Study quality was assessed independently by two investigators (P.W. and A.H.) using the updated version of the quality assessment of diagnostic accuracy studies (QUADAS-2) tool [199].

4.2.3 Statistical analysis

All outcomes were binary in nature. Meta-analysis methods were used to pool together the results from different studies for each outcome. The Freeman-Tukey double arcsine transformation was performed before analysis. This was used to stabilise the variances when the proportions were close to zero and one, and a Normal approximation to the binomial distribution did not hold.

The DerSimonian-Laird random-effects method was used for the analysis, regardless of the degree of heterogeneity between the study results.

4.2.4 Heterogeneity, subgroup analyses, and publication bias

The heterogeneity between studies was assessed based on the significance of the between-study heterogeneity, and also on the size of the I² value. Low, moderate and high inconsistency were associated with I² values of 25%, 50% and 75%, respectively [200]. Additional subgroup analyses were performed to examine if any factors could explain the heterogeneity between studies. We evaluated several factors a priori including: publication date (before and after Jan 2015), date of first recruitment

(before and after 2000), number of centres (single vs multicentre), sample size (<100 vs \geq 100), geographical location of study (USA, Europe or Asia) and main histological subtype included (adenocarcinoma or SCC). Publication bias was assessed with the use of a Funnel plot and by Egger's test. Egger's test uses linear regression to assess the relation between the standard error and the inverse variance of the treatment effect. A p value of \leq 0.10 was considered to represent possible publication bias.

4.3 Objective 4: Results

4.3.1 Characteristics of included studies

After duplicates were removed the search strategy identified a total of 1,199 studies which were all screened by title and abstract. Fifty-six potentially eligible articles were identified which were all read in full. Twenty studies [60], [61], [62], [192], [201], [202], [203], [204], [205], [206], [207], [208], [209], [210], [211], [212], [213], [214], [215], [216] met the inclusion criteria (n=5,213 patients) (Figure 4.1). Of these studies, 16 (n=4,182 patients) [60], [62], [201], [202], [203], [204], [205], [206], [207], [208], [209], [211], [213], [214], [215], [216] reported accuracy of combined T and N staging. Eighteen studies (n=4,471 patients) [60], [61], [62], [192], [201], [202], [203], [204], [205], [206], [207], [208], [209], [212], [213], [214], [215], [216] provided data on accuracy of T stage and 18 studies (n=5,180 patients) [60], [62], [192], [201], [202], [203], [204], [205], [206], [207], [208], [209], [210], [211], [213], [214], [215], [216], presented data for accuracy of N stage.

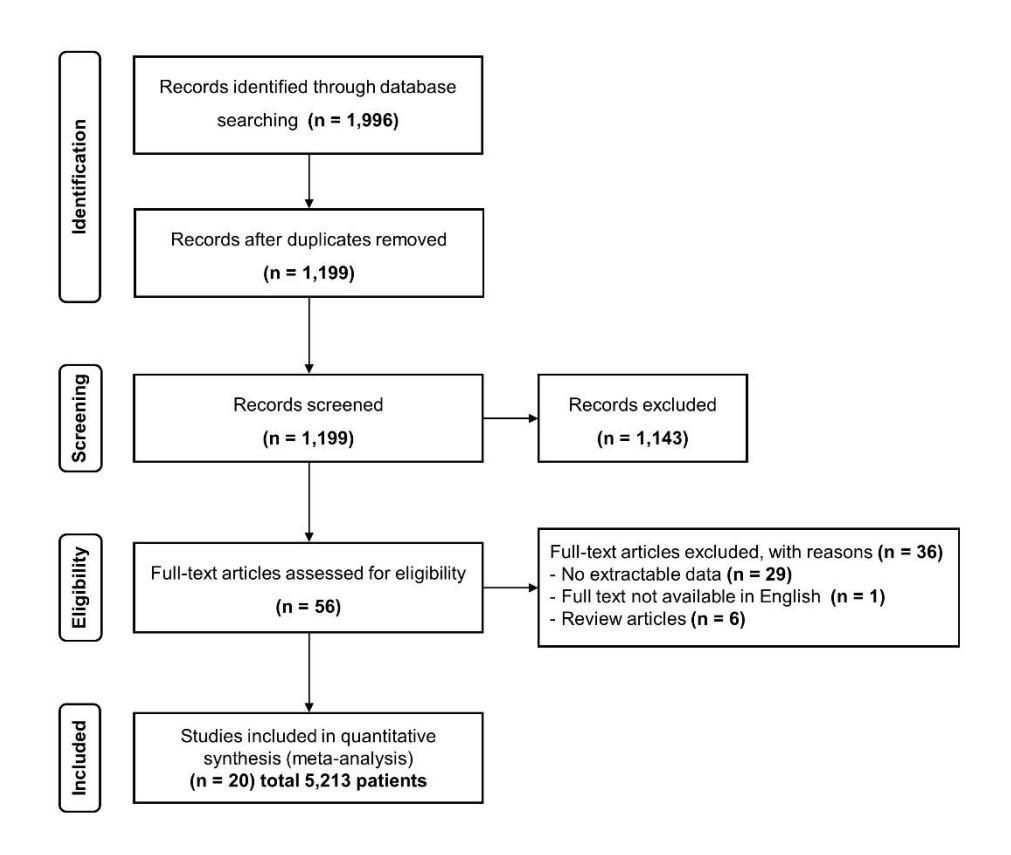


Figure 4.1: Flow diagram of the search strategy and selection of studies

A summary of the included studies is shown in Table 4.2. The characteristics of the patients included in the studies are shown in Table 4.3. Figure 4.2 displays the outcomes of the QUADAS-2 quality assessment [199].

Table 4.2: Summary of included studies (n=20)

Author and	Country	Modalities	No. of	%	%	% T-	% T-	% N
year	(Recruitme	used	pts	accuracy	accuracy	down-	up-	up-
	nt years)		(centres)	on T&N	on T	staged	staged	staged
				stage	stage			
Nishimaki T	Japan	CT/EUS,	23 (16)		43%	48%	9%	
[61] 1999	(1993-	abdominal US						
[0-]-000	1994)							
Rice TW	USA (1987-	PET/EUS/CT	53 (1)	13%	17%	62%	21%	25%
[201]	2005)							
2007								
Crabtree	USA (2000-	PET/EUS/CT	18 (1)	6%	28%	50%	22%	17%
TD et al	2008)							
[215]								
2011								
Stiles BM	USA (1992-	PET/EUS/CT	40 (1)	13%	30%	30%	40%	55%
[202]	2005)							
2011								

Chen WH [203] 2012	Taiwan (1995- 2005)	EUS/CT/bone scan/barium swallow	14 (1)	43%	50%	36%	14%	0%
Zhang JQ [204] 2012	USA (1989- 2009)	PET/EUS/CT/ Barium swallow	14 (1)	29%	50%	29%	21%	43%
Crabtree TD [205] 2013	USA (2002- 2011)	PET/EUS/CT	482 (multiple)	27%	40%	34%	26%	21%
Shin S [206] 2014	Korea (2005- 2010)	PET & EUS	66 (1)	15%	23%	61%	17%	39%
Tekola BD [207] 2014	USA (2003- 2013)	EUS & PET/CT	30 (1)	17%	20%	67%	13%	33%
Hardacker TJ [208] 2014	USA (1990- 2011)	EUS and "cross sectional imaging"	35 (1)	9%	17%	43%	40%	40%
Speicher PJ [209] 2014	USA (1998- 2011)	PET/EUS/CT	786 (multiple)	27%	27%	32%	42%	30%
Dolan JP [60] 2016	USA (1999- 2011)	all had PET,CT EUS	16 (1)	6%	19%	50%	31%	56%
Markar SR [192] 2016	France (2000- 2010)	PET/EUS/CT	285 (30)	NS	27%	39%	35%	48%
Samson P [210] 2016	USA (2006- 2012)	PET/EUS/CT	713 (multiple)	NS	NS	NS	32%	34%
Luu C [211] 2017	USA (2000- 2015)	PET/EUS/CT	29 (1)	21%	NS	NS	NS	24%
Winiker M [212] 2018	Switzerland (2000- 2006)	PET/EUS/CT	10 (1)	NS	10%	90%	0%	NS
Goense L [62] 2018	Netherland s (2005- 2014)	PET/EUS/CT/US neck	180 (multiple)	38%	53%	0%	47%	45%
Shridhar R [213] 2018	USA (2004- 2013)	Not specified (NS)	1840 (multiple)	31%	44%	31%	26%	34%
Barbetta A et al [216] 2018	USA (1997- 2016)	PET & EUS	80 (1)	9%	18%	61%	21%	35%
Atay SM [214] 2019	USA (2002- 2012)	PET/EUS/CT	499 (26)	14%	24%	44%	32%	39%

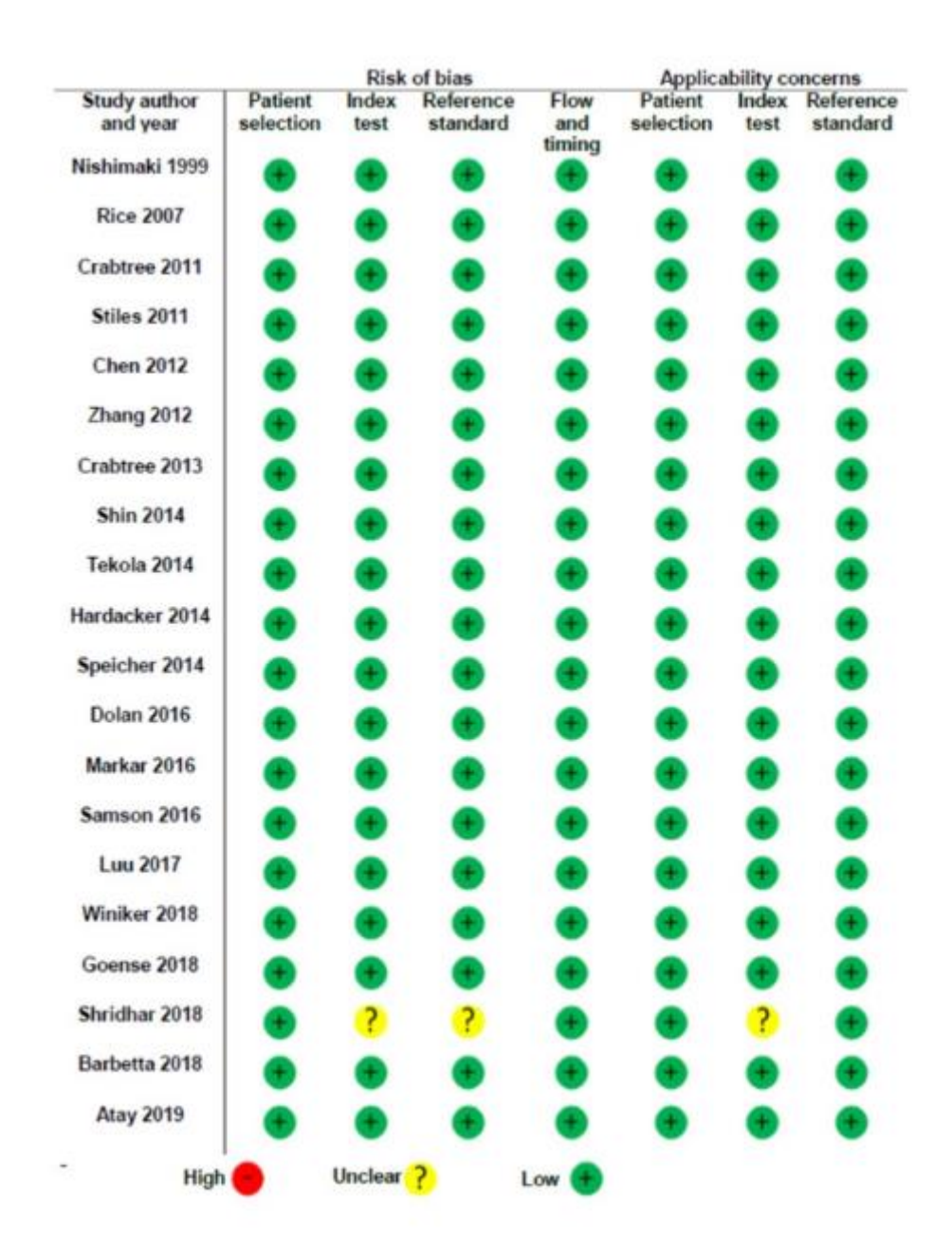


Figure 4.2: Quality Assessment of Diagnostic Accuracy Studies (QUADAS-2) tool for the 18 studies included in the meta-analysis.

Table 4.3: Summary of characteristics of patients included in the analysis

Author and year	Country	Mean age,	% Male	%	% SCC
	-	(years)		Adeno	
Nishimaki T [61] 1999	Japan	62	88.0%	0.4%	96.4%
Rice TW [201] 2007	USA	65	N/S	97.0%	3.0%
Crabtree TD et al					
[215] 2011	USA	NS	N/S	100.0%	0.0%
Stiles BM [202] 2011	USA	62.5	81.4%	71.6%	28.4%
Chen WH [203] 2012	Taiwan	60.9	78.6%	0.0%	100.0%
Zhang JQ [204] 2012	USA	69	85.7%	100.0%	0.0%
Crabtree TD [205]					
2013	USA	63.8	83.2%	86.3%	13.7%
Shin S [206] 2014	Korea	63.1	95.0%	1.3%	97.5%
Tekola BD [207] 2014	USA	NS	89.5%	N/S	N/S
Hardacker TJ [208]					
2014	USA	62.5	82.9%	82.9%	17.1%
Speicher PJ [209]					
2014	USA	66	82.5%	N/S	N/S
Dolan JP [60] 2016	USA	68	94.0%	93.8%	6.3%
Markar SR [192] 2016	France	NS	80.7%	49.5%	50.5%
Samson P [210] 2016	USA	65.6	82.3%	69.3%	30.7%
Luu C [211] 2017	USA	64.9	82.0%	92.8%	72.0%
Winiker M [212] 2018	Switzerland	65	74.5%	59.0%	41.0%
Goense L [62] 2018	Netherlands	66	77.0%	81.0%	19.0%
Shridhar R [213] 2018	USA	67	80.4%	87.5%	12.5%
Barbetta A [216]					
2018	USA	64	78.0%	100.0%	0.0%
Atay SM [214] 2019	USA	66	78.0%	88.0%	12.0%

4.3.2 Outcomes

4.3.2.1 T&N staging

Combined T and N staging was accurate in 19% of patients (95% confidence interval (CI), 15-24; 16 studies; n=4,182 patients; $l^2=88\%$; p<0.01) (Table 4.4 & Figure 4.3).

Table 4.4: Meta-analysis results for all studies combined

Outcome	Number	Heterog	eneity	Pooled %
	of	p-value	l ²	(95% CI)
	studies			
Combined T/N stage	16	<0.01	88%	19% (15%, 24%)
accuracy				
T stage accuracy	18	<0.01	91%	29% (24%, 35%)
T downstaged	18	<0.01	96%	41% (33%, 50%)
T upstaged	19	<0.01	86%	28% (24%, 32%)
N upstaged	18	<0.01	86%	34% (30%, 39%)

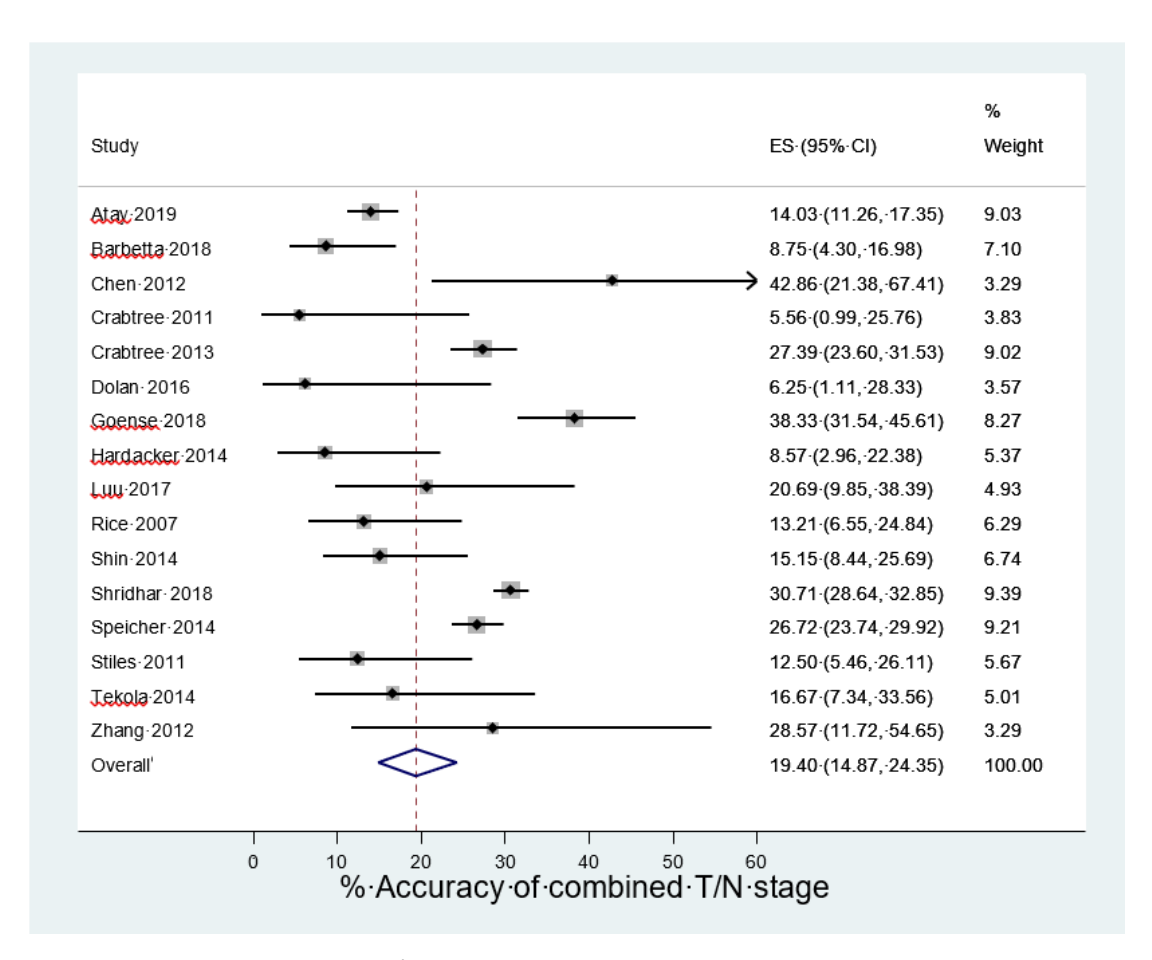


Figure 4.3: Forest plot for combined T/N stage accuracy

Potential sources of heterogeneity in accuracy of T&N staging are shown below in Table 4.5. Those sources of heterogeneity found to be significant were, the number of recruiting centres, the region in which the study was conducted, the most common histological subtype included in each study and the number of patients included. There was no significant evidence of publication bias (p=0.11) (Figure 4.4).

Table 4.5: Accuracy of combined T/N stage by study subgroup

Subgroup	Number	Heteroge	eneity	Pooled %	Subgroup
	studies	p-value	l ²	(95% CI)	p-value
Published ≤ 2014	10	<0.01	66%	19% (11%, 24%)	0.95
Published ≥ 2015	6	<0.01	95%	20% (11%, 30%)	
1 st recruitment < 2000	7	<0.01	79%	16% (9%, 25%)	0.34
1 st recruitment ≥ 2000	7	<0.01	92%	22% (15%, 30%)	
Single centre	11	0.17	29%	13% (9%, 18%)	<0.01
Multiple centres	5	<0.01	95%	27% (20%, 34%)	
USA	13	<0.01	89%	17% (13%, 23%)	<0.01
Asia	2	-	-	19% (10%, 28%)	
Europe	1	-	-	38% (32%, 46%)	
Adeno	6	0.29	20%	12% (7%, 18%)	<0.01
Mixed	6	<0.01	95%	22% (15%, 31%)	
SCC	2	-	-	19% (10%, 28%)	
Unknown	2	-	-	26% (23%, 29%)	
< 100 patients	11	0.24	29%	13% (9%, 18%)	0.01
100+ patients	5	<0.01	95%	27% (20%, 34%)	

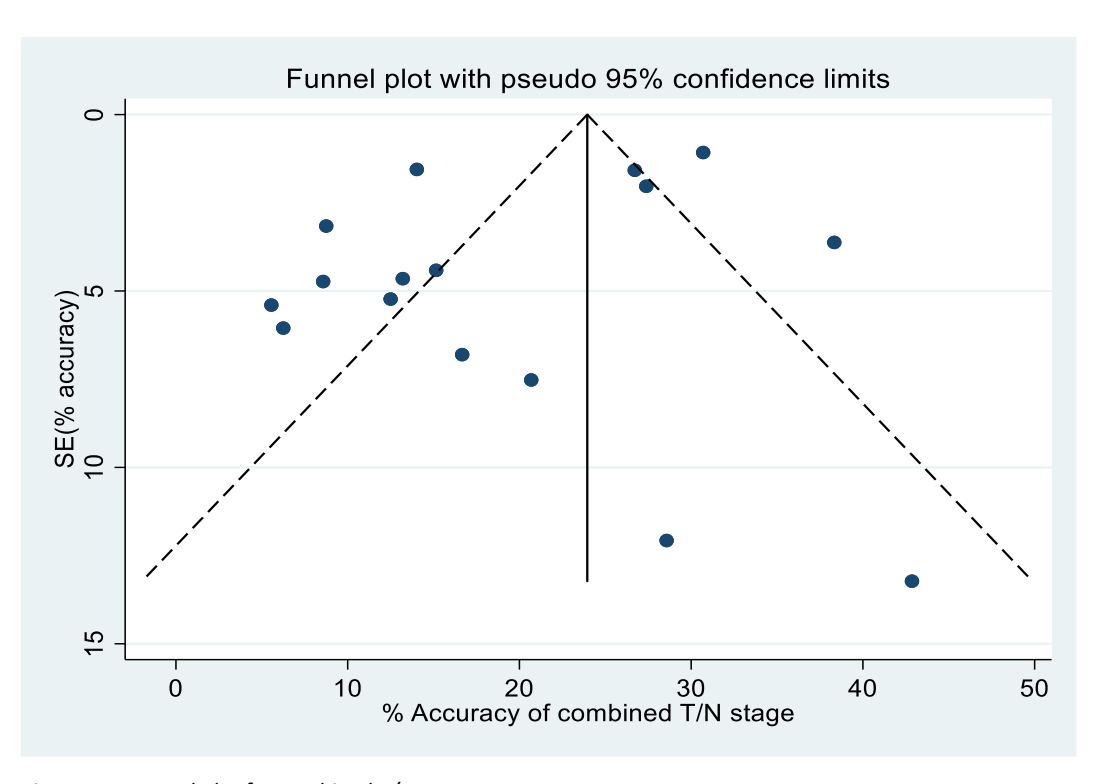
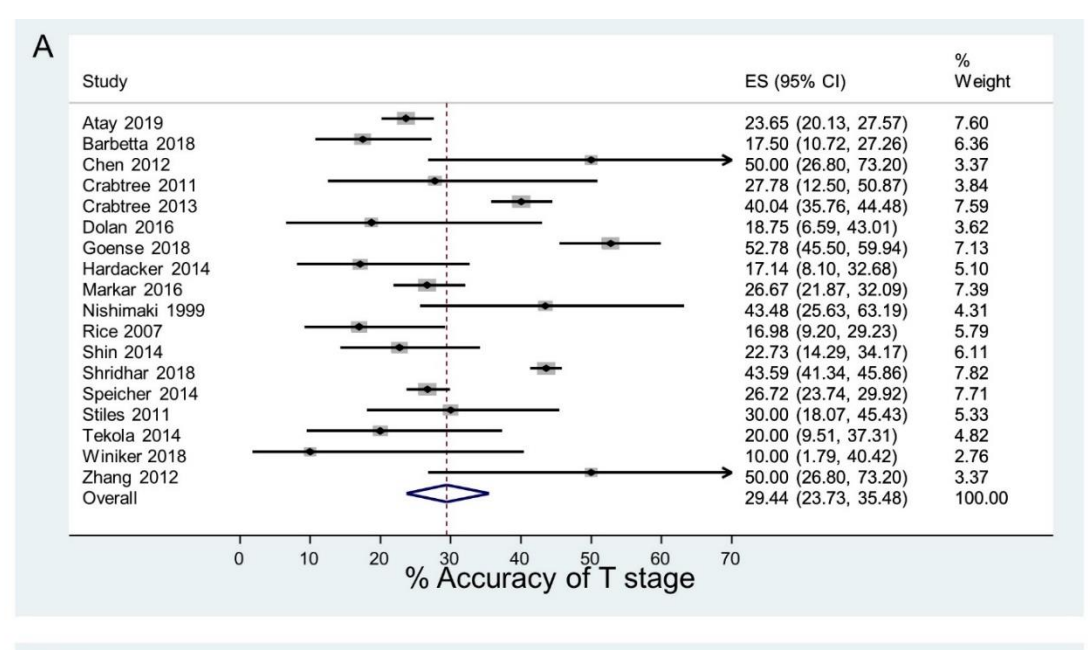


Figure 4.4: Funnel plot for combined T/N stage accuracy

4.3.2.2 T stage accuracy

T staging was accurate in 29% of patients (95%Cl 24-35; 18 studies; n=4,471 patients; $l^2=91\%$; p<0.01) (Table 4.4 & Figure 4.5A).



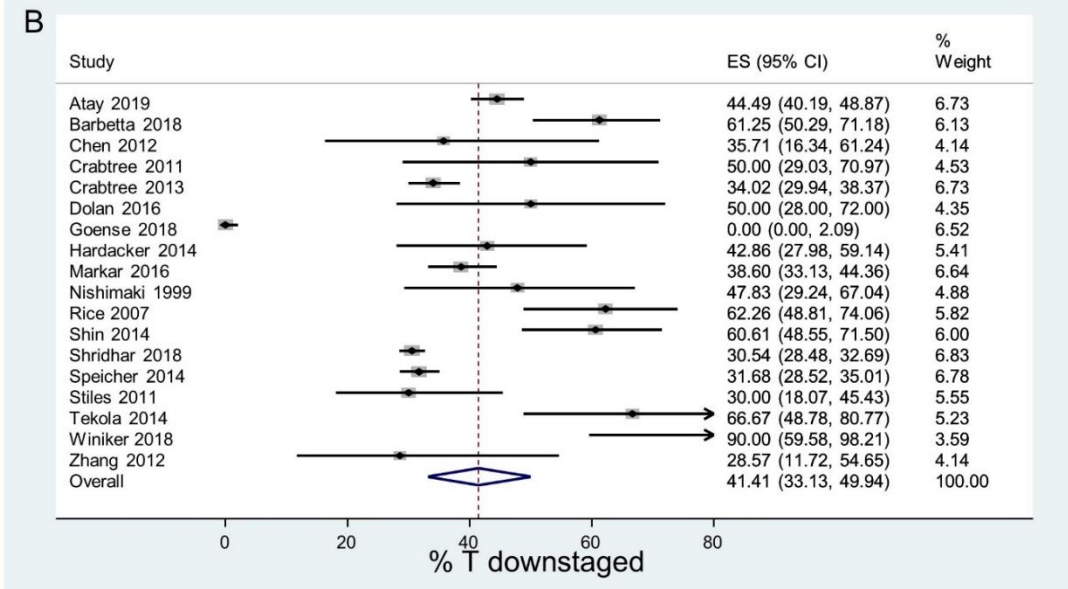


Figure 4.5: Forest plots for secondary outcomes. A, T stage accuracy; B, T downstaging.

Potential sources of heterogeneity in T stage accuracy are shown below in Table 4.2. Only the number of recruiting centres included in the study was found to be a significant source of heterogeneity. There was no significant evidence of publication bias (p=0.20) (Figure 4.6).

Table 4.6: Accuracy of T stage by study subgroup

Subgroup	Number	Heterog	eneity	Pooled %	Subgroup
	studies	p-value	l ²	(95% CI)	p-value
Published ≤ 2014	10	<0.01	79%	29% (23%, 36%)	0.73
Published ≥ 2015	6	<0.01	95%	31% (21%, 43%)	
1 st recruitment	8	0.04	52%	28% (21%, 35%)	0.50
2000		0.04	0.40/	220/ (2.40/ .400/)	
1 st recruitment	: 8	<0.01	94%	32% (24%, 40%)	
2000					
Single centre	9	0.12	37%	240/ /170/ 210/\	0.04
Single centre	_	_		24% (17%, 31%)	0.04
Multiple centres	7	<0.01	96%	36% (28%, 44%)	
USA	10	<0.01	94%	28% (21%, 36%)	0.74
Asia	3	_	-	36% (18%, 55%)	
Europe	3	-	-	32% (12%, 55%)	
Adeno	3	-	-	26% (9%, 46%)	0.38
Mixed	8	<0.01	94%	32% (24%, 41%)	
SCC	3	-	-	36% (18%, 55%)	
Unknown	2	-	-	26% (23%, 29%)	
< 100 patients	10	0.06	46%	26% (19%, 33%)	0.13
100+ patients	6	<0.01	97%	35% (27%, 44%)	

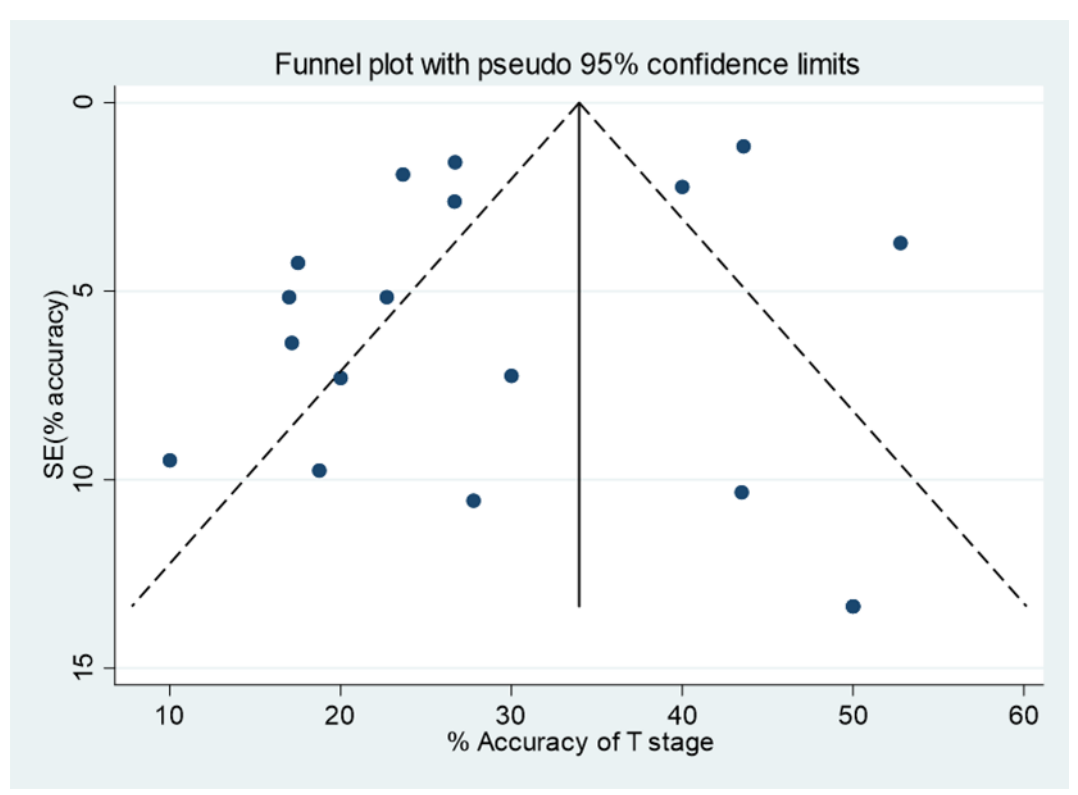


Figure 4.6: Funnel plot for T stage accuracy

4.3.2.3 T downstaging

The percentage of patients downstaged after surgery was 41% (95%CI, 33-50; 18 studies; n=4,471 patients; I²=96%; p<0.01) (Table 4.4 & Figure 4.5B).

Potential sources of heterogeneity in T downstaging are shown below in Table 4.7. Those sources of heterogeneity found to be significant were, the number of recruiting centres, the most common histological subtype included in each study and the number of patients included. There was evidence of publication bias as the Egger Test P-value was 0.02 (Figure 4.7).

Table 4.7: T downstaging by study subgroup

Subgroup		Number	Heteroge	eneity	Pooled %	Subgroup
		studies	p-value	l ²	(95% CI)	p-value
Published ≤ 2014		10	<0.01	66%	44% (36%, 52%)	0.36
Published ≥ 2015		6	<0.01	95%	34% (18%, 53%)	
1 st recruitment	<	8	<0.01	71%	41% (31%, 51%)	0.83
2000						
1 st recruitment	≥	8	<0.01	98%	39% (26%, 53%)	
2000						
Single centre		9	<0.01	70%	51% (40%, 63%)	<0.01
Multiple centres		7	<0.01	98%	29% (19%, 40%)	
USA		10	<0.001	87%	40% (34%, 46%)	0.28
Asia		3	-	-	51% (38%, 66%)	
Europe		3	-	-	33% (0%, 84%)	
Adeno		3	-	-	50% (30%, 69%)	0.02
Mixed		8	<0.01	95%	33% (21%, 46%)	
SCC		3	-	-	52% (38%, 66%)	
Unknown		2	-	-	33% (29%, 36%)	
		40	0.24	660/	E40/ /440/ C22/	.0.04
< 100 patients		10	0.24	66%	51% (41%, 62%)	<0.01
100+ patients		6	<0.01	98%	27% (17%, 38%)	

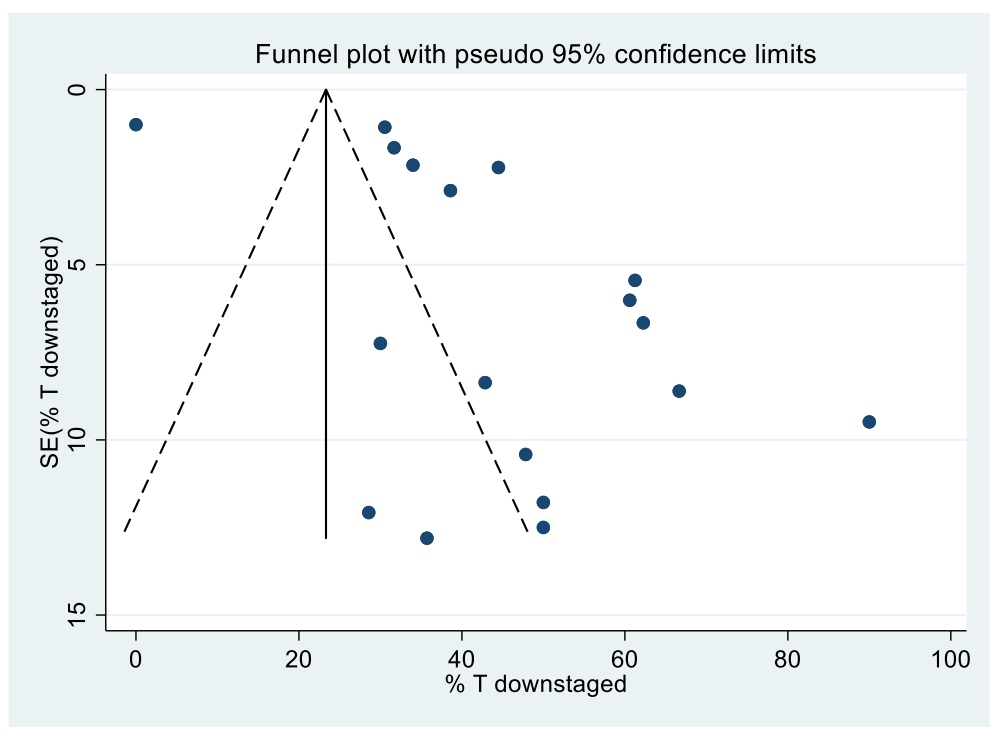


Figure 4.7: Funnel plot for T downstaging

4.3.2.4 Tupstaging

The percentage of patients T upstaged after surgery was 28% (95%Cl, 24-32; n=18 studies; 5,184 patients; I²=86%, p<0.01) (Table 4.4 & Figure 4.8A).

Potential sources of heterogeneity in T upstaging are shown below in Table 4.8. Those sources of heterogeneity found to be significant were, the number of recruiting centres, the most common histological subtype included in each study and the number of patients included. There was no significant evidence of publication bias (p=0.55) (Figure 4.9).

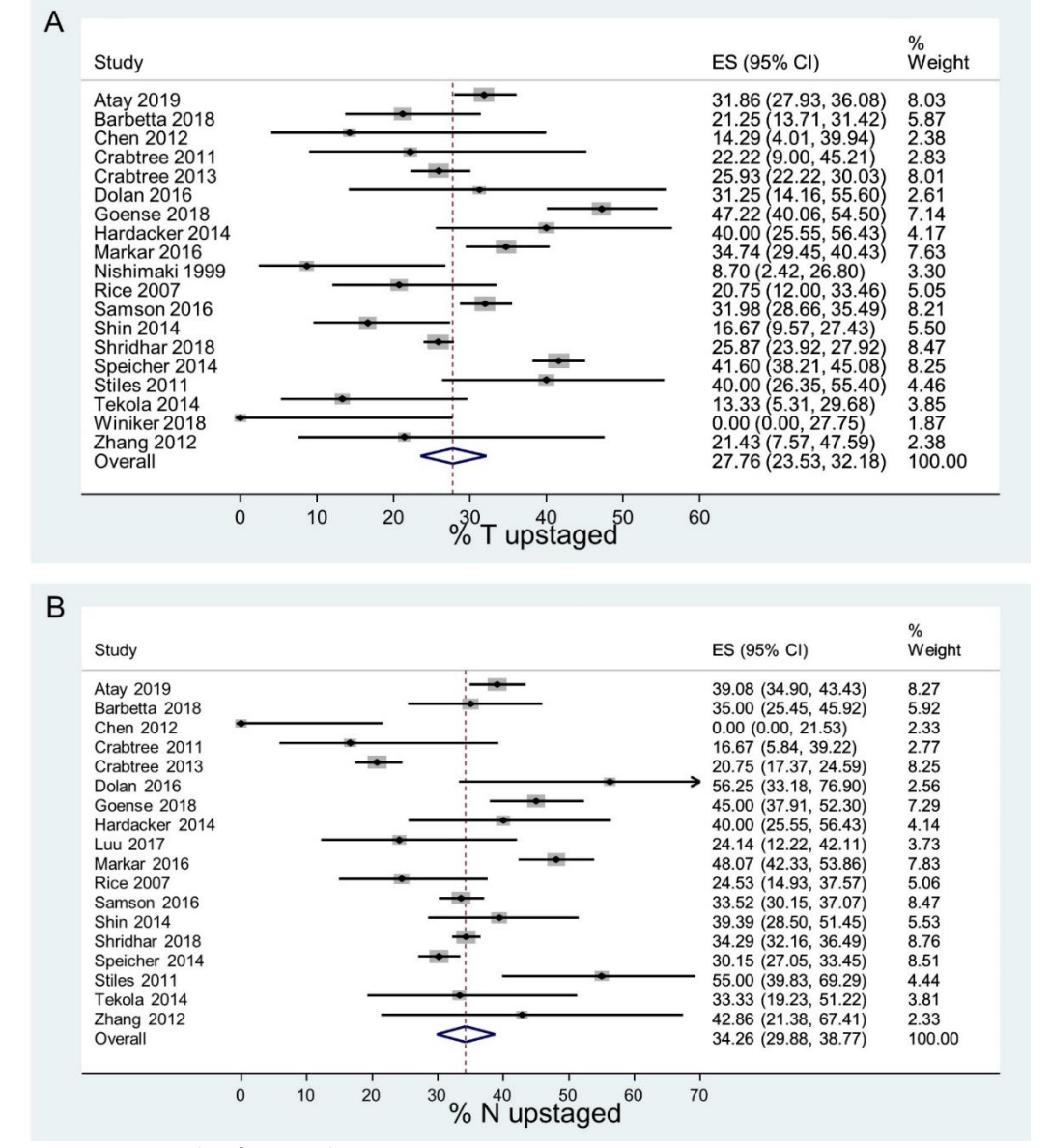


Figure 4.8: Forest plots for secondary outcomes. A, T upstaging; B, N upstaging.

Table 4.8: Tupstaging by study subgroup

Subgroup		Number	Heteroge	eneity	Pooled %	Subgroup
		studies	p-value	l ²	(95% CI)	p-value
Published ≤ 2014		10	<0.01	87%	24% (17%, 33%)	0.19
Published ≥ 2015		7	<0.01	88%	32% (26%, 38%)	
1 st recruitment	<	8	<0.01	75%	28% (19%, 39%)	0.95
2000						
1 st recruitment	≥	9	<0.01	87%	28% (24%, 33%)	
2000						
6: 1			0.24	50 0/	220/ /4.40/ 240/)	0.07
Single centre		9	0.24	59%	22% (14%, 31%)	0.07
Multiple centres		8	<0.01	93%	32% (27%, 38%)	
USA		11	<0.01	87%	30% (25%, 35%)	<0.01
Asia		3	-	-	14% (8%, 22%)	10.01
Europe		3	_	_	31% (16%, 48%)	
Ediope		3			3170 (1070, 1070)	
Adeno		3	_	_	22% (14%, 32%)	<0.01
Mixed		9	<0.01	86%	32% (27%, 37%)	
SCC		3	-	-	14% (8%, 22%)	
Unknown		2	-	-	40% (37%, 44%)	
< 100 patients		10	0.01	60%	20% (13%, 29%)	0.02
100+ patients		7	<0.01	93%	34% (28%, 39%)	

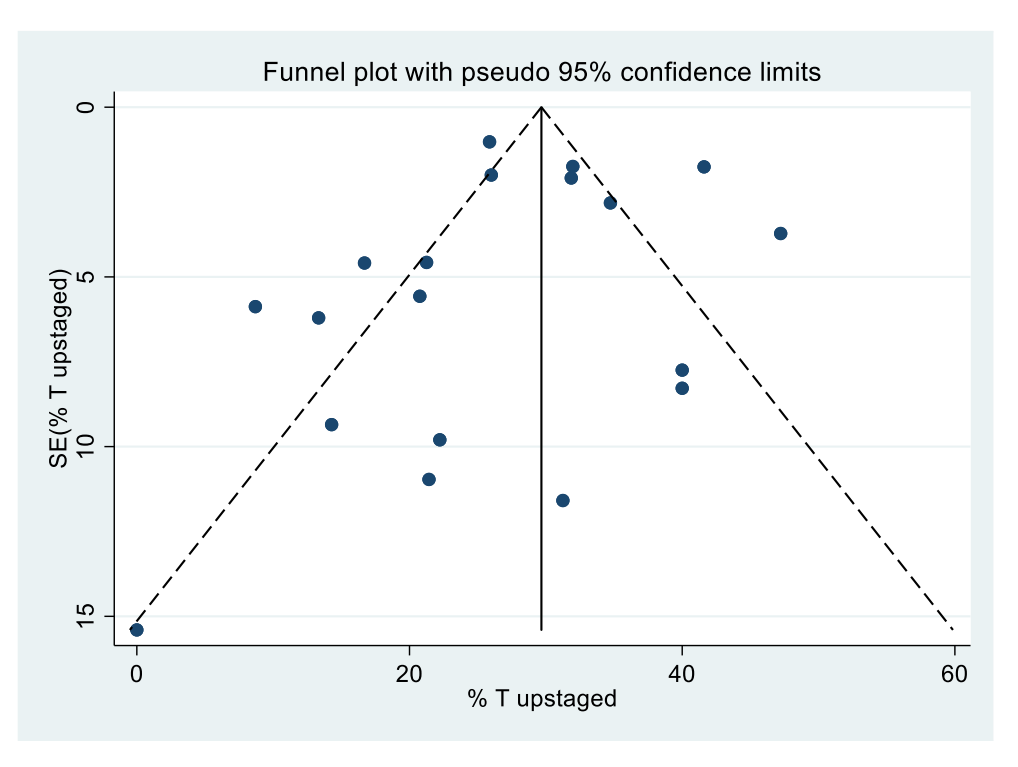


Figure 4.9: Funnel plot for T upstaging

4.3.2.5 N upstaging

The percentage of patients N upstaged after surgery was 34% (95%CI, 30-39; 18 studies; n=5,180 patients; $I^2=86\%$; p<0.01) (Table 4.4 & Figure 4.8B).

Potential sources of heterogeneity in T upstaging are shown below in Table 4.9. Only the region in which the study was conducted was found to be a significant source of heterogeneity. There was no significant evidence of publication bias (p=0.63) (Figure 4.10).

Table 4.9: N upstaging by study subgroup

Subgroup		Number	Heteroge	eneity	Pooled %	Subgroup
		studies	p-value	l ²	(95% CI)	p-value
Published ≤ 2014		9	<0.01	83%	30% (23%, 39%)	0.08
Published ≥ 2015		7	<0.01	82%	39% (34%, 44%)	
1 st recruitment	<	7	<0.01	80%	33% (22%, 46%)	0.81
2000						
1 st recruitment	≥	9	<0.01	90%	36% (30%, 41%)	
2000						
C'asla assis		0	.0.01	720/	220/ /220/ 450/\	0.07
Single centre		9	<0.01	73%	33% (23%, 45%)	0.87
Multiple centres		7	<0.01	93%	35% (30%, 41%)	
LICA		12	<0.01	070/	220/ /200/ 200/)	<0.01
USA			<0.01	87%	33% (29%, 38%)	<0.01
Asia		2	-	-	29% (20%, 40%)	
Europe		2	-	-	47% (42%, 51%)	
Adeno		4	0.08	55%	34% (20%, 49%)	0.16
Mixed		8	<0.01	92%	, , ,	0.10
			<0.01	92%	38% (32%, 44%)	
SCC		2	-	-	29% (20%, 40%)	
Unknown		2	-	-	30% (27%, 33%)	
< 100 patients		9	<0.01	73%	34% (23%, 45%)	0.87
•		7			, , ,	0.67
100+ patients		/	<0.01	93%	35% (30%, 41%)	

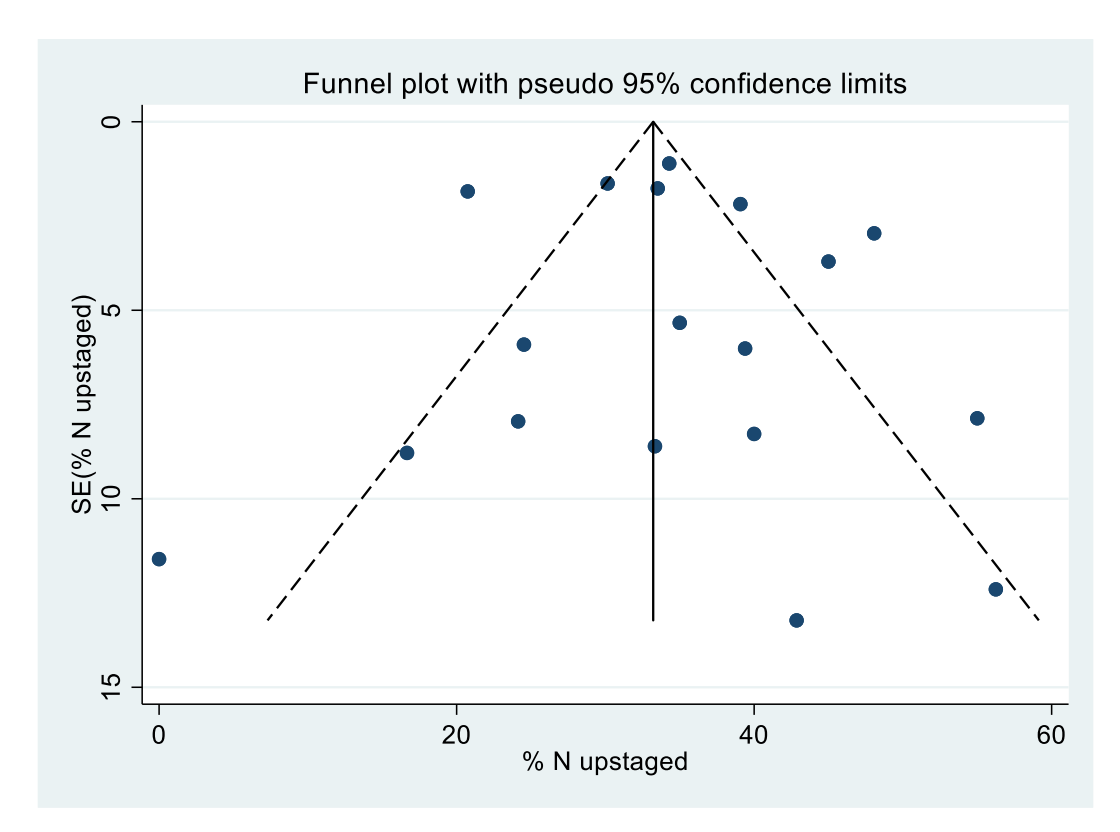


Figure 4.10: Funnel plot for N upstaging

4.4 Discussion

4.4.1 Principal findings

To my knowledge this is the first systematic review and meta-analysis evaluating the accuracy of current clinical staging tests of T2 oesophageal cancer. I only included studies using multimodality staging to reflect current day to day clinical practice. I demonstrate that combined T/N staging was accurate in only 19% of patients. Proportion with accurate T stage was 29%. Percentage of patients who had T downstaged, T upstaged, or N upstaged was 41%, 28%, and 34%, respectively. Small (n<100 patients), single-centre studies reported lower accuracy compared to larger (n>100 patients), multicentre studies. The latter study design has less biases and is therefore more likely to be representative of the truth rather than chance findings. Of note, I found no significant improvement in accuracy in the more recent studies (published after January 2015 and recruitment started after January 2000) compared to older studies (published before January 2015 and recruitment started before

January 2000). There was considerable heterogeneity between studies for all primary and secondary outcomes. This suggests that the study results should be interpreted with caution. I explored this further through subgroup analyses. One particular source of heterogeneity was from OSCC and OAC. Unfortunately, as individual studies did not publish accuracy of tumour staging by histological subtype excluding all patients with OSCC would have greatly reduced the number of patients included in the meta analysis.

This study highlights the urgent need to improve accuracy of clinical oesophageal cancer staging to improve patients' care as well as support therapeutic research in this field. The inaccuracy of staging T2 disease is thought to stem from missed occult nodal metastases, largely at EUS, resulting in under staging of the disease prior to surgery and subsequent upstaging following surgery [205]. However, the study shows that the accuracy for T stage only is equally poor (29%) with even higher rates of downstaging to T1 (41%) than upstaging (28%). The former suggests that a significant proportion of patients are perhaps over-treated with surgery instead of being offered organ-sparing endoscopic therapy. Similarly, a significant proportion are being undertreated and potentially missing out of life prolonging NAT.

Increasing the rates of EUS-guided FNA have been suggested as a way to improve node detection [217], whilst the use of higher frequency probes may improve detection of tumour depth, however, both these techniques will increase the technical complexity of the procedure and their efficacy has not been proven [218]. There are significant resources being applied to improving outcomes for oesophageal cancer patients [69]. For this research to be precise and for the findings from this research to be applicable to clinical practice, the clinical stage of the patients included in these studies must be accurate. EUS has been used in GI imaging since the 1980s [219]. It is used both for diagnostic and therapeutic reasons. Accuracy is highly operator dependent and yet despite improvements in the technology continues to be poor for T2 tumours [220]. Furthermore, approximately 30% of oesophageal tumours are not traversable with the EUS probe at diagnosis [221].

New technologies to aid staging include biomarkers and MRI. Despite the advances in biomarker research, none has become clinically viable for detection and staging of oesophageal cancers [54], [222]. MRI has been shown to be sensitive for T stage but is subject to significant technical challenges [223] such as: movement artefact; MRI bore diameters; and the longer imaging times [224]. Significant improvements have been made with respiratory and cardiac gating [225]. Optical coherence tomography is an advanced imaging technique which uses reflection of infrared light from the target tissue. Unfortunately, the light is only able to penetrate 3mm so it is unsuitable for providing accurate tumour stage.

4.4.2 Study strengths and limitations

This study includes a large number of patients with T2 oesophageal cancer which allows clinical staging accuracy to be assessed with high precision.

In this study, the majority of patients are from Western populations with adenocarcinoma. This accurately reflects the demographic of oesophageal cancer patients seen in Europe and the USA, but perhaps not in Asia.

Three studies included in the review primarily included patients with SCC histological subtype. I note that although the total number of included patients in these studies is 103, the T&N staging accuracy was similar across these three studies to studies primarily including adenocarcinomas, namely, 19% (95%CI 10-28%) for SCC studies compared to 12% (95%CI 7-18%) for adenocarcinoma studies (p<0.01).

It should also be noted that the majority of the studies are from tertiary referral centres. This is probably an accurate representation of the clinical pathway as oesophagectomies are increasingly done in high volume centres [226]. A large proportion of the cases reviewed came from four large USA based studies. These studies were all retrospective and used databases to collect the published data. This may limit some of the applicability of these findings to populations outside of the USA. Unfortunately, the time between index test (clinical staging) and reference standard (pathological staging) was rarely published which could lead to an incorrect

assessment of clinical staging accuracy. While unlikely, this could lead to clinical understaging of the disease status as T and N stage could progress during the time interval between clinical staging and surgery.

Values of heterogeneity indicate an inconsistency between the different studies which will compromise any reliable conclusions that can be drawn from this analysis. This issue is particularly evident in multicentre studies. There was a significant reduction in heterogeneity when calculations are restricted to smaller (n<100) and single centre studies.

Eighteen of the twenty included papers have been published in the past decade and use all imaging modalities currently available in clinical practice which increases the clinical relevance and external validity of this work.

4.4.3 Implications for clinical practice

Patient care and prognosis is fundamentally based around the staging of their cancer at diagnosis. If this staging is inaccurate, clinicians may be offering incorrect therapies or denying patients the correct therapies. The latter may be ineffective or even harmful. For under-staged patients, they may go on to have surgery with curative intent despite having more advanced disease. These patients may suffer unnecessary postoperative complications leading to significant mortality and morbidity as well as being exposed to long-lasting deterioration in quality of life [227], [228].

Individuals who have T or N upstaging following pathological assessment would have not received NAT and are therefore deprived of the additional survival benefit this therapy confers. The survival benefit of giving adjuvant chemotherapy after surgical resection remains unproven [229], [230], [231]. Similarly, Individuals that have T downstaging following pathological assessment may have potentially been candidates for organ preserving endoscopic therapy rather than subjecting them to unnecessary oesophagectomy.

4.4.4 Conclusions

The accuracy of clinical staging for oesophageal T2 cancers remains poor and is largely unchanged in recent years [213]. Patients that were downstaged after surgery may have successfully been treated with endotherapy. The 28% of patients who were upstaged would have been offered NAT according to current guidelines [67], [193], [194].

This data reinforces the need for further research directed at improving T2 oesophageal cancer staging. In addition, this may indicate a greater need beyond T2NO disease. The rationale for reviewing T2NO oesophageal cancer was to enable direct comparison between clinical staging and pathological staging in patients not undergoing neo-adjuvant therapy. This is not possible for patients with clinical staging >T2NO cancer (due to the downstaging effects of NAT) and so it remains a possibility that the inaccuracy I have detected may also affect patients with more advanced cancers.

It is possible that MRI may offer reliable staging in the future but the technical challenges of adapting this technology need to be resolved. Translational technologies such as XPCI which has been used in breast cancer imaging may provide more accuracy than those currently used [66], [232]. Ongoing work looking at adapting current imaging techniques with post processing techniques such as radiomics and artificial intelligence have shown promise in enhancing CT, MRI and PET [233].

Chapter 5 XPCI Methods

This chapter primarily describes the system setups used for XPCI, how tissue was

obtained and the development of specimen holders. The system setups were

designed and refined by Professor Sandro Olivo and his Advanced X-ray Imaging

Group (AXIm). Much of the refinement for this project was led by Dr Jinxing Jiang, Dr

Michela Esposito and Dr Tom Partridge. I led on all tissue acquirement and specimen

holder development.

5.1 Introduction

Having seen in the previous chapter the limitations of current clinical staging. I have

looked to introduce a new technology, namely XPCI, to stage and grade oesophageal

tissue.

This chapter provides a description of:

• The system setups used for XPCI

Methods for obtaining different specimens

Specimen holders

5.2 System setups

Four systems were used. These are listed below:

System 1:

UCL molybdenum system using EI. This used both:

166

a) Non-skipped masks

b) Skipped masks

System 2: HICF system using EI

System 3: UCL copper system using FSP

System 4: DLS Beamline i13-1 using FSP

El and FSP are described in section 1.5.1.1. This section describes the specific setups including different components. Precise parameters used during acquisitions are presented when these are discussed in later chapters.

5.2.1 UCL molybdenum system

This uses a custom-built breadboard scanner (Figure 5.1). The source is a rotating anode molybdenum source (Rigaku 007-HF Micro Max, Rigaku, Japan). This is operated at 40kVp with an applied current between 20mA and 30mA. This produces a broad polychromatic beam with a mean energy of 21keV. The detector is a flat panel detector (C9732DK-11, Hamamatsu, Japan). It has a total sensitive area of 120 x 120mm² and has a 50μ m pixel size. Two pairs of masks were used:

Non-skipped masks

- The sample mask is 5.5cm (horizontally) v 2.0 cm (vertically). The period size is 38 μ m and the aperture size is 12 μ m.

- The detector mask is 6.0cm (horizontally) v 2.5 cm (vertically). The period size is 48 μ m and the aperture size is 20 μ m.

Skipped masks

- The sample mask is 4.8cm (horizontally) v 4.8 cm (vertically). The period size is $79\mu m$ and the aperture size is $10\mu m$.

The detector mask is 6.0cm (horizontally) v 5.5cm (vertically). The period size is 98μm and the aperture size is 17μm.

These masks were manufactured by Microworks GmbH (Karlsruhe, Germany). They were fabricated by electroplating a layer of gold ~120µm thick on a 400µm thick graphite substrate.

(b)

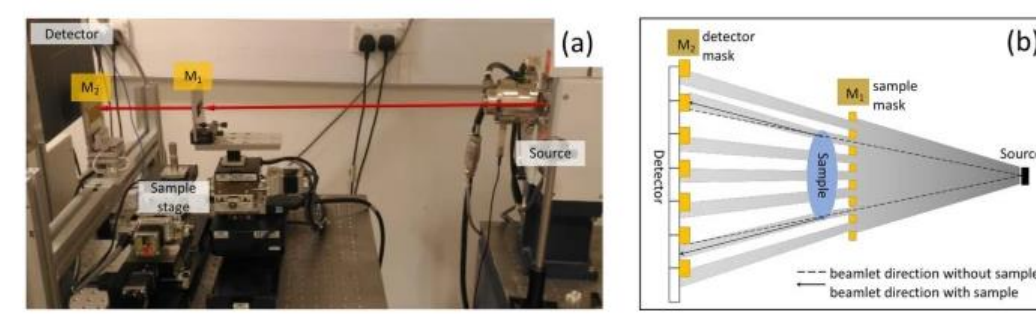


Figure 5.1: showing UCL XPCI- CT system [65]. A) A photograph of the system showing the source, sample mask (M1), sample stage, detector mask (M2) and detector. B) A top-down schematic representation of the system with non-skipped masks in place

5.2.2 HICF system using El

The HICF system is a standalone XPCI setup created for a previous project within UCL. This system was produced using a grant from the Health Innovation Challenge Fund (HICF). This system uses a very similar setup to that described above and shown in the schematic representation (Figure 5.1). The source and detector are largely the same as those used in for the UCL molybdenum system. The system is housed in a radiation shielded enclosure enabling transportation of the system (Figure 5.2). It was based Queen Mary's University (London, UK) and before being moved to Nikon X-TEK systems limited (Tring, UK). The source is run at 40kVp and 24mA.

The masks used are non-skipped with an identical aperture and period size to those used at UCL. The sample mask measures 9x9cm² and the detector mask measures 11.5x11.5cm². The manufacturing process for the masks was the same as for those used in the UCL molybdenum system.



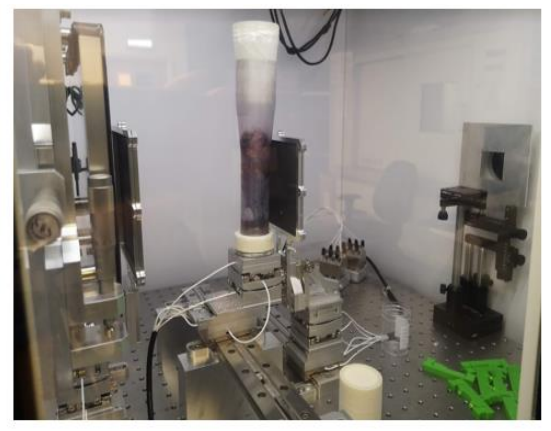


Figure 5.2: Images showing HICF machine. Left-hand image shows entire machine with radiation shielded enclosure. Right-hand image shows sample stage and masks.

The position of the sample, relative to the rest of the setup, can be adjusted with ease. The sample should always be positioned as close to the sample mask as possible. This maximises the distance between the sample and the detector so increasing the sensitivity to phase of the setup (Figure 5.3). The sample and detector masks were aligned before scans were commenced.

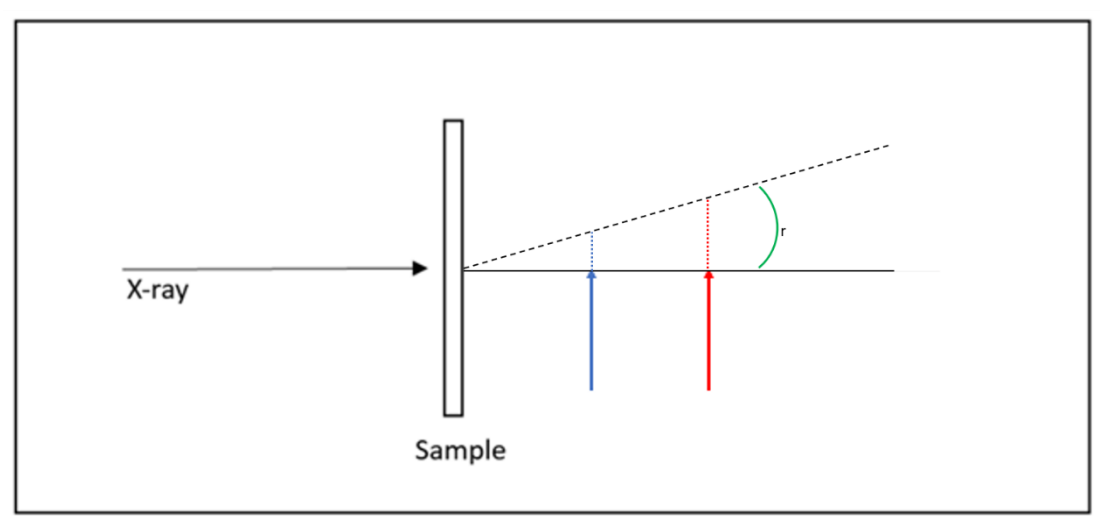


Figure 5.3: Schematic diagram to show the effect of increasing the distance between the sample and detector. Placing the detector at position 2 (red arrow) increases the sample to detector distance (relative to position 1 - blue arrow). This increases the x-ray deviation at position 2 relative to position 1 (shown by the relative difference in lengths of the blue and red dotted lines.

5.2.3 UCL copper system using Free Space Propagation

This system comprises of a Rigaku Multi-Max 9 rotating-anode source, featuring a copper anode. It is operated at 40kV and 20mA. The source is attached to a monochromator producing an x-ray beam at 8 KeV. This is connected to a vacuum tube 200cm in length to minimise photon attenuation. This creates a source-to-sample distance of 204cm. A CMOS (complementary metal-oxide semiconductor) detector with a pixel size of 0.65µm is coupled to a Gadox (Gadolinium oxysulfide) scintillator (Photonic Science). The total available FoV is 1x1mm^{2.} The propogation distance is fixed at 20mm. Identical acquisition parameters are used for all scans. This consisted of 1200 angular steps, each consisting of 6 frames with a 10s exposure time. The total acquisition time is ~18hours.

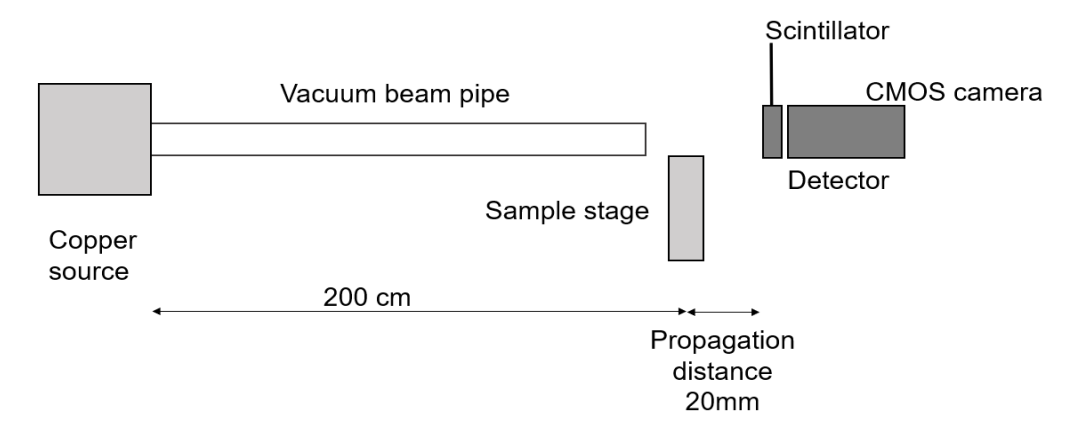


Figure 5.4: Schematic diagram of UCL copper source and monochromator for FSP

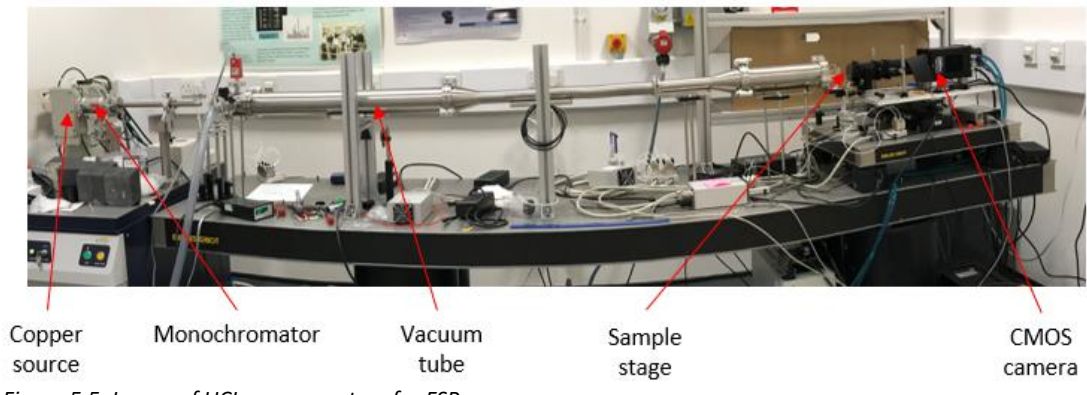


Figure 5.5: Image of UCL copper system for FSP

5.2.4 Diamond light source Beamline i13-1

The third system described is DLS beamline i13-1 (Figure 5.6). A narrow bandwidth polychromatic source centred around 15kV to maximise the available flux was used. The detector is a PCO Dimax CS1 coupled with a x10 optical lens. This produces an effective pixel size of $1.1\mu m$ and a FoV of $2.2x2.2mm^2$.

Identical acquisition parameters are used for all scans. These consisted of 1500 projections, with an exposure time of 3 secs/view. The total acquisition time is $1\,\%$ hours.



Figure 5.6: Image of DLS beamline i13-1

5.3 Human specimens

Our objective was to image multiple specimens using different systems. All human specimens were collected according to UK research guidelines. Ethical approval was granted by the London - Westminster Research Ethics Committee with UCL as the sponsor (ISRCTN registration 11347879). To obtain these specimens different

methods were used. Specimens were obtained either from the UCL biobank (see section 5.3.1) or "fresh" (see section 5.3.2).

The inclusion criteria were males and females over the age of 18 years and ability to provide written, informed consent. Specifically for biopsies, these were collected from patient with suspected or documented BO. For endoscopic resections, these were patients who were scheduled for a resection due to oesophageal dysplasia or an early stage oesophageal cancer. For oesophagectomies, these included patients with local oesophageal cancer who were scheduled for oesophagectomy.

The exclusion criteria were patients on anticoagulation, patients with oesophageal varices, patients who were pregnant and patients with a history of haemostasis disorder (including but not limited to haemophilia, thrombocytopaenia or coagulopathies).

For experimental purposes, four types of oesophageal biopsies were needed. These were normal (squamous), NDBO, DBO and OAC.

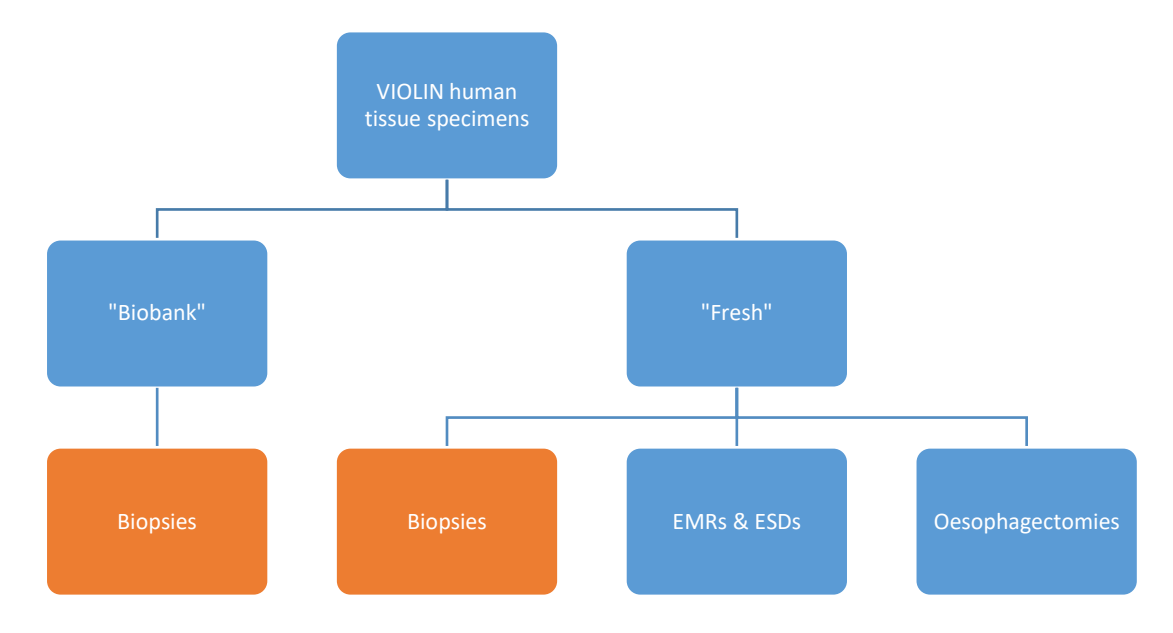


Figure 5.7: Diagram showing source of different specimens – note there were two sources of biopsies (highlighted in orange).

5.3.1 Biobank

The first group of biopsies, due to time constraints, were obtained from the UCL biobank. These were from patients that had previously given consent for additional research biopsies to be taken as part of the HALO study (Chapter 3). Fifteen biopsies of each tissue type, previously mentioned, were identified. The paraffin blocks in which these biopsies were stored were identified. The biopsy was punched out of the block before being returned to a formalin solution by reversing the process discussed in section 1.2.8.4. These are referred to as "biobank biopsies".

5.3.2 Fresh tissue

The second group of specimens were collected from patients attending UCLH for OGD or surgery. Endoscopy and surgical lists were screened prior to patient attendance to identify patients with relevant oesophageal pathology. Informed written consent was taken from patients prior to their procedure. Consent was taken using the trial consent form by myself or another member of the team. This was either on the day of admission for patients undergoing oesophagectomy or on the day of their procedure for patients having an OGD.

All biopsies obtained for this project were in addition to any required for the clinical pathway. EMR and oesophagectomy specimens remained part of the clinical workflow and therefore needed to be returned after imaging. All specimens were placed directly in formalin solution.

All patients recruited to the study were logged and given a unique identifier beginning with a letter referring to the type of tissue obtained. Biopsy patients were referred to as B01, B02 etc... Endoscopic resection patients were referred to as E01, E02 etc... Oesophagectomy patients were referred to as S01, S02 etc.

A Subject Identification Log allowing cross referencing of unique identifiers with subject hospital identification number, date of birth and full name was kept on a secure NHS computer.

5.4 Sample containers

The containers for each specimen and setup need to have the following three features:

- 1. Prevent specimen from moving
- 2. Fit into the field of view (FoV) of different XPCI systems
- 3. Minimise attenuation

5.4.1 Prevention of movement

I was concerned about two forms of movement. Firstly, movement as a result of drying of specimens and secondly movement of the specimen within the container. To minimise drying of the specimens I used sealable, water-tight containers that would enable a humidified micro-environment to be created around the specimen. In addition, drying of the specimens could compromise histology. As some of these specimens were still required for clinical care it was vital to avoid this.

Due to the variation in size of different specimens (biopsies, endoscopic resections and oesophagectomies) I aimed to produce containers for each specimen type.

5.4.2 Fit into the field of view of different XPCI systems

Another specification of any container would be ensuring it fit within the limited FoV of each XPCI setup. This will be discussed in more detail for each specimen and setup.

5.4.3 Minimise attenuation

Containers should cause minimal attenuation of photons during scanning. This is particularly important when using lower flux x-ray sources. This principle applies to all specimens I planned to image.

It should be noted that due to the very small FoV and high sensitivity to even small movements of the copper setup I used glass capillary tubes which had previously been shown to be reliable [234].

5.4.4 Sample types

5.4.4.1 Biopsies

Biopsies used for scanning were taken in addition to those required for clinical practice. Therefore, these biopsies could be cut to size to fit the system requirements. This is not an option for EMRs, ESDs or oesophagectomies which remained part of the clinical pathway.

5.4.4.1.1 CT imaging

5.4.4.1.1.1 Synchrotron setup

For imaging at DLS, biopsies were held in a pipette tip. Four biopsies were placed inside a pipette tip that had been mounted on a sample stage magnet (Figure 5.8). They were carefully placed in sequence to reduce the possibility of misplacing samples and to ensure a small gap remained between them. A small amount of liquid was transferred with each biopsy and left in situ. The top of the pipette tube was sealed with blue tack to minimise any sample drying.

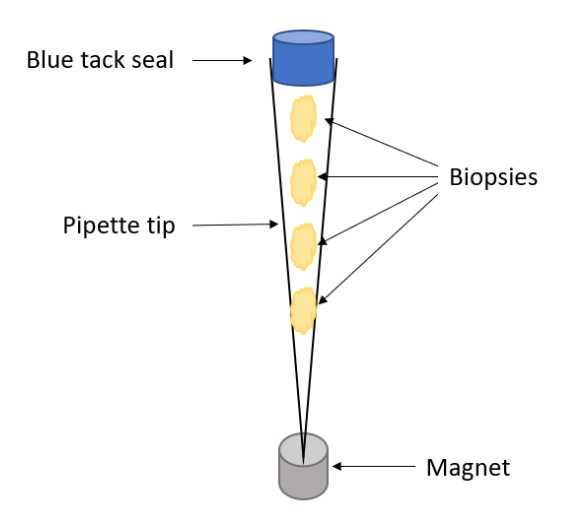


Figure 5.8: Pipette tip containing biopsies for CT imaging at DLS

5.4.4.1.1.2 UCL lab setup

At UCL the scan times are significantly longer due to the lower flux of a conventional x-ray source relative to a synchrotron source. Therefore, this setup needed to be more stable as the risk of movement increases with longer scan times. A glass capillary mounted on a brass pin and sealed with wax was used. The glass capillaries were supplied by Hampton Research and either measured 0.5mm or 1mm in diameter, with a 0.1mm thick wall.

To assist with reconstructions glass beads ~50μm in size were placed on the outside of the capillary to act as a reference for any movement. These were attached using molten wax. It was found that the smallest amount of heat would cause ethanol in the capillary to vaporise, creating bubbles which could introduce artefacts. To minimise the risk of this, the glass beads were attached prior to the capillary being filled with ethanol. Biopsies would be placed inside the capillary and held in place with a piece of nylon filament. The capillary was cut above the biopsies so any bubbles introduced to the capillary would remain above the biopsies and out of the FoV. The capillary was sealed with wax.

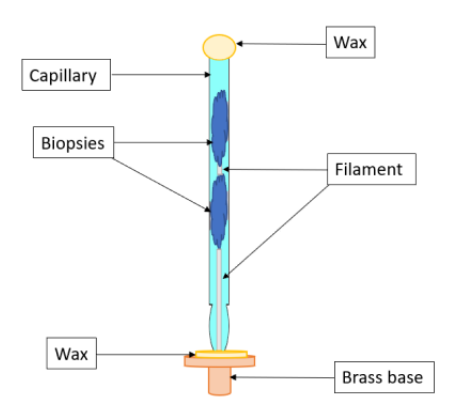


Figure 5.9: Schematic diagram showing biopsy setup for scanning. Microbeads were attached to the outside of the capillary. The setup could contain a single biopsy or two biopsies as depicted here.

After scanning, the glass capillary was cut just below each biopsy and the lowest extent of the biopsy was marked with red tissue marking die. This was done to assist with orientation of the biopsies when sent for histology. The biopsies were carefully removed from the glass capillary, marked with tissue marking dye and finally placed in formalin solution.

All biopsies were sent for serial sectioning. This involves the entire volume of the biopsy being sliced into 3-4 μ m sections.

5.4.4.2 Oesophagectomies

Dimensions of surgical specimens are recorded when received in histopathology. These measurements are taken at initial histological assessment before the specimen is cut up. Prior to designing an initial prototype, I reviewed the measurements of historical oesophagectomy specimens at UCLH. I identified 22 oesophagectomy pathology reports from the preceding two years. The measurements taken included oesophagus length, oesophagus width, greater curve length and lesser curve length (Figure 5.10). Tissue shrinks considerably after resection and also during fixation [235] but as all tissue would be fixed prior to imaging this would not affect this analysis.

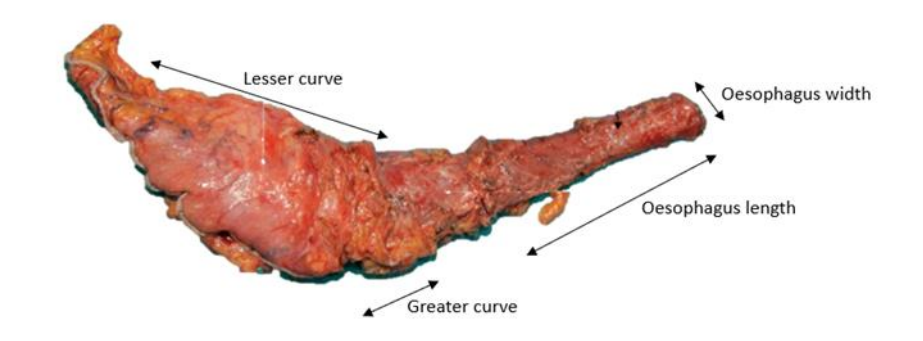


Figure 5.10: Oesophagectomy specimen with anatomical landmarks labelled.

A high level of variability across three of the four dimensions was identified (Figure 5.11). The length of the oesophagus, greater curve and lesser curve all had an interquartile range (IQR) greater than 10mm. The median length of a resected oesophagus was 62.5mm (IQR 55-75mm) and the median width was 25mm (IQR 20-30mm). The median length of the greater curve was 53.5mm (IQR 45-70mm) and the median length of the lesser curve was 54mm (IQR 40-75mm).

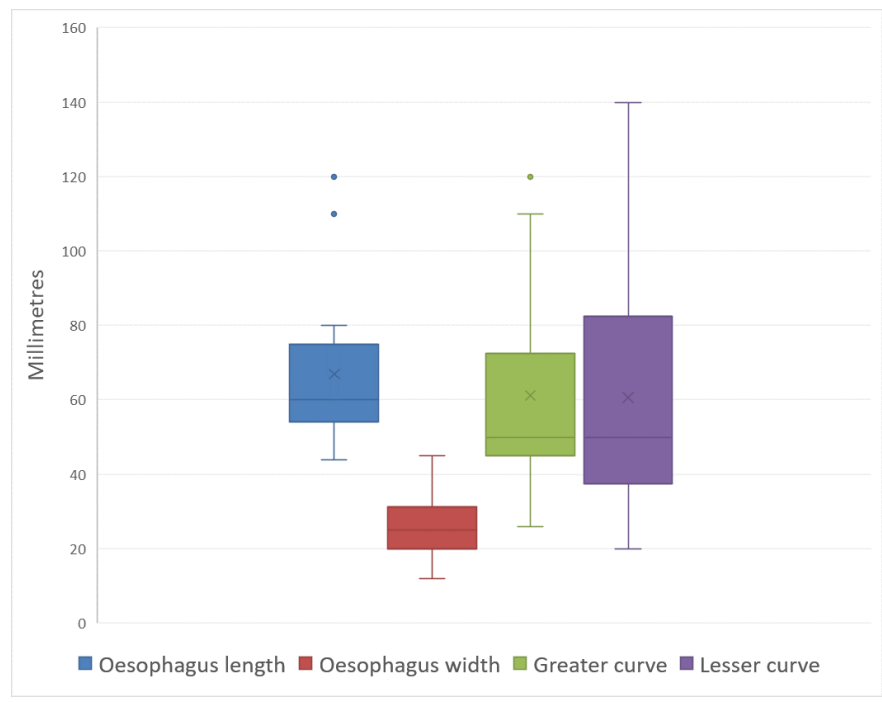


Figure 5.11: Graph showing distribution of measurements for oesophagectomy specimens

5.4.4.2.1 Prototypes

After discussion with members of the engineering department at UCL it was suggested that using 3D printing would enable bespoke containers to be produced in a timely fashion. I created designs using Fusion 360 (Autodesk, Ca, USA), a computer-aided design software. These were printed using Cura software (Ultimaker, Utrecht, Netherlands) in PLA (polylactic acid).

PLA was chosen as the material of choice after some initial trials with PLA, Acrylonitrile Butadiene Styrene (ABS), polycarbonate (PC) and high impact polystyrene (HIPS). Containers produced using PLA were considerably less likely to leak, when printed using Ultimaker S3 and S5 printers.

5.4.4.2.1.1 Prototype 1

The initial container produced is shown below (Figure 5.12). It was a single piece container and featured a central core to hold the specimen in place and a large funnel region to accommodate the stomach. This funnel extended above the sample mask. This allowed the specimen to be positioned close to the sample mask.

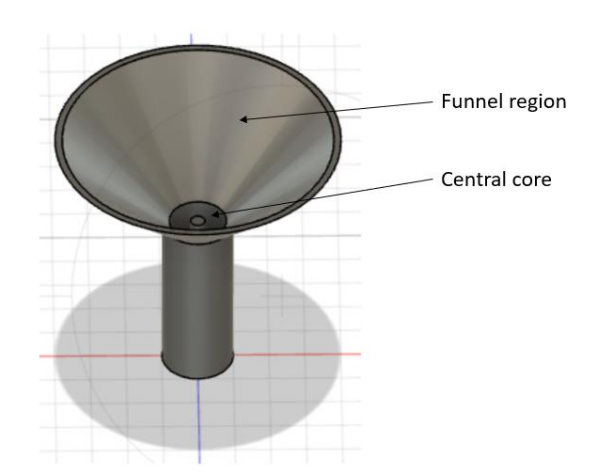


Figure 5.12: Prototype oesophagectomy holder – with central core and funnel region

I took single projection images of this container using the molybdenum setup. Unfortunately, I found the thickness of the walls and the central core led to \sim 40% attenuation of photons.

5.4.4.2.1.2 Prototype 2

The second design used a single piece container. Rather than having a central core a temporary scaffold was used to provide rigidity during fixation. This central scaffold was removed before imaging (Figure 5.13). The scaffold took the form of a 200mm hollow cylinder with holes printed into it. Sutures were passed through these to tie the oesophageal tissue to the scaffold. The holes were placed at different heights to accommodate specimens of different sizes.



Figure 5.13: Scaffold for oesophagectomies

In addition, after discussion with members of the engineering faculty I was advised to use a spiralised technique to print containers (Figure 5.14). This method lays a continuous line of filament which spirals upwards producing containers with thinner walls. By printing with this technique, I produced containers with 0.4mm thick walls.

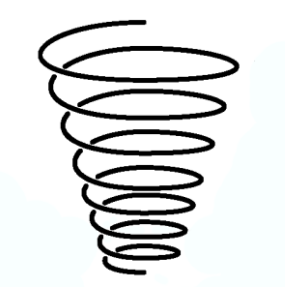


Figure 5.14: Image depicting spiralised 3D printing technique

The design for prototype 1 was adapted for producing this prototype (Figure 5.15). This continued to use a funnel at the top of the cylinder to hold the stomach. The design was adapted in three ways. Firstly, the walls were thinner (0.4mm vs >1mm). Secondly, the central core was removed. Finally, a vertical rim was added at the top of the funnel to allow a lid that would be able to sit within this region.

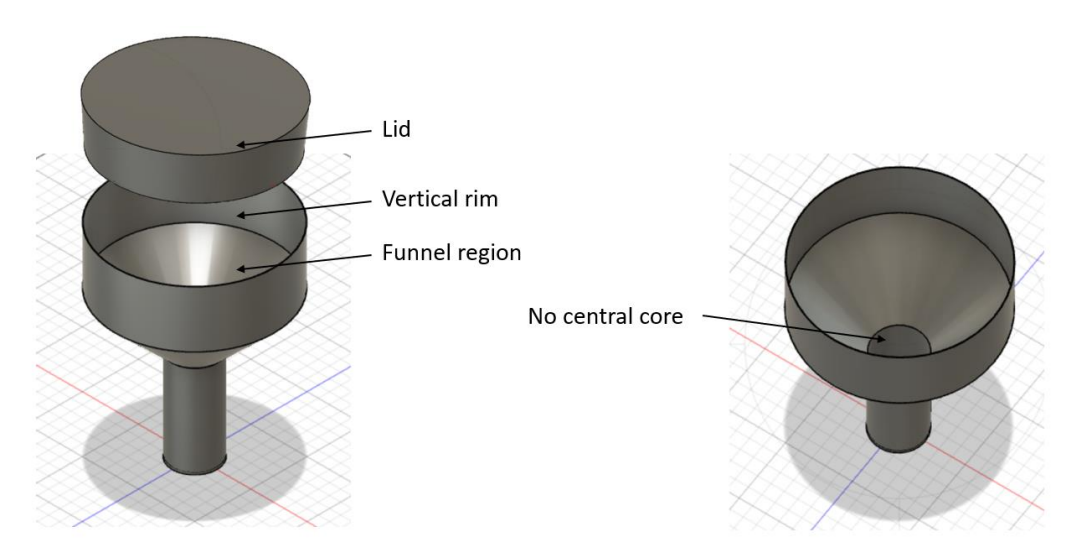


Figure 5.15: Prototype 2 container with lid. Printed with spiralised method.

Unfortunately, this container was found to be extremely weak at the points the container changed shape (Figure 5.16). The container cracked even before specimens were placed inside compromising the seal of the unit. The angles at these points were both ~45°.

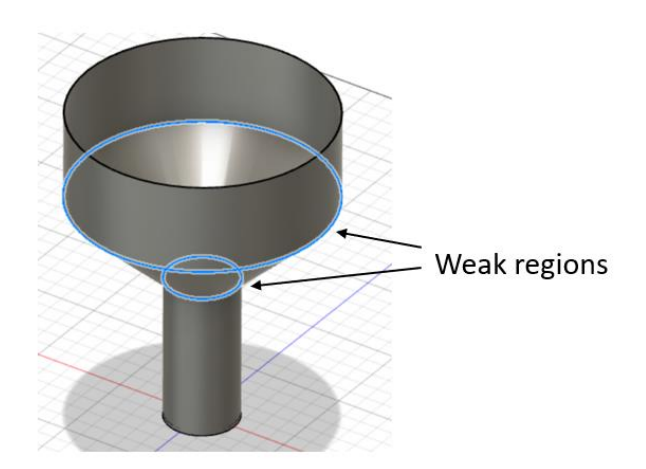


Figure 5.16: Image highlighting week regions of prototype 2.

5.4.4.2.1.3 Prototype 3

Given the weakness of prototype 2 a third prototype was developed (Figure 5.17). This used the same spiralised method (Figure 5.14). To increase the strength of the container the angles where the container changed shapes were reduced to ~5°. This reduced the volume of gastric tissue that could be accommodated within the container.

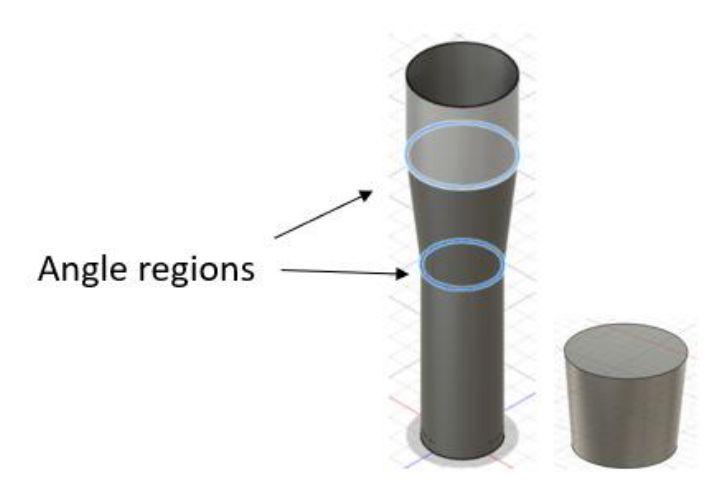


Figure 5.17: Prototype 3 and lid showing a less flared cone reducing the angle at the weak points seen in prototype

This was discussed with the team's pathologist (Prof Marco Novelli (MN)) who decided that as the distal gastric resection margin is significantly distal to the tumour some of the excess gastric tissue could be removed during histopathological assessment (Figure 5.18). This allowed the gastric tissue that remained contiguous with the oesophagus to be held in the smaller funnel region of prototype 3.

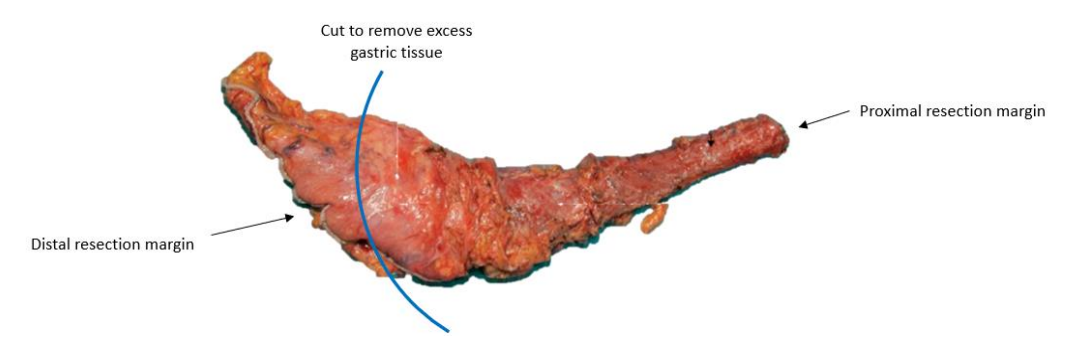


Figure 5.18: Oesophagectomy specimen showing area of gastric tissue that could be removed

Prototype 3 containers when combined with the temporary scaffold achieved the three objectives stated previously for oesophageal specimens imaged in the molybdenum XPCI setup.

To accommodate the variety in sizes of the specimens I printed different diameters of containers. These ranged from 28mm to 40mm (which is the maximum FoV of the molybdenum setup at UCL).

The specimens were placed in the smallest possible container (Figure 5.19). I ensured the proximal resection margin was resting on the base of the container and 20mls fluid (either ethanol or formalin solution) was left at the bottom of each container with the aim of maintaining a humidified environment. The lid was sealed using Parafilm® a waterproof stretchable thermoplastic.

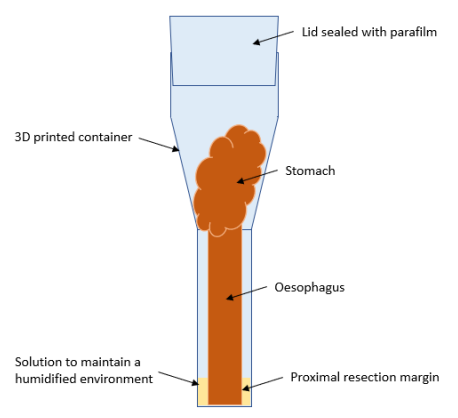


Figure 5.19: Schematic diagram showing how oesophagectomy specimens were held for imaging.

Further analysis of the degree of attenuation caused by different containers was performed by comparing four 3D printed containers against three that were commercially available. To compare the attenuation caused by different containers I took single projection images of each container using the UCL molybdenum setup (Section 5.2.1). I used the ratio between the mean photon counts inside (Figure 5.20B) and outside the container (Figure 5.20A). This was plotted on the graph below (Figure 5.21). These results show that the 3D printed container attenuate far fewer photons. On average the 3D printed containers attenuated 9% less photons than the commercially available containers.

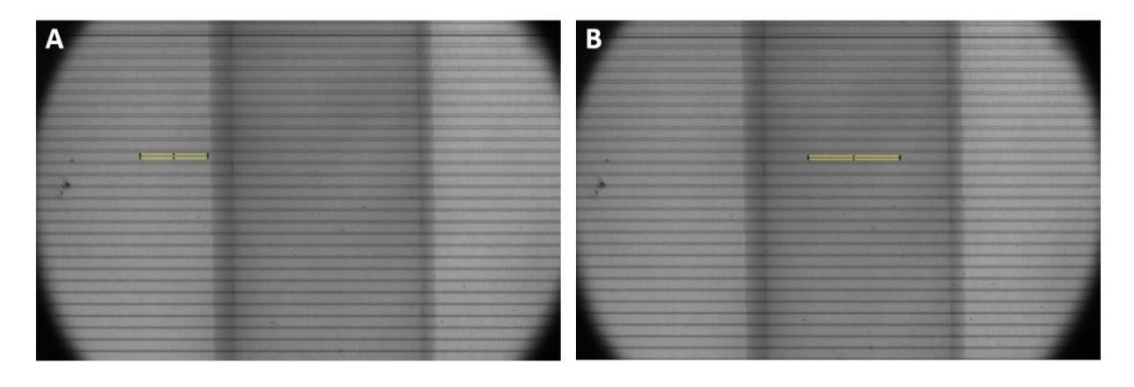


Figure 5.20: Projections of 3D printed PLA container. Image A yellow box shows an example area outside the container; Image B yellow box shows an example area inside the container.

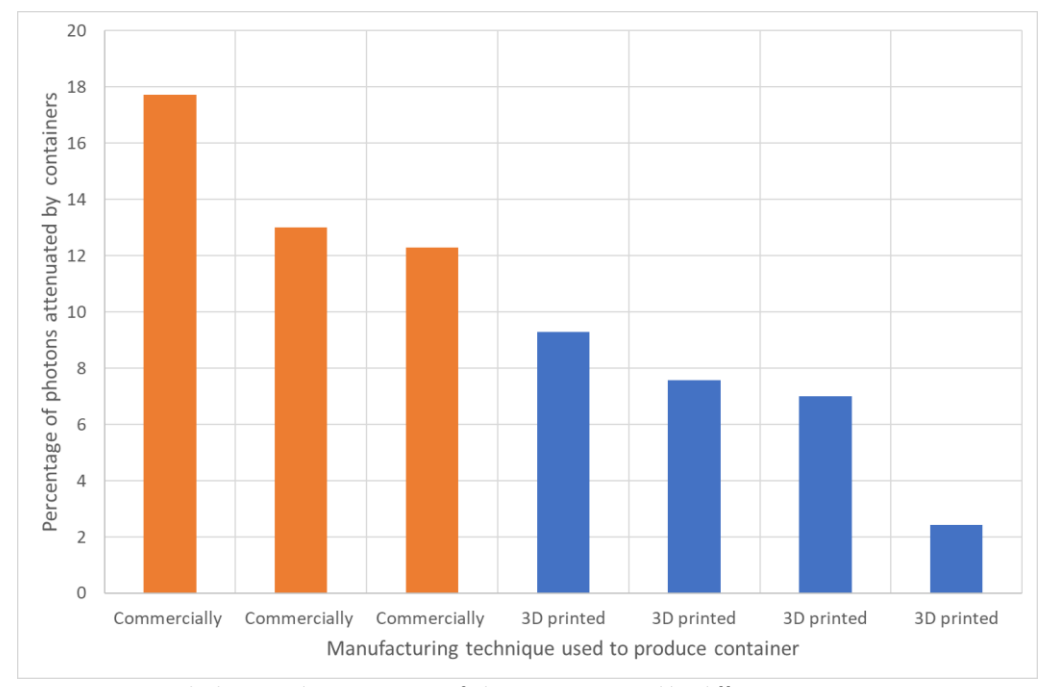


Figure 5.21: Graph showing the percentage of photons attenuated by different containers.

The commercially purchase pots were empty cosmetic jars produced by different manufacturers. The wall thickness of the containers were 1mm for two and 1.2mm for the third. These were all purchased online. The 3D printed sample containers were all made from PLA. Three were made using a standard technique with a three had a 0.4mm wall thickness and the container with the least attenuation was 0.25mm thick.

5.4.4.3 EMRs and ESDs

EMRs are resected using a standard piece of equipment (Figure 5.22) [236]. This leads to less variation in the specimen sizes than with oesophagectomies. EMRs are typically 6-10mm in diameter and 2-3mm in depth. If a lesion is larger than this multiple EMR specimens are resected.

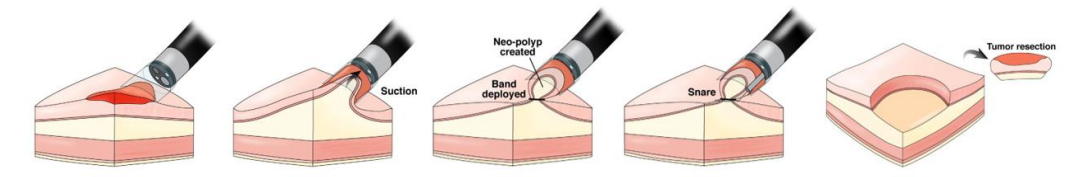


Figure 5.22: Cap and snare EMR technique highlighting relatively uniform size of resection specimens

There is more variation in size of ESD specimens. This is due to the endoscopist aiming to resect the lesion en-bloc, in one entire piece. These specimens range from 10mm to the entire cross-sectional area of the oesophagus (30mm). The thickness is very similar to EMRs.

Before designing a sample container, I needed to consider how these specimens would be orientated during scanning. Specimens could be scanned in one of three different positions as shown below (Figure 5.23).

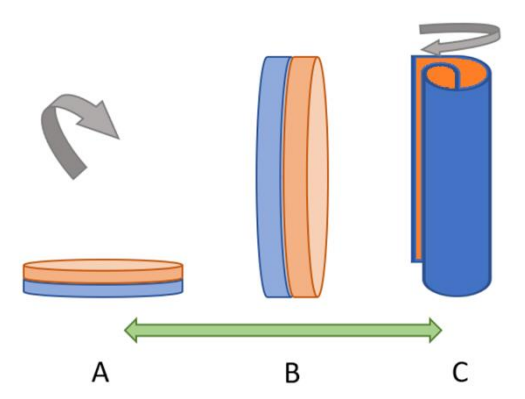


Figure 5.23: Schematic diagram showing different positions for imaging EMR and ESD specimens. The submucosa is illustrated in blue and mucosa in orange.

I planned to use the UCL molybdenum setup with skipped masks as described previously in section 5.2.1. To achieve the highest resolution image dithering steps, described previously in 1.5.1.1.1, would be performed by moving the sample horizontally with respect to the setup (i.e. source, masks and detector). This means

that the potential horizontal resolution of the setup is higher than the vertical resolution (as there is no dithering in this direction).

The aim was to see if tumour invasion could be visualised through the tissue layers (i.e between the orange and blue regions seen in Figure 5.23). If the specimen was placed as shown in image A this high resolution would not be in the direction of interest but if the specimen was placed vertically (as shown in image B) the high-resolution plane would be correctly orientated.

Placing a specimen in such a way creates a separate problem for CT imaging. If a specimen is significantly thicker in one direction than another there is much more attenuation of photons at certain projection angles compared to others. I have shown a theoretical example of this in Figure 5.24. In scenario A the specimen is placed at such a projection angle that photons (indicated by the arrows) need to pass through its smallest dimension. In this theoretical setup 2/3 of photons pass through the specimen. In scenario B, the specimen has been rotated such that the photons now need to pass through the longest dimension before reaching the detector. More photons are attenuated with only 2/9 reaching the detector. This creates a beam hardening artefact, plus photon starvation can occur at the angles corresponding to the highest attenuation.

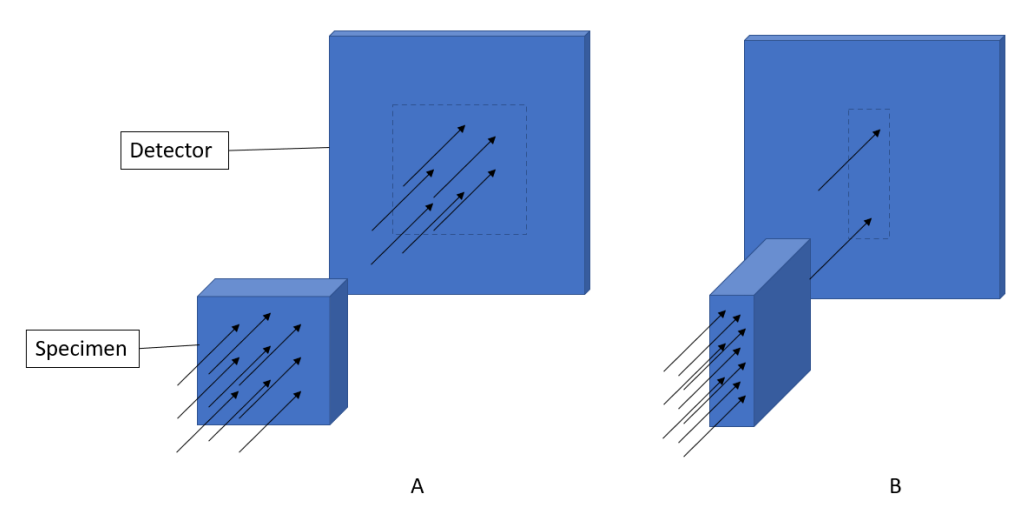


Figure 5.24: Schematic diagram of a theoretical setup that shows the effect of specimen orientation on photon attenuation

By rolling EMRs and ESDs I created a near cylindrical specimen (Figure 5.23C), thus avoiding these issues. It should also be noted that this would also enable the specimens to be placed in the smallest available container reducing movement and the risk of drying. As all tissue had been fixed prior to this rolling process once the scans had been completed the tissue could be returned to its normal flattened state for clinically histological assessment

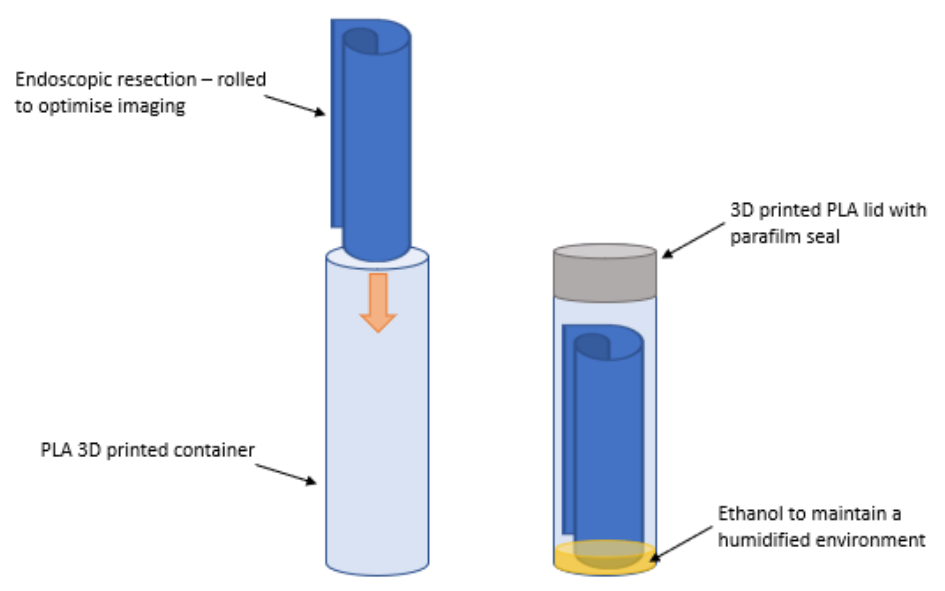


Figure 5.25: Schematic diagram showing how endoscopic resections were held for imaging

I created EMR/ESD containers as previously described using a spiralised technique (Figure 5.26). It was also possible to buy containers of varying sizes which would have possibly met the previously stated criteria. These containers were used for the porcine oesophagus preparatory work (Chapter 6).

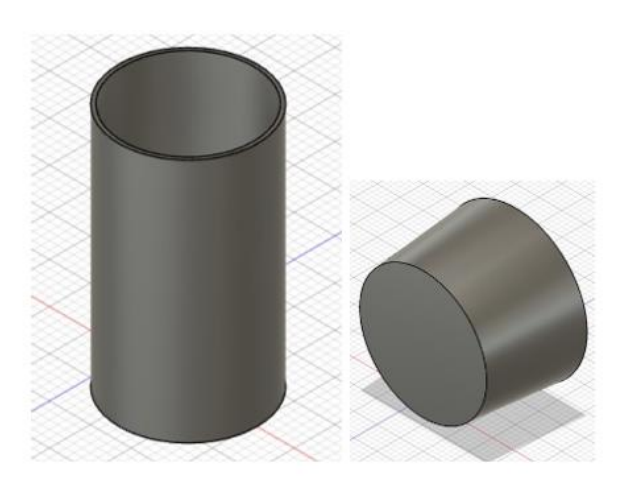


Figure 5.26: Container and lid for smaller specimens – EMRs, ESDs and porcine oesophagus

To accommodate the different sizes of specimens and to minimise the risk of movement artefact I printed containers with a range of diameters. These ranged from 6mm to 10mm.

5.5 Summary

This chapter shows how I have developed methods for tissue collection. It also shows how I have designed and produced containers tailored to both the system setups and the challenges of each specimen.

In the next chapter I will use these containers to develop tissue preparation and imaging techniques using porcine tissue.

Chapter 6 Preliminary oesophageal work

The following chapter describes early work to establish protocols for imaging human oesophageal tissue. I led much of this work with assistance from Dr Jinxing Jiang who launched many of the scans and performed most of the reconstructions.

6.1 Introduction

Prior to working with human tissue, preliminary experiments were performed. The rationale was 3-fold. Firstly, obtaining human tissue was complex (see section 5.4.4) as there was a finite supply of tissue, and the precise timing of specimen arrival could never be guaranteed. Secondly before handling human tissue, particularly specimens that remained vital for patient management, it was important to ensure no tissue damage occurred during this work. Finally, it was important to ensure that the tissue preparation techniques used and scan parameters were optimised.

XPCI has been used to image a wide spectrum of animal tissues ranging from rat oesophagus and liver [160] to mouse hearts and lungs [237]. However, to date, there are few cases in the literature on XPCI being used to image human tissue that has remained part of the clinical pathway. Published studies have used dried, formalin fixed and ethanol dehydrated tissues [65], [237], [238], [239].

It is not possible to dry tissues that are to be used for histological diagnosis due to the risk of inducing drying artefacts. Therefore, I prepared formalin fixed and ethanol dehydrated tissue for scanning. These results would be assessed prior to finalising the protocol for human tissue.

6.2 Aim

To test the hypothesis that it is possible to prepare tissue for XPCI without affecting later histological assessment.

6.3 Methods

I obtained fresh porcine oesophageal tissue from Medical Meats a private company specialising in providing animal tissue for research. The fresh tissue was collected from a commercial abattoir at the time of slaughter, chilled and couriered to UCL. On arrival this tissue was sutured to a scaffold (Figure 5.13 & Figure 6.1). This reduced tissue shrinkage during fixation and enabled the tissue to fix straight whilst maintaining a patent lumen.

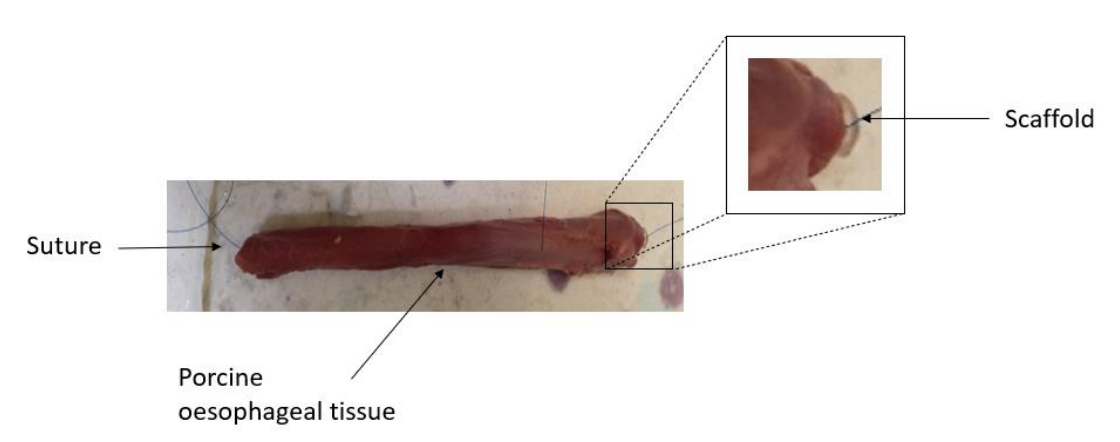


Figure 6.1: Porcine oesophageal tissue attached to scaffold with sutures

The tissue was placed in 10% formalin solution 6 days. After fixation was complete three rings of tissue 2cm in length were cut from one end of the oesophagus (Figure 6.2). These were labelled A, B and C.

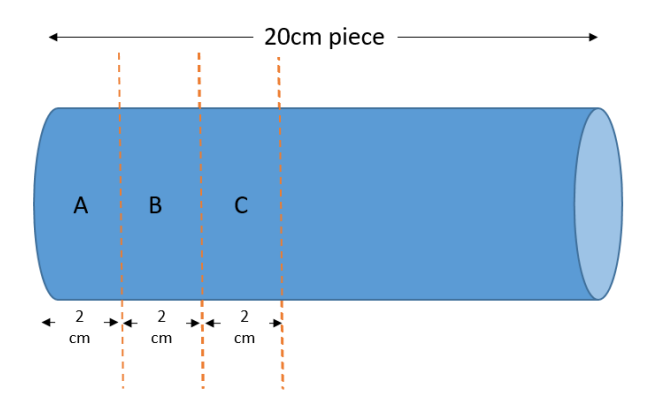


Figure 6.2: Schematic diagram showing sections of porcine oesophagus

Each of these samples were prepared according to the table below (Table 6.1). This was based on Godkar's tissue processing technique (section 1.2.8.4) [240]. Sample A underwent step 1, B steps 1-6 and C steps 1-9, respectively.

Table 6.1: Protocol for porcine oesophagus processing.

Step	Solution	Time	
1	4% formaldehyde	6 days	
2	80% ethanol	45mins	
3	80% ethanol	45mins	
4	90% ethanol	45mins	
5	100% ethanol	45mins	
6	100% ethanol	45mins	
7	100% ethanol	15hrs* (overnight)	
8	Xylene	45mins	
9	Xylene	45mins	

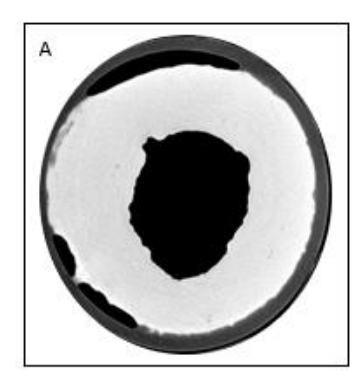
Each piece of tissue was placed inside a 20mm diameter 3D printed container, produced as described previously (section 5.4.4.3). A small amount of liquid was placed at the bottom of each container to maintain a humidified environment. The liquid for sample A was formalin, for B 100% ethanol and for C xylene. The container was sealed with a 3D printed PLA lid and parafilm (Figure 5.19).

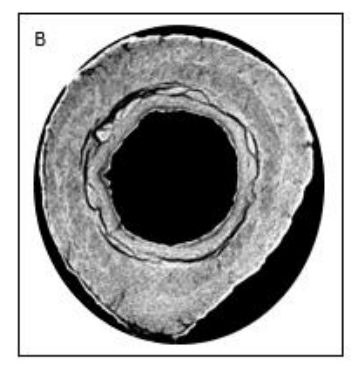
The samples were imaged using the molybdenum low resolution system with non-skipped masks (section 5.2.1) at 20mA. All the scans had identical parameters and took ~ 3hours. Each scan consisted of 1200 projections and 2 dithering steps. Each view had an exposure time of 1.5secs.

The samples were returned to formalin by performing the steps above in reverse (Table 6.1). They were then sent for histological processing. Reconstructions were performed using MATLAB software (Mathworks, USA).

6.4 Results

The results from these scans are seen below (Figure 6.3). Image A shows sample A saturated in formalin image B shows sample B saturated in ethanol and image C shows sample C saturated in xylene.





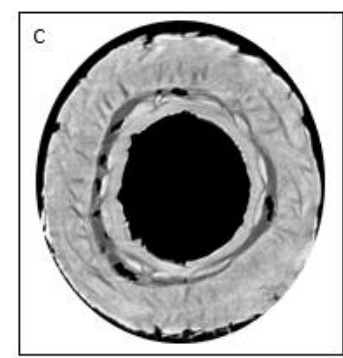


Figure 6.3: Reconstructed CT slice from samples A, B and C.

In sample A there is no contrast between the tissue layers. The entire thickness of the oesophagus is homogeneous with only some of the connective tissue surrounding the sample being distinguishable.

Both samples B and C show much improved contrast through the tissue. In sample B it is possible to clearly see the submucosa and muscle layers, furthermore, the mucosa appears bright. Sample C shows improved detail in the muscle layers compared with sample B but there is a loss of contrast of the mucosa. Although the images are adequate for this preliminary work the images all have a grainy appearance. This is likely due to excessive noise in the projections.

All samples were sent for histology. The tissue was unaffected by the processing before and after each scan.

6.5 Discussion

These experiments were useful and encouraging. I developed tissue processing methods which improved contrast in tissue layers whilst preserving the tissue for histology. Ethanol and xylene both improve contrast substantially. After review of the imaging the difference in contrast within samples B and C was felt to not be significant.

Xylene is a hazardous hydrocarbon with toxicity ranging from headache to loss of consciousness and even death [241]. It is known to cause skin irritation and hearing disorders. Xylene is also a potent solvent and can dissolve a large range of plastics. These factors add to the complexity of using xylene therefore it was decided to exclude xylene from further work.

The grainy appearance of the slices is likely due to low SNR (see section 1.4.4.1). In further scans attempts to increase the signal by altering the scan parameters (increasing the mA, number of projections and exposure time) will be made.

After discussion the plan was to examine these results using biopsies. I wanted to ensure these results were reproducible. In addition, I wanted to see if the increased contrast seen when tissue is saturated with ethanol remains once the tissue is returned to formalin. Could the physical composition of the tissue have been altered?

Chapter 7 Preliminary biopsy work

The following chapter describes early work to establish protocols for imaging human oesophageal biopsies. I led much of this work with assistance from Dr Jinxing Jiang who launched many of the scans and performed the reconstructions.

7.1 Introduction

Chapter 6 introduced the concept of saturating tissues with different solutions to improve contrast generated during XPCI scans. On reviewing the literature, a number of teams have used ethanol to improve image contrast.

One paper assessing white-matter injury in brain tissue hypothesised that the increased contrast, after water was removed, was due to a mismatch of the refractive indices between different tissues [242]. They suggest that this change occurs because different tissues have higher lipid content and are so less affected by dehydration than other tissues. Other hypotheses for the improved contrast are the increased rate of drying seen in ethanol saturated tissue or removal of some tissue elements [243], [244].

To understand better what causes the changes seen in Chapter 6 I would like to assess if these changes in contrast generated are reversable.

7.2 Aim

To test the hypothesis that the improved contrast seen after saturating a specimen in ethanol remains even when the tissue is returned to formalin solution?

7.3 Methods

A "Fresh" biopsy was obtained as previously discussed (see section 5.3.2). This biopsy was scanned three times (Figure 7.1) using identical parameters with the UCL copper

system (see section 5.2.3). Scan one was performed with the biopsy immersed in formalin. After this scan, the biopsy was placed in graded ethanol (Table 6.1 - steps 1-7) and returned to a glass capillary for scan 2. Each step was reduced to 15mins due to the smaller size of the tissue being processed. Following this the biopsy was returned to formalin using graded ethanol (Table 6.1 - steps 4-1). The biopsy was then returned to a glass capillary for scan 3.



Figure 7.1: Flow chart showing method for preliminary biopsy experiment

7.4 Results

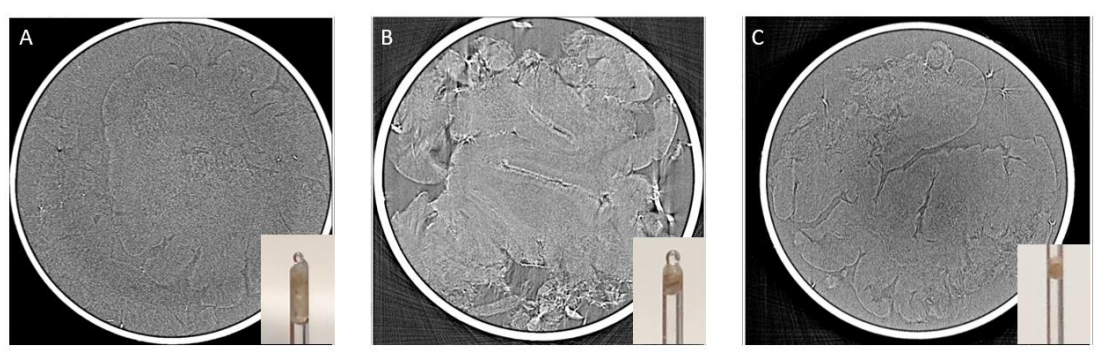


Figure 7.2: Results from preliminary biopsy work. Image A shows a slice from the first scan CT (biopsy in formalin). Image B shows a slice from the second scan CT (biopsy in ethanol). Image C shows a slice from the third scan CT (biopsy in formalin). The inserted pictures in the bottom right of each image show the biopsy mounted in the capillary.

Our results are shown above in Figure 7.2. Image A shows scan 1 with the specimen in formalin. The outline of the sample is visible but there is poor contrast within the biopsy. Image B shows scan 2 in which contrast can be seen throughout the specimen. The inserted picture of the biopsy held in the capillary shows the size of the specimen has reduced in size substantially. Image C shows scan 3 in which most of the contrast within the specimen has been lost. There is slightly more contrast than is seen in image A. The inserted picture of the biopsy held in the capillary shows the size of the specimen has reduced in size even further.

7.5 Discussion

There is increased contrast within the specimen when saturated with ethanol (Figure 7.2). Most of this contrast is lost when the specimen is returned to formalin solution. The volume of the specimen becomes smaller as the experiment proceeds making comparison of the images slightly harder, especially direct comparison of scan 1 and scan 3. However, given image B has the greatest contrast this suggests that ethanol alters the mismatch of the refractive indices between different tissues. If some of the contrast generated in ethanol is due to removal of lipids then the effect of this is minimal as image C would retain more contrast relative to the contrast seen in image B.

Both this work and Chapter 6 have provided positive findings. This has enabled the experimental methods to be refined for subsequent work. The benefit of ethanol in tissue preparation has been shown along with achieving more reproducible results which can be taken forward for further work on human tissue.

Chapter 8 VIOLIN – Oesophagectomies and Endoscopic Resections

This chapter was a collaboration of many individuals. The original grant was awarded to Professor Sandro Olivo, Professor Laurence Lovat and Professor Marco Novelli, who provided support and advice throughout. I identified and consented all patients. I prepared oesophagectomy specimens with the assistance of histopathologists from UCL, launched and reconstructed many of the scans and matched these to histology. Dr Jinxing Jiang and Dr Tom Partridge assisted with scanning specimens and improving the many reconstructions.

8.1 Aims

Objective 5: Can novel XPCI imaging identify if complete removal of OACs (clear margins) has been achieved and to identify the number, position and possible infiltration state of surrounding lymph nodes.

Objective 6: If it is possible to image entire oesophageal cancer specimens, can XPCI also identify more subtle abnormalities? Specifically, can it determine if the entire region of BO related dysplasia or neoplasia has been removed following endoscopic therapy, and whether it has penetrated into the submucosa?

8.2 Introduction

Cancer of the oesophagus is the 7th most common cause of cancer worldwide [190]. Its prevalence has continued to rise over the past 30 years. Clinical staging of OAC remains the most accurate reflection of prognosis, guiding therapy and acts as a survival reference point. Indeed, accurate staging has become increasingly important as the options for therapy have increased [58].

Current staging is based on several imaging modalities and includes any combination of EUS, CT, US, PET, and laparoscopy. While several studies have looked at the effectiveness of these techniques individually [195], [196], [197], I previously conducted (Chapter 4) a meta-analysis of T2NO staging accuracy using a combinations

of techniques. This identified an accuracy of T&N staging of just $19 \pm 4\%$ and T staging accuracy was $29 \pm 5\%$.

The lack of accuracy of conventional CT in staging early oesophageal cancers remains a significant limitation for clinical staging. In conventional CT the contrast is generated by differences in attenuation between the tissue types. Unfortunately, soft tissues, including muscle, submucosa and mucosa, along with tumours, have similar attenuation properties. This leads to poor differentiation between tissue layers and tumour, resulting in inaccurate clinical staging.

In addition, relapse rates following oesophagectomy remain high (section 1.1.3.3). This is partly due to circumferential resection margins frequently displaying tumour involvement [245], [246]. Having in-room, real-time assessment of margins and lymph nodes may facilitate improvements in outcomes. This technique could improve accuracy of clinical staging and offer both real-time results for surgeons, undertaking cancer resection surgery.

Endoscopic resection of BO dysplasia and early BO neoplasia is a well-established efficacious therapy. Enlarging the extent of resection increases the risk of complications, particularly post-resection stricturing [247]. Having real-time in-room results could enable practitioners to perform more conservative resections.

Here, I make use of XPCI, which uses phase rather than attenuation to generate contrast, to determine lesion extent in endoscopic resections and oesophagectomy specimens. This means that contrast between soft tissues and tumour may be greatly improved, allowing the assessment of tumour penetration with much greater precision.

8.3 Methods

As discussed previously (see section 5.3) I identified patients undergoing an endoscopic resection or oesophagectomy from endoscopy and surgical lists and informed written consent was completed.

Once resected, oesophagectomy specimens were immediately placed in formalin solution and transported from the operating theatres at ULCH to the UCLH histopathology laboratories at 60 Whitfield Street. The outer margins were inked by a histopathologist, and the specimen was photographed (as per routine histopathological processing). The histopathologist resected the distal stomach and attached the specimen to the scaffold (Figure 5.13) using prolene sutures. Specimens were left to fix in formalin solution overnight before being dehydrated in graded ethanol (Table 6.1). Each step was 1 hour long. The final 10 oesophagectomies were kept in ethanol for an extended period (>24hrs) to ensure complete ethanol penetration.

Each oesophagectomy specimen was transferred to the smallest sized PLA container possible, making sure the tissue was resting at the base of the container (Figure 5.19). Parafilm and a 3D printed lid was used to seal the container. If the HICF machine was going to be used the specimen was transferred to Tring or QMUL.

Endoscopic resections were left to fix in formalin solution overnight. Samples were dehydrated in graded ethanol (Table 6.1) using 30min steps. Specimens were rolled as shown previously and inserted into the smallest sized PLA container possible (Figure 5.25).

After mounting the specimen on the sample stage of either the HICF (see section 5.2.2) or UCL molybdenum system (see section 5.2.1), scans were delayed for a minimum of 2 hours, to ensure the specimen was fully stabilised before any acquisition commenced.

The scan parameters used varied according to the system used and the specimen imaged. These are shown below in Table 8.1. All scans were based on continuous sample rotation meaning the sample mask and detector masks remained in a constant position throughout all the scans.

Table 8.1: Showing scan parameters for endoscopic resection and oesophagectomy specimens

	Endoscopic resections	Oesophagectomy	Oesophagectomy
System	UCL	UCL	HICF
Masks	Skipped	Skipped	Non-skipped
Projections	1200-2500	3600	12,000-90,000
Time/view	1.2secs	1.8secs	0.6secs
Dithering	8 steps	4 steps	n/a
Scan time	6hrs-16hrs	16hrs	2hrs-15hrs

For oesophagectomy acquisitions the primary concern was improving the SNR. This was achieved by ensuring the photon count through the tissue were sufficient as the larger tissue volumes are more attenuating. Therefore, the number of projections or time per view were increased at the expense of more dithering steps and higher resolution.

The HICF system had a limited time/view of 0.6secs (due to detector saturation after this point). Therefore, many more projections per scan relative to the scans performed with the UCL molybdenum system were used.

For endoscopic resections a higher level of resolution was required to determine dysplasia or early neoplasia extent. Therefore, a higher number of dithering steps was used (described in 1.5.1.1.1). The smaller volume of tissue was less attenuating so the number of projections and time per view could be reduced.

Either Matlab software (Mathworks, USA) or software provided by Nikon was used for both phase retrieval and CT reconstruction. This uses a series of algorithms to retrieve both absorption and refraction images from each projection.

8.4 Results

8.4.1 Oesophagectomies

Twenty-seven oesophagectomy specimens were imaged. The HICF system was primarily used due to greater system stability and less competing users. Due to system and specimen instability each specimen was scanned multiple times to ensure a complete data set was obtained for each one. Early scans failed to show sufficient soft tissue contrast making tissue layers and tumour hard to identify (Figure 8.1).

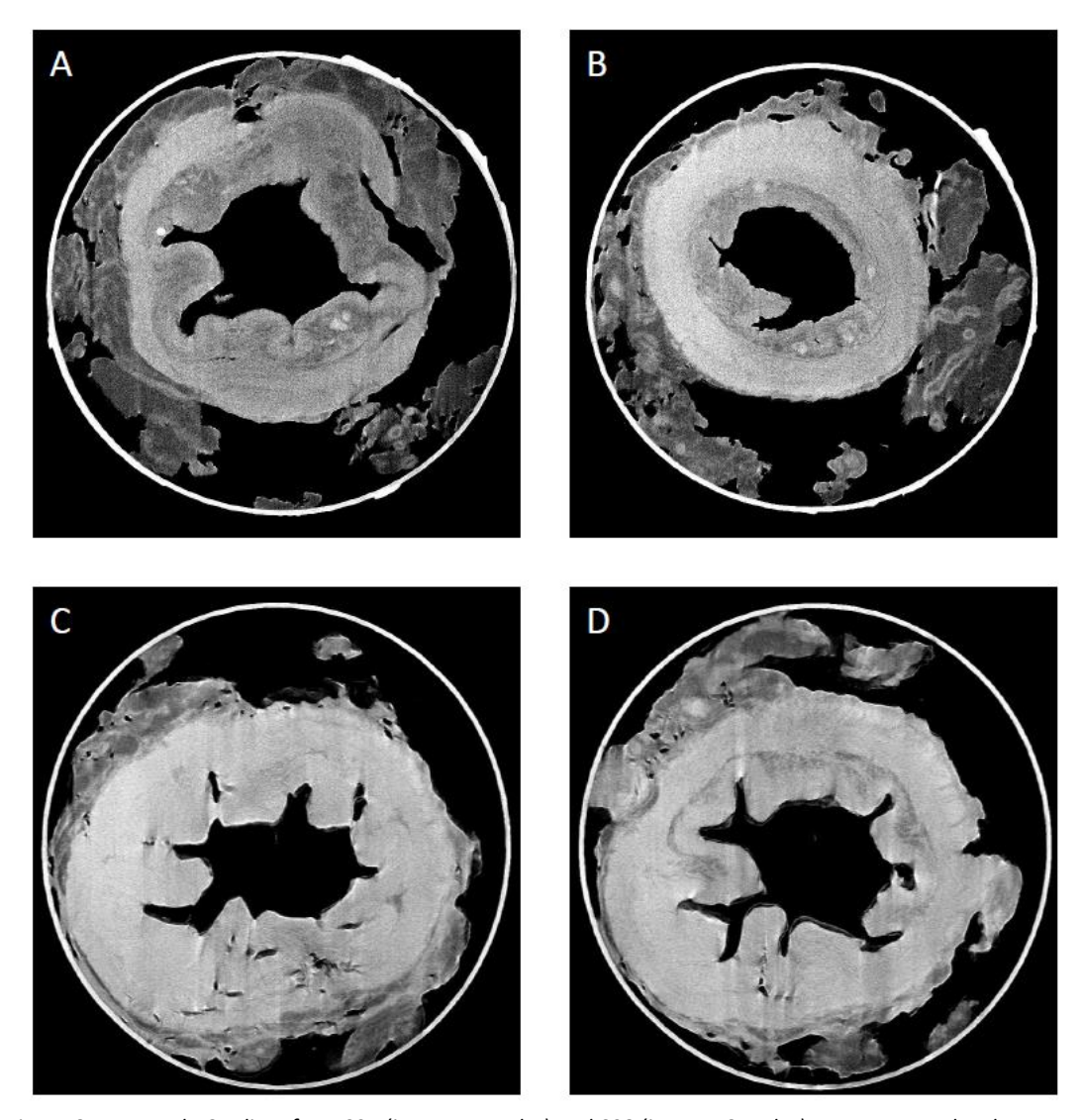


Figure 8.1: Example CT slices from S07 (images A and B) and S08 (images C and D). Images A and B show some degree of contrast through the soft tissue although not enough to identify tissue layers clearly or tumour. Images C and D show minimal contrast. In addition, motion artifacts can be observed in images C and D.

Figure 8.1 images A and B show two slices from an early scan. There is limited contrast through the soft tissue, not enough to clearly identify tissue layers or tumour, in this case a ypT1a. Figure 8.1 images C and D are images from a similar scan. Again, there is limited contrast through the tissue layers making identification of a pT1a tumour impossible. In addition, movement of the specimen during imaging has induced motion artefact seen as vertical streaks at some image locations.

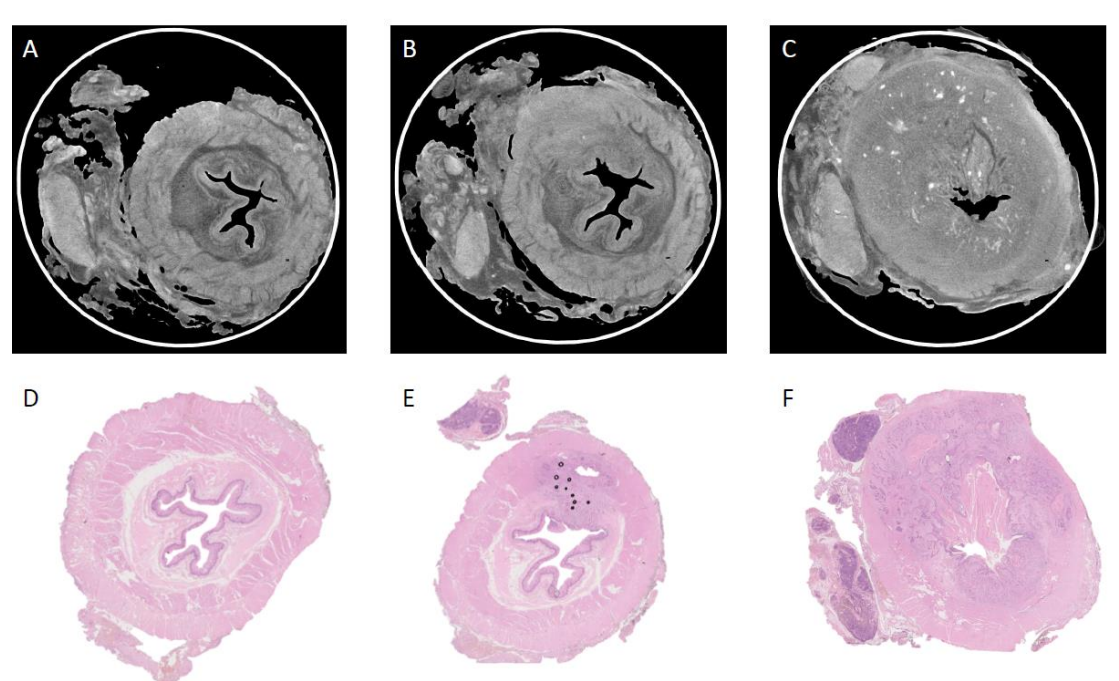


Figure 8.2: CT slices from an oesophagectomy that showed clear contrast throughout the tissue layers. Image A shows normal oesophageal tissue with matched histology in image D. Image C shows tumour starting to destroy the tissue layers between 10 and 12 o'clock. These changes are matched in the histology shown in image E. Image C shows near complete loss of tissue layers circumferentially (most marked in the top half of the specimen). This is matched to histology in image F.

Image 4.2 shows slices from the first oesophagectomy in which tissue layers are clearly defined. The specimen was kept in ethanol for an extended period due to a lack of availability of scanning facilities. Image A clearly demonstrates the normal mucosa, submucosa and muscle layers of the oesophagus. This is matched with histology in image D.

CT slices B and C with corresponding histology slices E and F show a tumour extending through the muscle layers. Image B shows gradual loss of the internal muscle layer due to the presence of tumour infiltration between 10 and 12 o'clock. Images C and

F show more extensive tumour. This extends through both muscle layers in the top image with some tumour extending below the lumen as well.

Histological assessment confirmed the presence of a T3 SCC. The high-density regions, seen in white, in image C are likely caused by keratin deposition within the tumour.

Note that although the shape of the tissue and lumen are good matches it was never possible to achieve a perfect match. This was due to slight variation in the orientation of specimens during cutting and mild deformation of tissues both during insertion of the specimen into the container for scanning and during histology processing. This deformation particularly affects the outside regions of the tissue partly due to the compression coming externally. In addition, the external layer of tissue is frequently less securely attached to the oesophagus as it contains connective tissue and lymph nodes.

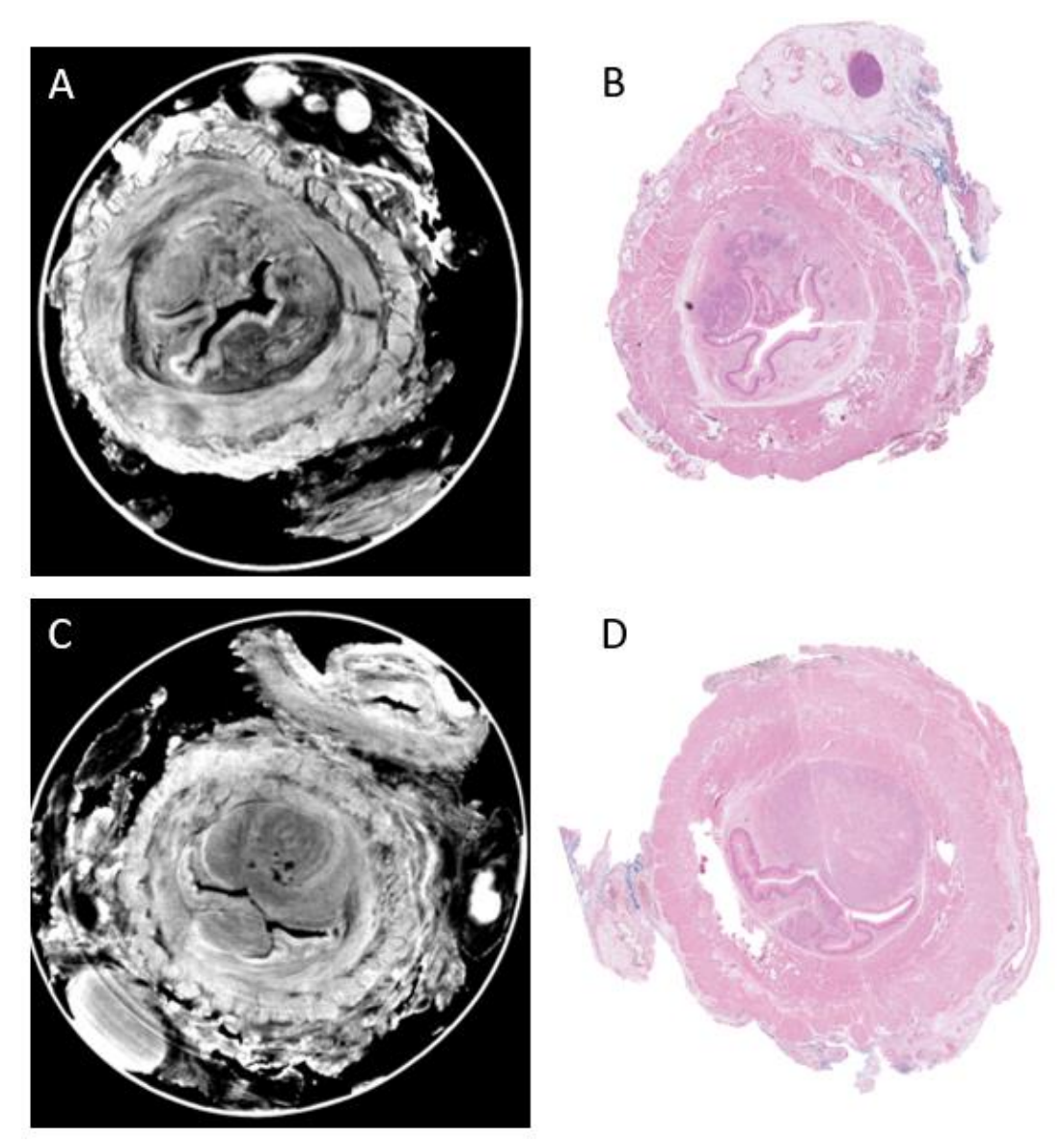


Figure 8.3: This shows CT slices from two different specimens. Image A shows a T1b tumour extending from 9 o'clock to 11 o'clock. Image B shows matching histology. Image C shows an early T2 tumour extending from 11 o'clock to 3 o'clock. Image D shows matching histology.

Figure 8.3 shows two specimens. These along with all subsequent specimens were subjected to extended ethanol dehydration (>24hrs). Image A with matched histology shown in image B shows a T1b OAC. The tumour extends from 9 to 11 o'clock but does not extend through into the muscle layers. In addition, at 12 o'clock the presence of a lymph node can be identified. Images C and D show an early T2 tumour as this extends to the junction of the submucosa and muscle layers.

In image C there are some ring artefacts especially over the tumour region. These are common artefacts that affect CT reconstruction, including in the clinical setting. They are secondary to miscalibration or failure of one or more detector elements.

Although some correction for these can be made it may not always be possible to eliminate them completely.

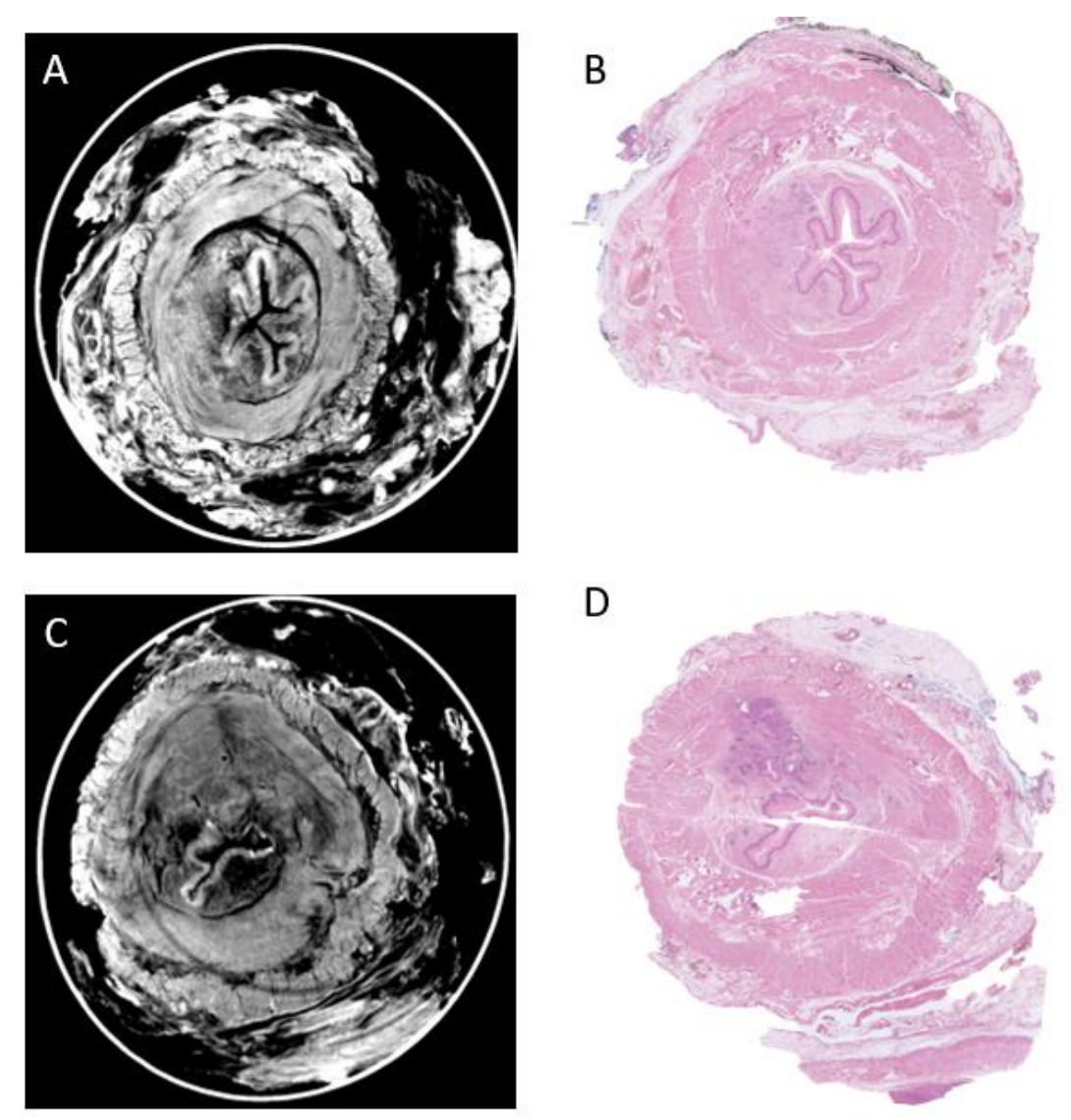


Figure 8.4: Shows CT slices from two different specimens. Image A shows a T2 tumour extending from 7 o'clock to 11 o'clock. Image B shows matching histology. Image C shows a T3 tumour extending from 10 o'clock to 12 o'clock. Image D shows matching histology.

Figure 8.4 shows two further specimens. Image A with matched histology shown in image B shows a T2 OAC. The tumour extends from 7 to 11 o'clock and invades into the muscle layers. Images C and D show a T3 tumour extending through the muscle layers into the adventitia.

All the images above are from "long" scans 10 hours or greater. As part of the protocol, a range of scans was performed. Figure 8.5 and Figure 8.6 show serial scans of the same specimen. In both figures image A is a slice from a 2 hour scan, image B

is a slice from a 4 hour scan, image C is a slice from a 10 hour scan and image D is a slice from a 15 hour scan.

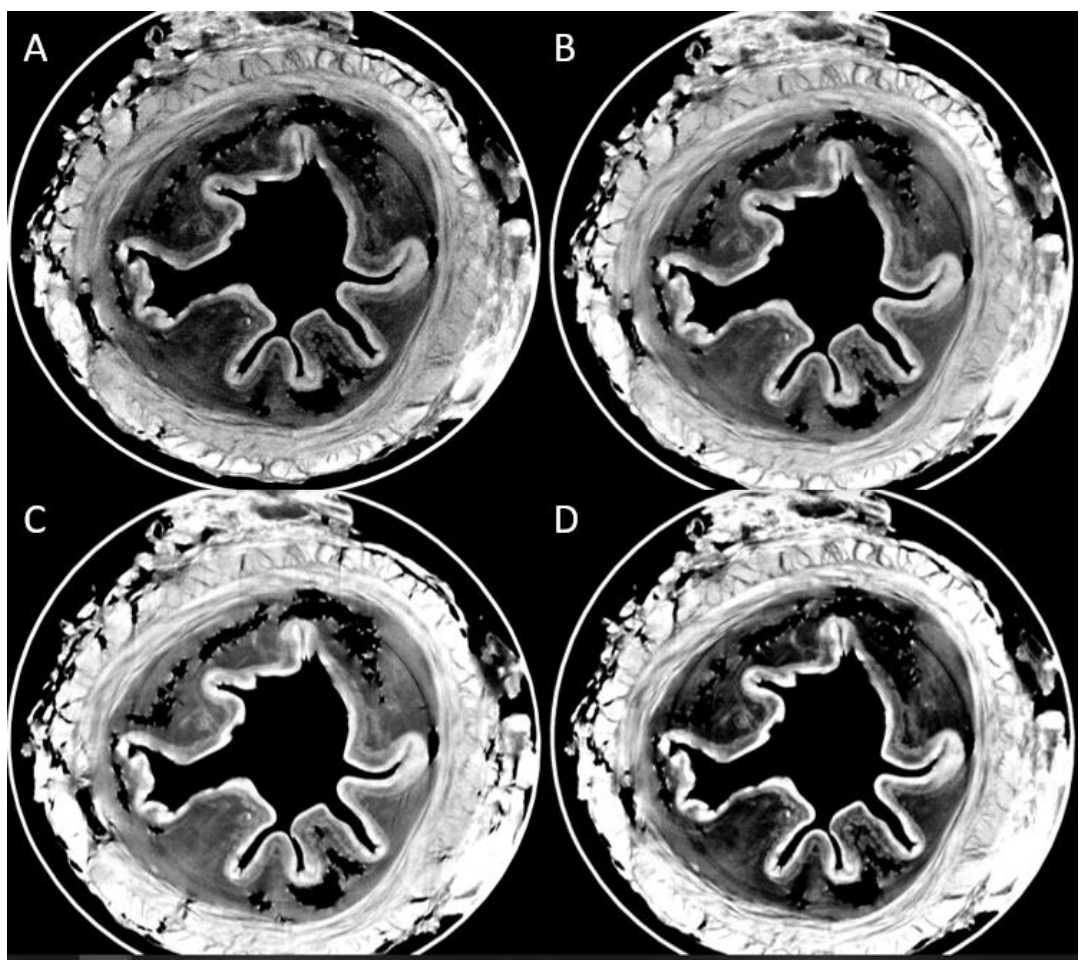


Figure 8.5: CT slices from a normal region of oesophagectomy. Each image depicts the same region. Images A, B, C and D show slices from 2, 4, 10 and 15 hour CT scans.

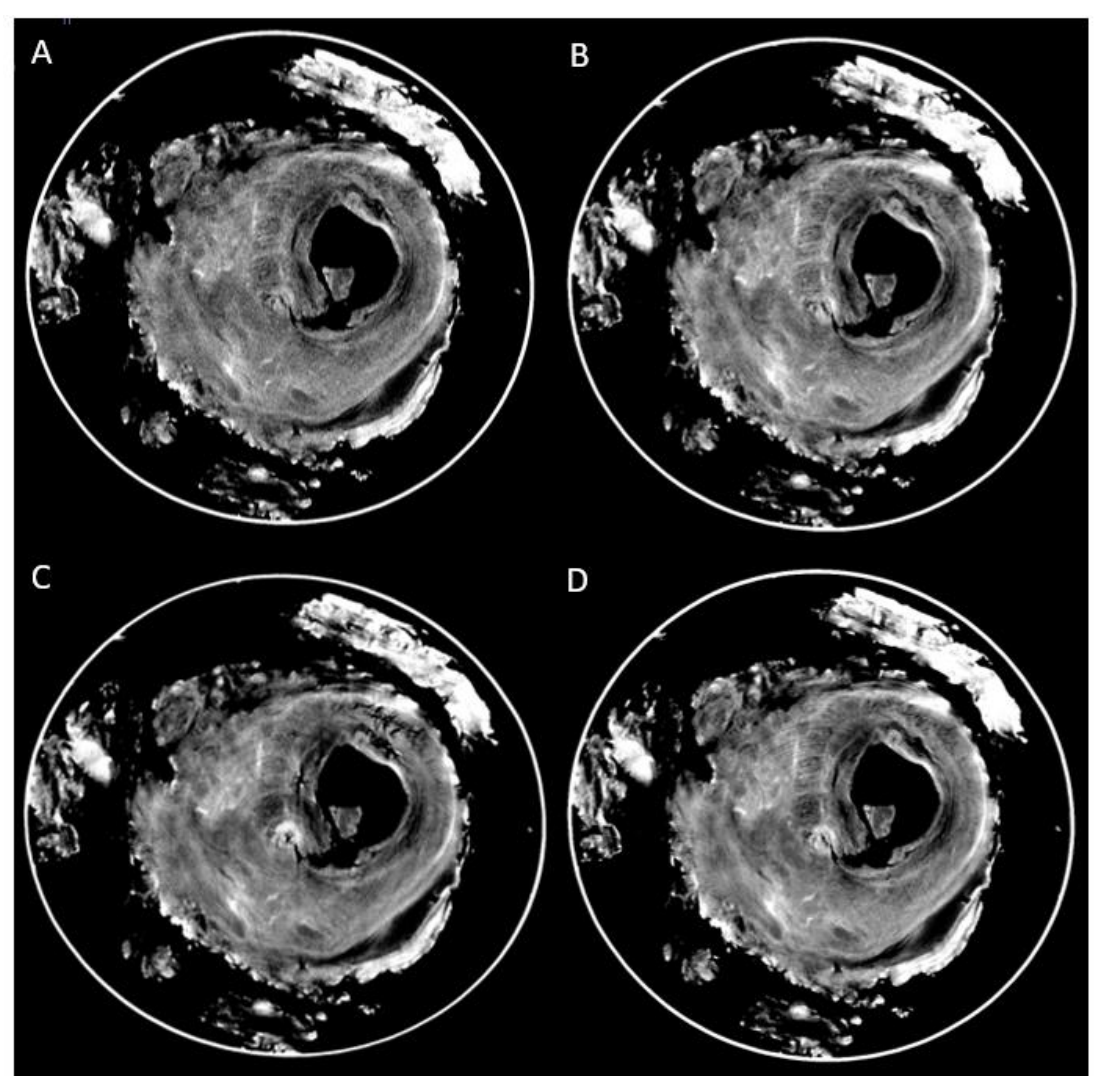


Figure 8.6: CT slices from an abnormal region of oesophagectomy. Each image depicts the same region. Images A, B, C and D show slices from 2, 4, 10 and 15 hour CT scans.

In both Figure 8.5 and Figure 8.6 image A appears grainy. This reflects the reduction in SNR resulting from lower x-ray statistics. Images B, C and D all appear sharper.

8.4.2 Endoscopic resections

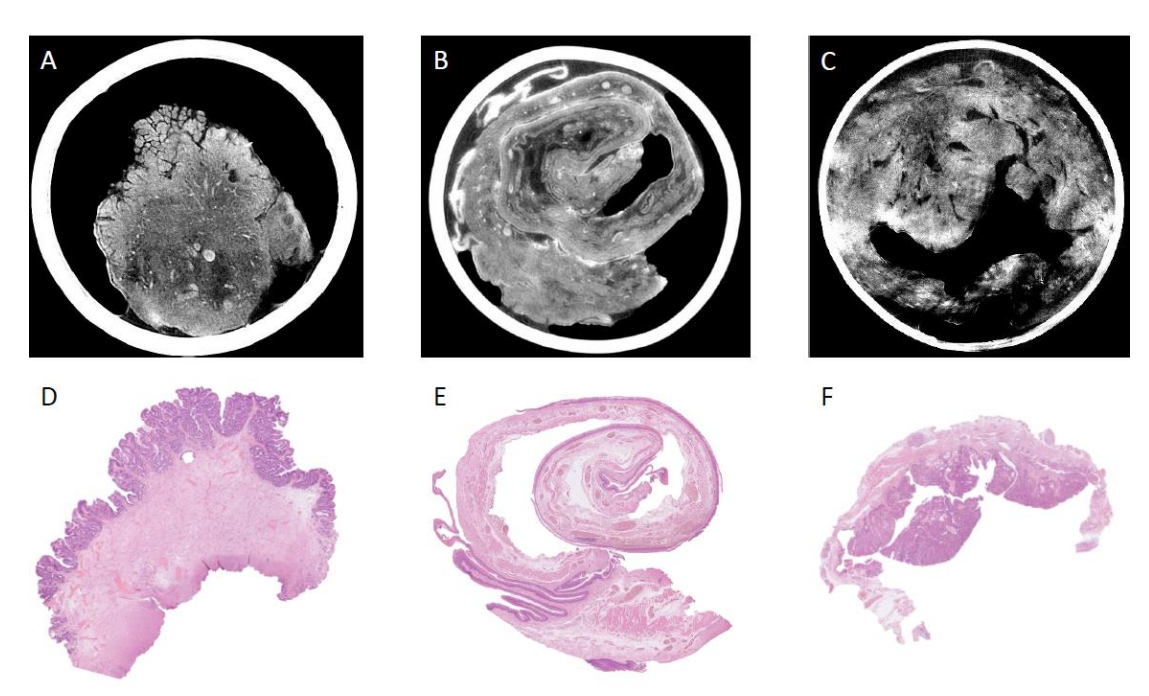


Figure 8.7: Shows endoscopic resections. Image A is an EMR with matching histology in image D. Images B and C show two ESD specimens with matching histology in images E and F, respectively.

Sixteen endoscopic resections were imaged on the UCL molybdenum system. Images A and D show an EMR specimen. Images B, C, E and F show two ESD specimens. The specimen shown in image C and F contains a pedunculated tumour. Imaging these small samples was challenging but the results shown in Figure 8.7 show contrast through the imaged tissue (images A, B and C) matched to histology sections (D, E and F).

Image A shows a CT slice with mucosa, which is glandular, and submucosa. There are regions of high density (seen in white) which correspond to vessels in the histology (imaged). Image B shows a CT slice of an ESD. In this it is possible to identify high density regions, blood vessels, mucosa and the submucosa which is matched to histology in image E. Image C shows an ESD containing a pedunculated pT1a tumour. This tumour region is shown by the darker region in the histology slice. It is harder to delineate this difference in the CT slice. There is some ringing throughout the slice and possibly some movement artefact.

8.5 Discussion

This chapter shows it is possible to stage oesophageal tumours using XPCI. I have matched these results to the gold-standard histopathology. Although these results are yet to be published, I have reviewed images with clinical radiologists who have correctly staged tumours using CT slices. This shows the potential benefits XPCI could offer both as an adjunct to conventional staging and as a tool to enable real-time assessment of surgical resection margins. The resolution achieved with the UCL molybdenum setup was insufficient to identify dysplasia and neoplasia extent in endoscopic resections.

This is the first time XPCI has been used to detect human oesophageal pathology. Previous work with XPCI in the oesophagus has used animal tissue [238], [248]. This has either been normal tissue or decellularised scaffolds. Much of this and other work has used synchrotron radiation. Using EI has enabled this work to be conducted using a conventional x-ray source, potentially opening this technique to a non-research setting.

8.5.1 Oesophagectomies

These results were variable with multiple scans failing for a number of reasons. There were several reasons for the failure of scans. Reasons included instability of the systems with several scans failing due to software and hardware malfunctions, human error in launching scans and movement of specimens during scanning.

As the setup methods became more established, the number of failed scans was reduced. In addition, once the specimen dehydration time was increased the results became more reliable achieving meaningful results in 8 of the final 10 specimens compared with just 1 of the first 17.

Unfortunately, matching lymph nodes seen during imaging to lymph nodes at histology was challenging. Although, a matched node in Figure 8.3 is visible, this was not reproducible. In part this was due to the challenges throughout the project

leading to the prioritisation of image quality in the primary organ, the oesophagus. The inability to provide nodal staging is a major limitation of the technology. We hope that further refinements of our methodology may allow imaged nodes to be compared to pathology in the future.

8.5.2 Endoscopic resections

I have shown it is possible to generate contrast through endoscopic resection specimens and achieved a resolution of ~25 μ m. The majority of endoscopic resections are performed to remove dysplastic tissue and IMC. There is rarely the substantial tumour or disruption of the normal tissue layers that is seen in invasive oesophageal cancers. To identify intramucosal pathology one would need to visualise the tissues at a cellular level, <5 μ m. The UCL molybdenum system with skipped masks has a theoretical resolution of 12 μ m, the aperture size. For this reason, with the system configured as it currently is I was unable to detect these intramucosal abnormalities.

One of the challenges with this project was the difficulty in making continual small adjustments to the methods. This was for two main reasons, namely the finite number of appropriate specimens and also the size of the data generated.

I calculated ~ 30 oesophagectomies per year were performed at UCLH. Some of these were not appropriate for the experimental needs, due to benign pathology or dysplasia that was not endoscopically treatable. Others were performed on patients from other hospitals meaning the histology specimens would be returned to a different institution. In addition to these challenges, I faced complexities due to the SARS-CoV-2 pandemic. For periods of time during this project endoscopies and surgeries were rescheduled as resources were redeployed to cope with increased acute healthcare burdens. This particularly impacted on the number of available oesophagectomy specimens, as major cancer surgery was halted for 4 months.

Another complexity centred around the data transfer and reconstructions. Some of the acquisitions produced on the HICF system consisted of 90,000 individual projections. This generated a total data set of nearly 1Tb. Copying, transferring, and manipulating this data was challenging and laborious with reconstructions often taking several days to complete. This made it harder to make small, considered adjustments to these methods.

If these techniques are to be used as an intraoperative staging technique the turnaround time needs to be shortened. This would require both reduction in sample preparation and scanning time. This would likely require unfixed specimens to be optimally scanned. The exact manner in which scans could be optimised is beyond the scope of this work but as newer technology becomes available this may enable contrast to be developed through oesophagectomy specimens without the need for dehydration.

Massimi et al [65] have shown in breast tissue XPCI-CT shows a higher sensitivity than conventional specimen imaging for detection of lesions at surgical margins. This work was performed on fixed non-dehydrated tissue. It is possible this additional contrast was generated to the physical properties of breast tissue, which contains a high proportion of fat [249]. In the oesophagus generating sufficient contrast, in non-dehydrated tissue, to delineate normal and abnormal tissue may be a greater challenge. With optimisation of both the system and these methods this may be achievable.

Chapter 9 VIOLIN – Biopsies

As for the previous chapter the work included was a collaboration of many individuals. The original grant was awarded to Professor Sandro Olivo, Professor Laurence Lovat and Professor Marco Novelli, who provided support and advice throughout. I identified and consented all patients. I prepared many of the biopsy samples and matched these to histology. Many members of AXIm assisted with both developing the technique and imaging the biopsies.

9.1 Aims

Objective 7: Finally, given that XPCI can image tissue on multiple scales, can it differentiate four types of oesophageal tissue from biopsy samples: squamous, NDBO, dysplastic Barrett's Oesophagus (DBO) and adenocarcinoma.

Specifically, I aim to show these tissue types can be identified both using synchrotron radiation and a conventional x-ray source. I aim to compare these results with the current gold-standard, histopathology.

9.2 Introduction

As discussed previously (section 1.2.7), histology is an essential tool in clinical diagnostics, for detecting cancers and pre-cancerous lesions. However, it is a complex, labour intensive and expensive process. Surveillance in BO (section 1.2.4), is performed using Seattle protocol biopsies. This involves taking quadrantic biopsies every 2 cm throughout the metaplastic oesophagus (

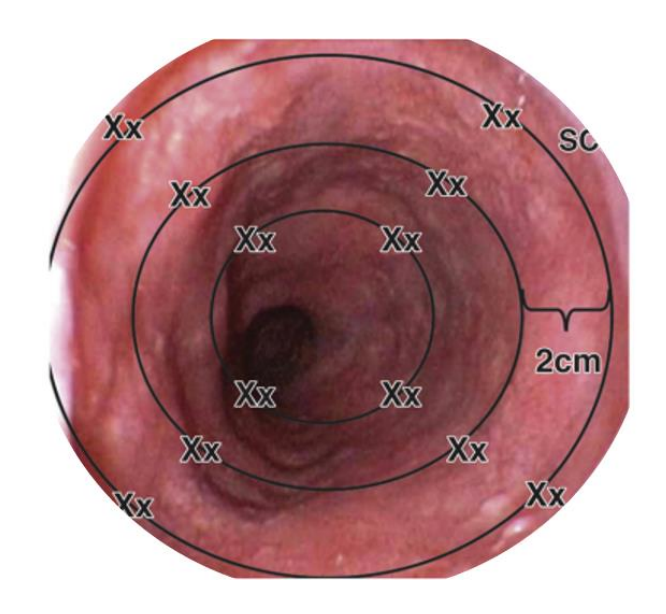


Figure 1.6).

There are several concerns with surveillance in BO. Firstly, there is a lack of evidence from RCTs to demonstrate the efficacy of surveillance, although results are awaited from the BOSS trial. Secondly, although Seattle protocol biopsies are recommended by national guidelines, adherence ranges from 10% to 79% with poorer compliance in longer BO segments [103], [104], [105]. Performing Seattle protocol biopsies only samples up to 5% of the BO segment meaning focal dysplasia can be missed. Another drawback of taking Seattle protocol biopsies is the high cost generated by processing multiple biopsies [80]. Reducing reliance on histological assessment may assist with some of these issues.

Turnaround times for histology can extend into weeks, in part due to the complex processing techniques discussed earlier but also due to the high demand for these diagnostic tests. Histological diagnosis is required before some therapeutic options can be considered [80]. This can lead to additional procedures and delays in therapy, which can be associated with increased cost, anxiety and worse outcomes [250].

Frozen sectioning, an existing real-time histological technique, requires skilled technicians and clinicians to produce and interpret slides [251]. In addition, histological confirmation of dysplasia in BO requires consensus between two expert GI pathologists [80].

One technique to reduce reliance on conventional histology may be x-ray microscopy using XPCI. As discussed previously this is a growing field making use of XPCI to generate contrast through soft tissues. FSP is particularly suited to this purpose. Discussed previously this uses a coherent source and a highly specialised setup to generate soft tissue contrast as photons waves pass through a specimen. Much of this work has been conducted at synchrotrons. For this technique to provide value beyond the research field, conventional sources need to be utilised.

Here, I use XPCI, to identify four different tissue types from the human oesophagus. I attempted to achieve this using a synchrotron source and a conventional x-ray source before comparing these results with the gold-standard, histopathology.

9.3 Methods

As described previously (section 5.3) biopsies were obtained from the UCL biobank and directly from newly recruited patients in endoscopy. All these biopsies were additional biopsies and so were not required for the clinical pathway. Informed written consent was obtained prior to these biopsies being taken. Biopsies collected were one of four subtypes; squamous, NDBO, DBO and OAC. All biopsies were held in formalin.

Fifteen biopsies of each histological subtype were taken to DLS. These were prepared as described in section 5.4.4.1.1.1. They were imaged in beamline i13-1 using the setup described in section 5.2.4. Following this, specimens were returned to formalin and returned to UCL. Reconstructions of these acquisitions were performed using software provided by DLS.

On return to UCL these biopsies were dehydrated in graded ethanol (Table 6.1). Each step was 15 mins long due to the small tissue volume. Biopsies were placed in 1mm glass capillaries as previously described in section 5.4.4.1.1.2 and the acquisition was performed as described in section 5.2.3. Following completion of the acquisition the biopsies were removed from the capillary and the base of each biopsy was stained with tissue marking dye. Biopsies were stained to assist with co-registration and

orientation of the reconstructed CT slices and histology sections. Biopsies were returned to formalin solution before being sent for serial sectioning in histology. CT reconstructions were performed using MATLAB software (Mathworks, USA).

Following completion of the serial sectioning and the CT reconstructions I attempted to match sections from the synchrotron imaging, lab imaging and histology sections.

9.4 Results

Twelve biopsies were successfully scanned at DLS during the 72 hours of beamtime. These were brought back to UCL and scans were attempted on 9 specimens. Three were not scanned at UCL; 1 was lost on transfer and 2 CTs performed at DLS contained significant artefacts so comparison between UCL and DLS scans was not possible.

I was able to match four of the DLS CTs to lab CTs performed using a conventional source (Figure 9.1).

Figure 9.1: Images from matched scans. Images on the left side are synchrotron CT slices and images on the right side are CT slices using a conventional source. Images A and B show a squamous biopsy, images C and D show a biopsy containing NDBO; images E and F show a biopsy containing DBO; images G and H show a biopsy containing adenocarcinoma

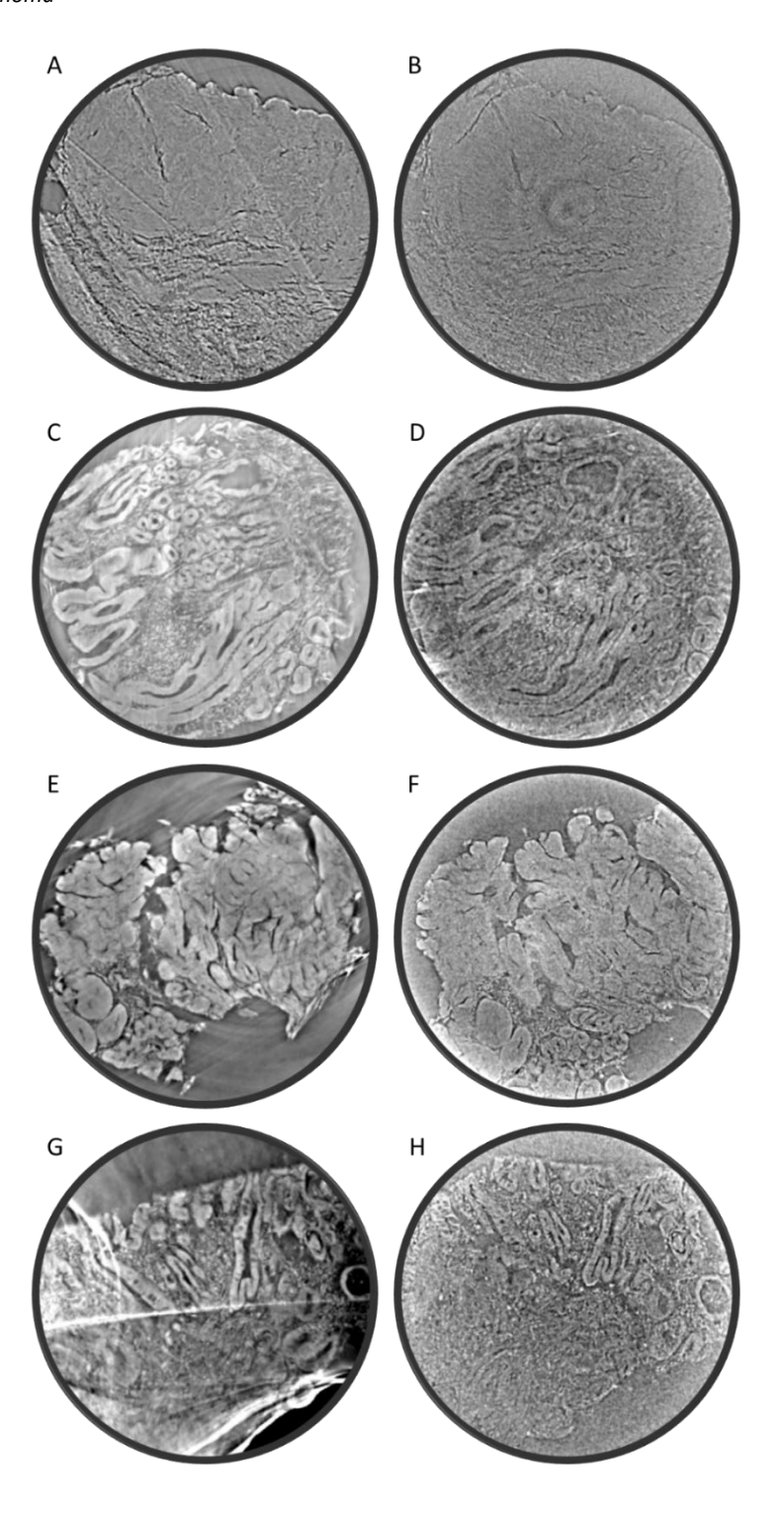


Image A shows a slice from a CT of a squamous biopsy acquired at DLS. In this the tissue layers can be seen. The stratified squamous sample is visible showing the mucosa at the top and submucosa below. The tissue is relatively featureless, with no obvious structure as is seen with metaplastic and dysplastic tissue. Image B shows a matched slice from a CT acquired at UCL. This shows comparable contrast and resolution to the synchrotron slice although there is some ring artefact present.

Image C shows a slice from a CT of a biopsy containing NDBO acquired at DLS. In this a piece of columnar epithelium metaplastic glandular tissue with goblet cells is clearly visible. The muscularis mucosa is visible in the middle of the tissue sample. Image D shows a matched slice from a CT acquired at UCL. Again, this shows comparable contrast and resolution to the synchrotron slice whilst also identifying and matching many of the features.

Image E shows a slice from a CT of a biopsy containing DBO acquired at DLS. In this piece of columnar epithelium, architectural atypia with glandular crowding is visible. There is some ring artefact visible in this image. Image F shows a matched slice from a CT acquired at UCL. Again, this shows comparable contrast and resolution to the synchrotron slice whilst also identifying and matching many of the features.

Image G shows a slice from a CT of a biopsy containing OAC acquired at DLS. In this a piece of columnar epithelium is shown in which there is destruction of the tissue architecture. There is some artefact in the imaging due to the air water interface. Image H shows a matched slice from a CT acquired at UCL. This slice shows good resolution, but the contrast is slightly worse than that seen in the matched synchrotron slice.

The serial slices were reviewed with MN. Unfortunately, the biopsy believed to contain OAC did not show evidence of invasive cancer through any of the histology slices so matching between histology and CT slices was not performed. In addition,

the squamous biopsy due to the lack of features throughout the specimen has not been matched.

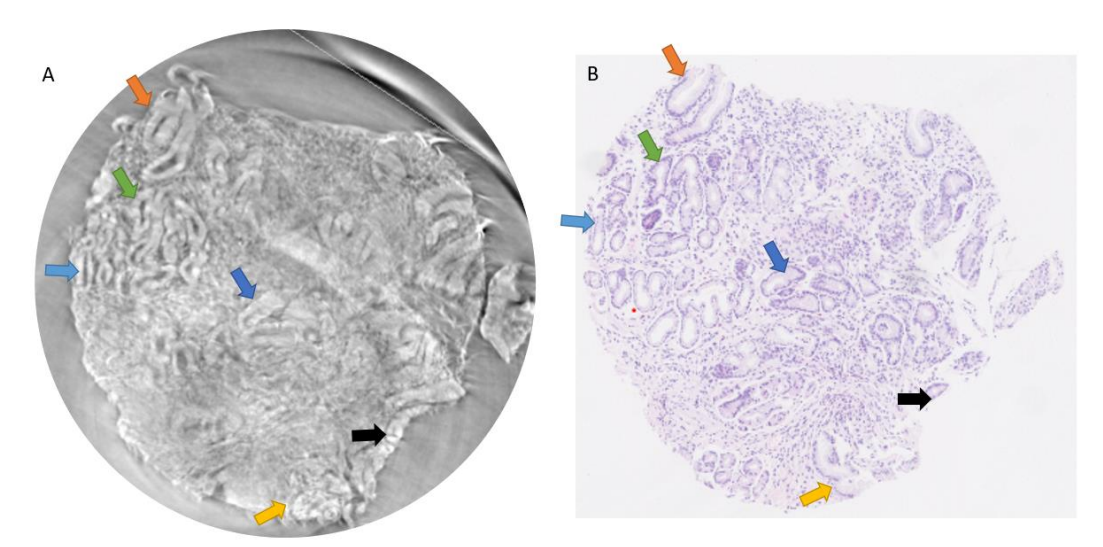


Figure 9.2: Images showing matched images of a NDE biopsy. The arrows highlight matched features. Image A shows a slice from the synchrotron CT. Image B shows a slice from serial sectioning of the biopsy.

Figure 9.2 shows matching synchrotron and histology slices for a biopsy containing non-dysplastic BO. Image A shows a slice from the synchrotron CT in which some ring artefact is visible. This has been matched with the H&E histology in image B. Several similar identifiable features are seen across both images as are shown by the arrows. Although the match is satisfactory there are areas such as the top right of the specimen which match less well.

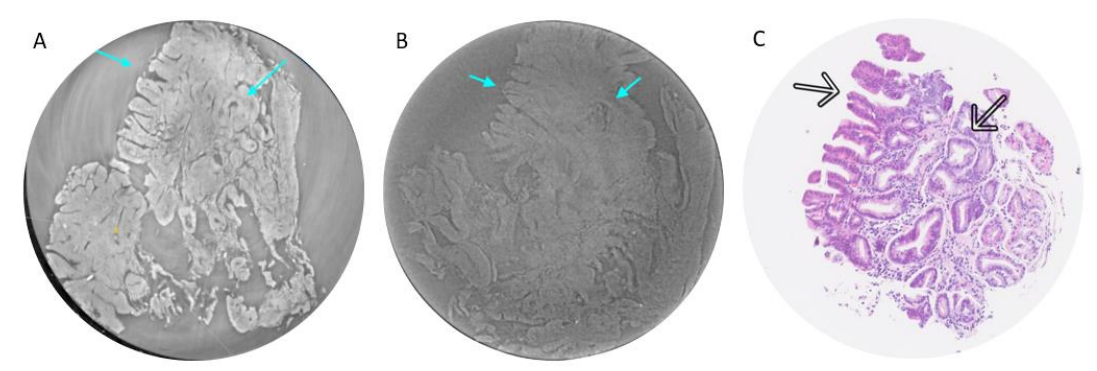


Figure 9.3: Images showing HGD. Image A shows a slice from the synchrotron CT. Image B shows a slice from the lab CT. Image C shows a slice from serial sectioning of the biopsy

Figure 9.3 shows matching synchrotron, lab CT and histology slices from a biopsy containing dysplastic BO. The features indicated by the arrows highlight matched regions. The orientation is matched showing the columnar epithelium in the top left of each image. Image A shows a slice from the synchrotron CT. Image B shows a slice

from the lab CT with slightly inferior contrast seen through the tissue. Image C shows a histology slice from the biopsy. Note the volume of tissue is reduced in the histology, likely due to some tissue loss in transfer from glass capillary to histology sectioning.

9.5 Discussion

This chapter shows it is possible to identify four different oesophageal tissue types using both synchrotron radiation and a conventional x-ray source. Although these CT volumes have not been independently verified the different tissue types appear substantially different.

Currently there are no other clinical or research alternatives to conventional histological processing of biopsies. Other techniques such as, narrow band imaging or optical coherence tomography, attempt to make use of novel imaging techniques to improve diagnosis in upper gastrointestinal endoscopy[252]. These are both operator dependent techniques and as such are associated with interobserver variability.

This is a proof-of-concept study in which several challenges were experienced. Firstly, although the scanned biopsies were believed to contain pathology, the grade of histology in the imaged specimen was not confirmed until histology was performed. There is evidence that multiple biopsies from the same site are required to confirm a histological diagnosis due to the heterogeneous nature of BO mucosa[253]. The highest grade within that tissue is what is described within the histology report. For this reason, UK guidelines recommend taking six biopsies of a suspected cancer[53]. Our imaged specimens were samples of biopsies either because of tissue preparation for histological assessment or to fit within the FoV which is only 1mm. To allow for this biopsies were frequently cut during preparation. This meant that the imaged tissue carried an even smaller chance of containing the desired tissue type. This raises the possibility that our specimens did not contain the suspected tissue grade, leading to scans being performed on normal or non-dysplastic tissue.

Secondly, there were issues with tissue preparation and stability during scans. As my experimental aims were attempting to achieve a microscopic resolution any movement during the acquisition would compromise the reconstruction. The longer the acquisition time the more stable the specimen needs to be. This issue was compounded by the relative low flux of the UCL copper system requiring longer scan times to improve the CNR.

Lastly the matching process was a unique challenge. When the acquisitions were performed, no consideration was made to standardise the orientation of the biopsies for each technique. This meant that the original synchrotron, lab and histology slices were not in the same plane. Therefore, orientation of the different imaging techniques was performed manually by locating regions with identifiable features. This was not always possible due to the changing size of each volume as some of the tissue degraded during preparation and over time.

To apply XPCI to histology consideration of the role it would play and modifications according to this would be required. If this technique was to provide in-room histological diagnosis the turn around time would need to be reduced to 10s of minutes. This shorter scan time would enable less precise tissue preparation, as used for specimens imaged at DLS (see section 5.4.4.1.1.1). Using XPCI in the histopathology laboratory pathway may enable reprioritisation of resources to other more specialised tasks. In this manner XPCI could be used to identify routine, normal specimens generated not just in upper gastrointestinal endoscopy but also across all diagnostic pathology.

Chapter 10 Discussion

The aims of this thesis were to:

- 1) Assess existing technologies used in the treatment and staging of OAC
- 2) To use XPCI to both grade and stage dysplasia and invasive OAC

Oesophageal cancer remains the 7th most common cause of cancer death in the UK [4]. In men it is the 4th most common cause. Five-year survival remains low.

Improving outcomes depends on early treatment of precursor lesions, namely dysplastic BO and early cancers. Long term data regarding the efficacy of treatment for these lesions is lacking.

In addition, accurate staging is essential to establish prognosis and enable appropriate treatment of invasive cancers. Although clinical staging is a fundamental part of clinical practice, data regarding the accuracy of combined imaging modalities to stage invasive cancers is lacking. Questions remain regarding the suitability of current technologies used in clinical staging. Frequently, modalities are unable to visualise the entire lesion and others do not provide the level of contrast required to stage local tumour invasion precisely.

10.1 Assess existing technologies used in the treatment and staging of OAC

The initial aim of this thesis was to assess two existing methods used in the treatment and staging of OAC. Firstly, the efficacy of EET and durability of clinical endpoints in

the treatment of Barrett's dysplasia and early OAC. Secondly the accuracy of clinical staging of oesophageal cancers.

Regarding the long-term efficacy of EET. Initial work was undertaken to assess the method for determining clinical endpoints, CR-D and CR-IM. The question was whether a single biopsy was sufficient to determine clearance or if biopsies at two consecutive endoscopies offered a more reliable outcome measure.

Using the UK HALO RFA registry data I developed an algorithm through which it was possible to calculate these clinical endpoints using both single and two biopsies. Through this work I was able to show that using two biopsies gave a significantly more durable outcome. This work enabled me to move forward to assess the long-term outcomes for EET.

I proceeded to establish the rate of CR-D and CR-IM within the database using the two-biopsy method. I also established the rate of recurrence from these endpoints and the rate of successful repeat therapy (CR-D2 and CR-IM2). Furthermore, I established the rate of invasive cancer across the whole cohort.

I showed that RFA therapy reduces cancer risk by more than 90% compared to historical control data of 6-19% per annum [119], [179], [180]. The KM rate of progression to EAC in this cohort was <5% after 10 years. At the time of publication this was the largest data set with such extended follow up.

Clinical staging of oesophageal cancer is the most accurate reflection of cancer prognosis, it guides therapy and is a survival reference point [57]. Accurate staging

has become increasingly important as the options for therapy have increased [58]. Clinical staging uses a number of imaging modalities in combination. Although the accuracy of each modality is well established the data regarding the accuracy of combination modalities is lacking.

Accuracy of staging requires comparison of clinical staging with the gold standard, pathological staging. To assess this, I performed a systematic review of T2NO oesophageal cancers. This ensured patients did not receive NAT potentially altering the staging prior to resection.

I demonstrated that combined T and N staging was accurate in only 19% of patients. The proportion with accurate T stage was 29%. This highlighted the accuracy of clinical staging for oesophageal T2 cancers remains poor and is largely unchanged in recent years [213].

10.2 Using XPCI to grade and stage oesophageal cancers

After extensive preliminary work using porcine tissue to develop these techniques and specimen holders I began to address the challenge of staging and grading oesophageal cancers. This comprised of three different work streams. Firstly, for oesophagectomies, to identify if complete resection of oesophageal tumours and pathological lymph nodes has been achieved. Secondly for endoscopic resections (EMRs and ESDs), to identify if the entire region of BO related dysplasia or neoplasia has been removed, and the depth of invasion. Thirdly, using XPCI to identify four types of oesophageal tissue, squamous, NDBO, DBO and adenocarcinoma.

The work to look at surgical resection specimens involved imaging specimens using EI XPCI systems both at UCL and in Tring. Slices of these CTs were compared to pathological staging.

Although there were a number of failed scans, I was able to show staging of oesophageal tumours was possible using XPCI for T1-T3 tumours. Unfortunately, lymph nodes seen during imaging were not matched to lymph nodes at histology partly due to histological preparation but also due to specimen movement and stability during scans.

All the endoscopic resections were imaged at UCL due to the higher resolution of the system. I have shown it is possible to generate contrast through endoscopic resection specimens and achieved a resolution of ~25 μ m. Unfortunately to identify the cellular changes pathognomonic of dysplasia scans would have need to have a resolution of <5 μ m.

The attempts to identify four different oesophageal tissue types generated the most challenges of any part of this thesis. I aimed to image these biopsies at a synchrotron facility and at UCL before comparing the results with histology. I have shown it was possible to show substantial differences in the tissue structure although these CT volumes have not been independently verified.

It should be noted that the length of scans coupled with the aim of achieving microscopic resolution meant any movement compromised the scans. This along

with the complexity of maintaining orientation to match histology slices to the CT slices made replication of this process difficult.

10.3 Limitations

The 10-year follow-up results from the UK RFA registry added substantial data to the literature. Data of this nature is not without its limitations.

There was some variability in practice across the sites. To minimise the effect of this a substantial number of exclusions was required. This enabled a more accurate assessment of the long-term effects of EET in BE. A limitation is that patients were followed by their recruiting site. If patients presented to other hospitals with any of the outcomes or had further therapy, these data were not collected. In addition, approximately 25% of patients were excluded from the detailed analysis because of inadequate follow-up, defined as <18 months. This reflects the high number of patients who dropped out of surveillance programs, either because of older age or patient choice.

The major limitations of the meta-analysis relate to the data used. This was generally heterogeneous showing a possible inconsistency between studies. Furthermore, most of the large studies included were retrospective and used databases to collect the published data. In addition, the time between clinical staging being completed to surgery may lead to disease progression in the interim.

The experimental parts of this thesis have shown that it is possible grade and stage oesophageal cancers using XPCI it is possible. To my knowledge this is the first

attempt to use XPCI to image human oesophageal tissue. Despite these promising results, there are some important consideration and limitations of this work. These may create further research opportunities.

One of the greatest limitations was the lack of reproducibility of results. This was primarily due to the challenge of dealing with clinical specimens. By nature, these are clinically essential, irregular in shape, vary in size and are prone to drying. All of these features increased the chance of movement during scans. Movement artifact was a particular challenge when attempting higher resolution imaging due to higher scan times. Furthermore, due to the experimental nature of the imaging setups there were frequent failed scans caused by software and hardware instability.

The FSP at UCL for biopsies had a FoV of 1mm. This meant only extremely small tissue specimens could be imaged. Working with such tissue was extremely challenging and made orientation and therefore co-registration of histology and CT slices more challenging.

10.4 Ideas for future work

It is highly unlikely further large-scale studies will publish purely on the efficacy and durability of RFA in BE given the nature of this work and the recently published work from the Dutch group [182]. Further work to compare the efficacy of differing technologies such as cryoablation to RFA may offer different treatment options in the future. Both to potentially reduce the discomfort associated with RFA treatment and for refractory BE.

Staging of oesophageal cancers remains challenging. For two reasons I suspect further work to improve accuracy is limited. Firstly, the trend to offering more NAC means comparing clinical staging to the reference standard is not useful. Also, given the technologies used for staging have not changed significantly in the past few decades there is unlikely to be much further data to add to this work. Hopefully, as new enhanced imaging modalities such as MRI with gating or more narrow EUS scopes improve comparison of clinical staging to pathological staging at this point will offer more valuable data.

Regarding the use of XPCI, I have shown the time required for each scan introduced problems in itself. Increasing scan time increased the chance of a system failure, a relatively common occurrence with such an experimental setup. Furthermore, increasing scan time increased the chance of sample movement. If efforts could be made to reduce this time this could improve the likelihood of successful imaging. The increasing introduction of liquid-metal-jet sources within the research community may facilitate this.

I would like to see XPCI used across more tissue types. If the scanning time could be reduced further this may open the potential for intraoperative imaging of biopsy or resection specimens. One way this could happen is further development and use of advanced x-ray sources such as liquid-metal-jet sources. This may enable surgical a reduction in the volume of resected tissues and techniques such as lymph node sampling specimens to be reduced which may minimise the morbidity seen with such procedures.

Although the challenges are extensive, using XPCI to improve in vivo tumour staging may go some way to improving the accuracy of oesophageal cancer staging.

10.5 Conclusions

Introducing new imaging techniques is vital for ongoing management of oesophageal cancer. As more novel therapies are introduced efforts need to be made to improve clinical diagnostics.

The introduction of XPCI to oesophageal cancer grading and staging was a unique project. It was extraordinarily challenging. Further work is needed to show that this technique can achieve reproducible results. With the aim of improving outcomes in oesophageal cancer.

Chapter 11 References

- P. Wolfson *et al.*, "Endoscopic eradication therapy for Barrett's esophagus–related neoplasia: a final 10-year report from the UK National HALO Radiofrequency Ablation Registry," *Gastrointest Endosc*, vol. 96, no. 2, pp. 223–233, Aug. 2022, doi: 10.1016/J.GIE.2022.02.016.
- [2] P. Wolfson *et al.*, "Accuracy of clinical staging for T2N0 oesophageal cancer: Systematic review and meta-analysis," *Diseases of the Esophagus*, vol. 34, no. 8, pp. 1–12, 2021, doi: 10.1093/dote/doab002.
- T. Partridge *et al.*, "T staging esophageal tumors with x rays," *Optica*, vol. 11, no. 4, p. 569, Apr. 2024, doi: 10.1364/OPTICA.501948.
- [4] "Oesophageal cancer incidence statistics | Cancer Research UK." Accessed: Jan. 29, 2019. [Online]. Available: https://www.cancerresearchuk.org/health-professional/cancer-statistics/statistics-by-cancer-type/oesophageal-cancer/incidence#heading-Three
- [5] M. Arnold, I. Soerjomataram, J. Ferlay, and D. Forman, "Global incidence of oesophageal cancer by histological subtype in 2012," *Gut*, vol. 64, no. 3, pp. 381–387, Mar. 2015, doi: 10.1136/GUTJNL-2014-308124.
- (6) "Cancer | Detect Cancer Early | Health Topics | ISD Scotland." Accessed: Jan.
 29, 2019. [Online]. Available: https://www.isdscotland.org/Health-Topics/Cancer/Detect-Cancer-Early/

- [7] "Queen's University Belfast | N. Ireland Cancer Registry | Official Statistics."
 Accessed: Jan. 29, 2019. [Online]. Available: http://www.qub.ac.uk/research-centres/nicr/CancerInformation/official-statistics/
- [8] National Cancer Registration and Analysis Service, "Survival by stage," Stage
 Breakdown by CCG 2014. London: NCIN; Accessed: Jan. 29, 2019. [Online].
 Available: http://www.ncin.org.uk/publications/survival_by_stage
- [9] "Welsh Cancer Intelligence and Surveillance Unit." Accessed: Jan. 29, 2019.[Online]. Available: http://www.wcisu.wales.nhs.uk/
- (10) "Cancer registration statistics, England Statistical bulletins Office for National Statistics." Accessed: Jan. 29, 2019. [Online]. Available: https://www.ons.gov.uk/peoplepopulationandcommunity/healthandsocialca re/conditionsanddiseases/bulletins/cancerregistrationstatisticsengland/previousReleases
- [11] J. Steevens, A. A. M. Botterweck, M. J. M. Dirx, P. A. Van Den Brandt, and L. J. Schouten, "Trends in incidence of oesophageal and stomach cancer subtypes in Europe," *Eur J Gastroenterol Hepatol*, vol. 22, no. 6, pp. 669–678, Jun. 2010, doi: 10.1097/MEG.0b013e32832ca091.
- [12] M. B. Cook *et al.*, "Cigarette Smoking and Adenocarcinomas of the Esophagus and Esophagogastric Junction: A Pooled Analysis From the International BEACON Consortium," vol. 102, no. 17, Sep. 2010.

- [13] M. B. Cook *et al.*, "Cigarette Smoking Increases Risk of Barrett's Esophagus: An Analysis of the Barrett's and Esophageal Adenocarcinoma Consortium," *Gastroenterology*, vol. 142, no. 4, pp. 744–753, Apr. 2012, doi: 10.1053/J.GASTRO.2011.12.049.
- [14] H. Nordenstedt and H. El-Serag, "The influence of age, sex, and race on the incidence of esophageal cancer in the United States (1992–2006)," Scand J Gastroenterol, vol. 46, no. 5, pp. 597–602, May 2011, doi: 10.3109/00365521.2011.551890.
- [15] J. Lagergren' and O. Nyr#{233}n, "Do Sex Hormones Play a Role in the Etiology of Esophageal Adenocarcinoma? A New Hypothesis Tested in a Population-based Cohort of Prostate Cancer Patients," 1998.
- [16] M. H. Derakhshan, S. Liptrot, J. Paul, I. L. Brown, D. Morrison, and K. E. L. Mccoll, "Oesophageal and gastric intestinal-type adenocarcinomas show the same male predominance due to a 17 year delayed development in females", doi: 10.1136/gut.2008.161331.
- [17] D. P. Cronin-Fenton *et al.*, "Reproductive and sex hormonal factors and oesophageal and gastric junction adenocarcinoma: A pooled analysis HHS Public Access," *Eur J Cancer*, vol. 46, no. 11, pp. 2067–2076, 2010, doi: 10.1016/j.ejca.2010.03.032.
- [18] C. Bodelon, G. L. Anderson, M. A. Rossing, R. T. Chlebowski, H. M. Ochs-Balcom, and T. L. Vaughan, "Hormonal Factors and Risks of Esophageal Squamous Cell

- Carcinoma and Adenocarcinoma in Postmenopausal Women," *Cancer Prev Res*, vol. 4, no. 6, 2011, doi: 10.1158/1940-6207.CAPR-10-0389.
- [19] N. D. Freedman, J. V Lacey, A. R. Hollenbeck, M. F. Leitzmann, ; Arthur Schatzkin, and C. C. Abnet, "The Association of Menstrual and Reproductive Factors With Upper Gastrointestinal Tract Cancers in the NIH-AARP Cohort", doi: 10.1002/cncr.24880.
- [20] M. Lindblad, L. A. García Rodríguez, E. Chandanos, and J. Lagergren, "Hormone replacement therapy and risks of oesophageal and gastric adenocarcinomas," *Br J Cancer*, vol. 94, pp. 136–141, 2006, doi: 10.1038/sj.bjc.6602906.
- [21] Z. Hui, Yu; Guiyun, Liu; Peng, Zhao; Liying, "Hormonal and Reproductive Factors and Risk of Esophageal Cancer in Chinese Postmenopausal Women: a Case-control Study," 2011.
- [22] K. Lagergren, J. Lagergren, and N. Brusselaers, "Hormone replacement therapy and oral contraceptives and risk of oesophageal adenocarcinoma: A systematic review and meta-analysis," *UICC International Journal of Cancer IJC*, vol. 135, pp. 2183–2190, 2014, doi: 10.1002/ijc.28869.
- [23] G. R. Locke, N. J. Talley, S. L. Fett, A. R. Zinsmeister, and L. J. Melton, "Risk Factors Associated with Symptoms of Gastroesophageal Reflux."

- [24] J. Kotzan, W. Wade, and H. H. Yu, "Assessing NSAID Prescription Use as a Predisposing Factor for Gastroesophageal Reflux Disease in a Medicaid Population," 2001.
- [25] G. Richard *et al.*, "Prevalence and Clinical Spectrum of Gastroesophageal Reflux: A Population-Based Study in Olmsted County, Minnesota," 1997.
- [26] M. B. Cook, C. P. Wild, and D. Forman, "A Systematic Review and Meta-Analysis of the Sex Ratio for Barrett's Esophagus, Erosive Reflux Disease, and Nonerosive Reflux Disease," *Am J Epidemiol*, vol. 162, no. 11, pp. 1050–1061, Dec. 2005, doi: 10.1093/aje/kwi325.
- [27] V. Bagnardi *et al.*, "Alcohol consumption and site-specific cancer risk: a comprehensive dose–response meta-analysis," *Br J Cancer*, vol. 112, no. 3, pp. 580–593, Feb. 2015, doi: 10.1038/bjc.2014.579.
- [28] D. Praud *et al.*, "Cancer incidence and mortality attributable to alcohol consumption," *UICC International Journal of Cancer IJC*, vol. 138, pp. 1380–1387, 2016, doi: 10.1002/ijc.29890.
- [29] K. F. Brown *et al.*, "The fraction of cancer attributable to modifiable risk factors in England, Wales, Scotland, Northern Ireland, and the United Kingdom in 2015," *Br J Cancer*, vol. 118, no. 8, pp. 1130–1141, Apr. 2018, doi: 10.1038/s41416-018-0029-6.

- [30] N. D. Freedman *et al.*, "Alcohol intake and risk of oesophageal adenocarcinoma: a pooled analysis from the BEACON Consortium", doi: 10.1136/gut.2010.233866.
- [31] F. Turati, I. Tramacere, C. La Vecchia, and E. Negri, "A meta-analysis of body mass index and esophageal and gastric cardia adenocarcinoma," *Annals of Oncology*, vol. 24, pp. 609–617, 2013, doi: 10.1093/annonc/mds244.
- [32] C. Hoyo *et al.*, "Body mass index in relation to oesophageal and oesophagogastric junction adenocarcinomas: a pooled analysis from the International BEACON Consortium.," *Int J Epidemiol*, vol. 41, no. 6, pp. 1706–1718, Dec. 2012, doi: 10.1093/ije/dys176.
- [33] Q. Zhang and Y. Wang, "Trends in the Association between Obesity and Socioeconomic Status in U.S. Adults: 1971 to 2000," *Obes Res*, vol. 12, no. 10, pp. 1622–1632, Oct. 2004, doi: 10.1038/oby.2004.202.
- [34] J. A. Abrams, R. Z. Sharaiha, L. Gonsalves, C. J. Lightdale, and A. I. Neugut, "Dating the rise of esophageal adenocarcinoma: analysis of Connecticut Tumor Registry data, 1940-2007.," *Cancer Epidemiol Biomarkers Prev*, vol. 20, no. 1, pp. 183–186, Jan. 2011, doi: 10.1158/1055-9965.EPI-10-0802.
- [35] H. Hampel, N. S. Abraham, and H. B. El-Serag, "Meta-Analysis: Obesity and the Risk for Gastroesophageal Reflux Disease and Its Complications," *Ann Intern Med*, vol. 143, no. 3, p. 199, Aug. 2005, doi: 10.7326/0003-4819-143-3-200508020-00006.

- [36] N. Barak, E. D. Ehrenpreis, J. R. Harrison, and M. D. Sitrin, "Gastro-oesophageal reflux disease in obesity: pathophysiological and therapeutic considerations," *Obesity Reviews*, vol. 3, no. 1, pp. 9–15, Feb. 2002, doi: 10.1046/j.1467-789X.2002.00049.x.
- [37] A. Maddox, M. Horowitz, J. Wishart, and P. Collins, "Gastric and Oesophageal Emptying in Obesity," *Scand J Gastroenterol*, vol. 24, no. 5, pp. 593–598, Jan. 1989, doi: 10.3109/00365528909093095.
- [38] P. Moayyedi, M. B. B. Ch, and F. R. C. P. (London, "Barrett's Esophagus and Obesity: The Missing Part of the Puzzle", doi: 10.1111/j.1572-0241.2007.01618.x.
- [39] D. C. Whiteman *et al.*, "Combined effects of obesity, acid reflux and smoking on the risk of adenocarcinomas of the oesophagus," *Gut*, vol. 57, no. 2, pp. 173–180, Feb. 2008, doi: 10.1136/GUT.2007.131375.
- [40] J. Lagergren, R. Bergström, and O. Nyrén, "Association between Body Mass and Adenocarcinoma of the Esophagus and Gastric Cardia," *Ann Intern Med*, vol. 130, no. 11, p. 883, Jun. 1999, doi: 10.7326/0003-4819-130-11-199906010-00003.
- [41] S. Singh *et al.*, "Central Adiposity Is Associated With Increased Risk of Esophageal Inflammation, Metaplasia, and Adenocarcinoma: A Systematic Review and Meta-analysis," 2013, doi: 10.1016/j.cgh.2013.05.009.

- [42] Y. Lin, E. Ness-Jensen, K. Hveem, Jesper Lagergren, Y. Lu, and Y. L. Se, "Metabolic syndrome and esophageal and gastric cancer," *Cancer Causes & Control*, vol. 26, pp. 1825–1834, 2015, doi: 10.1007/s10552-015-0675-4.
- [43] J. Maret-Ouda, W. Tao, F. Mattsson, N. Brusselaers, H. B. El-Serag, and J. Lagergren, "Esophageal adenocarcinoma after obesity surgery in a population-based cohort study," *Surgery for Obesity and Related Diseases*, vol. 13, no. 1, pp. 28–34, Jan. 2017, doi: 10.1016/j.soard.2015.09.016.
- [44] H. G. Coleman, S.-H. Xie, and J. Lagergren, "The Epidemiology of Esophageal Adenocarcinoma," 2017, doi: 10.1053/j.gastro.2017.07.046.
- [45] C. Duggan, L. Onstad, S. Hardikar, P. L. Blount, B. J. Reid, and T. L. Vaughan, "Association Between Markers of Obesity and Progression From Barrett's Esophagus to Esophageal Adenocarcinoma BACKGROUND & Esophageal & Es
- [46] J. Drahos, W. Ricker, R. M. Pfeiffer, and M. B. Cook Phd, "Metabolic Syndrome and Risk of Esophageal Adenocarcinoma in Elderly Patients in the United States: An Analysis of SEER-Medicare Data", doi: 10.1002/cncr.30365.
- [47] A. Ruol *et al.*, "Intestinal metaplasia is the probable common precursor of adenocarcinoma in Barrett esophagus and adenocarcinoma of the gastric

- cardia," *Cancer*, vol. 88, no. 11, pp. 2520–2528, Jun. 2000, doi: 10.1002/1097-0142(20000601)88:11<2520::AID-CNCR13>3.0.CO;2-L.
- [48] F. Hvid-Jensen, L. Pedersen, A. M. Drewes, H. T. Sørensen, and P. Funch-Jensen, "Incidence of Adenocarcinoma among Patients with Barrett's Esophagus,"

 New England Journal of Medicine, vol. 365, no. 15, pp. 1375–1383, Oct. 2011.
- [49] D. M. Nguyen, H. B. El-Serag, L. Henderson, D. Stein, A. Bhattacharyya, and R. E. Sampliner, "Medication Usage and the Risk of Neoplasia in Patients With Barrett's Esophagus," *Clinical Gastroenterology and Hepatology*, vol. 7, no. 12, pp. 1299–1304, Dec. 2009, doi: 10.1016/J.CGH.2009.06.001.
- [50] P. A. C. Gatenby, J. R. Ramus, C. P. J. Caygill, A. Charlett, M. C. Winslet, and A. Watson, "Treatment modality and risk of development of dysplasia and adenocarcinoma in columnar-lined esophagus," *Diseases of the Esophagus*, vol. 22, no. 2, pp. 133–142, Apr. 2009, doi: 10.1111/j.1442-2050.2008.00886.x.
- [51] T. K. Desai *et al.*, "The incidence of oesophageal adenocarcinoma in non-dysplastic Barrett's oesophagus: a meta-analysis," *Gut*, vol. 61, no. 7, pp. 970–976, Jul. 2012.
- [52] V. Switzer-Taylor, M. Schlup, R. Lübcke, V. Livingstone, and M. Schultz, "Barrett's esophagus: A retrospective analysis of 13 years surveillance," 2008, doi: 10.1111/j.1440-1746.2008.05311.x.

- [53] W. H. Allum, J. M. Blazeby, S. M. Griffin, D. Cunningham, J. A. Jankowski, and R. Wong, "Guidelines for the management of oesophageal and gastric cancer," *Gut*, vol. 60, no. 11, pp. 1449–1472, 2011, doi: 10.1136/gut.2010.228254.
- [54] J. Lagergren, E. Smyth, D. Cunningham, and P. Lagergren, "Oesophageal cancer," *The Lancet*, vol. 390, no. 10110, pp. 2383–2396, Nov. 2017, doi: 10.1016/S0140-6736(17)31462-9.
- [55] N. J. Curtis, F. Noble, I. S. Bailey, J. J. Kelly, J. P. Byrne, and T. J. Underwood, "The Relevance of the Siewert Classification in the Era of Multimodal Therapy for Adenocarcinoma of the Gastro-Oesophageal Junction," *The Authors. Journal of Surgical Oncology*, vol. 109, pp. 202–207, 2014, doi: 10.1002/jso.23484.
- [56] J. A. Ajani, J. Lee, T. Sano, Y. Y. Janjigian, D. Fan, and S. Song, "Gastric adenocarcinoma," *Nature Reviews Disease Primers 2017 3:1*, vol. 3, no. 1, pp. 1–19, Jun. 2017, doi: 10.1038/nrdp.2017.36.
- [57] T. W. Rice, D. T. Patil, and E. H. Blackstone, "8th edition AJCC/UICC staging of cancers of the esophagus and esophagogastric junction: application to clinical practice.," *Ann Cardiothorac Surg*, vol. 6, no. 2, pp. 119–130, Mar. 2017, doi: 10.21037/acs.2017.03.14.
- [58] C. Mariette, G. Piessen, N. Briez, C. G.-T. lancet oncology, and undefined 2011, "Oesophagogastric junction adenocarcinoma: which therapeutic approach?," *Elsevier*.

- [59] "TNM staging | Oesophageal cancer | Cancer Research UK." Accessed: Aug.13, 2021. [Online]. Available: https://www.cancerresearchuk.org/about-cancer/oesophageal-cancer/stages-types-and-grades/tnm-staging
- [60] J. P. Dolan *et al.*, "Significant understaging is seen in clinically staged T2N0 esophageal cancer patients undergoing esophagectomy," *Diseases of the Esophagus*, vol. 29, no. 4, pp. 320–325, May 2016, doi: 10.1111/dote.12334.
- [61] T. Nishimaki *et al.*, "Evaluation of the accuracy of preoperative staging in thoracic esophageal cancer," *Ann Thorac Surg*, vol. 68, no. 6, pp. 2059–2064, Dec. 1999, doi: 10.1016/S0003-4975(99)01171-6.
- [62] L. Goense *et al.*, "Role of neoadjuvant chemoradiotherapy in clinical T2N0M0 esophageal cancer: A population-based cohort study," *European Journal of Surgical Oncology*, vol. 44, no. 5, pp. 620–625, May 2018, doi: 10.1016/j.ejso.2018.02.005.
- [63] E. Vazquez-Sequeiros *et al.*, "Impact of EUS-guided fine-needle aspiration on lymph node staging in patients with esophageal carcinoma," *Gastrointest Endosc*, vol. 53, no. 7, pp. 751–757, 2001, doi: 10.1067/mge.2001.112741.
- [64] G. W. de Graaf, A. A. Ayantunde, S. L. Parsons, J. P. Duffy, and N. T. Welch, "The role of staging laparoscopy in oesophagogastric cancers," *European Journal of Surgical Oncology*, vol. 33, no. 8, pp. 988–992, Oct. 2007, doi: 10.1016/j.ejso.2007.01.007.

- [65] L. Massimi *et al.*, "Detection of involved margins in breast specimens with X-ray phase-contrast computed tomography," *Scientific Reports 2021 11:1*, vol. 11, no. 1, pp. 1–9, Feb. 2021, doi: 10.1038/s41598-021-83330-w.
- [66] E. Castelli *et al.*, "Mammography with synchrotron radiation: First clinical experience with phase-detection technique," *Radiology*, vol. 259, no. 3, pp. 684–694, Jun. 2011, doi: 10.1148/radiol.11100745.
- [67] F. Lordick, C. Mariette, K. Haustermans, R. Obermannová, and D. Arnold, "Oesophageal cancer: ESMO Clinical Practice Guidelines for diagnosis, treatment and follow-up+," *Annals of Oncology*, vol. 27, no. suppl_5, pp. v50–v57, Sep. 2016, doi: 10.1093/annonc/mdw329.
- [68] P. Van Hagen *et al.*, "Preoperative Chemoradiotherapy for Esophageal or Junctional Cancer," 2012.
- [69] E. C. Smyth et al., "Oesophageal cancer," Nat Rev Dis Primers, vol. 3, no. 1, p. 17048, Dec. 2017, doi: 10.1038/nrdp.2017.48.
- [70] A. D. Wagner *et al.*, "Chemotherapy for advanced gastric cancer," *Cochrane Database of Systematic Reviews*, vol. 2017, no. 8, Aug. 2017, doi: 10.1002/14651858.CD004064.PUB4/EPDF/FULL.
- [71] D. Cunningham *et al.*, "Capecitabine and Oxaliplatin for Advanced Esophagogastric Cancer," 2008.

- [72] I. C. Noordzij, M. L. Hazen, G. A. P. Nieuwenhuijzen, R. H. A. Verhoeven, and E. J. Schoon, "Endoscopic therapy replaces surgery for clinical T1 oesophageal cancer in the Netherlands: a nationwide population-based study," *Surg Endosc*, vol. 37, no. 6, pp. 4535–4544, Jun. 2023, doi: 10.1007/S00464-023-09914-X/TABLES/4.
- [73] "Surgery to remove your oesophagus | Oesophageal cancer | Cancer Research
 UK." Accessed: Oct. 11, 2021. [Online]. Available:
 https://www.cancerresearchuk.org/about-cancer/oesophagealcancer/treatment/surgery/surgery-remove-your-oesophagus
- [74] I. Gockel, C. Exner, and T. Junginger, "Morbidity and mortality after esophagectomy for esophageal carcinoma: A risk analysis," *World J Surg Oncol*, vol. 3, p. 37, Jun. 2005, doi: 10.1186/1477-7819-3-37.
- [75] B. Rim Kim *et al.*, "The association between hospital case-volume and postoperative outcomes after esophageal cancer surgery: A population-based retrospective cohort study," 2021, doi: 10.1111/1759-7714.14096.
- [76] N. Patel *et al.*, "Cardiopulmonary fitness predicts postoperative major morbidity after esophagectomy for patients with cancer," *Physiol Rep*, vol. 7, no. 14, p. e14174, Jul. 2019, doi: 10.14814/PHY2.14174.
- [77] S. M. Griffin *et al.*, "Evolution of Esophagectomy for Cancer Over 30 Years: Changes in Presentation, Management and Outcomes," *Ann Surg Oncol*, vol. 28, doi: 10.1245/s10434-020-09200-3.

- [78] E. Gottlieb-Vedi, J. H. Kauppila, G. Malietzis, M. Nilsson, S. R. Markar, and J. Lagergren, "Long-term survival in esophageal cancer after minimally invasive compared to open esophagectomy: A systematic review and meta-analysis," *Ann Surg*, vol. 270, no. 6, pp. 1005–1017, Dec. 2019, doi: 10.1097/SLA.0000000000003252.
- [79] C. Kondoh *et al.*, "Efficacy of palliative radiotherapy for gastric bleeding in patients with unresectable advanced gastric cancer: a retrospective cohort study," *BMC Palliat Care*, 2015, doi: 10.1186/s12904-015-0034-y.
- [80] R. C. Fitzgerald *et al.*, "British Society of Gastroenterology guidelines on the diagnosis and management of Barrett's oesophagus," *Gut*, vol. 63, no. 1, pp. 7–42, Jan. 2014, doi: 10.1136/gutjnl-2013-305372.
- [81] S. J. Spechler, P. Sharma, R. F. Souza, J. M. Inadomi, and N. J. Shaheen, "American gastroenterological association technical review on the management of Barrett's esophagus," 2011, W.B. Saunders. doi: 10.1053/j.gastro.2011.01.031.
- [82] D. B. Skinner, B. C. Walther, R. H. Riddell, H. Schmidt, C. Iascone, and T. R. Demeester, "Barrett's Esophagus Comparison of Benign and Malignant Cases."
- [83] "The spectrum of carcinoma arising in Barrett's esophagus: A...: The American Journal of Surgical Pathology." Accessed: Mar. 03, 2021. [Online]. Available: https://journals.lww.com/ajsp/Abstract/1984/08000/The_spectrum_of_carcinoma_arising_in_Barrett_s.1.aspx

- [84] K. Takubo *et al.*, "Cardiac rather than intestinal-type background in endoscopic resection specimens of minute Barrett adenocarcinoma," *Hum Pathol*, vol. 40, no. 1, pp. 65–74, Jan. 2009, doi: 10.1016/j.humpath.2008.06.008.
- [85] C. J. Kelty, M. D. Gough, Q. Van Wyk, T. J. Stephenson, and R. Ackroyd, "Barrett's oesophagus: Intestinal metaplasia is not essential for cancer risk," *Scand J Gastroenterol*, vol. 42, no. 11, pp. 1271–1274, 2007, doi: 10.1080/00365520701420735.
- [86] Z. R. Edelstein, M. P. Bronner, S. N. Rosen, and T. L. Vaughan, "Risk factors for Barrett's esophagus among patients with gastroesophageal reflux disease: A community clinic-based case-control study," *Am J Gastroenterol*, vol. 104, no. 4, p. 834, Apr. 2009, doi: 10.1038/AJG.2009.137.
- [87] Z. R. Edelstein, D. C. Farrow, M. P. Bronner, S. N. Rosen, and T. L. Vaughan, "Central Adiposity and Risk of Barrett's Esophagus," *Gastroenterology*, vol. 133, no. 2, pp. 403–411, Aug. 2007, doi: 10.1053/J.GASTRO.2007.05.026.
- [88] L. A. Anderson *et al.*, "Risk factors for Barrett's oesophagus and oesophageal adenocarcinoma: Results from the FINBAR study," *World Journal of Gastroenterology: WJG*, vol. 13, no. 10, p. 1585, Mar. 2007, doi: 10.3748/WJG.V13.I10.1585.
- [89] A. Chak *et al.*, "Familiality in Barrett's Esophagus, Adenocarcinoma of the Esophagus, and Adenocarcinoma of the Gastroesophageal Junction," *Cancer*

- *Epidemiology and Prevention Biomarkers*, vol. 15, no. 9, pp. 1668–1673, Sep. 2006, doi: 10.1158/1055-9965.EPI-06-0293.
- [90] A. Chak *et al.*, "Familial aggregation of Barrett's oesophagus, oesophageal adenocarcinoma, and oesophagogastric junctional adenocarcinoma in Caucasian adults," *Gut*, vol. 51, no. 3, pp. 323–328, Sep. 2002, doi: 10.1136/GUT.51.3.323.
- [91] A. Rosenfeld *et al.*, "Development and validation of a risk prediction model to diagnose Barrett's oesophagus (MARK-BE): a case-control machine learning approach," *Lancet Digit Health*, vol. 2, no. 1, pp. e37–e48, Jan. 2020, doi: 10.1016/S2589-7500(19)30216-X.
- [92] "Dysplasia | Definition of Dysplasia by Merriam-Webster." Accessed: Aug. 10,2021. [Online]. Available: https://www.merriam-webster.com/dictionary/dysplasia
- [93] J. A. Jankowski *et al.*, "Molecular evolution of the metaplasia-dysplasia-adenocarcinoma sequence in the esophagus," 1999, *American Society for Investigative Pathology Inc.* doi: 10.1016/S0002-9440(10)65346-1.
- [94] J. W. Van Sandick, J. J. B. Van Lanschot, B. W. Kuiken, G. N. J. Tytgat, G. J. A. Offerhaus, and H. Obertop, "Impact of endoscopic biopsy surveillance of Barrett's oesophagus on pathological stage and clinical outcome of Barrett's carcinoma," *Gut*, vol. 43, no. 2, pp. 216–222, 1998, doi: 10.1136/gut.43.2.216.

- [95] K. Geboes and P. Van Eyken, "The diagnosis of dysplasia and malignancy in Barrett's oesophagus," *Histopathology*, vol. 37, no. 2, pp. 99–107, Aug. 2000, doi: 10.1046/J.1365-2559.2000.00960.X.
- [96] R. J. Schlemper *et al.*, "The Vienna classification of gastrointestinal epithelial neoplasia," 2000.
- [97] E. Montgomery, C. A. Arnold, D. Lam-Himlin, K. Salimian, and K. Waters, "Some observations on Barrett esophagus and associated dysplasia," Dec. 01, 2018, *W.B. Saunders*. doi: 10.1016/j.anndiagpath.2018.09.013.
- [98] F. Schlottmann and M. G. Patti, "Current Concepts in Treatment of Barrett's Esophagus With and Without Dysplasia," *Journal of Gastrointestinal Surgery* 2017 21:8, vol. 21, no. 8, pp. 1354–1360, Mar. 2017, doi: 10.1007/S11605-017-3371-8.
- [99] "PII: S0046-8177(83)80175-0 | Elsevier Enhanced Reader." Accessed: Mar. 09, 2021. [Online]. Available: https://reader.elsevier.com/reader/sd/pii/S0046817783801750?token=FBF0 340EDD50C0C306A47AFFE20322A3E615BCA2C4FE4C43FDF901CBD78207CFE 213C531AA4AF6F8D5DB87F182202A0B
- [100] O. Old *et al.*, "Barrett's Oesophagus Surveillance Versus Endoscopy at Need Study (BOSS): A Randomized Controlled Trial," *Gastroenterology*, 2025, doi: 10.1053/j.gastro.2025.03.021.

- [101] N. Gupta, S. Gaddam, S. B. Wani, A. Bansal, A. Rastogi, and P. Sharma, "Longer inspection time is associated with increased detection of high-grade dysplasia and esophageal adenocarcinoma in Barrett's esophagus," *Gastrointest Endosc*, vol. 76, no. 3, pp. 531–538, Sep. 2012, doi: 10.1016/J.GIE.2012.04.470.
- [102] V. R. Muthusamy *et al.*, "AGA Clinical Practice Update on New Technology and Innovation for Surveillance and Screening in Barrett's Esophagus: Expert Review," *Clinical Gastroenterology and Hepatology*, vol. 20, no. 12, pp. 2696-2706.e1, 2022, doi: 10.1016/j.cgh.2022.06.003.
- [103] J. R. Ramus, C. P. J. Caygill, P. A. C. Gatenby, and A. Watson, "Current United Kingdom practice in the diagnosis and management of columnar-lined oesophagus: results of the United Kingdom National Barrett Oesophagus Registry endoscopist questionnaire," *European Journal of Cancer Prevention*, vol. 17, no. 5, pp. 422–425, Oct. 2008, doi: 10.1097/CEJ.0B013E3282B6FD1E.
- [104] D. Das *et al.*, "ORIGINAL CONTRIBUTIONS Esophagus Management of Barrett's Esophagus in the UK: Overtreated and Underbiopsied but Improved by the Introduction of a National Randomized Trial," *Am J Gastroenterol*, vol. 103, pp. 1079–1089, 2008, doi: 10.1111/j.1572-0241.2008.01790.x.
- [105] W. L. Curvers *et al.*, "Quality of Barrett's surveillance in The Netherlands: A standardized review of endoscopy and pathology reports," *Eur J Gastroenterol Hepatol*, vol. 20, no. 7, pp. 601–607, Jul. 2008, doi: 10.1097/MEG.0B013E3282F8295D.

- [106] "Surgical Endoscopy A new simplified technique of endoscopic esophageal mucosal resection using a cap-fitted panendoscope (EMRC)".
- [107] D. Alzoubaidi *et al.*, "Comparison of two multiband mucosectomy devices for endoscopic resection of Barrett's esophagus-related neoplasia," *Surg Endosc*, vol. 33, no. 11, p. 3665, Nov. 2019, doi: 10.1007/S00464-018-06655-0.
- [108] M. Conio et al., "Endoscopic mucosal resection for high-grade dysplasia and intramucosal carcinoma in Barrett's esophagus: An Italian experience," http://www.wjgnet.com/, vol. 11, no. 42, pp. 6650–6655, Nov. 2005, doi: 10.3748/WJG.V11.I42.6650.
- [109] C. V. Lopes *et al.*, "Circumferential endoscopic resection of Barrett's esophagus with high-grade dysplasia or early adenocarcinoma," *Surgical Endoscopy 2007 21:5*, vol. 21, no. 5, pp. 820–824, Feb. 2007, doi: 10.1007/S00464-006-9187-3.
- [110] A. May et al., "Intraepithelial High-Grade Neoplasia and Early Adenocarcinoma in Short-Segment Barrett's Esophagus (SSBE): Curative Treatment Using Local Endoscopic Treatment Techniques," *Endoscopy*, vol. 34, no. 08, pp. 604–610, Aug. 2002, doi: 10.1055/S-2002-33236.
- [111] A. May *et al.*, "A prospective randomized trial of two different endoscopic resection techniques for early stage cancer of the esophagus," *Gastrointest Endosc*, vol. 58, no. 2, pp. 167–175, Aug. 2003, doi: 10.1067/MGE.2003.339.

- [112] R. E. Pouw *et al.*, "Randomized trial on endoscopic resection-cap versus multiband mucosectomy for piecemeal endoscopic resection of early Barrett's neoplasia," *Gastrointest Endosc*, vol. 74, no. 1, pp. 35–43, Jul. 2011, doi: 10.1016/J.GIE.2011.03.1243.
- [113] S. Komanduri, V. R. Muthusamy, and S. Wani, "Controversies in Endoscopic Eradication Therapy for Barrett's Esophagus," *Gastroenterology*, vol. 154, no. 7, pp. 1861-1875.e1, May 2018, doi: 10.1053/J.GASTRO.2017.12.045.
- [114] J. Chennat *et al.*, "Complete Barrett's eradication endoscopic mucosal resection: An effective treatment modality for high-grade dysplasia and intramucosal carcinoma An American single-center experience," *American Journal of Gastroenterology*, vol. 104, no. 11, pp. 2684–2692, 2009, doi: 10.1038/ajg.2009.465.
- [115] A. Larghi *et al.*, "Long-term follow-up of complete Barrett's eradication endoscopic mucosal resection (CBE-EMR) for the treatment of high grade dysplasia and intramucosal carcinoma," *Endoscopy*, vol. 39, no. 12, pp. 1086–1091, Aug. 2007, doi: 10.1055/S-2007-966788.
- [116] A. Y. Cao *et al.*, "Meta-analysis of endoscopic submucosal dissection versus endoscopic mucosal resection for tumors of the gastrointestinal tract," 2009, doi: 10.1055/s-0029-1215053.
- [117] O. BF *et al.*, "Photodynamic therapy with porfimer sodium for ablation of high-grade dysplasia in Barrett's esophagus: international, partially blinded,

- randomized phase III trial," *Gastrointest Endosc*, vol. 62, no. 4, pp. 488–498, Oct. 2005, doi: 10.1016/J.GIE.2005.06.047.
- [118] D. JM *et al.*, "A randomised controlled trial of ALA vs. Photofrin photodynamic therapy for high-grade dysplasia arising in Barrett's oesophagus," *Lasers Med Sci*, vol. 28, no. 3, pp. 707–715, May 2013, doi: 10.1007/S10103-012-1132-1.
- [119] B. F. Overholt *et al.*, "Five-year efficacy and safety of photodynamic therapy with Photofrin in Barrett's high-grade dysplasia," *Gastrointest Endosc*, vol. 66, no. 3, pp. 460–468, Sep. 2007, doi: 10.1016/j.gie.2006.12.037.
- [120] Y. P. P. WP, and N. NS, "Patient predictors of esophageal stricture development after photodynamic therapy," *Clin Gastroenterol Hepatol*, vol. 6, no. 3, pp. 302–308, Mar. 2008, doi: 10.1016/J.CGH.2007.12.001.
- [121] D. E. Fleischer *et al.*, "Endoscopic ablation of Barrett's esophagus: a multicenter study with 2.5-year follow-up," *Gastrointest Endosc*, vol. 68, no. 5, pp. 867–876, Nov. 2008, doi: 10.1016/J.GIE.2008.03.008.
- [122] "RF Ablation Catheter Treating Barrett's Esophagus." Accessed: Oct. 21, 2021.
 [Online]. Available:
 https://www.todaysmedicaldevelopments.com/article/covidien-barrx-channel-rfa-endocscopic-medical-device-081713/
- [123] R. J. Haidry *et al.*, "Improvement over time in outcomes for patients undergoing endoscopic therapy for Barrett's oesophagus-related neoplasia: 6-

- year experience from the first 500 patients treated in the UK patient registry," *Gut*, vol. 64, no. 8, doi: 10.1136/gutjnl-2014-308501.
- [124] N. J. Shaheen *et al.*, "Durability of radiofrequency ablation in Barrett's esophagus with dysplasia," *Gastroenterology*, vol. 141, no. 2, pp. 460–468, Aug. 2011, doi: 10.1053/j.gastro.2011.04.061.
- [125] M. H. Johnston, J. A. Eastone, J. D. Horwhat, J. Cartledge, J. S. Mathews, and J. R. Foggy, "Cryoablation of Barrett's esophagus: a pilot study," *Gastrointest Endosc*, vol. 62, no. 6, pp. 842–848, Dec. 2005, doi: 10.1016/J.GIE.2005.05.008.
- [126] J. A. Dumot, J. J. Vargo, G. W. Falk, L. Frey, R. Lopez, and T. W. Rice, "An open-label, prospective trial of cryospray ablation for Barrett's esophagus high-grade dysplasia and early esophageal cancer in high-risk patients,"

 Gastrointest Endosc, vol. 70, no. 4, pp. 635–644, 2009, doi: 10.1016/j.gie.2009.02.006.
- [127] M. I. Canto et al., "Safety and efficacy of carbon dioxide cryotherapy for treatment of neoplastic Barrett's esophagus," Endoscopy, vol. 47, pp. 582–591, 2015, doi: 10.1055/s-0034-1391734.
- [128] F. H. Ramay, Q. Cui, and B. D. Greenwald, "Outcomes after liquid nitrogen spray cryotherapy in Barrett's esophagus—associated high-grade dysplasia and intramucosal adenocarcinoma: 5-year follow-up," *Gastrointest Endosc*, vol. 86, no. 4, pp. 626–632, Oct. 2017, doi: 10.1016/J.GIE.2017.02.006.

- [129] M. Fasullo *et al.*, "Outcomes of Radiofrequency Ablation Compared to Liquid Nitrogen Spray Cryotherapy for the Eradication of Dysplasia in Barrett's Esophagus," *Digestive Diseases and Sciences 2021*, vol. 1, pp. 1–7, May 2021, doi: 10.1007/S10620-021-06991-7.
- [130] M. F. Peerally *et al.*, "566 BRIDE (Barrett's Randomised Intervention for Dysplasia by Endoscopy)-Results of a Feasibility Study Comparing Argon Plasma Coagulation (APC) With Radiofrequency Ablation (RFA) After Endoscopic Resection of Patients With High Grade Dysplasia or T1 Adenocarcinoma in Barrett's Esophagus," 2016, doi: 10.1016/j.gie.2016.03.105.
- [131] E. S. ORMAN, N. LI, and N. J. SHAHEEN, "Efficacy and Durability of Radiofrequency Ablation for Barrett's Esophagus: Systematic Review and Meta-analysis," *Clin Gastroenterol Hepatol*, vol. 11, no. 10, pp. 1245–1255, Oct. 2013, doi: 10.1016/J.CGH.2013.03.039.
- [132] K. N. Phoa *et al.*, "Multimodality endoscopic eradication for neoplastic Barrett oesophagus: results of an European multicentre study (EURO-II).," *Gut*, pp. 1–8, 2015, doi: 10.1136/gutjnl-2015-309298.
- [133] M. Desai *et al.*, "Systematic review with meta-analysis: the long-term efficacy of Barrett's endoscopic therapy—stringent selection criteria and a proposal for definitions," *Aliment Pharmacol Ther*, vol. 54, no. 3, pp. 222–233, Aug. 2021, doi: 10.1111/APT.16473.

- [134] M. B. Loughrey and N. A. Shepherd, "The indications for biopsy in routine upper gastrointestinal endoscopy," *Histopathology*, vol. 78, no. 1, pp. 215–227, Jan. 2021, doi: 10.1111/his.14213.
- [135] B. Qumseya *et al.*, "ASGE guideline on screening and surveillance of Barrett's esophagus Prepared by: ASGE STANDARDS OF PRACTICE COMMITTEE," 2019. doi: 10.1016/j.gie.2019.05.012.
- [136] A. Bas Weusten *et al.*, "Endoscopic management of Barrett's esophagus: European Society of Gastrointestinal Endoscopy (ESGE) Position Statement," 2017, doi: 10.1055/s-0042-122140.
- [137] M. A. Everson *et al.*, "Virtual chromoendoscopy by using optical enhancement improves the detection of Barrett's esophagus—associated neoplasia," *Gastrointest Endosc*, vol. 89, no. 2, pp. 247-256.e4, Feb. 2019, doi: 10.1016/J.GIE.2018.09.032.
- [138] "Histology | Definition of Histology by Merriam-Webster." Accessed: Dec. 16,2020. [Online]. Available: https://www.merriam-webster.com/dictionary/histology
- [139] "Histopathology | Definition of Histopathology by Merriam-Webster."

 Accessed: Dec. 16, 2020. [Online]. Available: https://www.merriam-webster.com/dictionary/histopathology

- [140] R. Thavarajah, V. K. Mudimbaimannar, J. Elizabeth, U. K. Rao, and K. Ranganathan, "Chemical and physical basics of routine formaldehyde fixation," Sep. 2012, Wolters Kluwer -- Medknow Publications. doi: 10.4103/0973-029X.102496.
- [141] C. by Lord Carter of Coles, "Report of the Review of NHS Pathology Services in England," 2006.
- [142] "Report of the Second Phase of the Review of NHS Pathology Services in England Report of the Second Phase of the Independent Review of NHS Pathology Services in England Chaired by Lord Carter of Coles An Independent Review for the Department of Health."
- [143] N. A. Shepherd and R. M. Valori, "The effective use of gastrointestinal histopathology: guidance for endoscopic biopsy in the gastrointestinal tract", doi: 10.1136/flgastro-2013-100412.
- [144] "TESTING TIMES TO COME? AN EVALUATION OF PATHOLOGY CAPACITY ACROSS THE UK," 2016.
- [145] B. J. Williams, D. Bottoms, and D. Treanor, "Future-proofing pathology: The case for clinical adoption of digital pathology," *J Clin Pathol*, vol. 70, no. 12, pp. 1010–1018, Dec. 2017, doi: 10.1136/jclinpath-2017-204644.
- [146] R. J. Haidry *et al.*, "Radiofrequency ablation and endoscopic mucosal resection for dysplastic Barrett's esophagus and early esophageal adenocarcinoma:

- Outcomes of the UK national halo RFA registry," *Gastroenterology*, vol. 145, no. 1, pp. 87–95, Jul. 2013, doi: 10.1053/j.gastro.2013.03.045.
- [147] M. F. Peerally *et al.*, "Radiofrequency ablation compared with argon plasma coagulation after endoscopic resection of high-grade dysplasia or stage T1 adenocarcinoma in Barrett's esophagus: a randomized pilot study (BRIDE)," *Gastrointest Endosc*, vol. 89, no. 4, pp. 680–689, 2019, doi: 10.1016/j.gie.2018.07.031.
- [148] R. J. Haidry *et al.*, "Comparing outcome of radiofrequency ablation in Barrett' s with high grade dysplasia and intramucosal carcinoma: a prospective multicenter UK registry," *Endoscopy*, vol. epub Jun 3, no. 11, pp. 980–987, Jul. 2015, doi: 10.1055/s-0034-1392414.
- [149] S. W. Webb and R. M. Henkelman, "Physics of Medical Imaging ," Phys Today, vol. 43, no. 4, pp. 77–78, Apr. 1990, doi: 10.1063/1.2810532.
- [150] A. Olivo and E. Castelli, "X-ray phase contrast imaging: From synchrotrons to conventional sources", doi: 10.1393/ncr/i2014-10104-8.
- [151] Jones and Bartlett, "Light and the electromagnetic spectrum," *Physics (College Park Md)*, pp. 95–122, 1964.
- [152] "Full details and actions for Introduction to medical imaging [electronic resource]: physics, engineering and clinical applications / Nadine Barrie Smith,

- Andrew Webb." Accessed: Jun. 08, 2021. [Online]. Available: https://www.vlebooks.com/Vleweb/Product/Index/2007614?page=0
- [153] N. Smith, Introduction to medical imaging: physics, engineering and clinical applications / Nadine Barrie Smith, Andrew Webb.
- [154] S. Balter and G. T. Barnes, "AAPM T utorial Contrast and Scatter in X-ray Imaging1."
- [155] U. Bonse and M. Hart, "An X-ray interferometer," *Appl Phys Lett*, vol. 6, no. 8, pp. 155–156, Nov. 1965, doi: 10.1063/1.1754212.
- [156] A. Olivo *et al.*, "Low-dose phase contrast mammography with conventional x-ray sources.," *Med Phys*, vol. 40, no. 9, p. 090701, Sep. 2013, doi: 10.1118/1.4817480.
- [157] T. Takeda, A. Momose, Y. Itai, W. Jin, and K. Hirano, "Phase-contrast imaging with synchrotron x-rays for detecting cancer lesions," *Acad Radiol*, vol. 2, no. 9, pp. 799–803, Sep. 1995, doi: 10.1016/S1076-6332(05)80490-8.
- [158] F. A. Vittoria *et al.*, "Beam tracking phase tomography with laboratory sources," in *Journal of Instrumentation*, Institute of Physics Publishing, Apr. 2018, p. C04008. doi: 10.1088/1748-0221/13/04/C04008.
- [159] "Edge-illumination x-ray phase-contrast imaging," 2021, doi: 10.1088/1361-648X/ac0e6e.

- [160] C. K. Hagen *et al.*, "High contrast microstructural visualization of natural acellular matrices by means of phase-based x-ray tomography," *Sci Rep*, vol. 5, no. 1, pp. 1–10, Dec. 2015, doi: 10.1038/srep18156.
- [161] M. Marenzana et al., "Visualization of small lesions in rat cartilage by means of laboratory-based x-ray phase contrast imaging," Phys Med Biol, vol. 57, no. 24, p. 8173, Nov. 2012, doi: 10.1088/0031-9155/57/24/8173.
- [162] M. J. Kitchen et al., "Phase contrast X-ray imaging of mice and rabbit lungs: a comparative study," http://dx.doi.org/10.1259/bjr/13024611, vol. 78, no. 935, pp. 1018–1027, Jan. 2014, doi: 10.1259/BJR/13024611.
- [163] K. Mori et al., "Application of synchrotron X-ray imaging to phase objects in orthopedics," urn:issn:0909-0495, vol. 9, no. 3, pp. 143–147, Apr. 2002, doi: 10.1107/S0909049502004624.
- [164] H. Nguyen Thi *et al.*, "Preliminary in situ and real-time study of directional solidification of metallic alloys by x-ray imaging techniques," *J. Phys. D: Appl. Phys*, vol. 36, pp. 83–86, 2003.
- [165] "International Year of Light How do they work?" Accessed: Oct. 26, 2021.
 [Online]. Available:
 https://www.light2015.org/Home/LearnAboutLight/Lightsources-of-the-world/How-does-it-work-.html

- [166] P. Wolfson *et al.*, "Endoscopic eradication therapy for Barrett's esophagus–related neoplasia: a final 10-year report from the UK National HALO Radiofrequency Ablation Registry," *Gastrointest Endosc*, vol. 96, no. 2, pp. 223–233, Aug. 2022, doi: 10.1016/J.GIE.2022.02.016.
- [167] M. B. Cook, W. H. Chow, and S. S. Devesa, "Oesophageal cancer incidence in the United States by race, sex, and histologic type, 1977-2005," *Br J Cancer*, vol. 101, no. 5, pp. 855–859, Sep. 2009, doi: 10.1038/sj.bjc.6605246.
- [168] E. Paulus *et al.*, "Esophagectomy for cancer in octogenarians: should we do it?," *Langenbecks Arch Surg*, vol. 402, no. 3, pp. 539–545, 2017, doi: 10.1007/s00423-017-1573-x.
- [169] J. Ohn et al., "Special Article 1128 ·," 2002.
- [170] T. R. Semenkovich *et al.*, "Trends in Treatment of T1N0 Esophageal Cancer," *Ann Surg*, vol. 270, no. 3, pp. 434–443, Sep. 2019, doi: 10.1097/SLA.0000000000003466.
- [171] K. N. Phoa *et al.*, "Multimodality endoscopic eradication for neoplastic Barrett oesophagus: results of an European multicentre study (EURO-II).," *Gut*, pp. 1–8, 2015, doi: 10.1136/gutjnl-2015-309298.
- [172] K. N. Phoa *et al.*, "Remission of Barrett's esophagus with early neoplasia 5 years after radiofrequency ablation with endoscopic resection: A Netherlands

- cohort study," *Gastroenterology*, vol. 145, no. 1, pp. 96–104, Jul. 2013, doi: 10.1053/j.gastro.2013.03.046.
- [173] O. Pech *et al.*, "Long-term results and risk factor analysis for recurrence after curative endoscopic therapy in 349 patients with high-grade intraepithelial neoplasia and mucosal adenocarcinoma in Barrett's oesophagus," *Gut*, vol. 57, no. 9, pp. 1200–1206, Sep. 2008, doi: 10.1136/gut.2007.142539.
- [174] M. F. Peerally *et al.*, "Radiofrequency ablation compared with argon plasma coagulation after endoscopic resection of high-grade dysplasia or stage T1 adenocarcinoma in Barrett's esophagus: a randomized pilot study (BRIDE)," *Gastrointest Endosc*, vol. 89, no. 4, pp. 680–689, 2019, doi: 10.1016/j.gie.2018.07.031.
- [175] M. di Pietro and R. C. Fitzgerald, "Revised British Society of Gastroenterology recommendation on the diagnosis and management of Barrett's oesophagus with low-grade dysplasia," 2018. doi: 10.1136/gutjnl-2017-314135.
- [176] S. Wani *et al.*, "Endoscopic eradication therapy for patients with Barrett's esophagus—associated dysplasia and intramucosal cancer," *Gastrointest Endosc*, vol. 87, no. 4, pp. 907-931.e9, 2018, doi: 10.1016/j.gie.2017.10.011.
- [177] Y. Gibbens and P. G. Iyer, "What Is the Optimal Surveillance Strategy for Non-dysplastic Barrett's Esophagus?," *Current Treatment Options in Gastroenterology 2020 18:3*, vol. 18, no. 3, pp. 369–383, Jun. 2020, doi: 10.1007/S11938-020-00297-9.

- [178] D. Graham, G. Lipman, V. Sehgal, and L. B. Lovat, "Monitoring the premalignant potential of Barrett's oesophagus'," 2016. doi: 10.1136/flgastro-2016-100712.
- [179] R. E. Pouw *et al.*, "Radiofrequency ablation for low-grade dysplasia in Barrett's esophagus: long-term outcome of a randomized trial," *Gastrointest Endosc*, vol. 92, no. 3, pp. 569–574, Sep. 2020, doi: 10.1016/J.GIE.2020.03.3756.
- [180] N. J. Shaheen *et al.*, "Radiofrequency Ablation in Barrett's Esophagus with Dysplasia," *https://doi.org/10.1056/NEJMoa0808145*, vol. 6, no. 4, pp. 223–224, Dec. 2009, doi: 10.1056/NEJMOA0808145.
- [181] W. A. Wolf *et al.*, "Incidence of Esophageal Adenocarcinoma and Causes of Mortality after Radiofrequency Ablation of Barrett's Esophagus," *Gastroenterology*, vol. 149, no. 7, pp. 1752-1761.e1, 2015, doi: 10.1053/j.gastro.2015.08.048.
- [182] S. van Munster *et al.*, "Long-term outcomes after endoscopic treatment for Barrett's neoplasia with radiofrequency ablation ± endoscopic resection: results from the national Dutch database in a 10-year period," *Gut*, vol. 0, pp. 1–12, 2021, doi: 10.1136/gutjnl-2020-322615.
- [183] A. Rastogi, S. Puli, H. B. El-Serag, A. Bansal, S. Wani, and P. Sharma, "Incidence of esophageal adenocarcinoma in patients with Barrett's esophagus and high-grade dysplasia: a meta-analysis," *Gastrointest Endosc*, vol. 67, no. 3, pp. 394–398, Mar. 2008, doi: 10.1016/j.gie.2007.07.019.

- [184] P. Sharma, N. J. Shaheen, D. Katzka, and J. J. G. H. M. Bergman, "AGA Clinical Practice Update on Endoscopic Treatment of Barrett's Esophagus With Dysplasia and/or Early Cancer: Expert Review," *Gastroenterology*, vol. 158, no. 3, pp. 760–769, Feb. 2020, doi: 10.1053/J.GASTRO.2019.09.051.
- [185] D. Alzoubaidi *et al.*, "Quality indicators for Barrett's endotherapy (QBET): UK consensus statements for patients undergoing endoscopic therapy for Barrett's neoplasia," *Frontline Gastroenterol*, p. flgastro-2019-101247, Aug. 2019, doi: 10.1136/flgastro-2019-101247.
- [186] C. C. Cotton, R. Haidry, A. P. Thrift, L. Lovat, and N. J. Shaheen, "Development of Evidence-Based Surveillance Intervals After Radiofrequency Ablation of Barrett's Esophagus," *Gastroenterology*, vol. 155, no. 2, pp. 316-326.e6, 2018, doi: 10.1053/j.gastro.2018.04.011.
- [187] D. Alzoubaidi *et al.*, "Quality indicators for Barrett's endotherapy (QBET): UK consensus statements for patients undergoing endoscopic therapy for Barrett's neoplasia," *Frontline Gastroenterol*, p. flgastro-2019-101247, Aug. 2019, doi: 10.1136/flgastro-2019-101247.
- [188] P. H. Deprez, "Barrett's esophagus: The advocacy for ESD," *Endosc Int Open*, vol. 4, no. 6, p. E722, Jun. 2016, doi: 10.1055/S-0042-109599.
- [189] P. Wolfson *et al.*, "Accuracy of clinical staging for T2NO oesophageal cancer: Systematic review and meta-analysis," *Diseases of the Esophagus*, vol. 34, no. 8, pp. 1–12, 2021, doi: 10.1093/dote/doab002.

- [190] F. Bray, J. Ferlay, I. Soerjomataram, R. L. Siegel, L. A. Torre, and A. Jemal, "Global cancer statistics 2018: GLOBOCAN estimates of incidence and mortality worldwide for 36 cancers in 185 countries," CA Cancer J Clin, vol. 68, no. 6, pp. 394–424, Nov. 2018, doi: 10.3322/caac.21492.
- [191] J. Shapiro *et al.*, "Neoadjuvant chemoradiotherapy plus surgery versus surgery alone for oesophageal or junctional cancer (CROSS): long-term results of a randomised controlled trial," *Lancet Oncol*, vol. 16, no. 9, pp. 1090–1098, Sep. 2015, doi: 10.1016/S1470-2045(15)00040-6.
- [192] S. R. Markar *et al.*, "Role of neoadjuvant treatment in clinical T2N0M0 oesophageal cancer: results from a retrospective multi-center European study," *Eur J Cancer*, vol. 56, pp. 59–68, Mar. 2016, doi: 10.1016/J.EJCA.2015.11.024.
- [193] J. A. Ajani *et al.*, "NCCN Guidelines Version 2.2019 Esophageal and Esophagogastric Junction Cancers Continue NCCN," 2019.
- [194] H. Kuwano *et al.*, "Guidelines for Diagnosis and Treatment of Carcinoma of the Esophagus April 2012 edited by the Japan Esophageal Society.," *Esophagus*, vol. 12, no. 1, pp. 1–30, 2015, doi: 10.1007/s10388-014-0465-1.
- [195] N. Thosani *et al.*, "Diagnostic accuracy of EUS in differentiating mucosal versus submucosal invasion of superficial esophageal cancers: a systematic review and meta-analysis," *Gastrointest Endosc*, vol. 75, no. 2, pp. 242–253, Feb. 2012, doi: 10.1016/j.gie.2011.09.016.

- [196] S. Kelly *et al.*, "A systematic review of the staging performance of endoscopic ultrasound in gastro-oesophageal carcinoma," *Gut*, vol. 49, pp. 534–539, 2001, doi: 10.1136/gut.49.4.534.
- [197] S. R. Puli, J. B. Reddy, M. L. Bechtold, D. Antillon, J. A. Ibdah, and M. R. Antillon, "Staging accuracy of esophageal cancer by endoscopic ultrasound: A meta-analysis and systematic review ESOPHAGEAL CANCER," *World J Gastroenterol*, vol. 14, no. 10, pp. 1479–1490, 2008, doi: 10.3748/wjg.14.1479.
- [198] "Cochrane Handbook for Systematic Reviews of Interventions | Cochrane Training." Accessed: Jan. 28, 2020. [Online]. Available: https://training.cochrane.org/handbook/current
- [199] P. F. Whiting et al., "Quadas-2: A revised tool for the quality assessment of diagnostic accuracy studies," 2011, American College of Physicians. doi: 10.7326/0003-4819-155-8-201110180-00009.
- [200] J. P. T. Higgins, S. G. Thompson, J. J. Deeks, and D. G. Altman, "Measuring inconsistency in meta-analyses.," BMJ, vol. 327, no. 7414, pp. 557–560, Sep. 2003, doi: 10.1136/bmj.327.7414.557.
- [201] T. W. Rice et al., "T2N0M0 esophageal cancer," J Thorac Cardiovasc Surg, vol. 133, no. 2, pp. 317-324.e1, Feb. 2007, doi: 10.1016/J.JTCVS.2006.09.023.

- [202] B. M. Stiles *et al.*, "Clinical T2-T3N0M0 Esophageal Cancer: The Risk of Node Positive Disease," *Ann Thorac Surg*, vol. 92, no. 2, pp. 491–498, Aug. 2011, doi: 10.1016/J.ATHORACSUR.2011.04.004.
- [203] W.-H. Chen *et al.*, "Long-term outcomes following neoadjuvant chemoradiotherapy in patients with clinical T2NO esophageal squamous cell carcinoma," *Diseases of the Esophagus*, vol. 25, no. 3, pp. 250–255, Apr. 2012, doi: 10.1111/j.1442-2050.2011.01243.x.
- [204] J. Q. Zhang et al., "Neoadjuvant Chemoradiation Therapy Is Beneficial for Clinical Stage T2 NO Esophageal Cancer Patients Due to Inaccurate Preoperative Staging," Ann Thorac Surg, vol. 93, no. 2, pp. 429–437, Feb. 2012, doi: 10.1016/J.ATHORACSUR.2011.10.061.
- [205] T. D. Crabtree *et al.*, "Evaluation of the reliability of clinical staging of T2 N0 esophageal cancer: a review of the Society of Thoracic Surgeons database.," *Ann Thorac Surg*, vol. 96, no. 2, pp. 382–390, Aug. 2013, doi: 10.1016/j.athoracsur.2013.03.093.
- [206] S. Shin, H. K. Kim, Y. S. Choi, K. Kim, and Y. M. Shim, "Clinical stage T1–T2N0M0 oesophageal cancer: accuracy of clinical staging and predictive factors for lymph node metastasis†," *European Journal of Cardio-Thoracic Surgery*, vol. 46, no. 2, pp. 274–279, Aug. 2014, doi: 10.1093/ejcts/ezt607.
- [207] B. D. Tekola, B. G. Sauer, A. Y. Wang, G. E. White, and V. M. Shami, "Accuracy of Endoscopic Ultrasound in the Diagnosis of T2NO Esophageal Cancer," J

- Gastrointest Cancer, vol. 45, no. 3, pp. 342–346, Sep. 2014, doi: 10.1007/s12029-014-9616-9.
- [208] T. J. Hardacker *et al.*, "Treatment of Clinical T2N0M0 Esophageal Cancer," *Ann Surg Oncol*, vol. 21, no. 12, pp. 3739–3743, Nov. 2014, doi: 10.1245/s10434-014-3929-6.
- [209] P. J. Speicher *et al.*, "Induction Therapy Does Not Improve Survival for Clinical Stage T2N0 Esophageal Cancer," *Journal of Thoracic Oncology*, vol. 9, no. 8, pp. 1195–1201, Aug. 2014, doi: 10.1097/JTO.000000000000228.
- [210] P. Samson *et al.*, "Clinical T2N0 Esophageal Cancer: Identifying Pretreatment Characteristics Associated With Pathologic Upstaging and the Potential Role for Induction Therapy," *Ann Thorac Surg*, vol. 101, no. 6, pp. 2102–2111, Jun. 2016, doi: 10.1016/J.ATHORACSUR.2016.01.033.
- [211] C. Luu *et al.*, "Endoscopic ultrasound staging for early esophageal cancer: Are we denying patients neoadjuvant chemo-radiation?," *World J Gastroenterol*, vol. 23, no. 46, pp. 8193–8199, Dec. 2017, doi: 10.3748/wjg.v23.i46.8193.
- [212] M. Winiker, S. Mantziari, S. G. Figueiredo, N. Demartines, P. Allemann, and M. Schäfer, "Accuracy of preoperative staging for a priori resectable esophageal cancer," *Diseases of the Esophagus*, vol. 31, no. 1, Jan. 2018, doi: 10.1093/dote/dox113.

- [213] R. Shridhar, J. Huston, and K. L. Meredith, "Accuracy of endoscopic ultrasound staging for T2NO esophageal cancer: a National Cancer Database analysis," *J Gastrointest Oncol*, vol. 9, no. 5, p. 887, 2018, doi: 10.21037/JGO.2018.01.16.
- [214] S. M. Atay *et al.*, "Predictors of staging accuracy, pathologic nodal involvement, and overall survival for cT2N0 carcinoma of the esophagus," *J Thorac Cardiovasc Surg*, vol. 157, no. 3, pp. 1264-1272.e6, Mar. 2019, doi: 10.1016/J.JTCVS.2018.10.057.
- [215] T. D. Crabtree *et al.*, "Endoscopic ultrasound for early stage esophageal adenocarcinoma: Implications for staging and survival," *Annals of Thoracic Surgery*, vol. 91, no. 5, pp. 1509–1516, May 2011, doi: 10.1016/j.athoracsur.2011.01.063.
- [216] A. Barbetta *et al.*, "Predictors of Nodal Metastases for Clinical T2N0 Esophageal Adenocarcinoma," *Annals of Thoracic Surgery*, vol. 106, no. 1, pp. 172–177, Jul. 2018, doi: 10.1016/j.athoracsur.2018.02.087.
- [217] E. Vazquez-Sequeiros *et al.*, "Routine vs. selective EUS-guided FNA approach for preoperative nodal staging of esophageal carcinoma," *Gastrointest Endosc*, vol. 63, no. 2, pp. 204–211, Feb. 2006, doi: 10.1016/j.gie.2005.08.053.
- [218] S. Yoshinaga, "Endoscopic ultrasound using ultrasound probes for the diagnosis of early esophageal and gastric cancers," World J Gastrointest Endosc, vol. 4, no. 6, p. 218, 2012, doi: 10.4253/wjge.v4.i6.218.

- [219] S. R. Friedberg and J. Lachter, "Endoscopic ultrasound: Current roles and future directions," *World J Gastrointest Endosc*, vol. 9, no. 10, pp. 499–505, Oct. 2017, doi: 10.4253/wjge.v9.i10.499.
- [220] T. Krill *et al.*, "Accuracy of endoscopic ultrasound in esophageal cancer staging," *J Thorac Dis*, vol. 11, no. S12, pp. S1602–S1609, Aug. 2019, doi: 10.21037/jtd.2019.06.50.
- [221] P. R. Pfau, G. G. Ginsberg, R. J. Lew, D. O. Faigel, D. B. Smith, and M. L. Kochman, "Esophageal dilation for endosonographic evaluation of malignant esophageal strictures is safe and effective," *American Journal of Gastroenterology*, vol. 95, no. 10, pp. 2813–2815, 2000, doi: 10.1016/S0002-9270(00)01101-1.
- [222] C. Tan *et al.*, "Potential biomarkers for esophageal cancer.," *Springerplus*, vol. 5, p. 467, 2016, doi: 10.1186/s40064-016-2119-3.
- [223] F. Giganti *et al.*, "Prospective comparison of MR with diffusion-weighted imaging, endoscopic ultrasound, MDCT and positron emission tomography-CT in the pre-operative staging of oesophageal cancer: results from a pilot study," *Br J Radiol*, vol. 89, no. 1068, p. 20160087, Dec. 2016, doi: 10.1259/bjr.20160087.
- [224] G. Linder, N. Korsavidou-Hult, T. Bjerner, H. Ahlström, and J. Hedberg, "18F-FDG-PET/MRI in preoperative staging of oesophageal and gastroesophageal

- junctional cancer," *Clin Radiol*, vol. 74, no. 9, pp. 718–725, Sep. 2019, doi: 10.1016/j.crad.2019.05.016.
- [225] P. S. N. van Rossum *et al.*, "Imaging strategies in the management of oesophageal cancer: what's the role of MRI?," *Eur Radiol*, vol. 23, no. 7, pp. 1753–1765, Jul. 2013, doi: 10.1007/s00330-013-2773-6.
- [226] S. R. Markar and D. E. Low, "The Volume-Outcome Relationship, Standardized Clinical Pathways, and Minimally Invasive Surgery for Esophagectomy," in *Minimally Invasive Foregut Surgery for Malignancy*, Cham: Springer International Publishing, 2015, pp. 25–34. doi: 10.1007/978-3-319-09342-0 3.
- [227] J. M. Daly *et al.*, "Esophageal cancer: results of an American College of Surgeons patient care evaluation study," *J Am Coll Surg*, vol. 190, no. 5, pp. 562–572, May 2000, doi: 10.1016/S1072-7515(00)00238-6.
- [228] M. Jacobs *et al.*, "Meta-analysis shows clinically relevant and long-lasting deterioration in health-related quality of life after esophageal cancer surgery," *Quality of Life Research*, vol. 23, no. 4, pp. 1155–1176, May 2014, doi: 10.1007/s11136-013-0576-5.
- [229] S. Pasquali *et al.*, "Survival After Neoadjuvant and Adjuvant Treatments Compared to Surgery Alone for Resectable Esophageal Carcinoma," *Ann Surg*, vol. 265, no. 3, pp. 481–491, Mar. 2017, doi: 10.1097/SLA.0000000000001905.

- [230] X. Pouliquen, H. Levard, J. M. Hay, K. McGee, A. Fingerhut, and O. Langlois-Zantin, "5-Fluorouracil and cisplatin therapy after palliative surgical resection of squamous cell carcinoma of the esophagus. A multicenter randomized trial. French Associations for Surgical Research.," *Ann Surg*, vol. 223, no. 2, pp. 127–33, Feb. 1996, doi: 10.1097/00000658-199602000-00003.
- [231] N. A. Saeed *et al.*, "Adjuvant chemotherapy and outcomes in esophageal carcinoma.," *J Gastrointest Oncol*, vol. 8, no. 5, pp. 816–824, Oct. 2017, doi: 10.21037/jgo.2017.07.10.
- [232] P. Wolfson *et al.*, "OTU-18 Using X-ray phase contrast imaging to identify oesophageal pathology," *Gut*, vol. 68, no. Suppl 2, pp. A134–A134, Jun. 2019, doi: 10.1136/gutjnl-2019-bsgabstracts.253.
- [233] P. S. N. van Rossum, C. Xu, D. V Fried, L. Goense, L. E. Court, and S. H. Lin, "The emerging field of radiomics in esophageal cancer: current evidence and future potential.," *Transl Cancer Res*, vol. 5, no. 4, pp. 410–423, Aug. 2016, doi: 10.21037/tcr.2016.06.19.
- [234] M. Esposito *et al.*, "Technical note: Cartilage imaging with sub-cellular resolution using a laboratory-based phase-contrast x-ray microscope," *Med Phys*, vol. 50, no. 10, pp. 6130–6136, 2023, doi: 10.1002/mp.16599.
- [235] K. F. Siu, H. C. Cheung, and J. Wong, "Shrinkage of the esophagus after resection for carcinoma," *Ann Surg*, vol. 203, no. 2, pp. 173–176, 1986, doi: 10.1097/00000658-198602000-00011.

- [236] V. Chandrasekhara and G. G. Ginsberg, "Endoscopic mucosal resection: Not your father's polypectomy anymore," Jul. 01, 2011, W.B. Saunders. doi: 10.1053/j.gastro.2011.05.012.
- [237] L. Bailly *et al.*, "3D multiscale imaging of human vocal folds using synchrotron X-ray microtomography in phase retrieval mode," *Scientific Reports 2018 8:1*, vol. 8, no. 1, pp. 1–20, Sep. 2018, doi: 10.1038/s41598-018-31849-w.
- [238] C. K. Hagen *et al.*, "High contrast microstructural visualization of natural acellular matrices by means of phase-based x-ray tomography," *Scientific Reports 2015 5:1*, vol. 5, no. 1, pp. 1–10, Dec. 2015, doi: 10.1038/srep18156.
- [239] P. Garcia-Canadilla *et al.*, "Complex Congenital Heart Disease Associated With Disordered Myocardial Architecture in a Midtrimester Human Fetus," *Circ Cardiovasc Imaging*, vol. 11, no. 10, p. e007753, Oct. 2018, doi: 10.1161/CIRCIMAGING.118.007753/FORMAT/EPUB.
- [240] P. Jali, M. Donoghue, and M. Gadiwan, "A rapid manual processing technique for resource-limited small laboratories," *Journal of Oral and Maxillofacial Pathology*, vol. 19, no. 3, pp. 306–314, Sep. 2015, doi: 10.4103/0973-029X.174616.
- [241] R. Kandyala, S. P. C. Raghavendra, and S. T. Rajasekharan, "Xylene: An overview of its health hazards and preventive measures," *J Oral Maxillofac Pathol*, vol. 14, no. 1, p. 1, 2010, doi: 10.4103/0973-029X.64299.

- [242] M. Chourrout *et al.*, "Brain virtual histology with X-ray phase-contrast tomography Part I: whole-brain myelin mapping in white-matter injury models," *bioRxiv*, p. 2021.03.24.436852, Jul. 2021, doi: 10.1101/2021.03.24.436852.
- [243] J. Dudak *et al.*, "High-contrast X-ray micro-radiography and micro-CT of ex-vivo soft tissue murine organs utilizing ethanol fixation and large area photon-counting detector," *Scientific Reports 2016 6:1*, vol. 6, no. 1, pp. 1–9, Jul. 2016, doi: 10.1038/srep30385.
- [244] M. Reichardt, J. Frohn, A. Khan, F. Alves, and T. Salditt, "Multi-scale X-ray phase-contrast tomography of murine heart tissue," *Biomed Opt Express*, vol. 11, no. 5, p. 2633, 2020, doi: 10.1364/BOE.386576.
- [245] P. M. Sagar, D. Johnston, M. J. McMahon, M. F. Dixon, and P. Quirke, "Significance of circumferential resection margin involvement after oesophagectomy for cancer," *British Journal of Surgery*, vol. 80, no. 11, pp. 1386–1388, Dec. 2005, doi: 10.1002/BJS.1800801109.
- [246] J. R. O'Neill *et al.*, "Defining a positive circumferential resection margin in oesophageal cancer and its implications for adjuvant treatment," *Br J Surg*, vol. 100, no. 8, pp. 1055–1063, Jul. 2013, doi: 10.1002/BJS.9145.
- [247] R. E. Pouw *et al.*, "Stepwise radical endoscopic resection for eradication of Barrett's oesophagus with early neoplasia in a cohort of 169 patients," *Gut*, vol. 59, no. 9, pp. 1169–1177, Sep. 2010, doi: 10.1136/GUT.2010.210229.

- [248] L. Urbani et al., "Long-term cryopreservation of decellularised oesophagi for tissue engineering clinical application," PLoS One, vol. 12, no. 6, p. e0179341, Jun. 2017, doi: 10.1371/JOURNAL.PONE.0179341.
- [249] R. C. Boston, M. D. Schnall, S. A. Englander, J. R. Landis, and P. J. Moate, "Estimation of the content of fat and parenchyma in breast tissue using MRI T1 histograms and phantoms," *Magn Reson Imaging*, vol. 23, no. 4, pp. 591–599, May 2005, doi: 10.1016/J.MRI.2005.02.006.
- [250] K. M. A. Ho, A. Banerjee, M. Lawler, M. D. Rutter, and L. B. Lovat, "Predicting endoscopic activity recovery in England after COVID-19: a national analysis," *Lancet Gastroenterol Hepatol*, vol. 6, no. 5, pp. 381–390, 2021, doi: 10.1016/S2468-1253(21)00058-3.
- [251] H. L. Somerset and B. K. Kleinschmidt-DeMasters, "Approach to the intraoperative consultation for neurosurgical specimens," Adv Anat Pathol, vol. 18, no. 6, pp. 446–449, Nov. 2011, doi: 10.1097/PAP.0B013E3182169934.
- [252] W. L. Curvers, R. Kiesslich, and J. J. G. H. M. Bergman, "Novel imaging modalities in the detection of oesophageal neoplasia," *Best Pract Res Clin Gastroenterol*, vol. 22, no. 4, pp. 687–720, Aug. 2008, doi: 10.1016/J.BPG.2008.01.001.
- [253] R. C. Fitzgerald, I. T. Saeed, D. Khoo, M. J. G. Farthing, and W. Rodney Burnham, "Rigorous Surveillance Protocol Increases Detection of Curable Cancers Associated with Barrett's Esophagus," 2001.